Wear Simulation Study

I. Persson[1], L-O. Jönsson[2], M. Asplund[3], P. Söderström[4], M. Li[5], E. Aggestam[6], J. Dolk[7], M. Berg[8], E. Khoramzad[9]

[1] AB DEsolver, Östersund, Sweden. ingemar.persson@desolver.se
[2] Analytical Dynamics, Lund, Sweden. lars-ove.jonsson@anadyn.se
[3] Trafikverket, Technology & Environment, Luleå, Sweden. matthias.asplund@trafikverket.se
[4] SJ AB, Rolling Stock Division, Stockholm, Sweden. par.soderstrom@sj.se
[5] Trafikverket, Technology & Environment, Göteborg, Sweden. martin.li@ trafikverket.se
[6] Trafikverket, Technology & Environment, Trollhättan, Sweden. emil.aggestam@ trafikverket.se
[7] A-Train, Stockholm, Sweden. johanna.dolk@atrain.se
[8] KTH, Department of Engineering Mechanics, Stockholm, Sweden. mabe@kth.se
[9] KTH, Department of Engineering Mechanics, Stockholm, Sweden. elhamk@kth.se

Abstract

The conditions at wheel and rail contact have a major impact on the economy of the whole railway system, as frequent reprofiling of wheels and rails due to wear and rolling contact fatigue are major cost drivers. This extensive study investigates the impact of different factors on wheel wear and risk of rolling contact fatigue (RCF). A large number of iterative wear simulations are compared to a reference case in terms of development of equivalent conicity, and risk of surface and subsurface RCF. The reference case is chosen to be representative of a typical vehicle operation in Sweden today.

Keywords: Wear prediction loop, Wheel profile, Rail profile, Conicity, EN15302, GIP, GIPw, GIPr1435, RCF.

Table of Contents

1. Introduction

The wheel and rail contact is of vital importance for the total economy of the railway system. A poorly performing wheel-rail contact leads to immense costs in terms of frequent reprofiling of wheels to keep vehicle dynamics acceptable and tread damage under control, and to frequent rail grinding to ensure that rolling contact fatigue does not cause safety issues, or rail replacements due to wear.

The focus in this investigation is on wheel wear. The reasoning is that wheels wear faster than rails since the steel grade in rails is usually harder than the steel grade in wheels and since each point around the circumference of the wheel is in contact every wheel revolution, whereas it takes longer to accumulate the same number of contacts for the rail.

This project started as an investigation to find a wheel profile as an option to the ever-present S1002 profile, but it turns out there are many parameters that influence the change of the wheel profile with wear. Thus, the scope was widened to investigate which factors have the greatest influence on wear, equivalent conicity in the wheel-rail contact, and rolling contact fatigue.

The basis for the investigation is wear loop simulations, where a generic vehicle is simulated on a collection of representative tangent and curved track sections. The positions and forces in the wheel-rail contact are collected throughout the simulations, and the wear on the wheel profile is determined. The shape of the wheel profile is updated, and the process is repeated. Typically, around 1500 wear iterations (generations) are followed for each set of simulation parameters. In a postprocessing step, equivalent conicity and indexes for the initiation of surface and subsurface rolling contact fatigue (RCF) are calculated. The method is described in detail in [2].

The Gradient Index Profile set of indexes are used to describe the rail and wheel profiles in this report. These are described in section 3.

A large number of wear loop simulations have been made, but not all are presented in this report. It is a challenge to summarize an investigation of this size, and it has been necessary to limit the number of variations presented. The factors that are varied are presented in section 2. More detailed descriptions are presented in sections 4 to 8.

The results are interpreted in relation to a reference case, which is chosen to be representative of a typical operation in Sweden today. The reference case and simulation results are presented in section 9.

The wheel-rail contact must fulfil many requirements, and it is a challenge to fulfil all of them. In particular, there are often contradicting actions required in order to improve different vehicle/track responses. As an example, it is a challenge to obtain low risk for instability due to high conicity and at the same time low risk for RCF since if the wheel/rail profiles are good for avoiding RCF they may instead lead to vehicle instability and bad ride, or vice versa. Generally, the parameters available for change are limited. For example, the wear simulations show that the wheel profile mainly influences the results at the beginning of the wear cycle. In section 11, the idea of using different rail profiles in curves versus on tangent track is proposed as a possible solution for minimizing the risks for both RCF and vehicle instabilities at the same time.

Finally, a summary of the findings in this report is given in section 12.

This work is part of the project "A systematic approach to improve passenger ride comfort" [1]. This collaboration project between the infrastructure manager Trafikverket and operators SJ AB and A-Train AB, together with external partners, aims to improve the handling of bad ride comfort. The current rules and regulations are centred on safety and are often poorly adapted to handle ride comfort issues, especially for factors shared between track and rolling stock such as the wheel-rail contact conditions. The project is part of the In2Track2 [3] and In2Track3 [4] initiatives in the EU Innovation Programme 3.

2. Parameters

Parameters that have been varied in this study are presented in Table 2.

Table 1: Parameters varied in this wear simulation study

Pos	Variable	Comment
1	Rprof	Used rail profiles. This field can look a bit different depending how many rail profiles that have been used. See section 4
2	mu	Wheel/rail friction. Average value during one year.
3	SAb	Bogie steering ability, see section 5 and ref [2].
4	Wprof	Initial wheel profile, see section 6
5	Cdist	Curve distribution of the track, see section 7.1
6	Tirr_file	Track irregularity file, see section 7.2
7	Gauge	Track gauge, see section 7.3
8	Tirr_ampl	Track irregularity amplitudes, see section 7.4
9	Lat_acc	Uncompensated lateral acceleration in curves, see section 8
10	Wear_fact	Wear factor on high rail in curves. Due to track lubrication the wear is lower in curves < 700 m, see T. Jendel [6]
11	Brake	Wear due to braking.
12	Accel	Wear due to acceleration. (Has not been studied yet)
13	Wear_chart	Wear chart used when calculating the wear, see Archard [5] and Jendel [6].

3. Using GIP to describe rail and wheel profiles

Gradient Index Profile, or GIP, is a set of indexes that is used to assess the wheel-rail interface that have been developed within the framework of this collaboration project. The definitions are given in [7]. It has been presented at international conferences [8][9], and also in a CEN report [10].

A summary is given in Figure 1, with a definition of the parameters in Table 2.

$$GIPw = 100 \cdot \frac{dZw}{dYw}; GIPr = 100 \cdot \frac{dZr}{dYr}$$

$$GIP = \frac{GIPwL - GIPrL}{GIPwL + GIPrL} + \frac{GIPwR - GIPrR}{GIPwR + GIPrR}$$

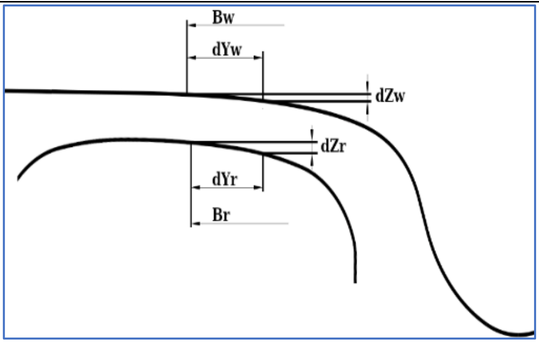

Figure 1.Definitions of GIP, GIPr and GIPw.

Table 2. The definitions of the parameters in Figure 1.

Parameter	Definition
GIPw	GIP for wheel, GIPwL and GIPwR, left and right side respectively
GIPr	GIP for rail, GIPrL and GIPrR, left and right side respectively
GIP	GIP combined, a combination of the four values above (wheel and rail, left and right)
Bw	750 mm, the lateral distance of the reference point from centre of wheelset
dYw	15 mm, for finding the vertical position to determine dZw
Br	751 mm, the lateral distance of the reference point from centre of track
dYr	16 mm, for finding the vertical position to determine dZr

The inclination (gradient) of the wheel profile at the running circle is called GIPw, and the corresponding inclination of the rail profile is GIPr. The combined index GIP is closely related to the equivalent conicity, as demonstrated for example by [8]. As an example, if the inclination of the rail GIPr is larger than the inclincation of the wheel GIPw, the wheel-rail contact is normally situated towards the field side, and the conicity is generally low.

In this report, the rail and wheel profiles are sorted and described by their GIPr and GIPw values. The development of GIPw as the wheel profiles wear is also shown in diagrams. The GIPr values are calculated at track gauge 1435 mm, which is indicated by using the term GIPr1435. The wheelset back-to-back distance 1360 mm has been used in all calculations.

4. Rail profiles

In this study, the rail profiles are sorted according to their GIPr1435 value. The tested rail profiles are presented in Table 3.

Table 3: Studied rail profiles, sorted on their GIPr1435-value

GIPr1435	Rail profile
06.76	SL TUB1, a profile optimized with the genetic algorithm

07.34	60E2i40_grind060_outwards, same as rail profile 60E2 with an inclination of 1/40, but the field side of the profile is ground 0.6[mm]. In order to shift the lateral position of the contact patch.
07.63	60E1i40
07.89	bv50i30
07.94	60E1i35
07.99	60E2i40_grind030_outwards, same as rail profile 60E2 with an inclination of 1/40, but the field side of the profile is ground 0.3[mm]. In order to shift the lateral position of the contact patch.
08.21	60E2i40_grind020_outwards, same as rail profile 60E2 with an inclination of 1/40, but the field side of the profile is ground 0.2[mm]. In order to shift the lateral position of the contact patch.
08.33	Same profile as SL TUB1 but with another rail inclination.
08.34	60E1i30
08.36	60E2i40_grind013_outwards, same as rail profile 60E2 with an inclination of 1/40, but the field side of the profile is ground 0.13[mm]. In order to shift the lateral position of the contact patch.
08.42	60E2i40_grind010_outwards, same as rail profile 60E2 with an inclination of 1/40, but the field side of the profile is ground 0.1[mm]. In order to shift the lateral position of the contact patch.
08.64	60E2i40
08.78	60E1i26
08.80	Bdl416_U_km0163_0331.000_L_MP_XXXmgt_180620, a profile measured 2018-06-20 on the left rail on the up track of Bdl416, km 163 and meter 331.
09.05	60E1i24
09.33	60E2i30
09.52	60E2i28
09.74	60E2i26
09.76	60E1i20
09.80	Bdl416_U_km0163_0219.810_L_IMV100Xm5_XXXmgt_180913, a profile measured 2018-09-13 on the left rail on the up track of Bdl416, km 163 and meter 219.810.
10.00	60E2i24
10.05	Bdl512_D_km0222_586.7900_L_IMV200Nm5_XXXmgt_210324, a profile measured 2021-03-24 on the left rail on the down track of Bdl512, km 222 and meter 586.790.
10.30	60E2i22
10.32	Bdl416_U_km0138_0375.000_R_MP_XXXmgt_181025, a profile measured 2018-10-25 on the right rail on the up track of Bdl416, km 138 and meter 375.

10.34	Bdl416_U_km163_184.9307_L_180913_f5, a profile measured 2018-10-25 on the left rail on the up track of Bdl416, km 138 and meter 375.
10.66	60E2i20
10.81	MB4_smooth2. Same as MB4 but the facets from the grinding have been smoothed.
12.80	Bdl416_D_km0163_0399.000_L_MP_XXXmgt_180620, a profile measured 2018-06-20 on the left rail on the down track of Bdl416, km 163 and meter 399.

The rail profiles 60E1 and 60E2 are defined according to EN13674.

The notation 60E1i40 stands for a 60E1 rail profile with an inclination of 1/40. Similarly, the notation 60E1i30 stands for a 60E1 rail profile with an inclination of 1/30 and so on.

In the studies, different profiles has been used in curves and on tangent track. Variable “Rprof” in Table 1 is defined as:

1) If the same rail profile has been used on both tangent track and in curves. Variable “Rprof” is defined as:
   [GIPr1435]
   Where GIPr1435 is the profile used both on tangent track and in all curves.

2) If different profiles have been used on tangent track and in curves. Variable “Rprof” is defined as:
   [GIPr1435t “t_” GIPr1435c CurveCode]

   Where: GIPr1435t = Rail profile on tangent track

   GIPr1435c = Rail profile in curves

   CurveCode = Code that tells in which curves the curve profiles shall be used:

   ”c” Curves from 400m up to 1400m

   ”c2500” All curves under 2500m

3) If different profiles have been used on tangent track and in curves. In curves different profiles has been used on high and low rail. Variable “Rprof” is defined as: [GIPr1435t “t_” GIPr1435h ”-” GIPr1435l CurveCode]

   Where: GIPr1435t = Rail profile on tangent track

   GIPr1435h = Rail profile on high rail

   GIPr1435l = Rail profile on low rail

   CurveCode = Code that tells in which curves the curve profiles shall be used:

   ”c” Curves from 400m up to 1400m

   ”c2500” All curves under 2500m

5. Bogie steering ability

The steering ability of a bogie depends on the longitudinal stiffness of the primary springs, track gauge, lateral distance to the primary springs, contact force between wheel and rail and wheelbase.

The bogie steering ability SAb s defined as:

$$SAb = \frac{kxbl \cdot WB \cdot (Bkxbl/bo)^2}{Fznom}$$

The Following values for SAb have been studied:

SAb	Comment
167	Very soft radial steering bogie.
360	Semi-soft bogie. A typical value used in modern railway vehicles.
900	Very stiff non-radial steering bogie. The primary suspension acts more or less as a constraint between the two wheelsets in the bogie.

For further information see ref [2].

6. Initial wheel profile

The initial wheel profile affects the wear on the wheel when the wheels are newly turned. However, after the first wear-in phase, the wheels are getting more and more similar to each other. The studied initial wheel profiles are:

GIPw	Wheel profile	Comment
2.50	1i40t32.5	Profile 1/40th acc. to EN13715, flange thickness 32.5 mm
4.27	ENS1002t29.0	Profile S1002 acc. to EN13715, flange thickness 29.0 mm
4.84	ENS1002t30.0	Profile S1002 acc. to EN13715, flange thickness 30.0 mm
5.14	ENS1002t30.5	Profile S1002 acc. to EN13715, flange thickness 30.5 mm
5.24	n33t32.8	Normalprofil, an old Swedish wheel profile
5.53	S1002t30.5	Profile S1002 according to UIC, flange thickness 30.5 mm
5.66	mix75t30.5	A mix of 75% ENS1002t30.5 and 25% EPSt30.5.
6.45	ENS1002t32.5	Profile S1002 according to EN13715 full flange 32.5 mm
6.86	ENXt30.3	New wheel profile developed at KTH 2023

7. Tracks

Different tracks lead to different wear pattern on the wheels.

7.1 Curve distribution

Tracks which have many and tight curves will lead to flange wear of the wheels. On the other hand, mainly tread wear of the wheels take place for tracks which have very few curves.

7.1.1 Cdist “1”

Is based on the track curve distribution on the main track from Stockholm to Gothenburg. The curve distribution was created by B. Dirks [11].

```
 R       Cant    Ltot %
 394   .112      0.5
 495   .106      0.3
 594   .127      3.4
 795   .108      2.8
1002   .134      9.8
1164   .113      5.3
1468   .090      5.2
1869   .081      4.4
2276   .070      2.9
1e99   .000     65.4
         Total  100%
```

7.1.2 Cdist “2”

Same as track “1” but with the transition curves included

```
   R   Lt      Lc      Cant   Ltot%
 394   69     289     .112    0.5
 495   90     161     .106    0.3
 594  117     191     .127    3.4
 795  115     158     .108    2.8
1002  197     272     .134    9.8
1164  161     230     .113    5.3
1468  150     155     .090    5.2
1869  131     182     .081    4.4
2276  107     170     .070    2.9
1e99   -       -        -    65.4
```

7.2 Track irregularity file

The wavelength distribution of the track irregularities may have an impact on the wear on the wheels. However, this hasn’t been studied yet. The analysis so far is made only on one track file.

7.2.1 Tirr_file “track_V200a.trac”

A track made for speeds up to 200 km/h, measured 1994-10-21 on Bdl 363 km 151-146. Track quality:

```
#
#       Bdl 363 Simonstorp-Strångsjö up km 151-146
#       Measured by Mauzin      941021
#       Class K0
#       Translated in trac-format by trc_imauz, 950201/IP
#  ----------------------------------------------------------------
#
#
#     Results according to UIC518 and CEN/TC 256 WG 10:
#                     Alignment       Level       Mean    Speed   Threshold
#     Distance         Sigma  MAX    Sigma  MAX   Gauge    200.    Level
#  ------------------------------------------------------------------------
#       0.-    250.   0.49   1.16   0.97   3.35  1432.36    QN<1
#     250.-    500.   0.85   2.54   0.95   3.46  1434.53  1<QN<2   Ys
#     500.-    750.   0.72   1.75   1.00   3.49  1433.92    QN<1
#     750.-   1000.   0.68   2.31   1.15   4.61  1434.20    QN<1
```

```
#    1000.-   1250.   0.77   2.61   1.07   5.77  1434.02  1<QN<2        Zm
#    1250.-   1500.   0.63   1.96   1.09   5.16  1435.45  1<QN<2        Zm
#    1500.-   1750.   0.74   2.15   0.92   3.27  1435.03    QN<1
#    1750.-   2000.   0.71   2.00   0.99   3.88  1434.03    QN<1
#    2000.-   2250.   0.84   2.28   0.98   3.10  1434.54  1<QN<2   Ys
#    2250.-   2500.   0.84   2.87   1.08   3.52  1433.51  1<QN<2   Ys
#    2500.-   2750.   0.31   2.61   0.95   4.29  1433.84    QN<1
#    2750.-   3000.   0.44   2.55   1.13   4.79  1434.98    QN<1
#    3000.-   3250.   0.53   2.60   1.01   3.29  1435.47    QN<1
#    3250.-   3500.   0.38   2.19   1.01   3.70  1432.93    QN<1
#    3500.-   3750.   0.43   2.69   0.87   3.50  1433.77    QN<1
#    3750.-   4000.   0.24   2.49   0.60   1.67  1432.77    QN<1
#    4000.-   4250.   0.34   2.51   0.59   2.38  1434.13    QN<1
#    4250.-   4500.   0.26   2.30   0.91   3.17  1435.29    QN<1
#    4500.-   4750.   0.36   1.83   1.05   4.63  1433.58    QN<1
#  -------------------------------------------------------------------------
#  In Total:
#       0.-   4997.   0.58   2.87   0.97   5.77  1434.17
#  -------------------------------------------------------------------------
#
#
# Summary for the total track
# ---------------------------
#   QN<1 Sections with good track standard        =  73.7 %  Should be > 50%
# 1<QN<2 Regularly planned maintenance operations =  26.3 %  Should be < 40%
# 2<QN<3 Short term maintenance action            =   0.0 %  Should be < 10%
# 3<QN   Sections to be excluded from the analysis=   0.0 %  Should be =  0%
#
#
#
#          Table MAX according to CEN/TC 256 WG 10
#                Alignment             Level
#     Max Speed   QN1    QN2    QN3    QN1    QN2    QN3
#  -----------------------------------------------------------------
#        80      12.0   14.0   18.3   12.0   16.0   20.8
#       120       8.0   10.0   13.0    8.0   12.0   15.6
#       160       6.0    8.0   10.4    6.0   10.0   13.0
#       200       5.0    7.0    9.1    5.0    9.0   11.7
#       300       4.0    6.0    7.8    4.0    8.0   10.4
#
#          Table RMS according to CEN/TC 256 WG 10
#                Alignment       Level
#     Max Speed   QN1    QN2    QN1    QN2
#  -----------------------------------------------------------------
#        80       1.5    1.8    2.3    2.6
#       120       1.2    1.5    1.8    2.1
#       160       1.0    1.3    1.4    1.7
#       200       0.8    1.1    1.2    1.5
#       300       0.7    1.0    1.0    1.3
#  -----------------------------------------------------------------
```

7.3 Track gauge

The average track gauge affects the value of GIPr. A wider gauge will give a greater GIPr, which affects the wear pattern on the wheels.

7.3.1 Gauge “0”

Gauge “0” gives a similar track as Gauge “1” but 2 mm tighter in all curves

7.3.2 Gauge “1”

When parameter “Gauge” is set equal to “1”, the following gauge distribution will apply:

R	Lt	Lc	Cant	Ltot %	Gauge=1
394	69	289	.112	0.5	1440.5
495	90	161	.106	0.3	1440.5
594	117	191	.127	3.4	1439.5
795	115	158	.108	2.8	1437.5
1002	197	272	.134	9.8	1437.5
1164	161	230	.113	5.3	1436
1468	150	155	.090	5.2	1436
1869	131	182	.081	4.4	1436
2276	107	170	.070	2.9	1436
1e99	-	-	-	65.4	1436

7.3.3 Gauge “2”

Gauge “2” gives a similar track as Gauge “1” but 2 mm wider in all curves.

7.4 Track irregularity amplitudes

Larger track irregularities lead to more even distributed wheel wear. Smaller amplitudes lead to more concentrated wear on the wheels.

7.4.1 Tirr_ampl “0”

Same track irregularity amplitudes factor= 1.0 in all curves:

R	Lt	Lc	h	Ltot %	Gauge1	Tirr0
394	69	289	.112	0.5	1440.5	1.0
495	90	161	.106	0.3	1440.5	1.0
594	117	191	.127	3.4	1439.5	1.0
795	115	158	.108	2.8	1437.5	1.0
1002	197	272	.134	9.8	1437.5	1.0
1164	161	230	.113	5.3	1436	1.0
1468	150	155	.090	5.2	1436	1.0
1869	131	182	.081	4.4	1436	1.0
2276	107	170	.070	2.9	1436	1.0
1e99	-	-	-	65.4	1436	1.0

7.4.2 Tirr_ampl “1”

Smaller track irregularity amplitudes on tangent track and in larger curves:

R	Lt	Lc	h	Ltot %	Gauge1	Tirr1
394	69	289	.112	0.5	1440.5	1.0
495	90	161	.106	0.3	1440.5	1.0
594	117	191	.127	3.4	1439.5	0.9
795	115	158	.108	2.8	1437.5	0.8
1002	197	272	.134	9.8	1437.5	0.7
1164	161	230	.113	5.3	1436	0.6
1468	150	155	.090	5.2	1436	0.5
1869	131	182	.081	4.4	1436	0.5
2276	107	170	.070	2.9	1436	0.5
1e99	-	-	-	65.4	1436	0.5

7.4.3 Tirr_ampl “2”

Larger track irregularity amplitudes according to the following table:

R	Lt	Lc	h	Ltot %	Gauge1	Tirr2
394	69	289	.112	0.5	1440.5	1.00

```
 495  90     161     .106  0.3     1440.5  1.40
 594 117     191     .127  3.4     1439.5  1.50
 795 115     158     .108  2.8     1437.5  1.50
1002 197     272     .134  9.8     1437.5  1.45
1164 161     230     .113  5.3     1436    1.40
1468 150     155     .090  5.2     1436    1.35
1869 131     182     .081  4.4     1436    1.30
2276 107     170     .070  2.9     1436    1.25
1e99  -       -        -  65.4     1436    1.25
```

8. Uncompensated lateral acceleration

Uncompensated lateral acceleration in curves is the same as cant deficiency, but expressed in [m/s^2]. The following table show the relation between uncompensated lateral acceleration and cant deficiency:

Kat	Cant deficiency [mm]	Uncompensated lateral acceleration [m/s^2]
A	100	0.65255
B	150	0.97613
C	180	1.16881
S	245	1.58134

9. Reference case

To see the effect of different factors on wheel wear. The problem is “linearized” around a reference case. The reference case is assumed to approximatively correspond to the case we currently have on the Swedish railway network today.

The reference case is denoted:

wl_09.33[1]_0.30[2]_360[3]_S1002t30.5[4]_2[5]_2[6]_1[7]_0[8]_0.98[9]_1[10]_0.74,11[11]_0[12]_5[13]

Which have the following meaning:

Pos	Variable	Value	Comment
1	GIPr1435	9.33	Rail profile 60E2i30 according to EN13674, on both tangent track and in curves. This rail profile has a GIPr1435 value of 9.33, see section 4
2	mu	0.30	Friction coefficient between wheel and rail. Average value during one year.
3	SAb	360	Steering ability of the vehicle. For the definition of SAb, see section 5 and ref [2].
4	Wprof	5.14	Initial wheel profile, see section 6
5	CurveD	“2”	Curve distribution “2” defined in section 7.1.2.
6	Tirr_file	“2”	Track irregularities. Tirr_file number “2” is defined in section 7.2.1.
7	Gauge	“1”	Track gauge “1” defined in section 7.3.2
8	Tirr_ampl	“0”	Track irregularity amplitude “0” defined in section 7.4.1.
9	Lat_acc	0.98	Uncompensated lateral acceleration in curves, see section 8.
10	Wear_fact	“1”	Wear factor on high rail in curves. Number “1” stands for a factor of 0.5 in all curves under 700m. A factor discovered by T.Jendel [6]
11	Braking	0.74,11	Retardation 0.74 [m/s^2], 11% of the time.
12	Accel	“0”	Wear due to acceleration and rolling resistance. Number “0” stands for no acceleration
13	Wear_chart	“5"	Wear chart according to T.Jendel [6] but without area 1 (seizure)

9.1 Reference case: Conicity development wheelset 1&4

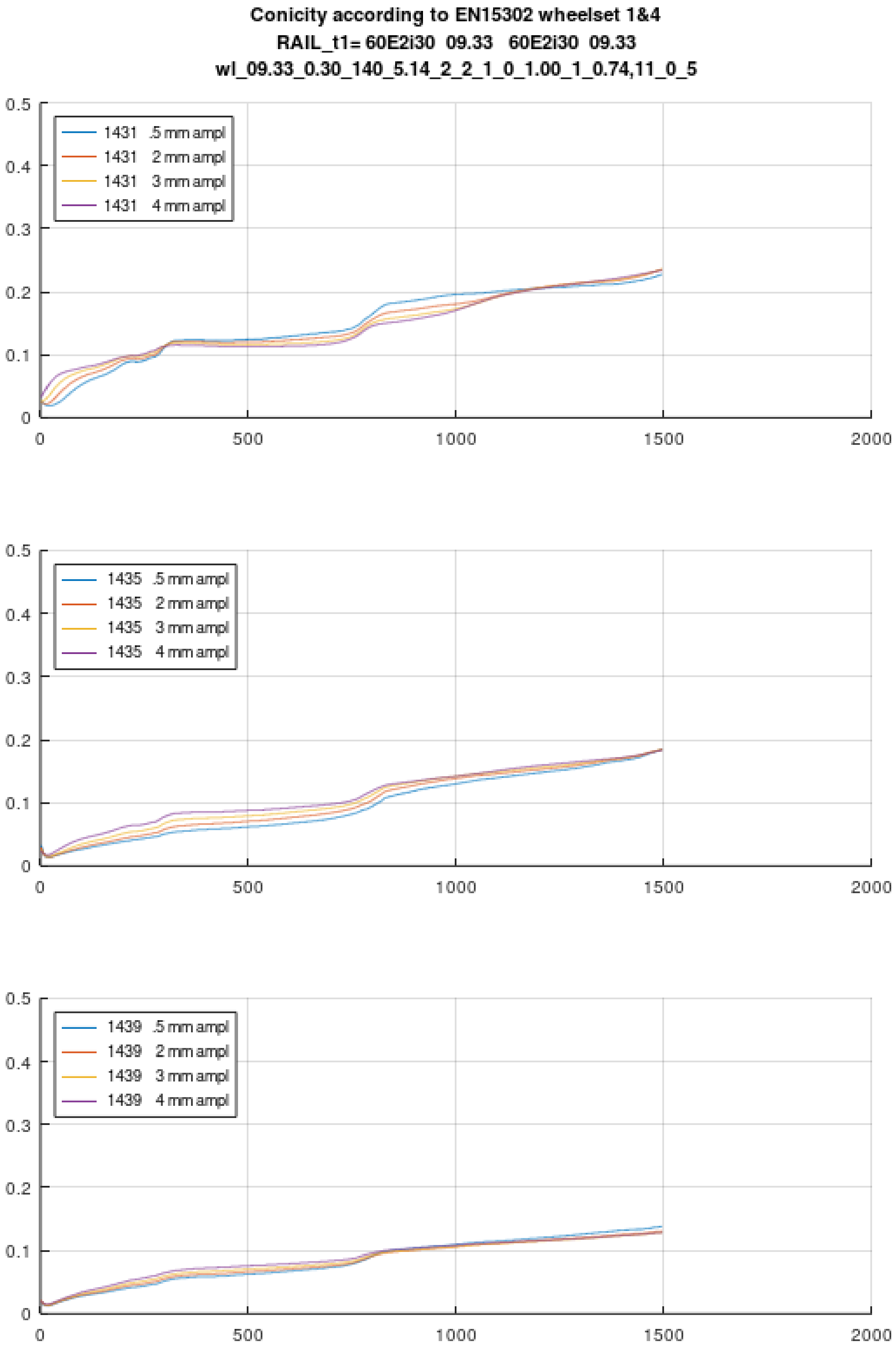

The figure above shows how the conicity according to UIC519 and EN15302 develops over time. Starting to the left with the initial wheel profile 0000, and ends to the right with the last update of the wheel profile. In this case, the wheel profiles have been updated ~1500 times.

With “outer wheels” means wheelset number 1&4 in the vehicle.
The top diagram shows the conicity for track gauge 1431mm.
The middle diagram shows the conicity for track gauge 1435mm.
The bottom diagram shows the conicity for track gauge 1439mm.
For each track gauge four curves are drawn:
Blue curve shows the conicity at 0.5mm wheelset lateral amplitude.
Red curve shows the conicity at 2mm wheelset lateral amplitude.
Yellow curve shows the conicity at 3mm wheelset lateral amplitude.
Purple curve shows the conicity at 4mm wheelset lateral amplitude.

As can be seen in all curves above, the conicity increases with travelled distance. This is typically what we often see on modern railway vehicles today which run on tracks with a great portion of tangent track sections.

9.2 Reference case: Conicity development for wheelset 2&3

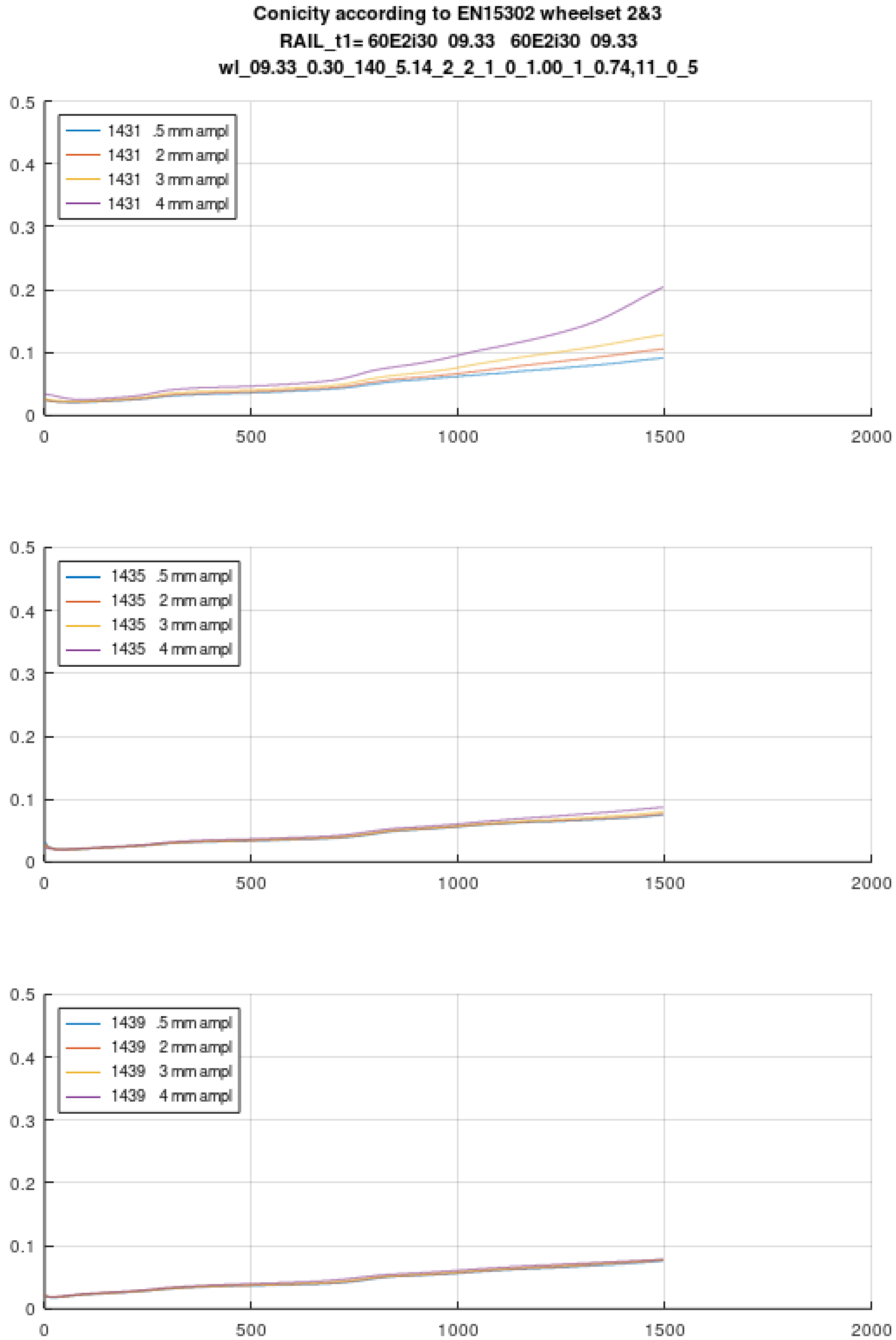

The figure above shows how the conicity according to UIC519 changes with travelled distance. Starting to the left with the initial wheel profile 0000, and ends to the right with the last update of the wheel profile. In this case, the wheel profiles have been updated approximatively ~1500 times.

The term “inner wheels” means the second and third wheelset in a four-axle bogie vehicle. Also here we can see that the conicity increases with travelled distance. However not as fast as for wheelset 1&4 in the vehicle.

9.3 Reference case: Wheel profile shapes wheelset 1&4

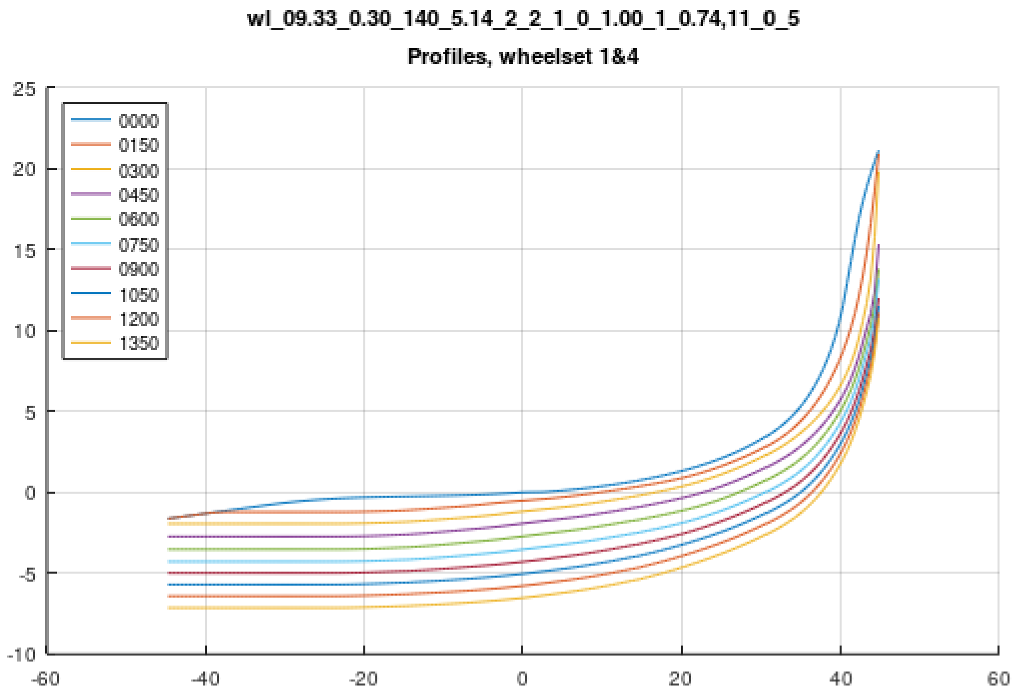

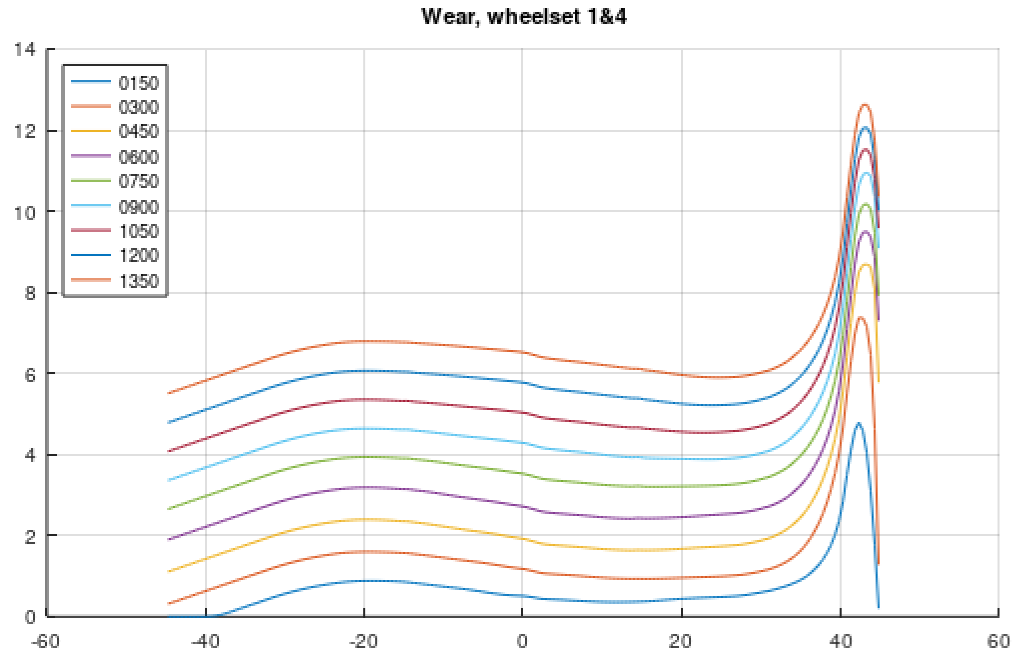

The upper diagram in the figure above shows how the shape of the wheel changes as the wheels are getting worn. Starting with the initial wheel profile 0000 (blue line), and ending with wheel profile 1350 (orange line).

The X-axis shows the Y-coordinates in mm on the wheel. Negative coordinates are towards the field side. Positive coordinates are toward the flange.

The Y-axis in the diagram shows the Z-coordinates in mm on the wheel.

The lower diagram in the above figure shows the difference between the worn wheel profile and the original initial wheel profile 0000. Starting with wheel profile 0200 (blue line), and ending with wheel profile 1350 (orange line).

In the beginning of the diagrams, it can be seen that the wheels have a lot of flange wear, but after a while, the flange wear is decreasing. In contrast to the tread wear, that seems to be more or less constant through the lifetime of the wheel.

9.4 Reference case: Wheel profile shapes wheelset 2&3

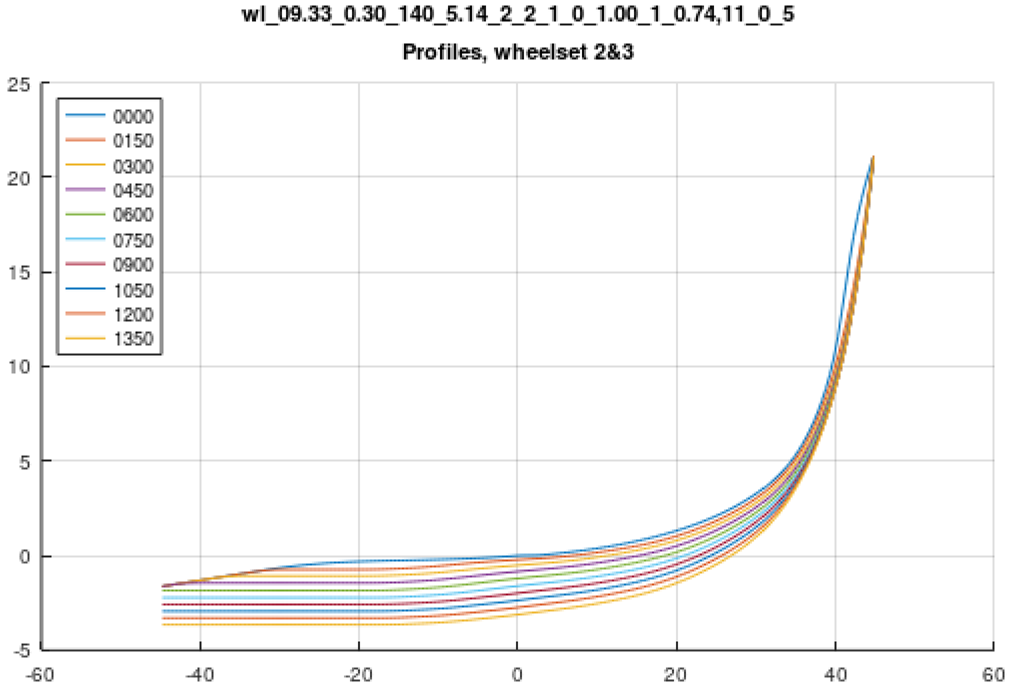

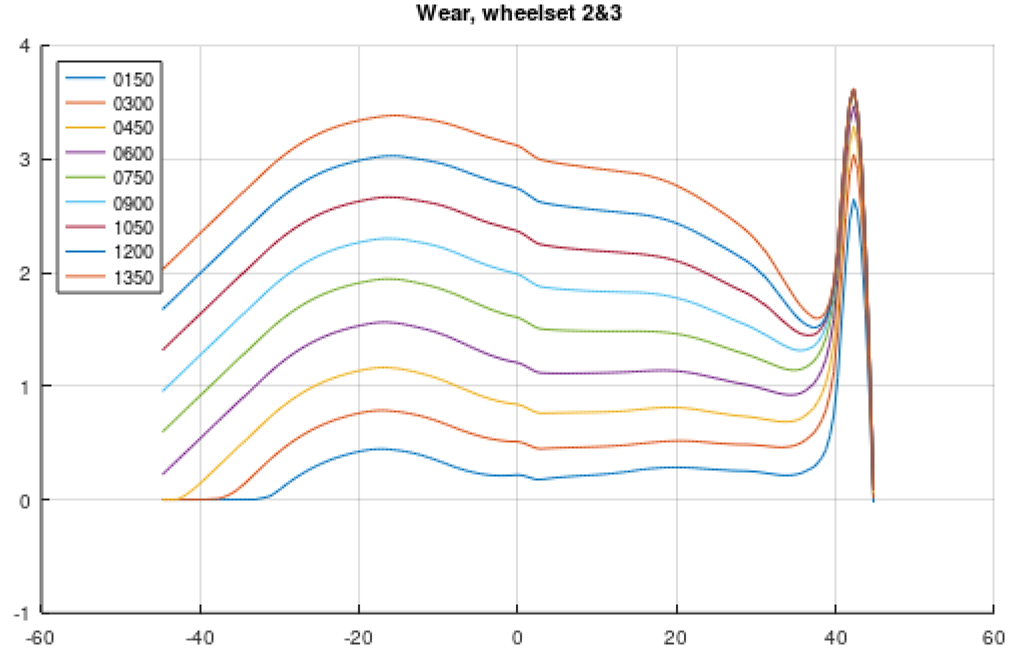

The figure above shows the wear on the wheel and wear depth on wheelset number 2&3 in a four axle bogie vehicle. As we can see, the wear is less on these two wheelsets compared to axle 1&4.

9.5 Reference case: Development of GIPw

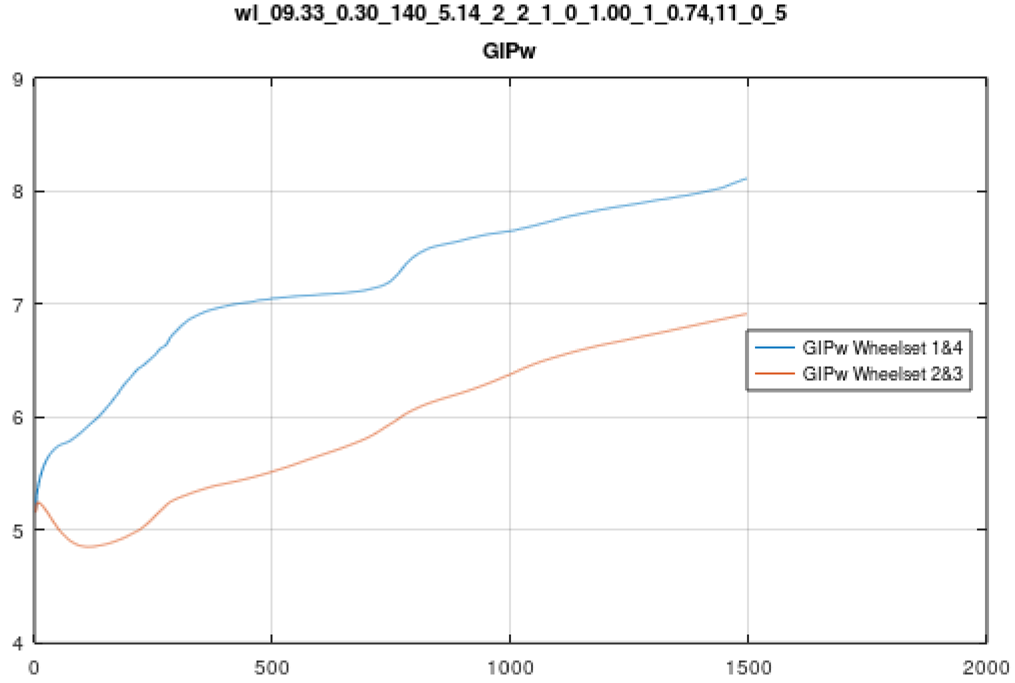

The figure above shows how GIPw changes with travelled distance. For new wheel profiles S1002t30.5 (profile #0000) the value for all wheels is the same 5.14, but as the wheels are getting worn, we can see that GIPw is increasing for all wheels. GIPw for wheelset 1&4 are increasing more than for wheelset 2&3.

In this case, GIPr for the rails are 9.33, and it looks like wheelset 1&4 is approaching this value.

9.6 Reference case: Development of Flange Thickness

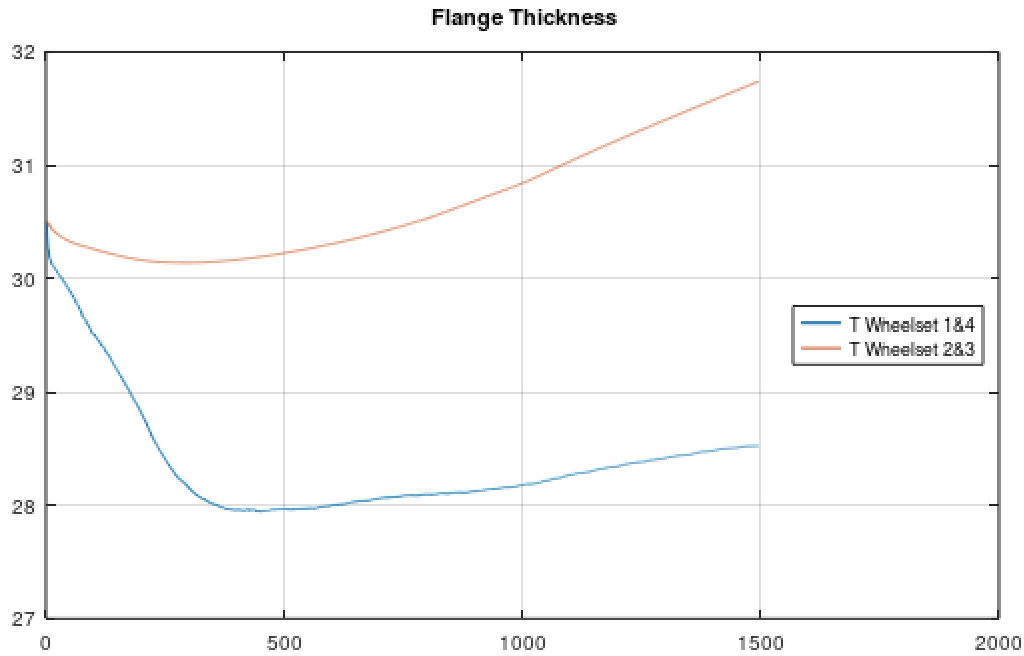

The figure above shows how the flange thickness changes with travelled distance. All wheels start with a flange thickness of 30.5 [mm]. Initially, the wheels have flange wear, we can see the thickness of the flanges is decreasing. However, after a while the shape of wheel profiles wears into a profile that steers better and after that, the flanges start to grow instead. The reason for growing flanges is that there is a tread wear which is lowering the nominal running circle (70 [mm] from inside wheel), this is also lowering the measuring position on the wheel flanges.

9.7 Reference case: Development of Flange flank qR

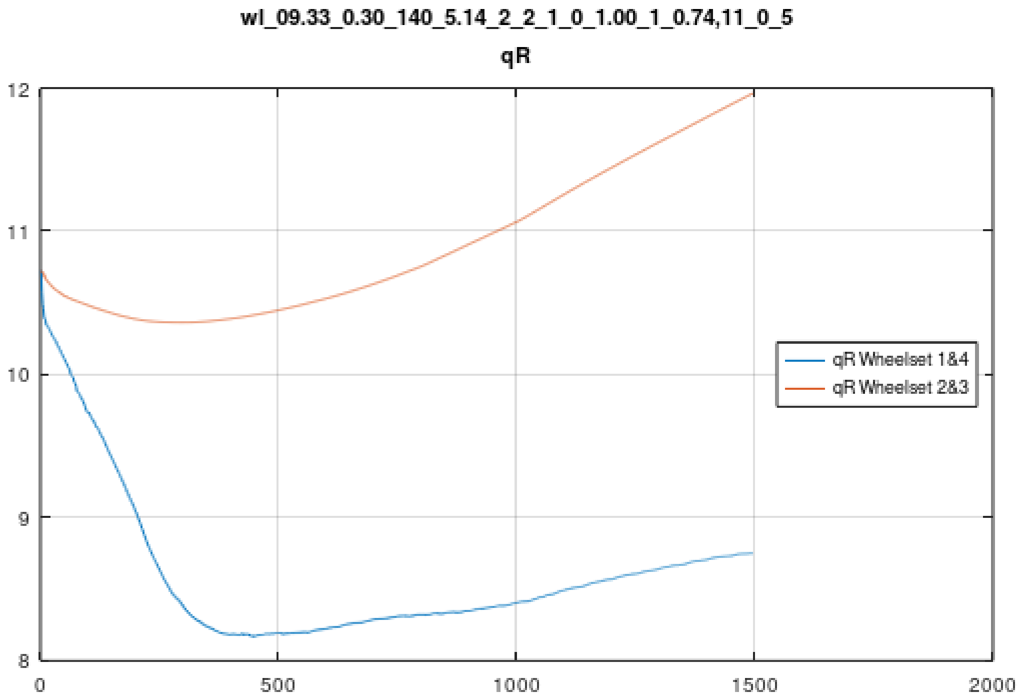

The figure above shows the qR value. The value of qR must be over 6.5 at all times. In this case there are no problems.

9.8 Reference case: Development of Wheelset Steering Ability

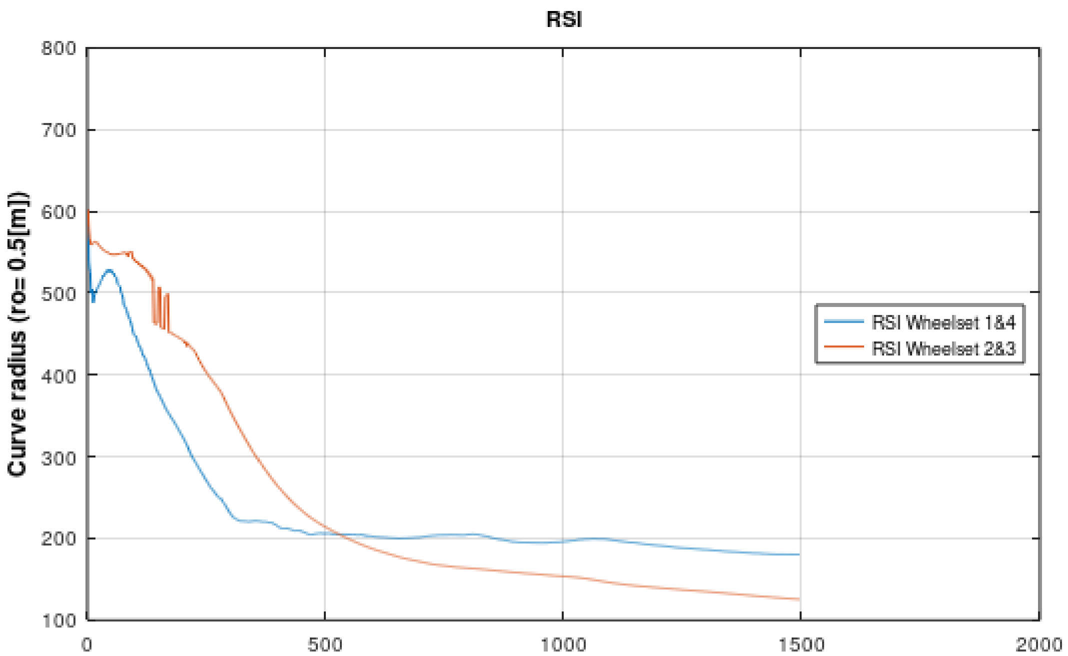

The figure above shows how tight curves the wheelsets can negotiate without flange contact. The diagram is based on the Radial Steering Index according to EN 14363. In the beginning, when the wheels are newly turned, the wheelsets can steer in curves down to ~600 [m]. When the wheels are getting worn, they are wearing into a shape so they steer better and better. Because of that, they can negotiate tighter and tighter curves without flange contact. Passing a curve without flange contact is only valid for a single wheelset that can steer freely in the curve. When the wheelset is mounted in a bogie the steering ability of the wheelset also depends on the properties of the bogie. If the bogie design is stiff there will always be flange contact, even if the wheelset itself is good at steering.

9.9 Reference case: Development of risk for RCF

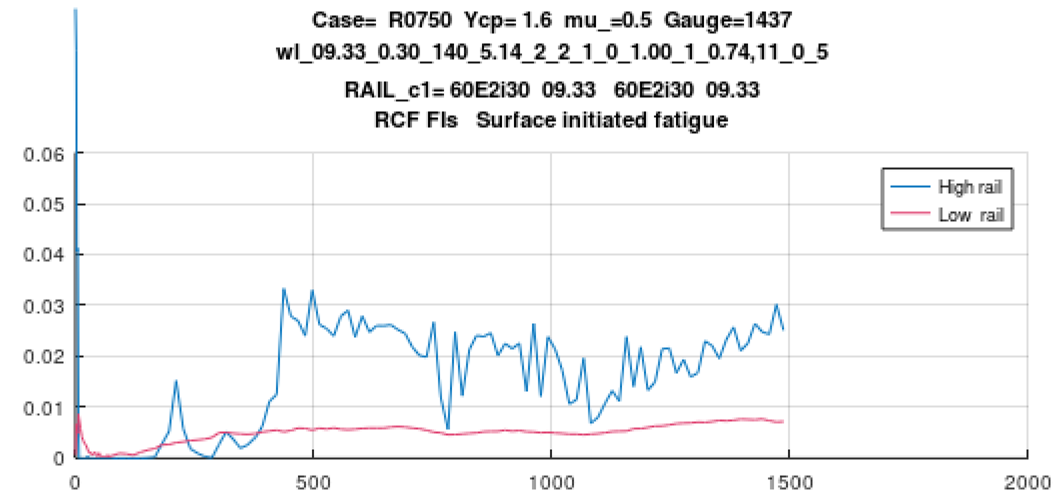

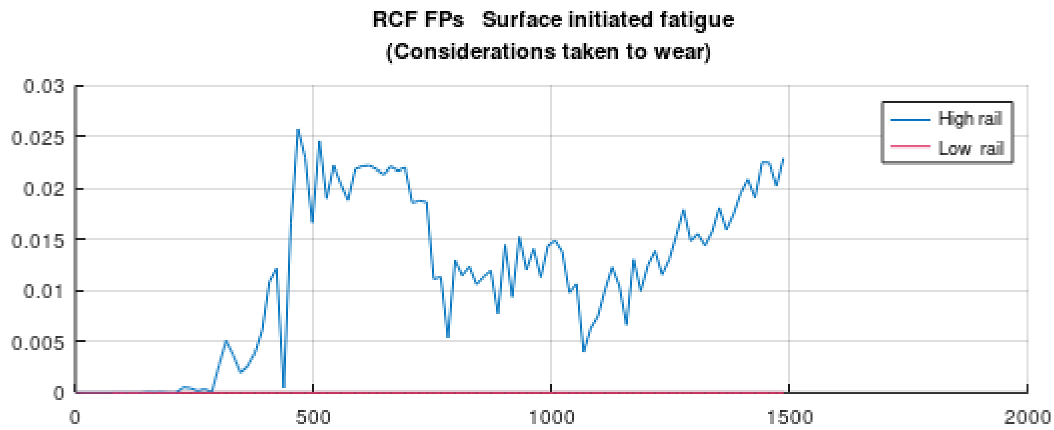

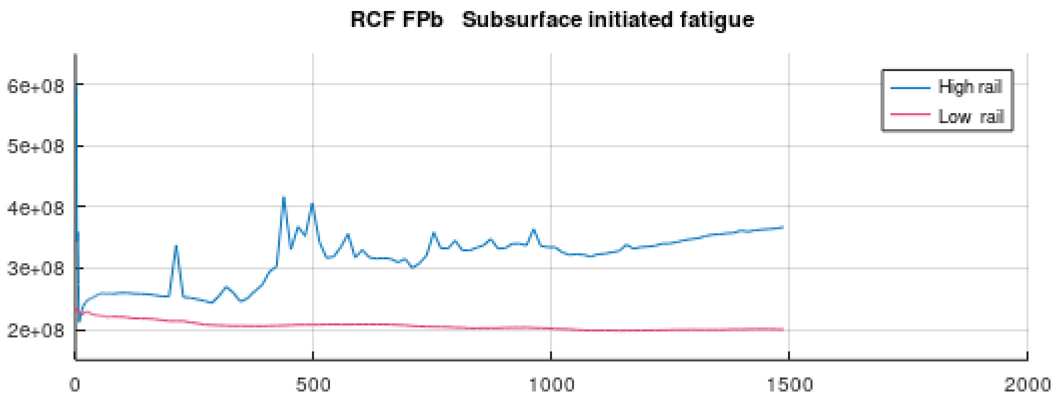

The diagrams above show the risk for RCF.

The top diagram shows the risk for surface-initiated RCF. The definition of this index is given in [2].

The middle diagram also shows the risk for surface-initiated RCF, but with considerations taken to wear.

The bottom diagram shows the risk for subsurface-initiated RCF. The definition of this index is given in [2].

The top diagram shows there is a risk for RCF both on high and low rail.

The middle diagram shows there is no risk for RCF on the lower rail because the wear rate is larger than the crack propagation rate. On the high rail, there is no risk for RCF when the wheels are newly turned, but unfortunately, the wheels wear into a shape that increases the risk for RCF after a while.

In the bottom diagram we can see that the risk for subsurface-initiated RCF also increases with travelled distance. Luckily it seems that the risk for subsurface-initiated RCF stops at ~400e6 [N/m^2]. The limit value for this index depends on the steel grade, but we think the limit value should be ~450e6 [N/m^2].

10. Different factors influence on wheel wear

In this report, only the variations we think are the most interesting are presented.

Variation #1 The influence on different rails with different values on GIPr1435.
Appendix A shows a case where GIPr1435 on the rails are 0.99 lower than the Reference case. The results show that the wheel/rail conicity is good, it is almost constant during the lifetime of the wheel. However, RCF is not 100% good. Especially when the wheels are newly turned RCF FPs are quite high.

Appendix B shows a case where GIPr1435 on the rails are 0.69 lower than the Reference case. The results show that the wheel/rail conicity is good, the conicity does not increase very fast. RCF is also good when the wheels are newly turned, but unfortunately after a little while the risk for RCF starts to increase.

Appendix C shows a case where GIPr1435 on the rails are 0.47 higher than the Reference case. The results in this case showed that the wheel/rail conicity increases very fast. The conicity became so high that the wear prediction loop was stopped prematurely.

Our understanding is that rails with lower GIPr lead to conicities that increase more slowly, but the risk for RCF is higher on rails with lower GIPr. For rail with high GIPr, the conicities are low when the wheels are newly turned, but as the wheels get worn, the conicities get high. The same applies also for the risk of RCF. When the wheels are newly turned, the risk of RCF is low, but the risk increases as the wheels are getting worn.

Variation #2 The influence on average friction coefficient between wheel and rail
Appendix D shows a case where the average friction coefficient is 0.05 lower than in the Reference case. We are a bit unsure how high the average friction coefficient is during one year. We assume a typical friction coefficient during one year is 0.30±0.05, where 0.30 was the value used in the Reference case.
The conicity looks much better compared to the reference case, it does not increase so much. Regarding RCF it looks good for newly turned wheels, but after a while when the wheels get worn the risk for RCF increases.
Appendix E shows a case where the average friction coefficient is 0.05 higher than in the Reference case. The conicity does not look good in this case. In this case, the conicity became so high that the wear prediction loop was stopped prematurely. The risk for RCF behaves in a similar manner as the reference case, but the levels in this case are lower.

Our understanding is that a lower friction coefficient allows the wheelset to move more easily on the track. Therefore, it leads to a more even distributed wear over the surface of the wheels, and the conicity therefore does not increase as fast as for the reference case. If the friction coefficient is higher, the opposite applies: the wheels steers better and the wear gets more concentrated on one location on the wheel which leads to higher conicities.

Variation #3 The influence on bogie steering ability SAb
Appendix F shows a case where the steering ability of the bogie is better, i.e. the bogie design is softer than the Reference case. The conicity doesn't look good in this case. Our understanding is that softer primary suspension leads to better steering of the wheelsets. When the wheelsets steer better, the wear gets more concentrated on one location, and the shape of the wheel therefore gets closer to the shape of the rail profile. This implies that for small lateral displacements of the wheelset, the contact patches can move very far, which leads to high conicities. In this case, the conicity became so high that the wear prediction

loop was stopped prematurely. However, the risk for RCF in this case looks very good. The soft bogie design does not create high creepage forces.

Appendix G shows a case where the steering ability of the bogie is worse, i.e. the bogie design is stiffer than the Reference case. The conicity develops very differently in this case. The conicity is decreasing instead of increasing. The wheels got a lot of wear on the flanges, so the wear prediction loop was stopped prematurely because of thin flanges. The risk for RCF also behaves differently. In this case, the risk for RCF is mainly on the low rail.

Our understanding is that the wear gets more concentrated on the same location when the bogie steers better, which explains why the conicity gets high. For a stiff bogie, the opposite applies. The stiff bogie does not steer well so the wear gets more even distributed.

Variation #4 The influence on initial wheel profiles

Appendix H shows a case where GIPw on the wheels is 0.87 lower than the Reference case. The results show that the conicity when the wheels are newly turned is lower than the reference case, so it takes a longer time until the conicity becomes very high. The risk for RCF also looks better as it takes longer time until the risk for RCF starts to increase.

Appendix I shows a case where GIPw on the wheels is 0.30 lower than the Reference case. The results show that the initial conicity is a little lower, therefore it also takes a little longer time before the conicity gets too high. The risk for RCF is approximately the same as for the Reference case.

Appendix J shows a case where GIPw on the wheels is 0.39 higher than the Reference case. The results show that the initial conicity is a little higher, and the conicity increases a little bit more. This case is a little bit longer than the reference case. This case comprises 2000 wear steps. The risk for RCF is approximately the same as for the Reference case.

Appendix K shows a case where GIPw on the wheels is 0.52 higher than the Reference case. The results show that the initial conicity is higher, and the conicity increases a bit more. The risk for RCF is approximately the same as for the Reference case.

Appendix L shows a case where GIPw on the wheels is 1.72 higher than the Reference case. The results show that the initial conicity is much higher, and the conicity from this point increases even more. The risk for RCF is approximately the same as for the Reference case. In this case, the conicity became so high that the wear prediction loop was stopped prematurely. However, the risk for RCF with this profile looks very, much less than for the reference case.

Our understanding is that it is GIPr that controls the slope of the conicity curve, and with GIPw you can control where on the conicity curve you want to start. If you choose a wheel profile with low GIPw there can be a risk of body hunting, but it will take longer time until the conicity gets too high. If you choose a wheel profile with high GIPw you will start higher up on the conicity curve, so the wheels will reach the high conicity region faster.

Appendix M shows a conical wheel profile where GIPw on the wheels is 2.64 lower than the Reference case. A wheel with a pure conical profile, with little or no flange root, behaves a bit differently. These types of wheel profiles have severe flange wear. The behaviour of the conicity curve is quite the same as for the reference case. But when looking at the flange thickness, we can its thickness reduces very fast in the beginning. In this case the qR value for the wheel does not look good, it goes down to a value less than 6.5.

Appendix N shows a conical wheel profile where GIPw on the wheels is 0.10 higher than the Reference case. The higher cone angle makes this profile higher up on the conicity curve. This profile also shows a lot of flange wear, and problem with a low qR value.

Variation #5 The influence on track irregularity amplitudes

Appendix O shows a case with better track alignment than the Reference case. A better track leads to more concentrated wear, and higher conicities. RCF behaves similarly to the reference case. We assume a track with larger track irregularities will have a positive effect on the conicities, but as it is detrimental to ride comfort it is not an option to achieve good wheel and rail economy. Therefore, larger track irregularities have not been studied.

Variation #6 The influence on lateral uncompensated acceleration

Appendix P shows a case with a lateral uncompensated acceleration that is 0.32 less than the Reference case. A lower lateral uncompensated acceleration is positive for the conicity. In this case, the conicity does not increase as in the reference case. The risk for RCF is approximately the same as for the reference case.

Appendix Q shows a case with a lateral uncompensated acceleration that is 0.19 greater than the Reference case. The conicity increases a little bit more in this case compared to the reference case. The risk for RCF is approximately the same as for the reference case.

Appendix R shows a case with a lateral uncompensated acceleration that is 0.60 greater than the Reference case. This case shows very good results for the conicity curve. The risk for RCF is different compared to the reference case. In this case, it is the low rail that has problems with high risk for RCF.

Our understanding is that the higher lateral uncompensated acceleration leads to higher lateral forces on the wheelsets, which makes the wheelsets steer better in the curves. When they steer better, the wear will be more concentrated and the conicity increases. However, there is an upper limit. If the lateral force gets too high, the vertical contact forces on the low rail become so low that the steering becomes worse instead.

11. Different rail profiles in curves and on tangent track

The wear prediction studies above show that it seems to be difficult to solve the problem with high conicities and risk for RCF at the same time. Therefore, a novel idea has been tested. The idea is to use different rail profiles in curves and on tangent track. The outcome from a test of this idea is showed in Appendix S.

Our understanding is that since the main part of the track consists of tangent track. It is the rails on the tangent track that controls the development of the wheel profiles. On tangent track, there is normally no problem with RCF, so it is possible to use rail profiles with low GIPr1435 in order to create an even distributed wear on the wheels. In curves on the other hand, the rail profiles should be chosen such that the risk for RCF is minimized, and for this profile, it is not necessary to take its effect on the wheel profiles into consideration.
At least this is valid for the chosen track section Stockholm-Gothenburg. For other tracks which consist of more curves, maybe the above statement cannot be made.

12. Summary

The analysis presented above is summarised as follows:

- GIPr:
  Lower GIPr values lead to wheel wear in the flange root, which leads to lower conicities. Higher GIPr values lead to wheel wear around the nominal running circle, which leads to a wheel wear that gives higher conicities.
  It is possible to change the rail profiles on the Swedish network. However, it will take a long time, because it entails a lot of grinding.
- Average friction during one year:
  A lower wheel/rail-friction coefficient doesn't connect the wheels so hard to the rail. The wheelsets are freer to move in the lateral direction, which causes a more even distributed wear over the wheel profiles, which leads to lower conicities. It is difficult to change the average friction value. Could be possible to find another type of steel that gives a lower average friction coefficient?
- Primary suspension stiffness:
  Stiffer bogies don't steer very well in curves and in track irregularities. This causes a more even distributed wear over the wheel profiles, which leads to lower conicities.
- Initial wheel profile:
  The shape of the initial wheel profile is of importance mainly in the beginning of a wheel's life.
- Curve distribution:
  (This has not been studied so well, but we expect that more curves and tighter curves will lead to a more even distributed wear over the wheel profiles, which in turn will lead to lower conicities)
- Track irregularities:
  (The influence of using different track irregularity files, hasn't been studied yet)
- Track Gauge:
  When the gauge gets wider, the value of GIPr increases, which leads to wear further out on the tread, which after a while leads to higher conicities.
- Track Irregularity amplitudes:
  What we have seen, is that smaller lateral track irregularities lead to more concentrated wear, which leads to higher conicities
- Cant deficiency:
  Results indicate that higher cant deficiencies lead to higher conicities. A higher speed in the curves leads to larger lateral forces, which leads to better steering of the wheelsets, which in turn leads to more concentrated wear in the flange root. However, if the cant deficiency gets too high, the steering ability of the wheelsets gets less again.
- Wear chart:
  All calculations have been made with wear chart 5, as Tomas Jendel's wear chart but without area 1 (seizure).

In principle, it means wheelsets that move more freely in the lateral direction gives a more even distributed wear over the surface of the wheel which leads to lower conicities.

13. Acknowledgements and disclaimer

This project has received funding from the European Union's Horizon 2020 research and innovation programme under grant agreements 826255 and 101012456. Funding has also been received from Trafikverket, SJ AB and A-Train AB.

This document reflects the views of the author(s) and does not necessarily reflect the views or policy of the European Commission. Whilst efforts have been made to ensure the accuracy and completeness of this document, the IN2TRACK2 and IN2TRACK3 consortiums shall not be liable for any errors or omissions, however caused.

14. References

[1] Asplund M. et al. (2023). Introduction to the Collaboration Project: A Systematic Approach to Improve Passenger Ride Comfort, Trafikverket TRV 2023/113404: 178508100-001.

[2] Asplund M. et al. (2023). *Methodology for Wheel Wear Simulations, RCF and Equivalent Conicity*, Trafikverket TRV 2023/113404: 178508100-006.

[3] S2R-IN2TRACK2 Webpage [Internet]. Available from: https://projects.shift2rail.org/s2r_ip3_n.aspx?p=IN2TRACK2.

[4] S2R-IN2TRACK3 Webpage [Internet]. Available from: https://projects.shift2rail.org/s2r_ip3_n.aspx?p=IN2TRACK3.

[5] Archard J.F. (1953). *Contact and Rubbing of Flat Surfaces*, Journal of Applied Physics, Volume 24, Issue 8, August.
doi: 10.1063/1.1721448

[6] Jendel T. (2000). *Prediction of wheel profile wear*, TRITA-FKT 200:49; ISRN KTH/FKT/L-00/49-SE.

[7] Asplund M. et al. (2023). *Gradient Index Profile, Definitions and Terminology*, Trafikverket TRV 2023/113404: 178508100-013.

[8] Persson I. and Jönsson L-O (2021). *Gradient Index Profile, a novel idea for predicting equivalent conicity*. The IAVSD International Symposium on Dynamics of Vehicles on Roads and Tracks. Cham: Springer International Publishing, 2021. p. 513-521.

[9] Li M. et al (2023). *Investigating Gradient Index Profile and its Correlations with Equivalent Conicity and Rail Surface Management.* IAVSD 2023: 28th IAVSD Symposium on the Dynamics of Vehicles on Roads and on Tracks, Ottawa, Canada, 2023.

[10] CEN/TR 17792:2022 (2022). Railway Applications - Wheel-rail contact geometry parameters - Technical report and background information about EN 15302

[11] Dirks B. (2003). *Vehicle Dynamics Simulation of Wheel Wear of Swedish High-Speed Train X2000*, TRITA AVE 2003:16; ISRN KTH/AVE/RTM-03/16-SE.

[12] Dirks B. (2015). *Simulation and Measurement of Wheel on Rail Fatigue and Wear*, TRITA AVE 2015:16; ISBN 978-91-7595-544-5.

[13] Ekberg A, Kabo E, & Andersson H, *An engineering model for prediction of rolling contact fatigue of railway wheels*, 2001,
doi: 10.1046/j.1460-2695.2002.00535.x

[14] Enblom R. (2006). *On Simulation of Uniform Wear and Profile Evolution in the Wheel – Rail Contact*, TRITA AVE 2006:83; ISBN 978-91-7178-605-3.

15. Revisions

Revision	Date	Description
1	2024-02-27	First issue.

16. Appendices

The following appendices are included:

Appendix A	Rails with 0.99 lower GIPr1435
Appendix B	Rails with 0.69 lower GIPr1435
Appendix C	Rails with 0.47 higher GIPr1435
Appendix D	Lower average friction coefficient
Appendix E	Higher average friction coefficient
Appendix F	Softer longitudinal primary stiffnesses in the bogies
Appendix G	Stiffer longitudinal primary stiffnesses in the bogies
Appendix H	Initial wheel profile with 0.87 lower GIPw
Appendix I	Initial wheel profile with 0.30 lower GIPw
Appendix J	Initial wheel profile with 0.39 higher GIPw
Appendix K	Initial wheel profile with 0.52 higher GIPw
Appendix L	Initial wheel profile with 1.72 higher GIPw
Appendix M	Initial wheel profile with GIPw-2.64 pure conical wheels
Appendix N	Initial wheel profile with GIPw+0.10 pure conical wheels
Appendix O	Lower amplitudes for the track irregularities
Appendix P	Lateral uncompensated acceleration 0.65
Appendix Q	Lateral uncompensated acceleration 1.17
Appendix R	Lateral uncompensated acceleration 1.60
Appendix S	Different rail profiles in curves

Appendix A. Rails with 0.99 lower $GIPr_{1435}$

This case is denoted:

wl_08.34_0.30_360_5.14_2_2_1_0_1.00_1_0.74,11_0_5

All data are the same as the reference case 9, except for $GIPr_{1435}$ 4. In this case rail profile 60E1i30 has been used. $GIPr_{1435}$ for this rail is 0.99 less than the reference case $GIPr_{1435}$= 9.33.

A.1 The conicity development diagrams for wheelset 1&4

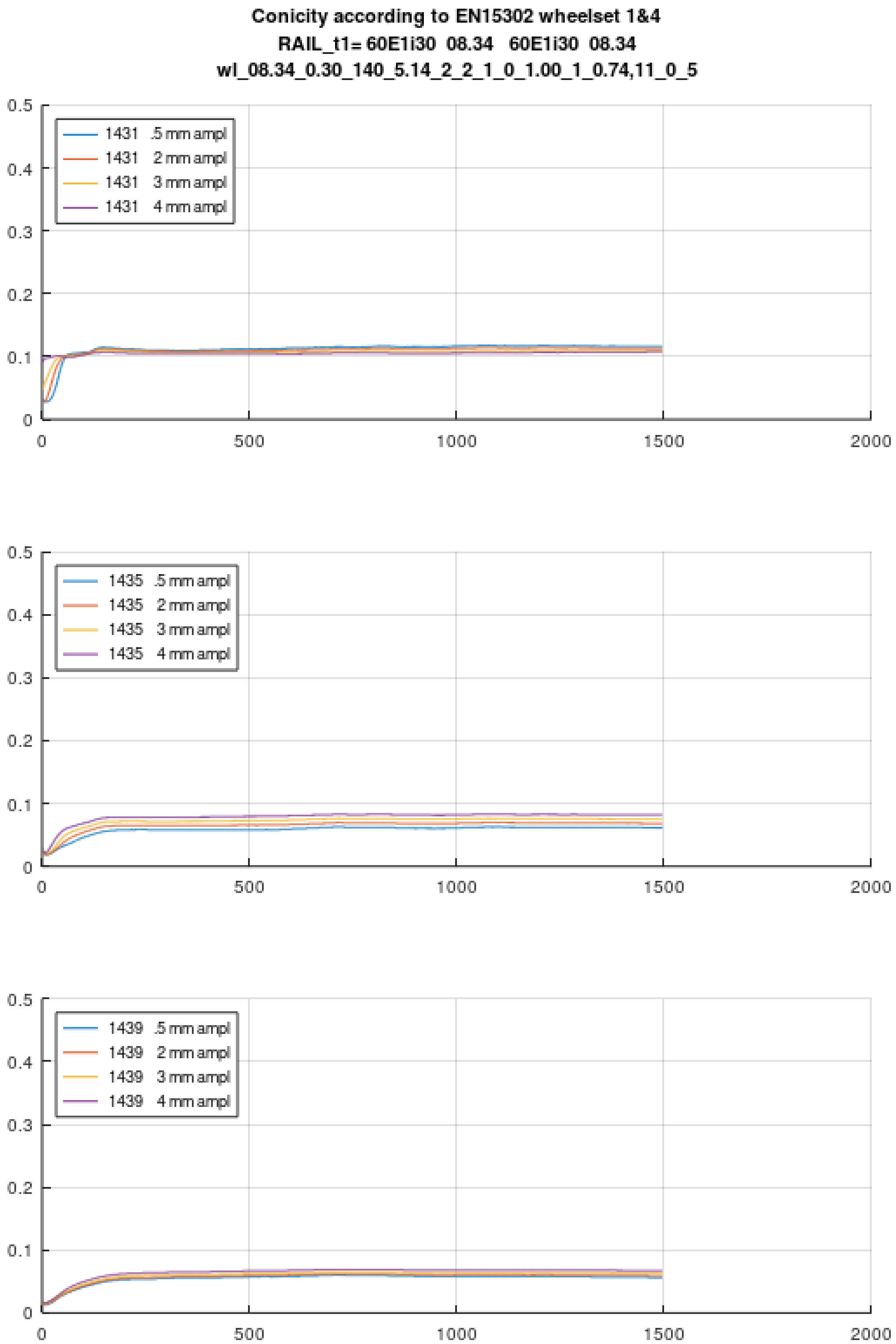

Rail profile 60E1i30 has a positive influence on the worn shape of the wheel profile. Which can be clearly seen if you compare with the reference case 9.1. With this rail profile the conicity according to EN 15302 is almost constant. There is only a short wear-in phase in the beginning.

A.2 Wheel profile shapes wheelset 1&4

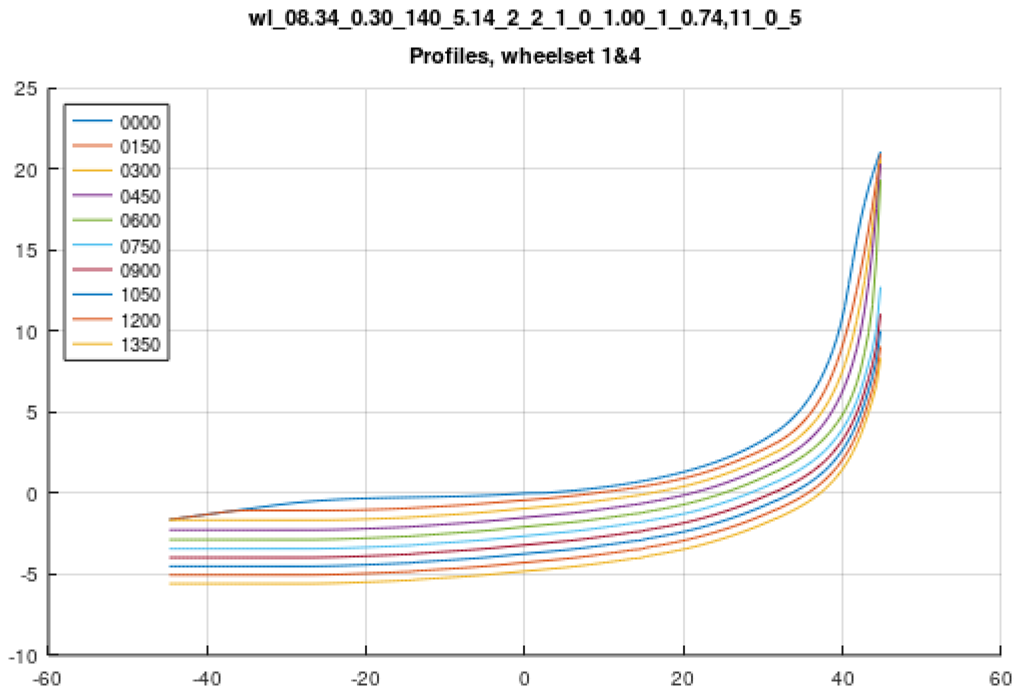

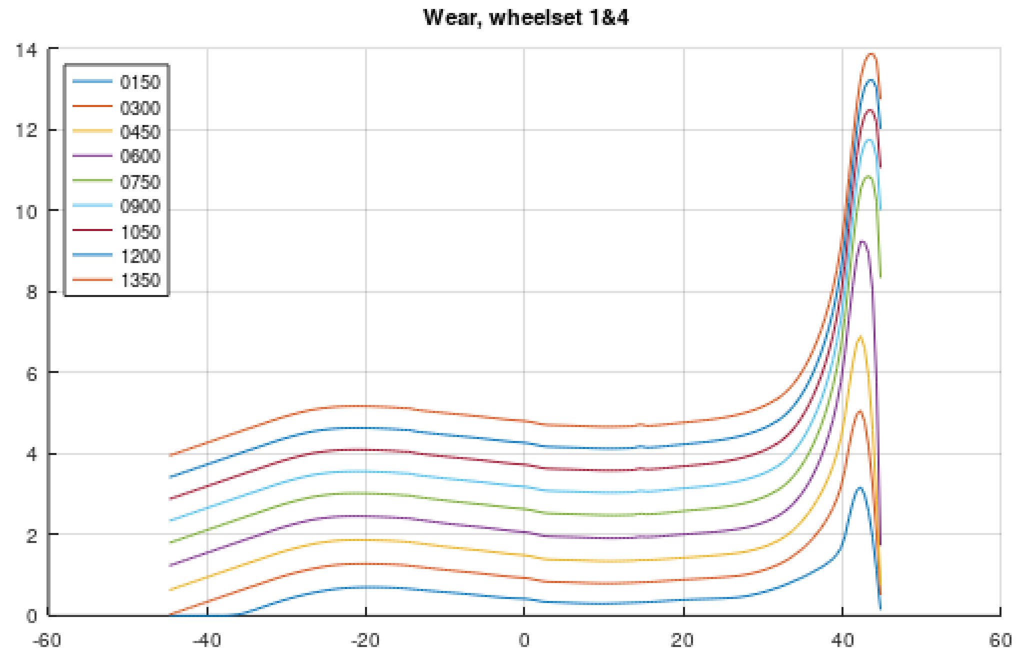

As can be seen in the above figure, the flange wear is larger than the reference case 9.3, which keeps the conicities at lower levels.

A.3 Development of GIPw

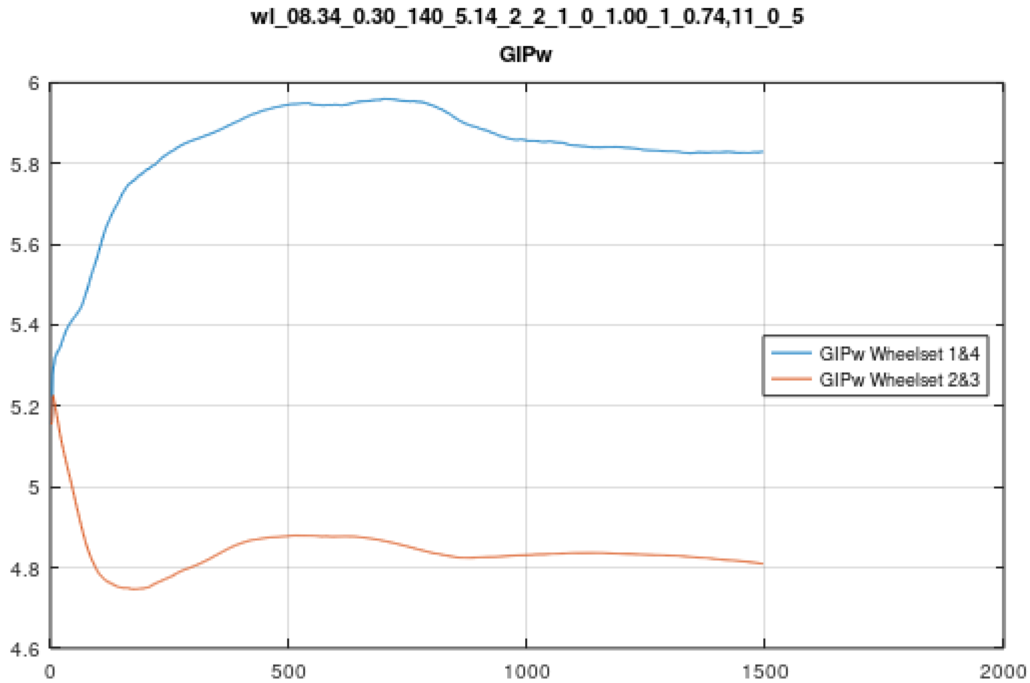

GIPw is not increasing so much as the reference case 9.5. With rail profile 60E1i30 it seems that GIPw finds its asymptotic value of ~5.8 for wheelsets 1&4, and ~4.8 for wheelsets 2&3, which is relatively far from the rail GIPr1435= 8.34.

A.4 Development of the Flange Thickness

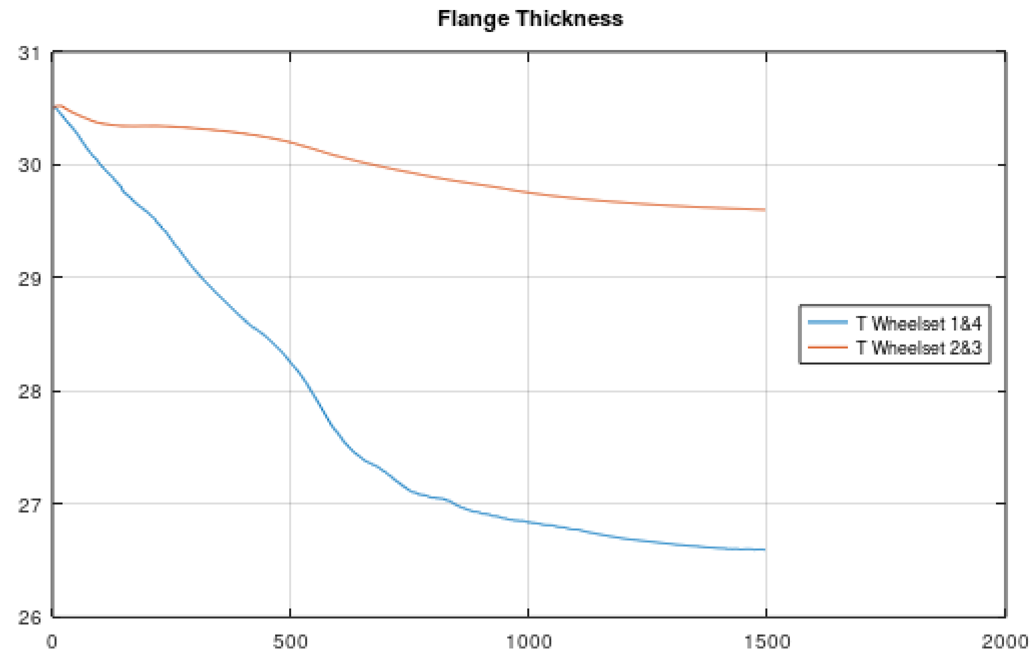

With this rail profile 60E1i30, the flanges are getting thinner as the wheels are getting worn, which is not the same as for the reference case 9.6. However, in the end of the wear prediction loop the rate of the flange thickness change seems to stabilize to a relatively constant value. Eventually the flanges will also start to grow if the simulation loop has been longer?

A.5 Development of the Flange Flank qR

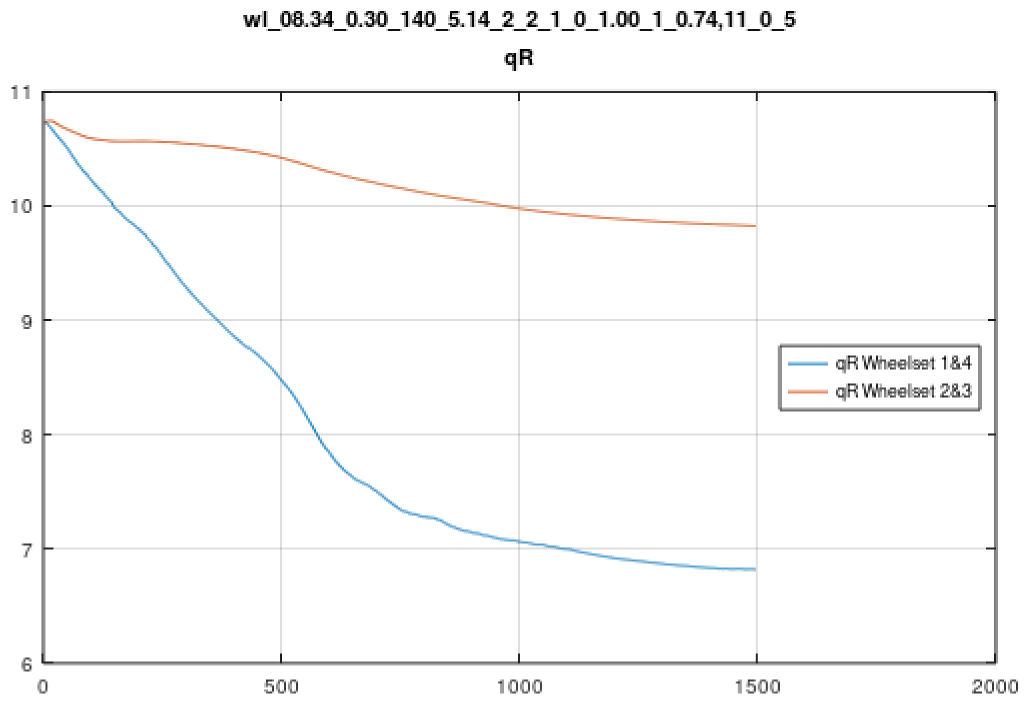

Flange flank qR is getting lower and lower as the wheels are getting worn. In contrast to the reference case 9.7, where the flange flank first goes quickly down, but after that the qR value starts to grow again. Maybe this will happen also on this rail profile if the simulation has been a little longer. The lower limit for the qR is 6.5. Luckily it looks that the wheels will not reach that value.

A.6 Development of the Wheelset Steering Ability

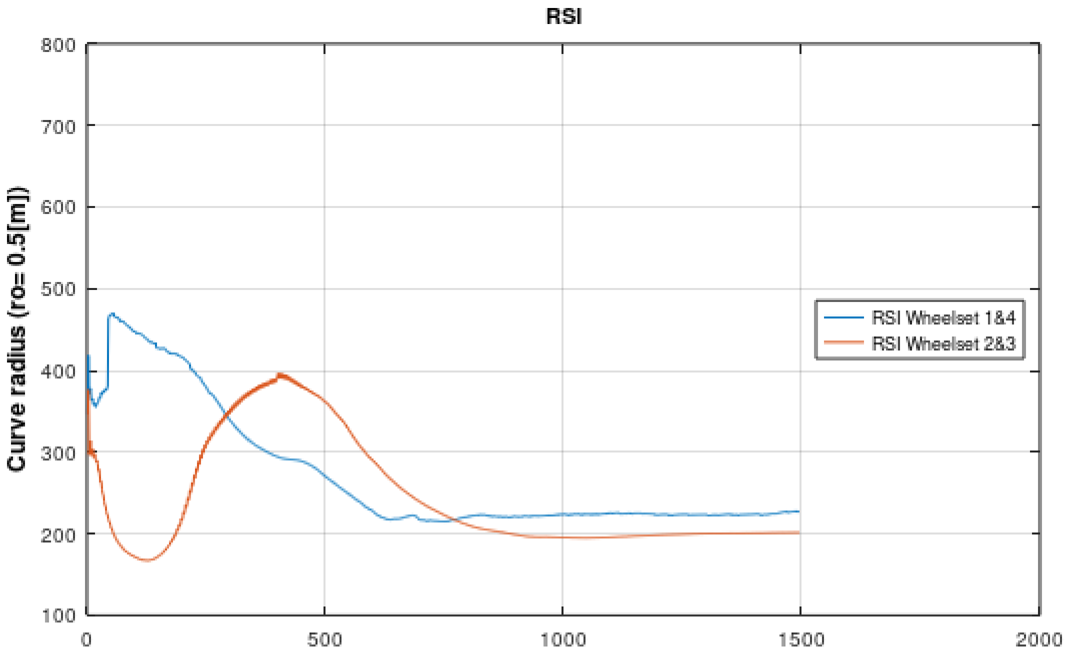

Compared to the reference case 9.8 this rails steers better than the reference case already for newly turned wheels. However, the worn wheelsets don’t steer as well as in the reference case 9.8.

A.7 Development of the risk for RCF

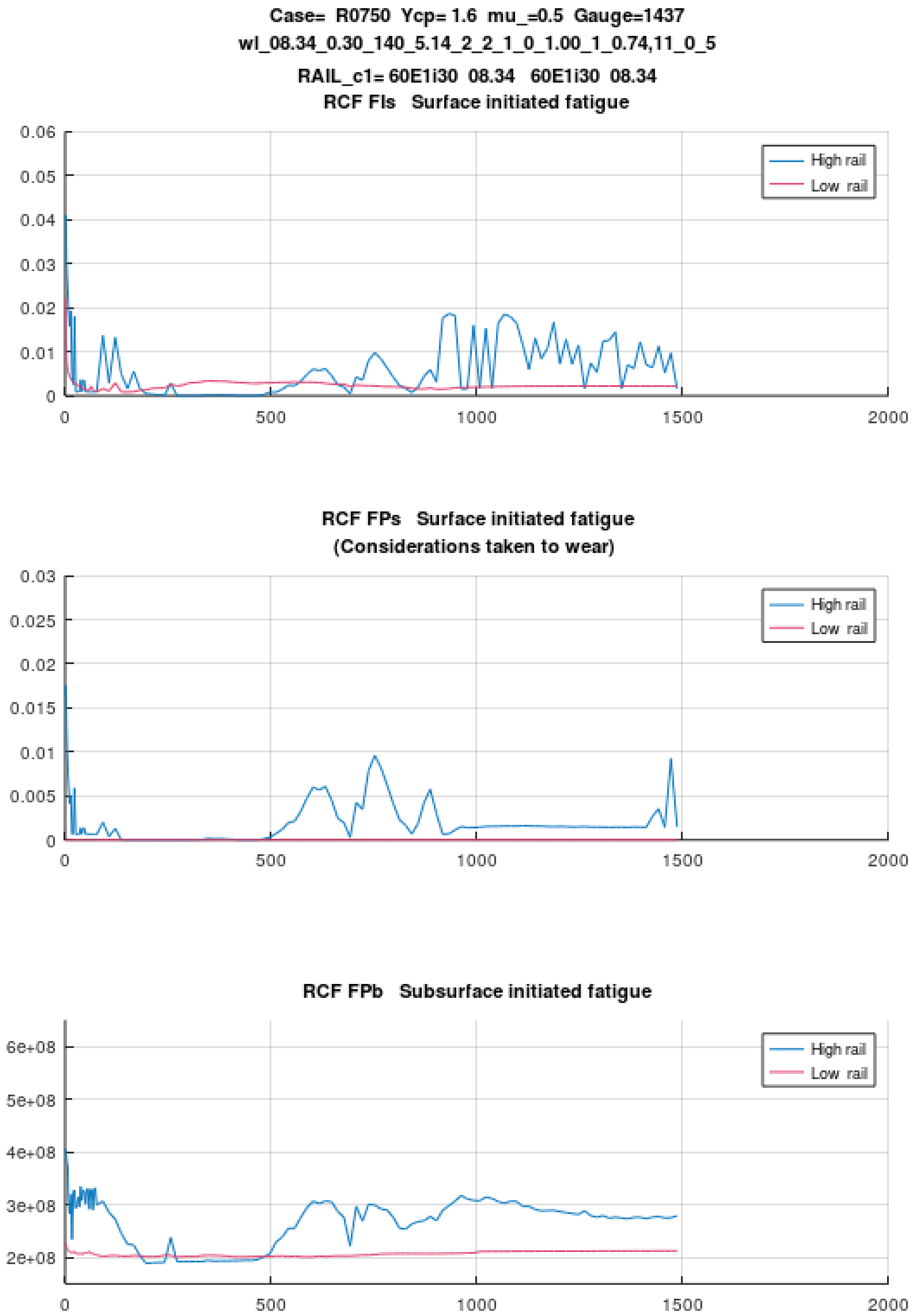

As can be seen in the middle diagram in the figure above. The risk for RCF on the lower rail is very low, but there are some problems with RCF FPs on the high rail. In contrast to the reference case 9.9 this rail profile is not safe for RCF FPs when the wheels are newly turned. However, after an initial wear-in period the risk for RCF is getting better, but after a while the risk for RCF FPs comes back again.

The lower diagram shows that the risk for RCF FPb is low for both new and worn wheels the curve is at all times lower than the limit value 450e6.

Appendix B. Rails with 0.69 lower $GIPr_{1435}$

This case is denoted:

wl_08.64_0.30_360_5.14_2_2_1_0_1.00_1_0.74,11_0_5

All data are the same as the reference case 9, except for $GIPr_{1435}$ 4. In this case rail profile 60E2i40 has been used. $GIPr_{1435}$ for this rail is 0.69 less than the reference case $GIPr_{1435}$= 9.33.

B.1 The conicity development diagrams for wheelset 1&4

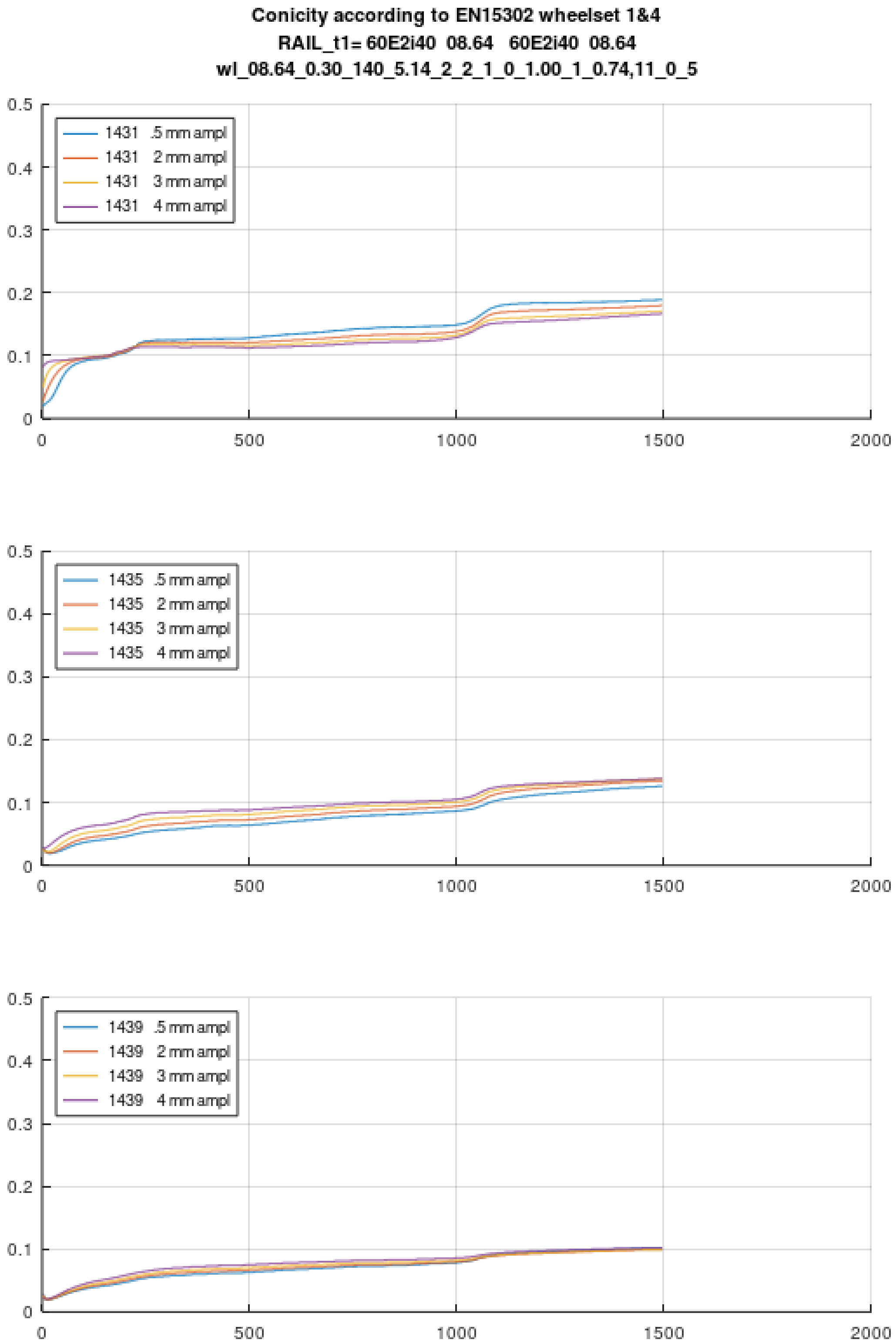

A rail inclination of 1/40 has a positive effect on the wheel/rail conicities. The conicities don't increase as fast as in the reference case 9.1.

B.2 Wheel profile shapes wheelset 1&4

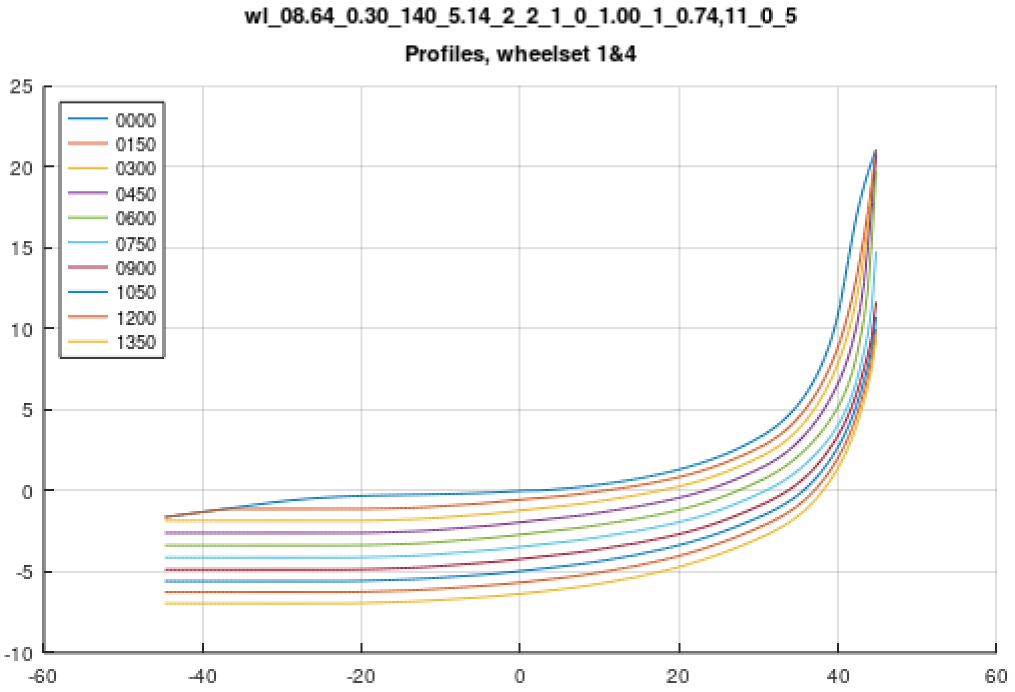

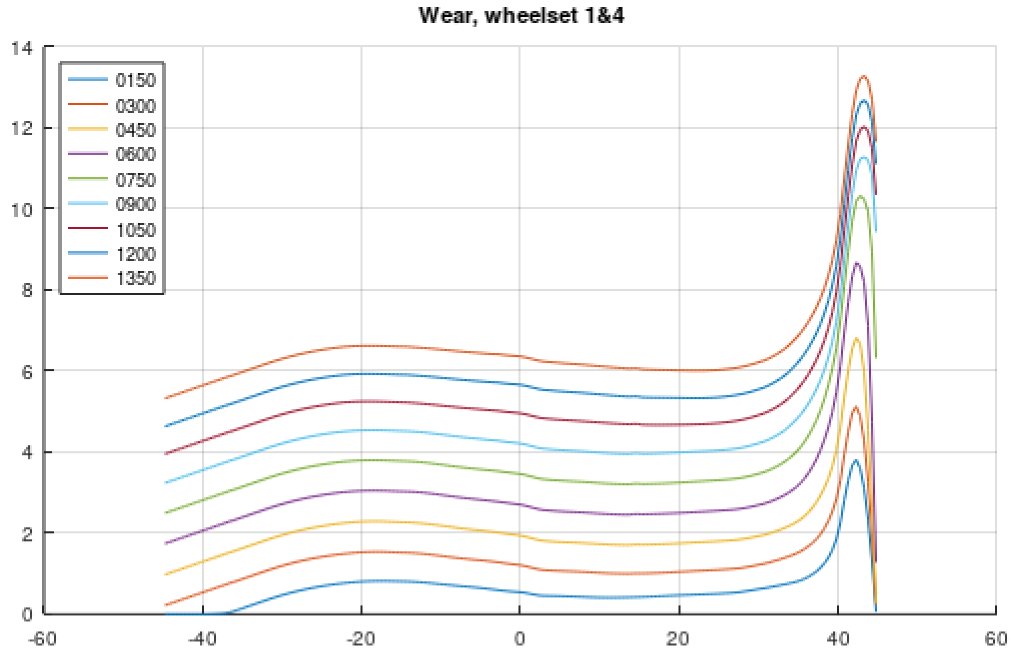

The worn shapes of the wheels look very similar to the reference case 9.3. However, when the wheel profiles and rail profiles are close to each other, a small change in the shape can have a significant impact on the conicity.

B.3 Development of GIPw

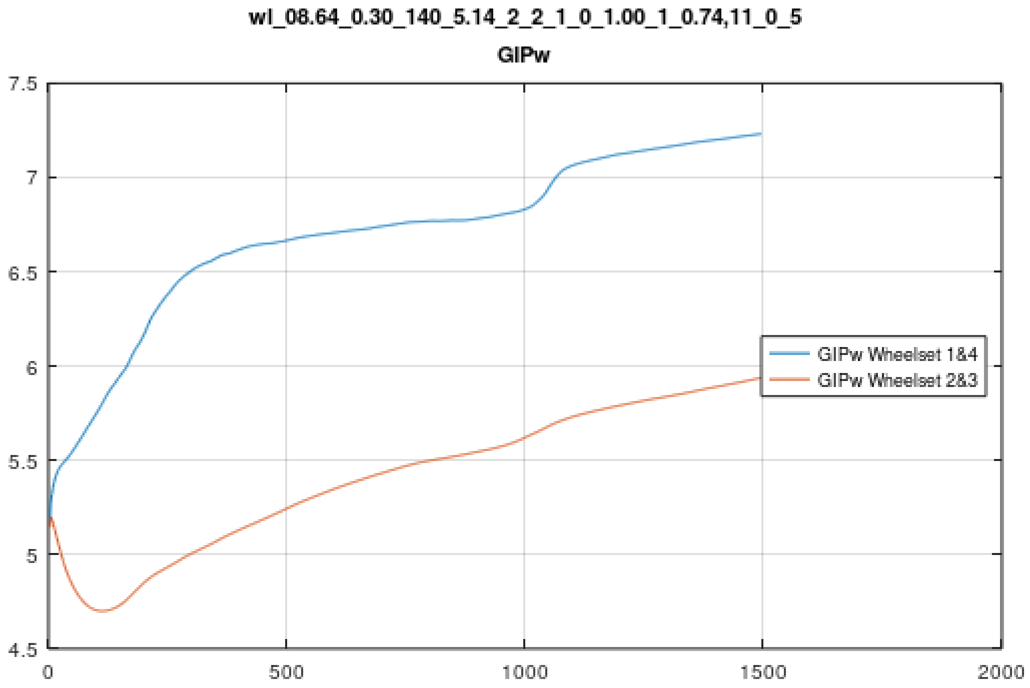

GIPw don't increase as fast as for the reference case 9.5.

B.4 Development of the Flange Thickness

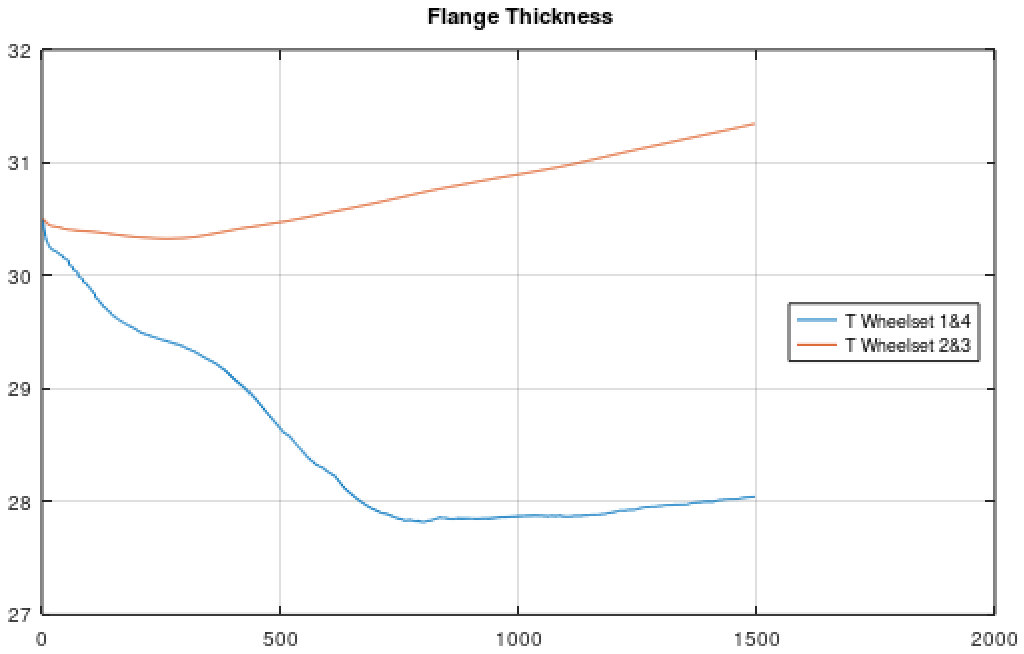

The thickness of the flange behaves in a similar way as in the reference case 9.6. The thickness goes down to ~28mm then it increases again. However, the flanges don't grow as fast as in the reference case.

B.5 Development of the Flange Flank qR

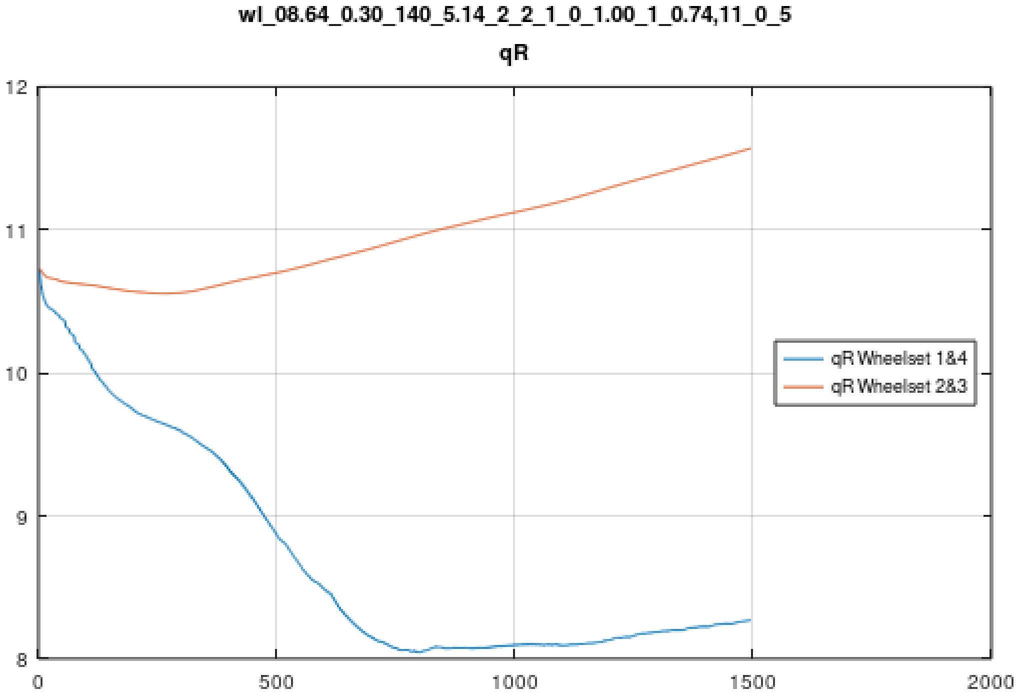

The flange flank behaves in a similar way as in the reference case 9.7. The flange flank goes down to ~8 then it increases again. However, the flange flanks don't grow as fast as in the reference case.

B.6 Development of the Wheelset Steering Ability

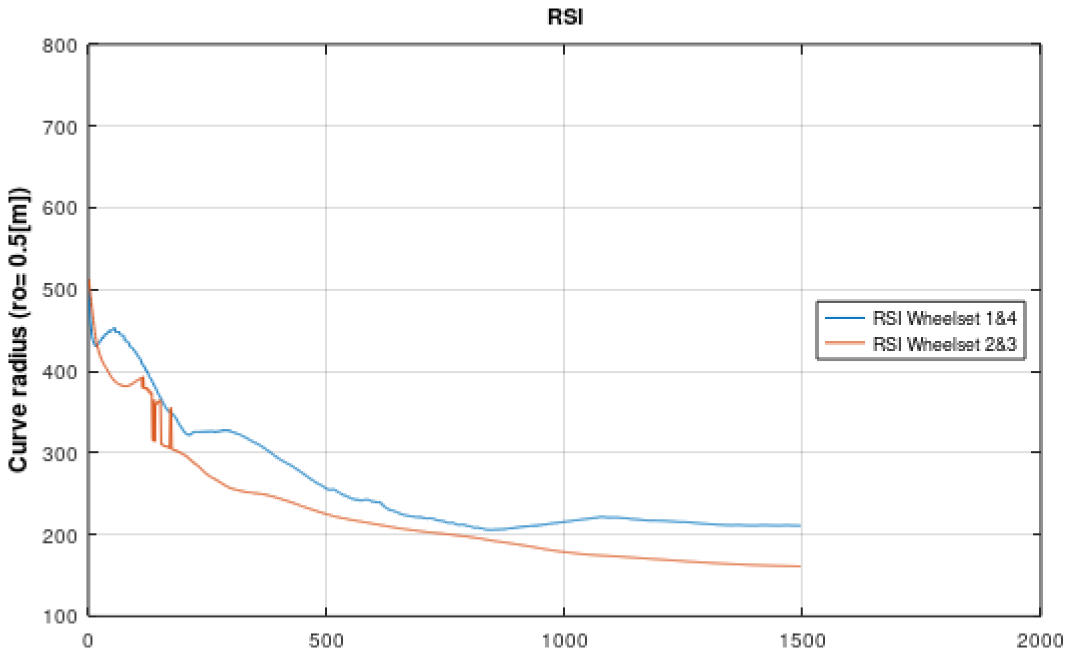

This rail inclination steers a little bit better than the reference case 9.8 when the wheels are newly turned, but when the wheels are getting worn this rail inclination is not as good as the reference case.

B.7 Development of the risk for RCF

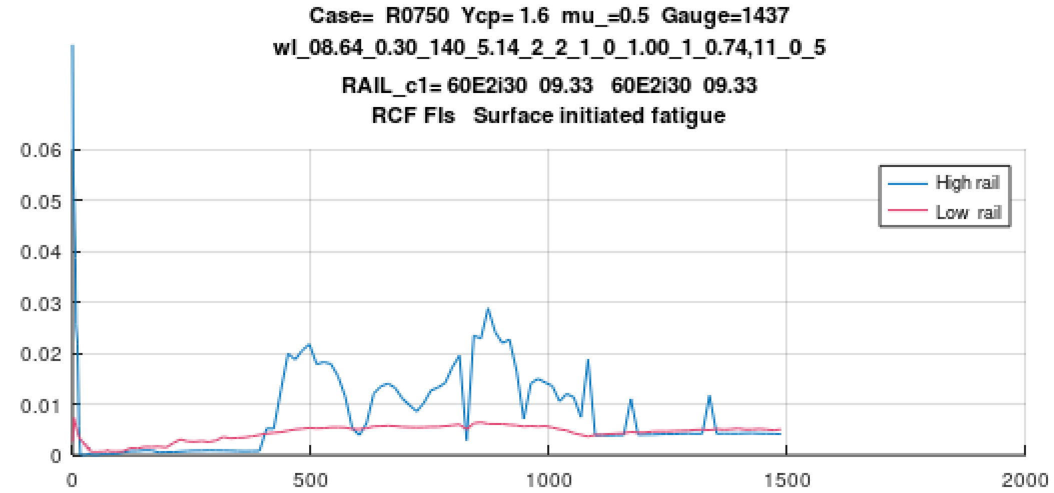

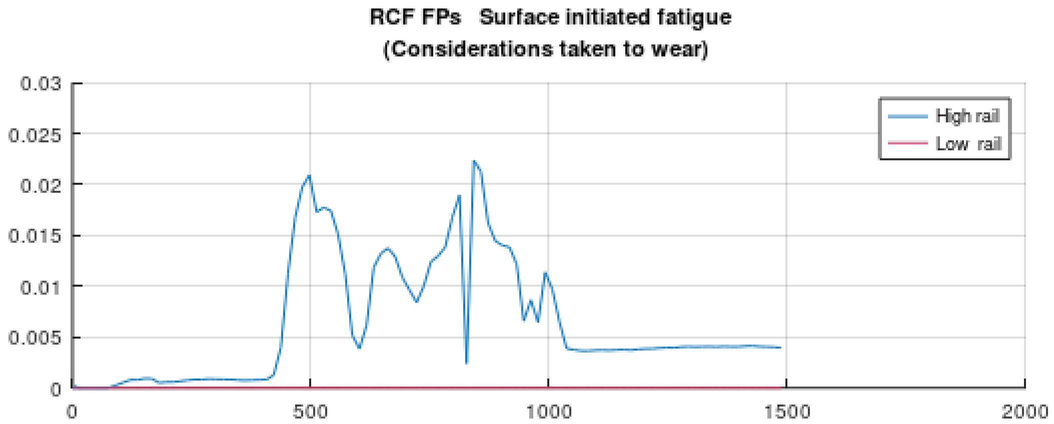

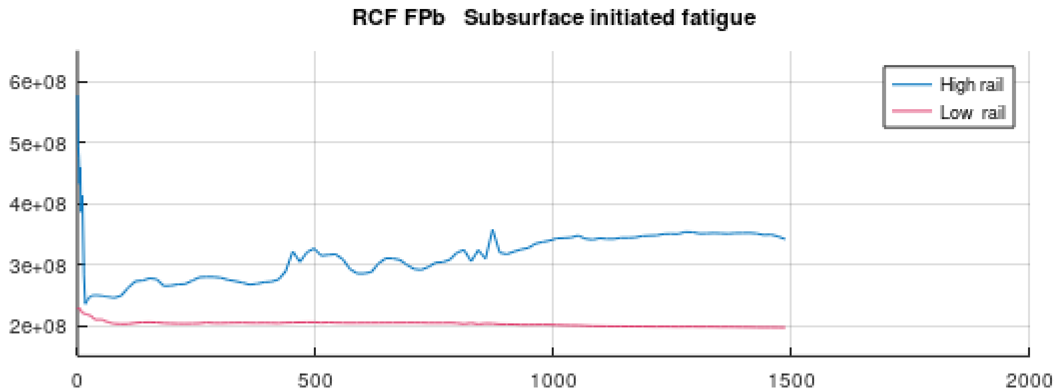

The risk for RCF behaves in a similar way as the reference case 9.9.

RCF FPs is low for newly turned wheels, but after a while the risk for RCF FPs increases. However, in the end the risk for RCF FPs seems to be low again.

RCF FPb is low for both new and worn wheels, the curve is at all times lower than the limit value 450e6.

Appendix C. Rails with 0.47 higher $GIPr_{1435}$

This case is denoted:

wl_09.80_0.30_360_5.14_2_2_1_0_1.00_1_0.74,11_0_5

All data are the same as the reference case 9, except for $GIPr_{1435}$ 4. In this case the rail profile is a measured rail profile from Bdl416. $GIPr_{1435}$ for this rail is 0.47 higher than the reference case $GIPr_{1435}$= 9.33.

C.1 Development of conicity wheelset 1&4

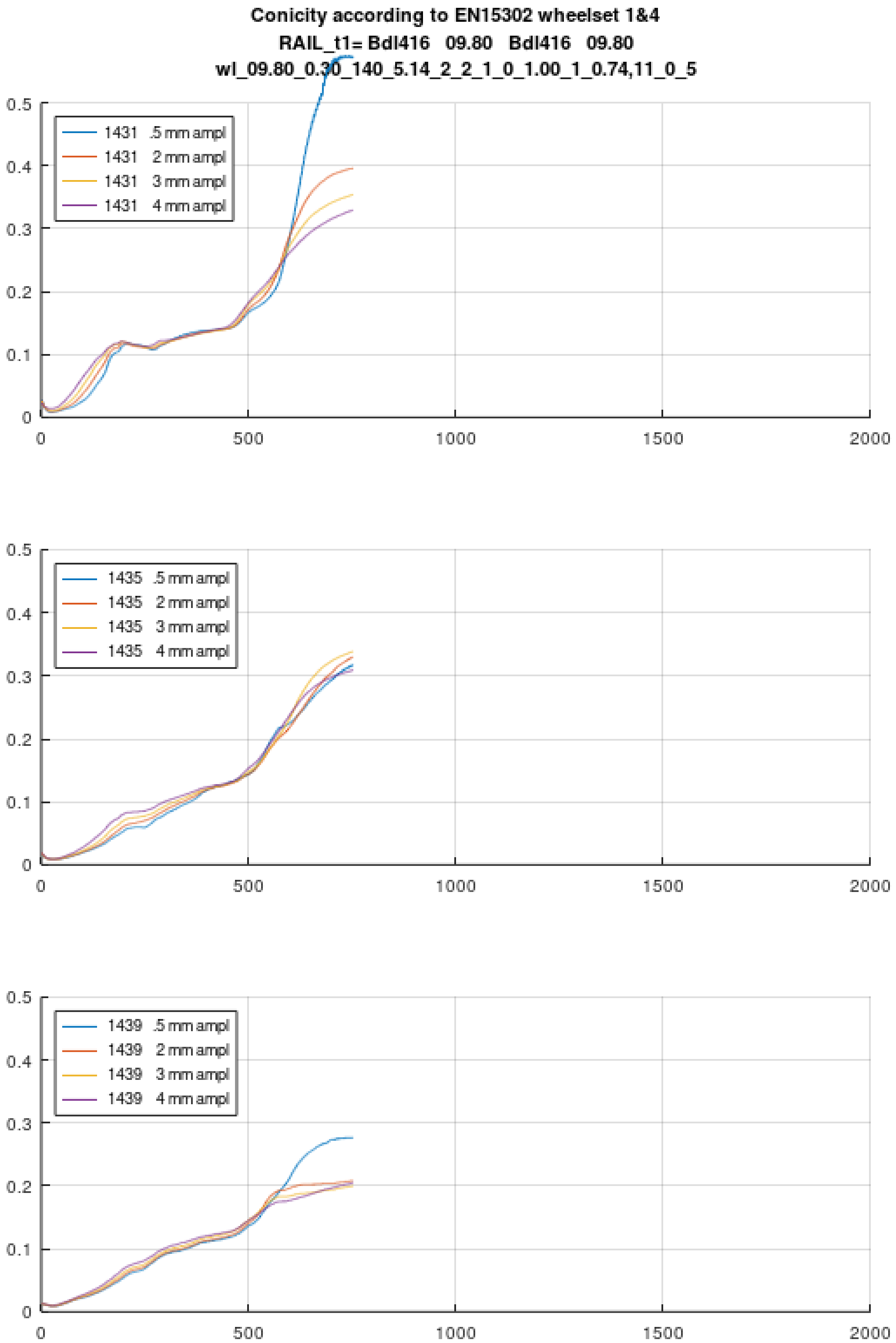

Compared to the reference case 9.1 the conicities for this rail profile increases very fast. The conicity become so high so the wear prediction loop was be stopped prematurely.

C.2 Development of wheel profile shapes wheelset 1&4

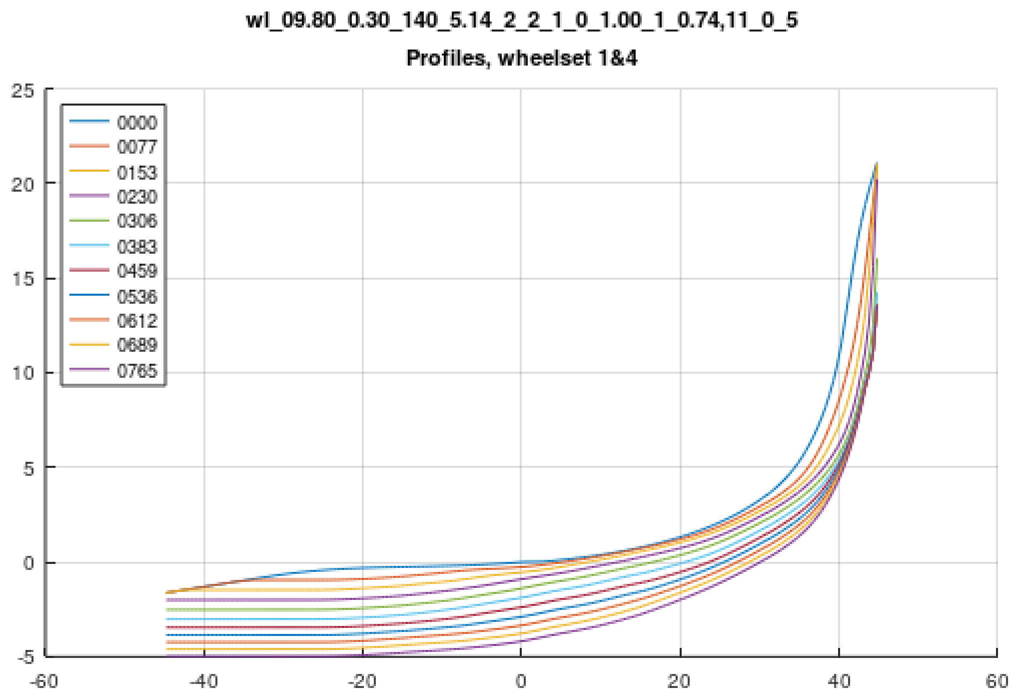

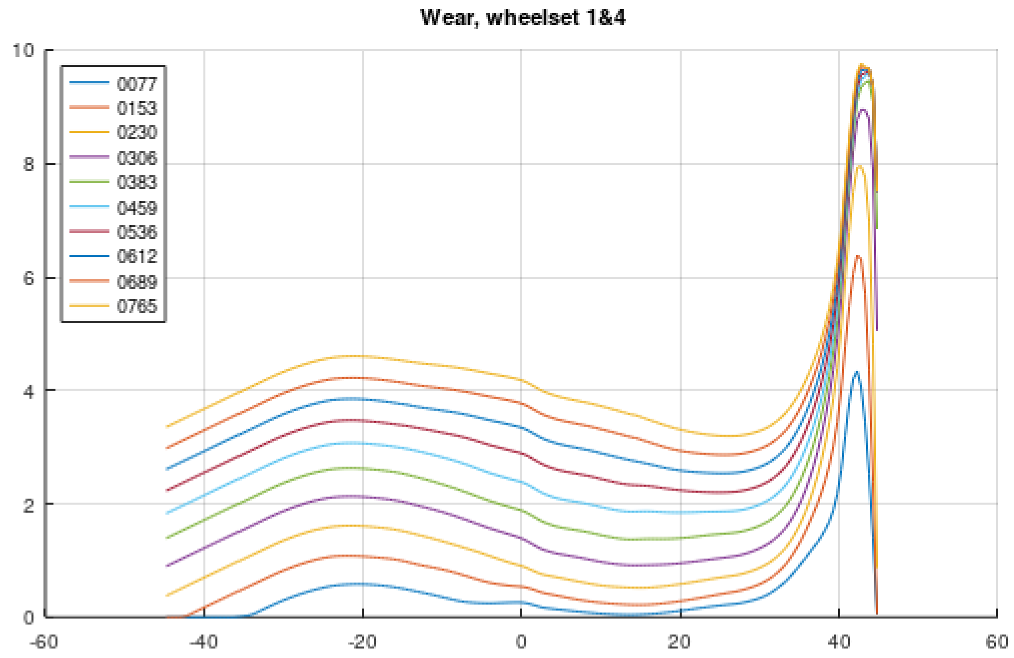

The worn shapes of the wheels look very similar to the reference case 9.3. However, when the wheel profiles and rail profiles are close to each other, a small change in the shape can have a significant impact on the conicity.

C.3 Development of GIPw

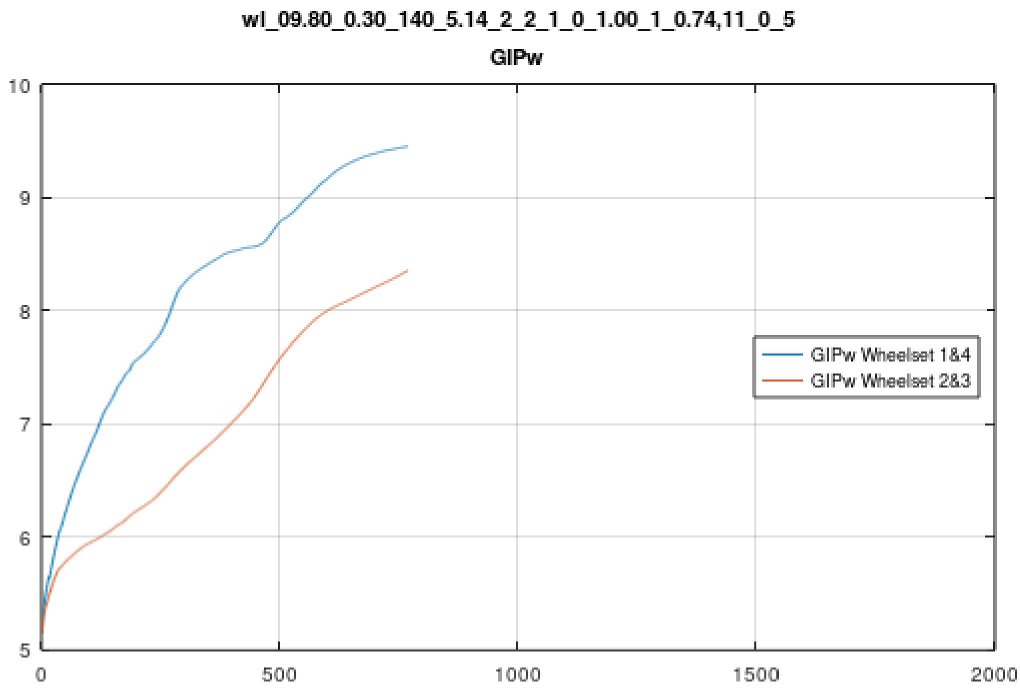

GIPw increases much faster than for the reference case 9.5. It looks like GIPw is asymptotically reaching the same GIP value as for the rail 9.80.

C.4 Development of the Flange Thickness

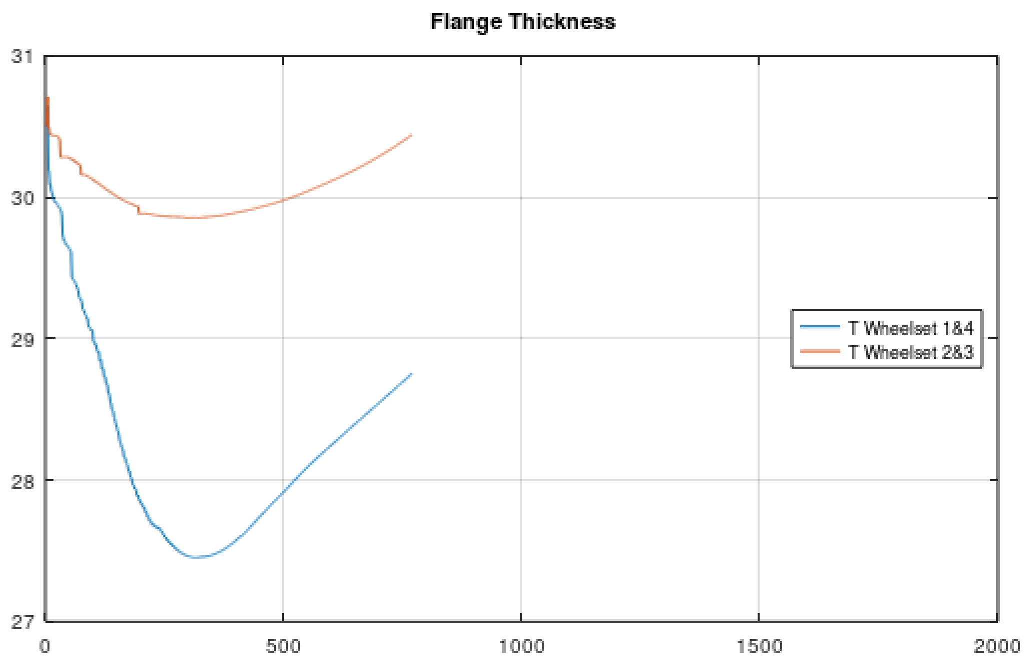

Compared to the reference case 9.6 the flange thicknesses goes down fast but after a while they goes up very fast.

C.5 Development of the Flange Flank qR

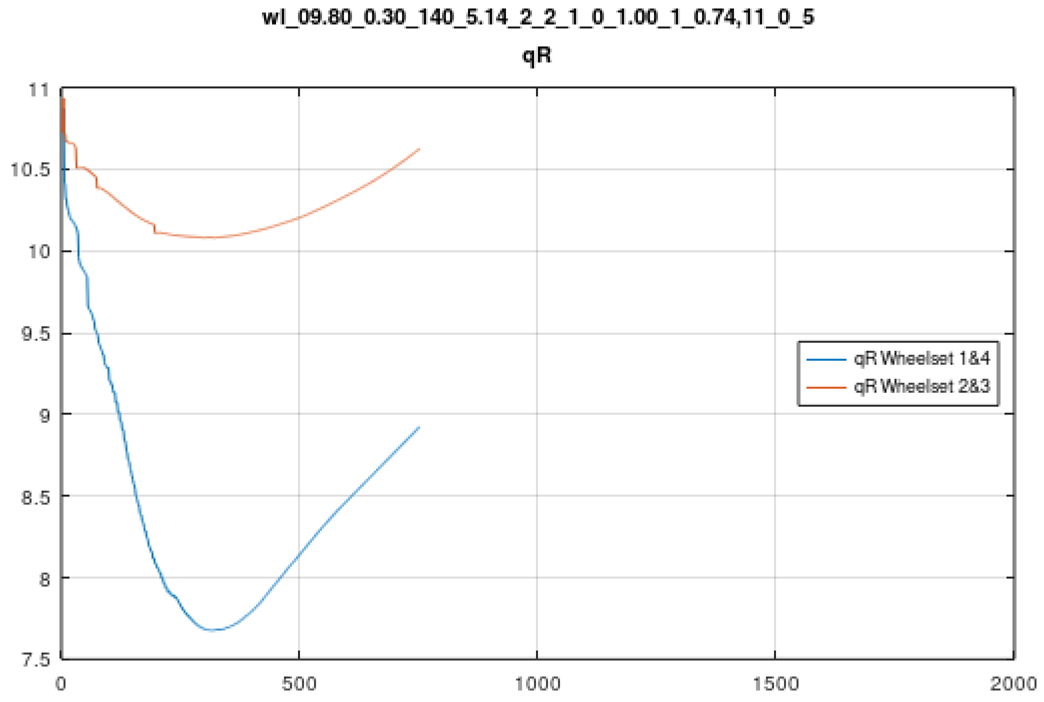

Compared to the reference case 9.7 the qR value goes down fast but then also goes up very fast.

C.6 Development of the Wheelset Steering Ability

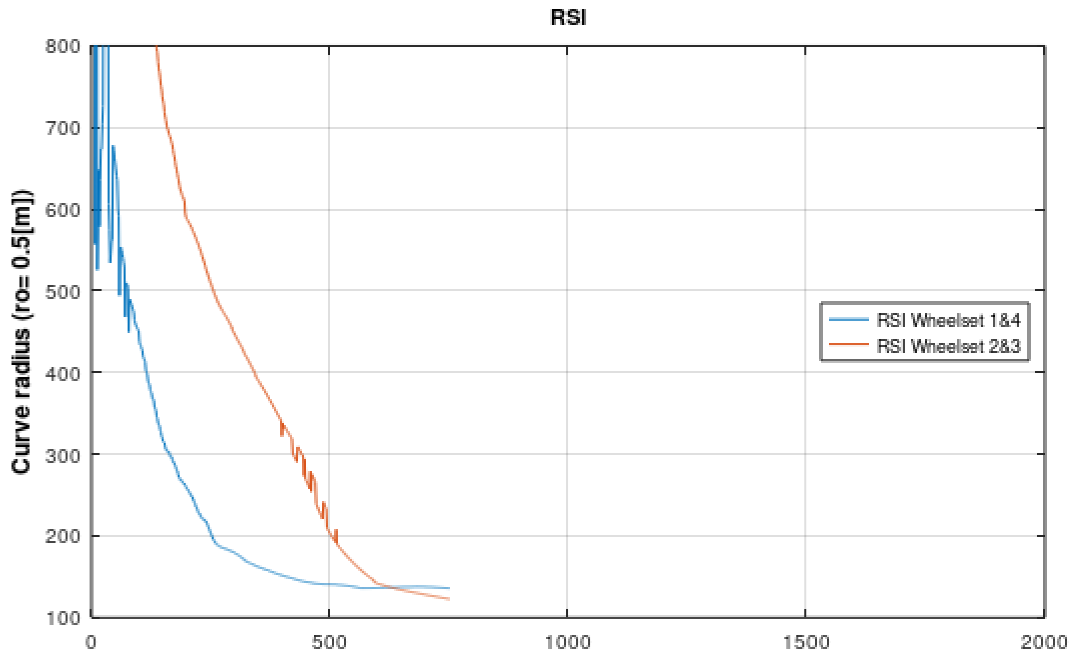

Compared to the reference case 9.8 the wheelsets the steers worse in the beginning, but after a short while their steering ability improves very fast.

C.7 Development of the risk for RCF

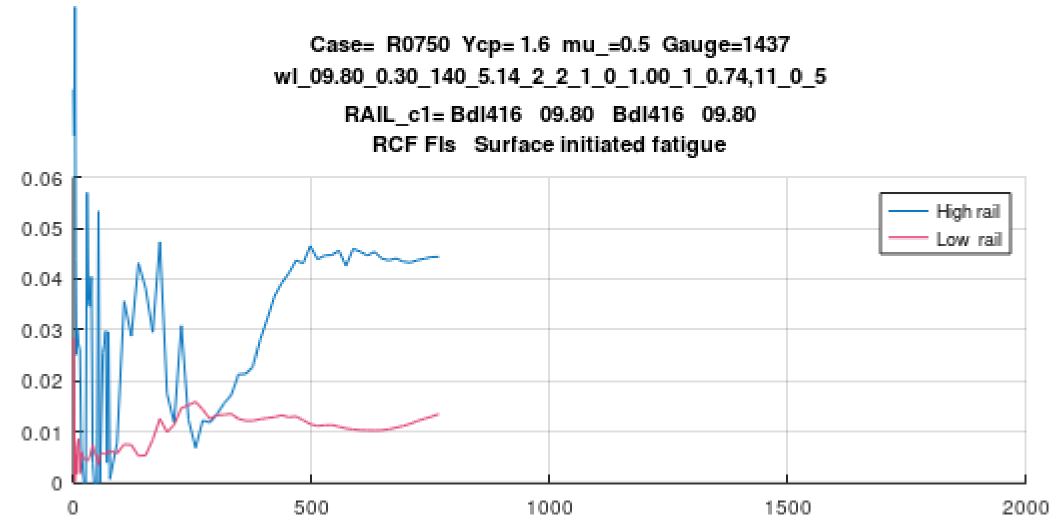

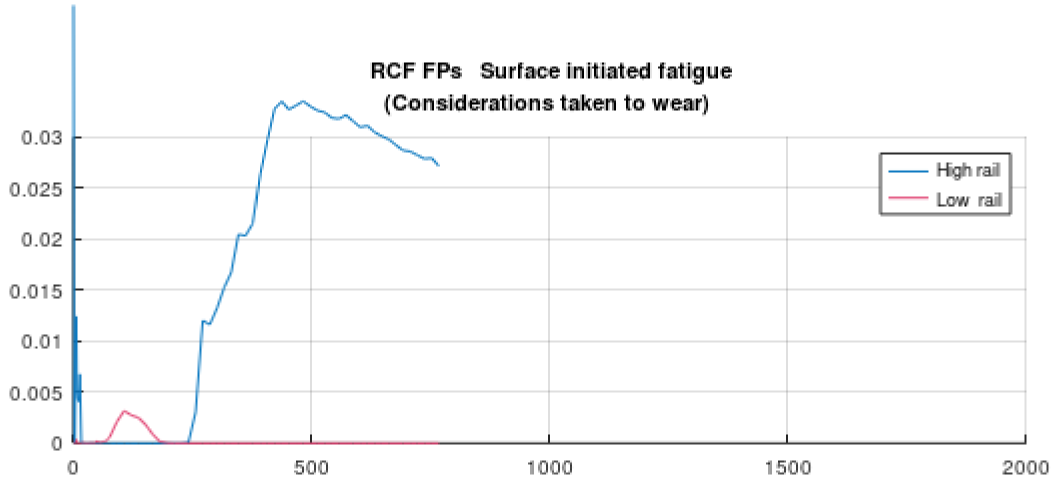

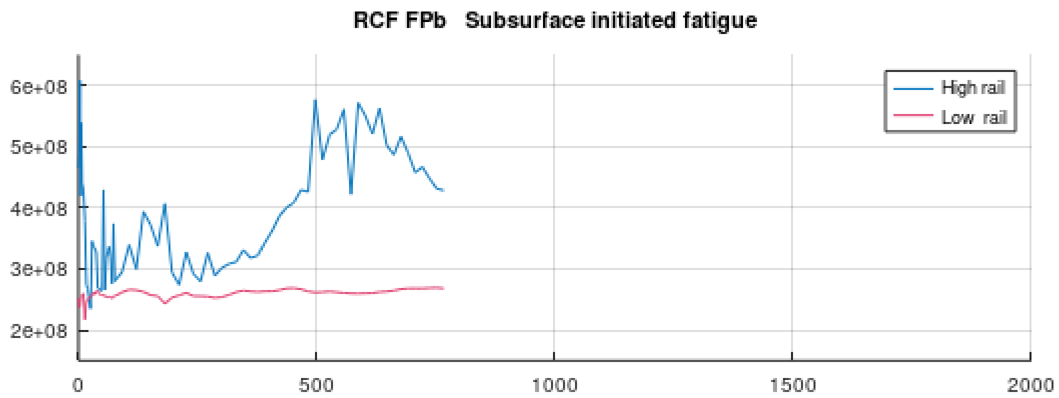

The risk for surface initiated RCF is similar to the reference case 9.9. When the wheels are newly turned the risk for RCF FPs is low, but after a wear-in period the risk for surface initiated RCF becomes big.

Also, the subsurface RCF FPb becomes big after a while. After ~500 updates of the wheel profile, RCF FPb exceeds the limits value 450e6.

Appendix D. Lower average friction coefficient

This case is denoted:

wl_09.33_0.25_360_5.14_2_2_1_0_1.00_1_0.74,11_0_5

All data are the same as the reference case 9, except the average friction coefficient between wheel and rail, that in this case is 0.25.

D.1 Development of conicity wheelset 1&4

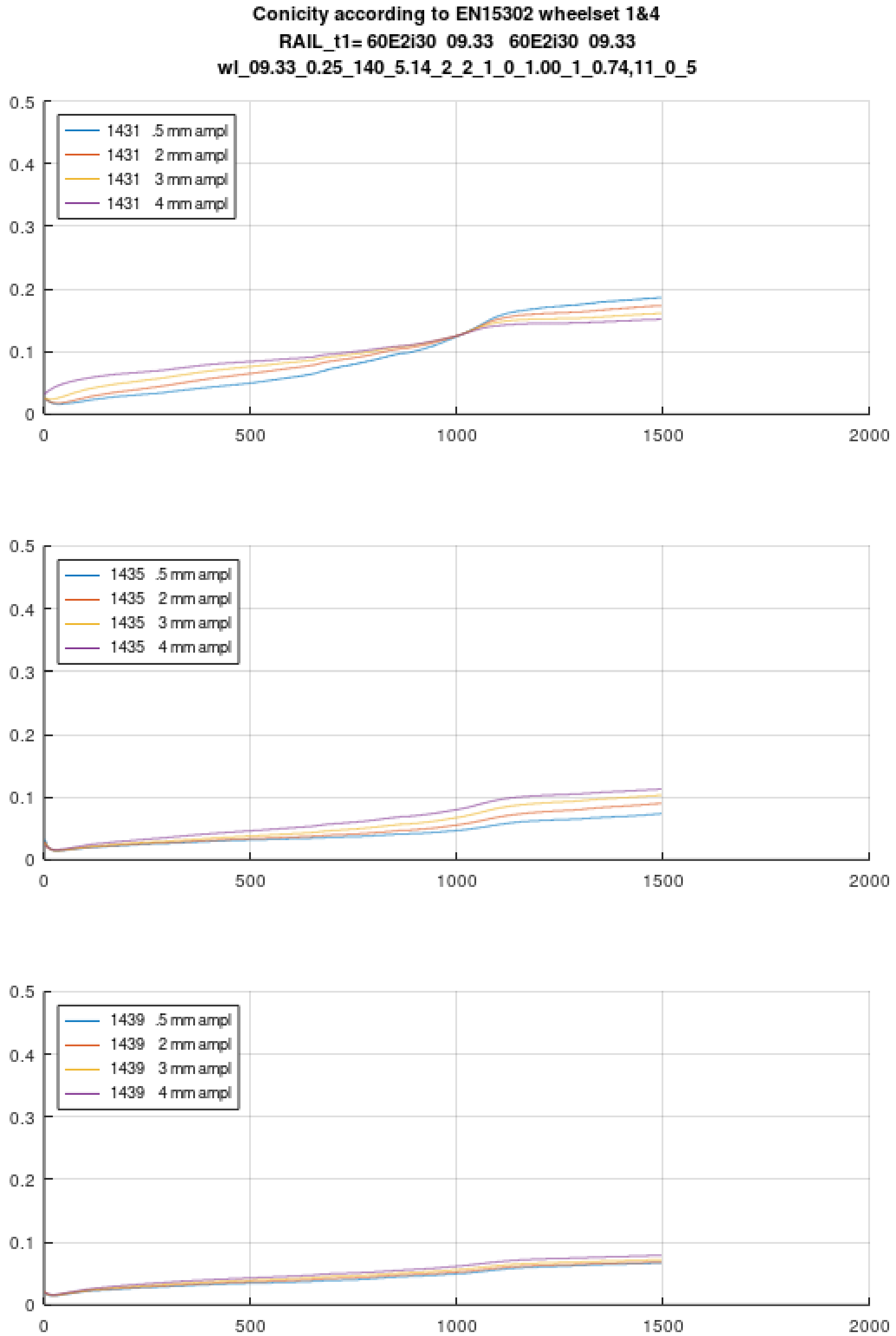

Compared to the reference case 9.1, it can be seen that the conicities increases more slowly. as fast for the reference case 9.1.

D.2 Development of wheel profile shapes wheelset 1&4

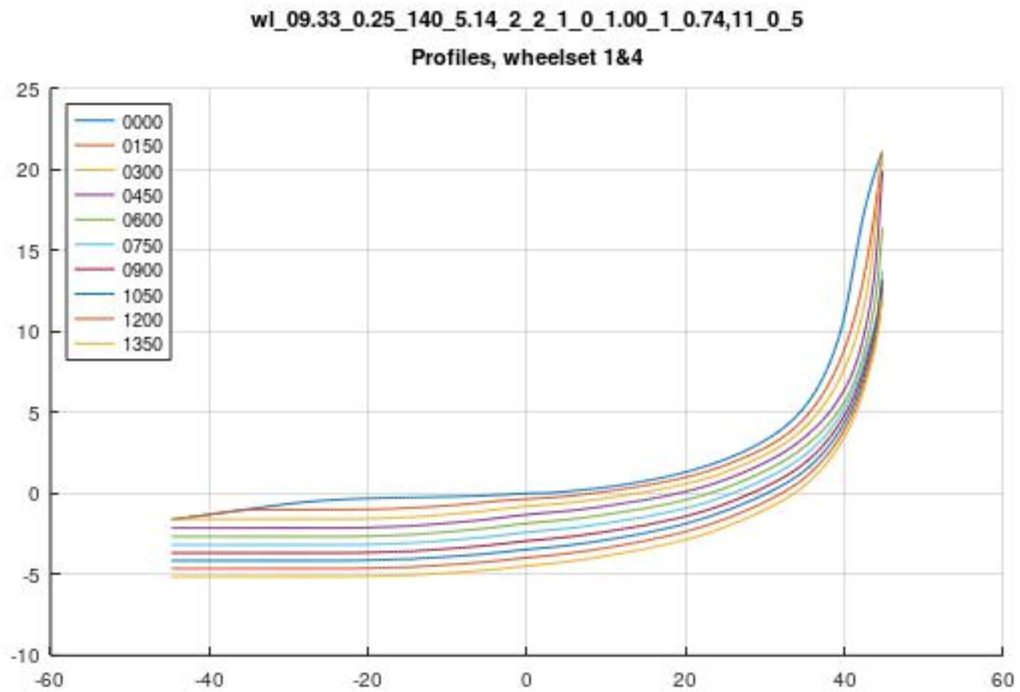

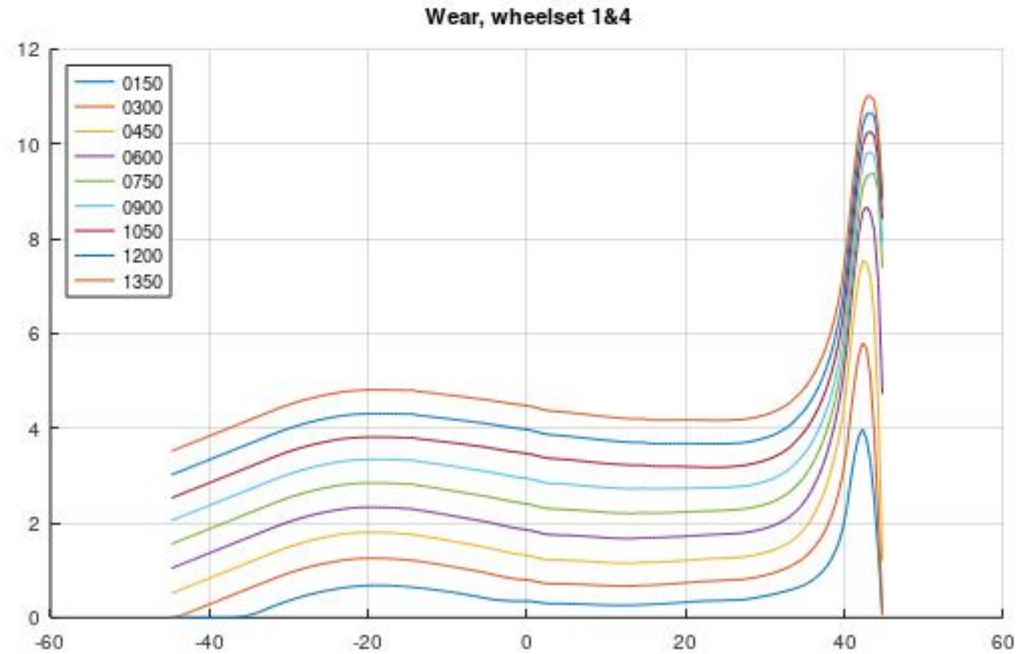

The worn shapes of the wheels look very similar to the reference case 9.3. However, when the wheel profiles and rail profiles are close to each other, a small change in the shape can have a significant impact on the conicity.

D.3 Development of GIPw

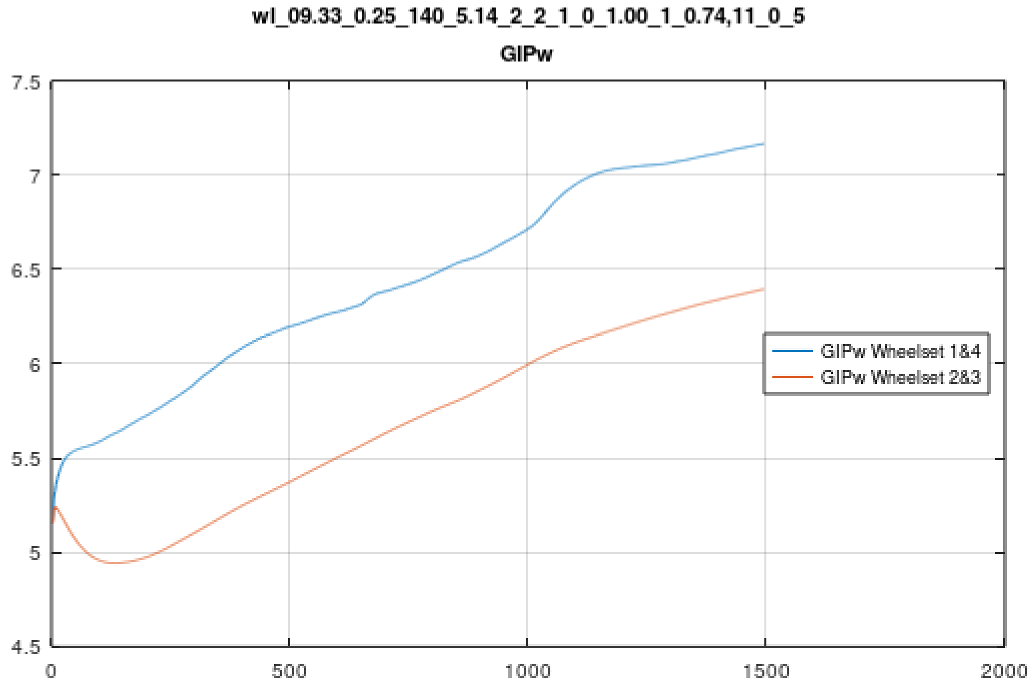

GIPw don’t increase as fast as for the reference case 9.5.

D.4 Development of the Flange Thickness

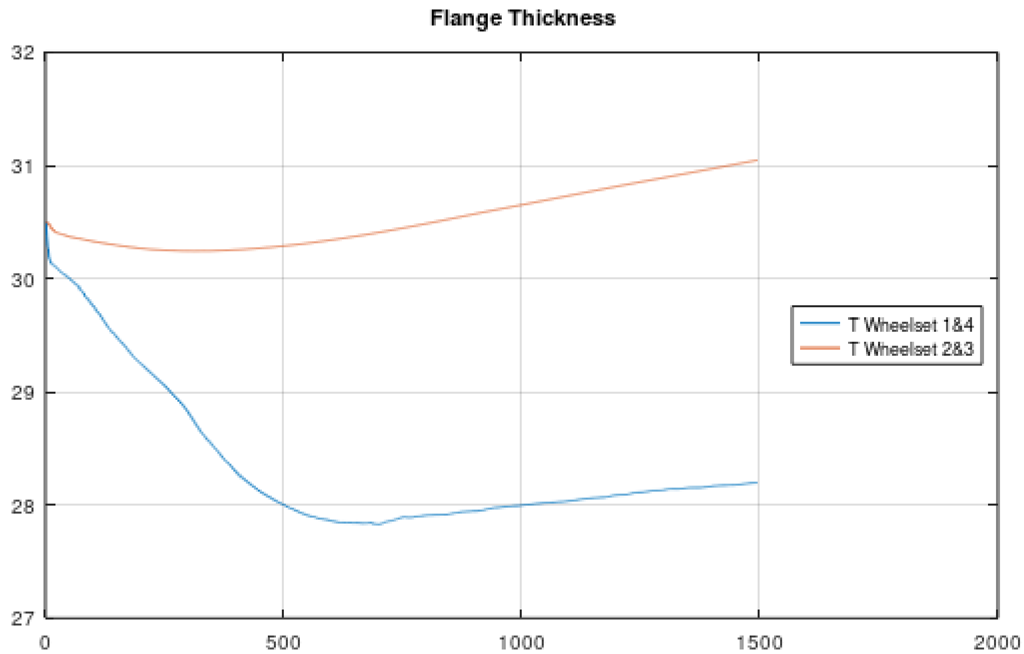

The thickness of the flange behaves in a similar way as in the reference case 9.6. The thickness goes down to ~28mm then it increases again. However, the flanges don’t grow as fast as in the reference case.

D.5 Development of the Flange Flank qR

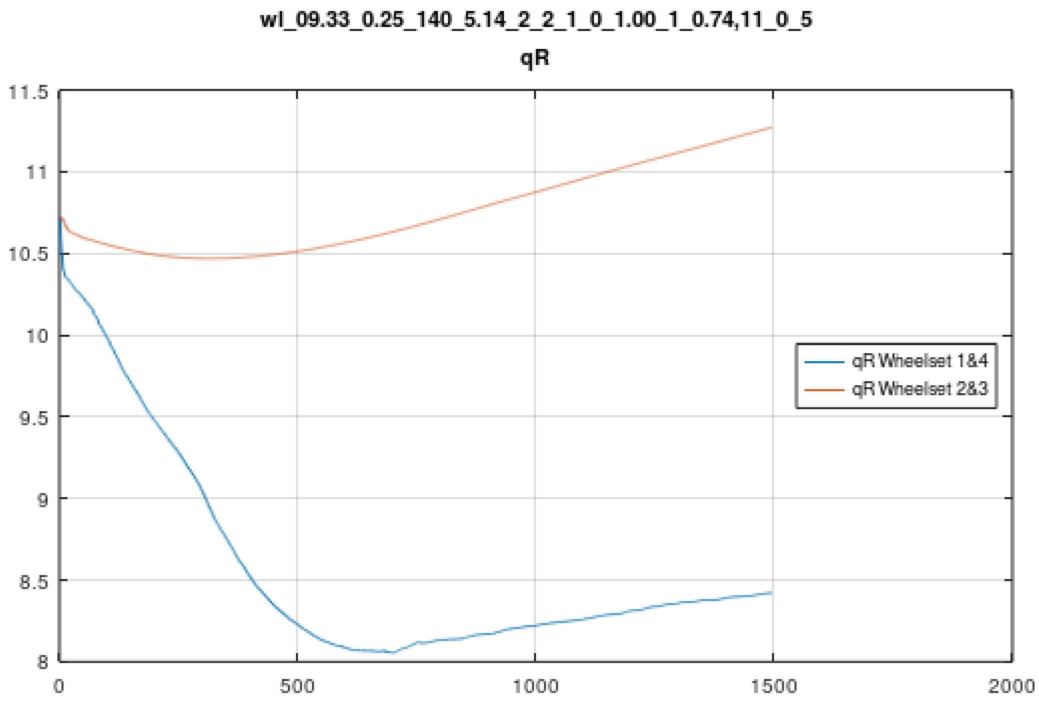

The flange flank behaves in a similar way as in the reference case 9.7. The flange flank goes down to ~8 then it increases again. However, the flange flanks don't grow as fast as in the reference case.

D.6 Development of the Wheelset Steering Ability

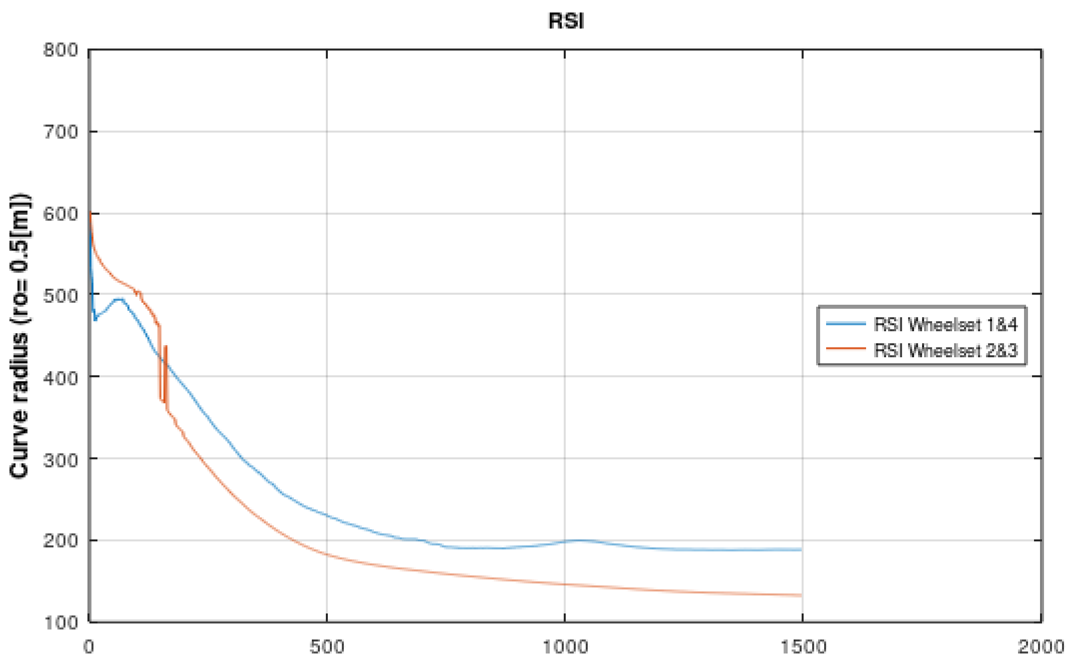

The wheelset steering ability behaves in a similar way as in the reference case 9.8. It only takes a little longer time to reach the asymptotic value.

D.7 Development of the risk for RCF

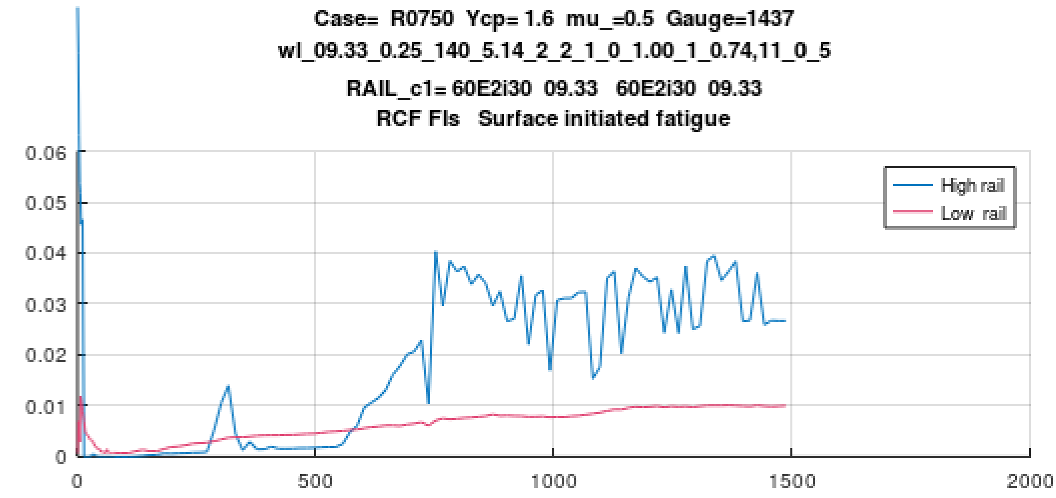

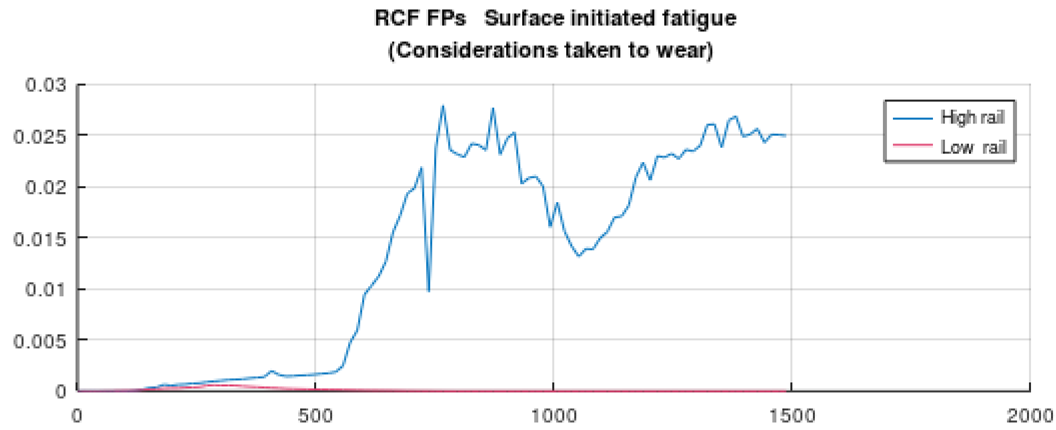

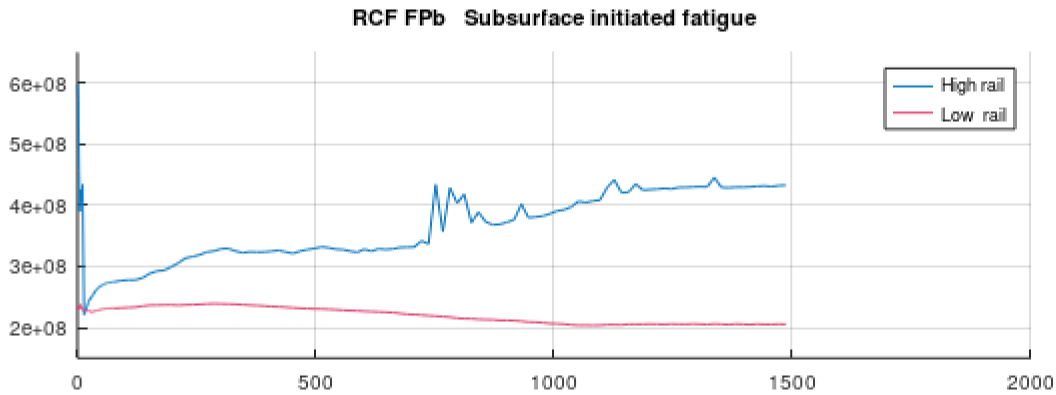

As in the reference case 9.9, the risk for RCF FPs is low for newly turned wheels, but after a while the risk for RCF FPs builds up. It this case RCF FPs in the end seems to be a little higher than in the reference case.

RCF FPb also is low when the wheels are newly turned, but over time the risk for RCF FPb increases. This case seems to be a little bit worse than the reference case, but luckily RCF FPb seems to be below the limit value 450e6 at all times.

Appendix E. Higher average friction coefficient

This case is denoted:

wl_09.33_0.35_360_5.14_2_2_1_0_1.00_1_0.74,11_0_5

All data are the same as the reference case 9, except the average friction coefficient between wheel and rail.

E.1 Development of conicity wheelset 1&4

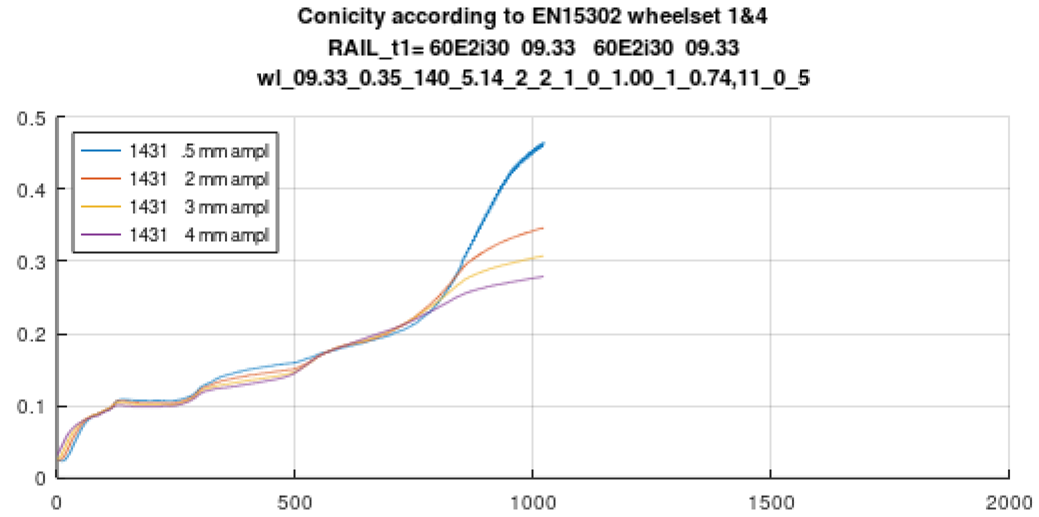

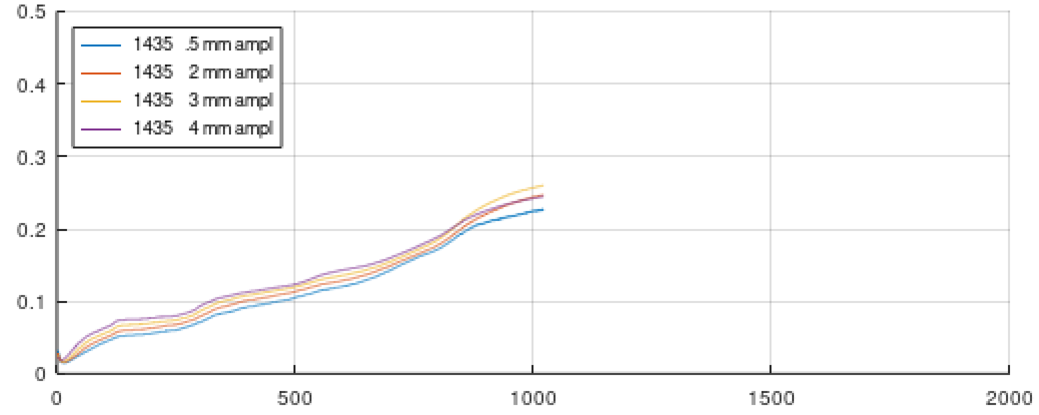

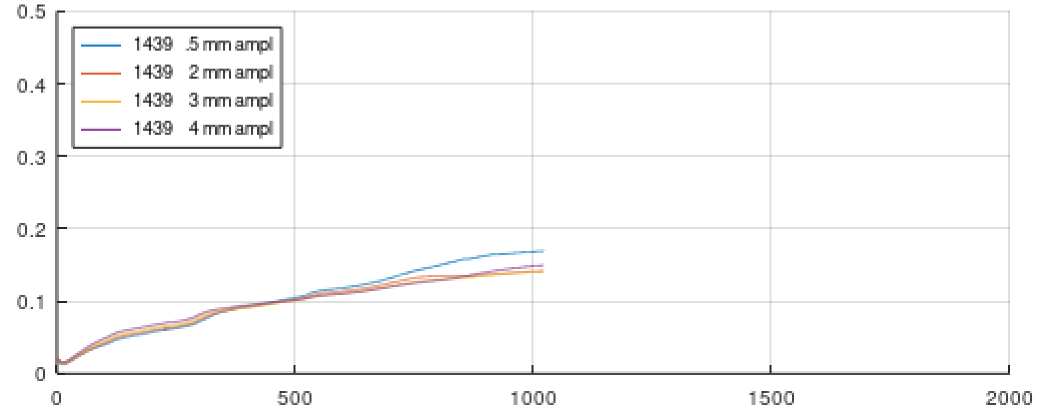

Compared to the reference case 9.1 the conicities for this rail profile increases very fast. The conicity become so high so the wear prediction loop was be stopped prematurely.

E.2 Development of wheel profile shapes wheelset 1&4

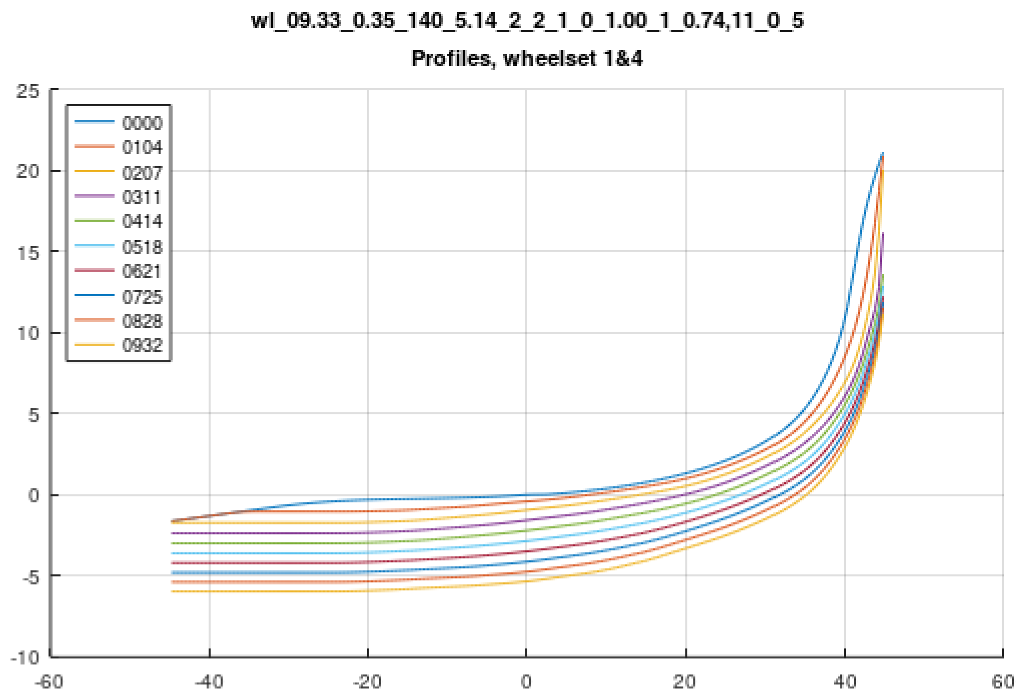

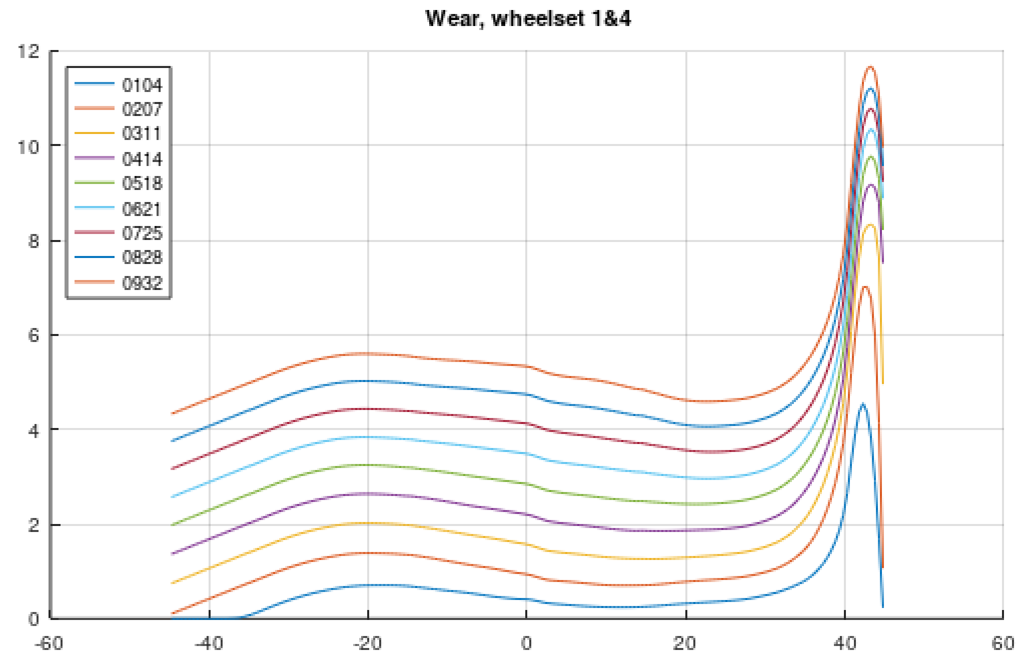

The worn shapes of the wheels look very similar to the reference case 9.3. However, when the wheel profiles and rail profiles are close to each other, a small change in the shape can have a significant impact on the conicity.

E.3 Development of GIPw

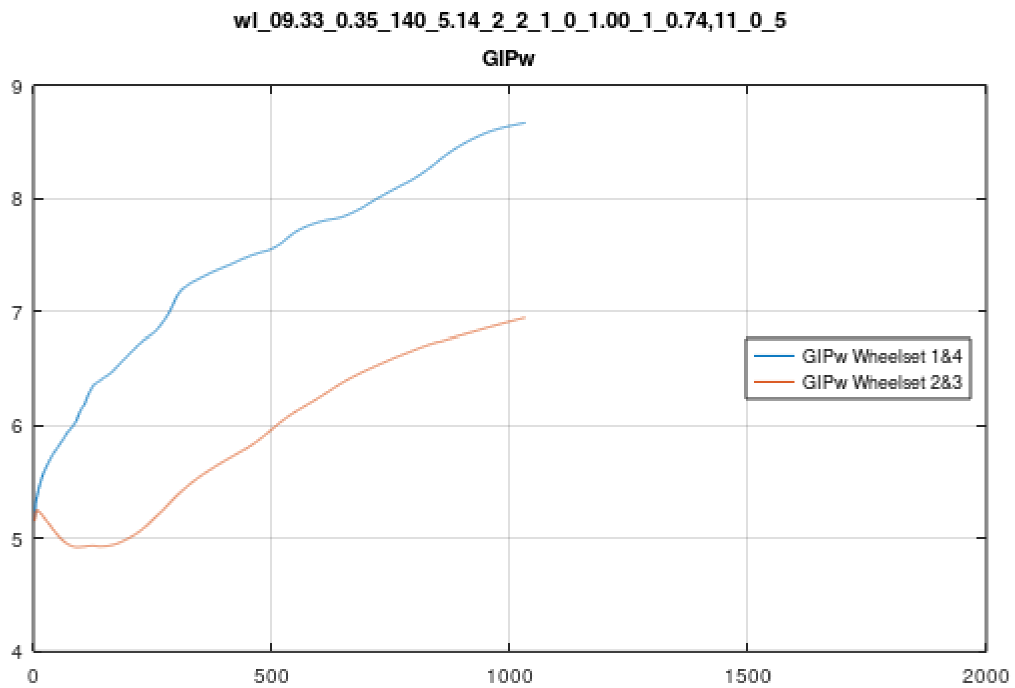

GIPw increases faster than for the reference case 9.5.

E.4 Development of the Flange Thickness

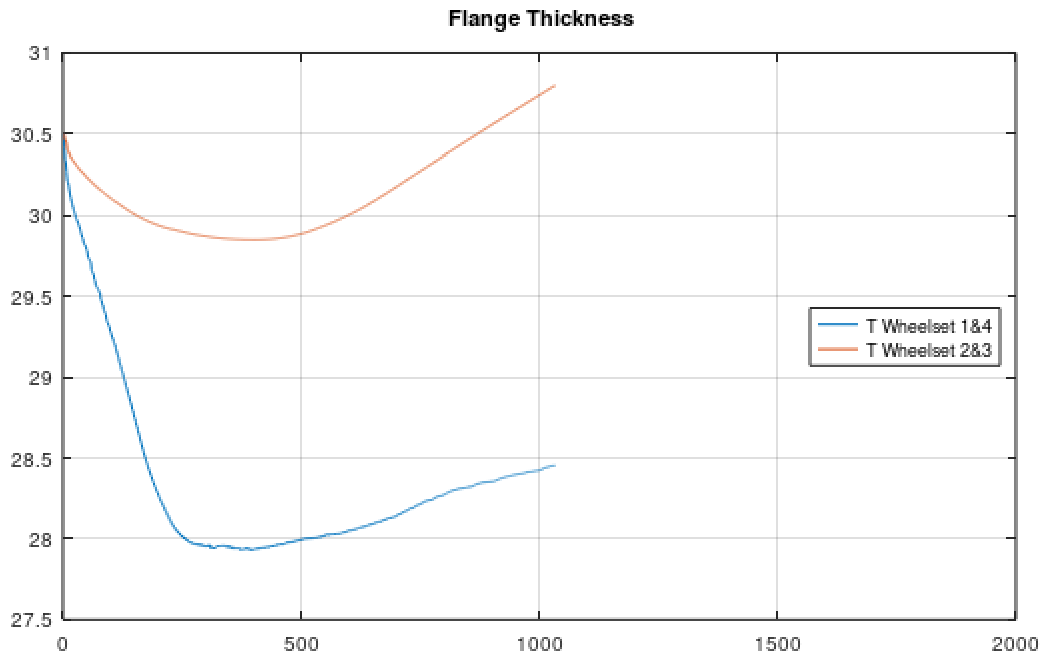

The flange thickness has a similar behaviour as the reference case 9.6.

.

E.5 Development of the Flange Flank qR

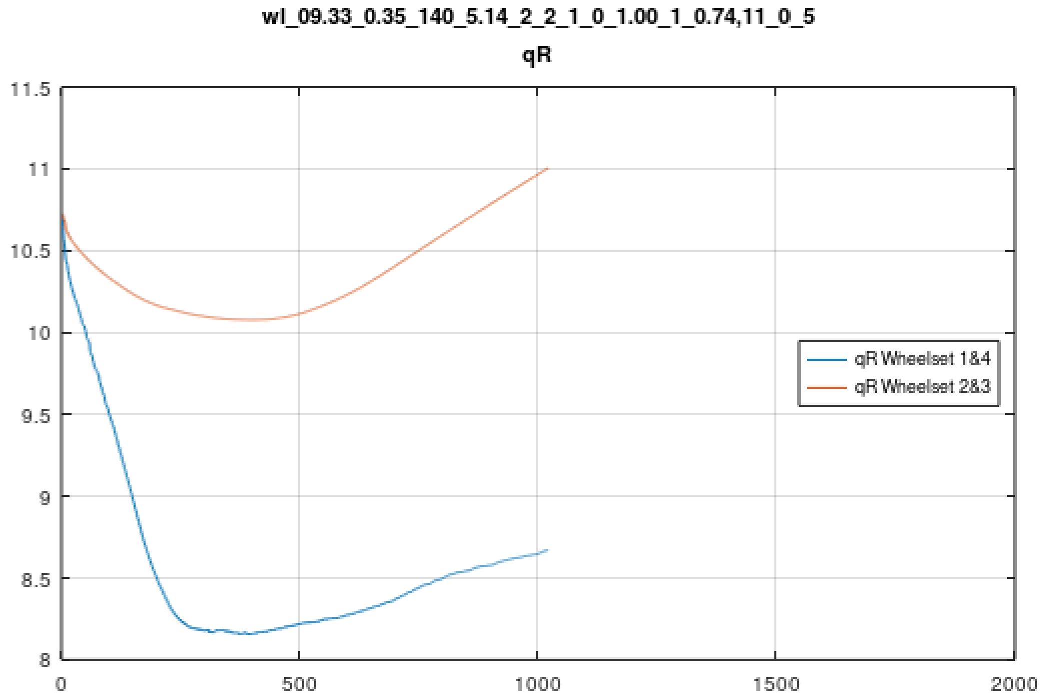

Compared to the reference case 9.7 the qR value goes down and up faster. The results are OK, the value of qR is over 6.5 at all times.

E.6 Development of the Wheelset Steering Ability

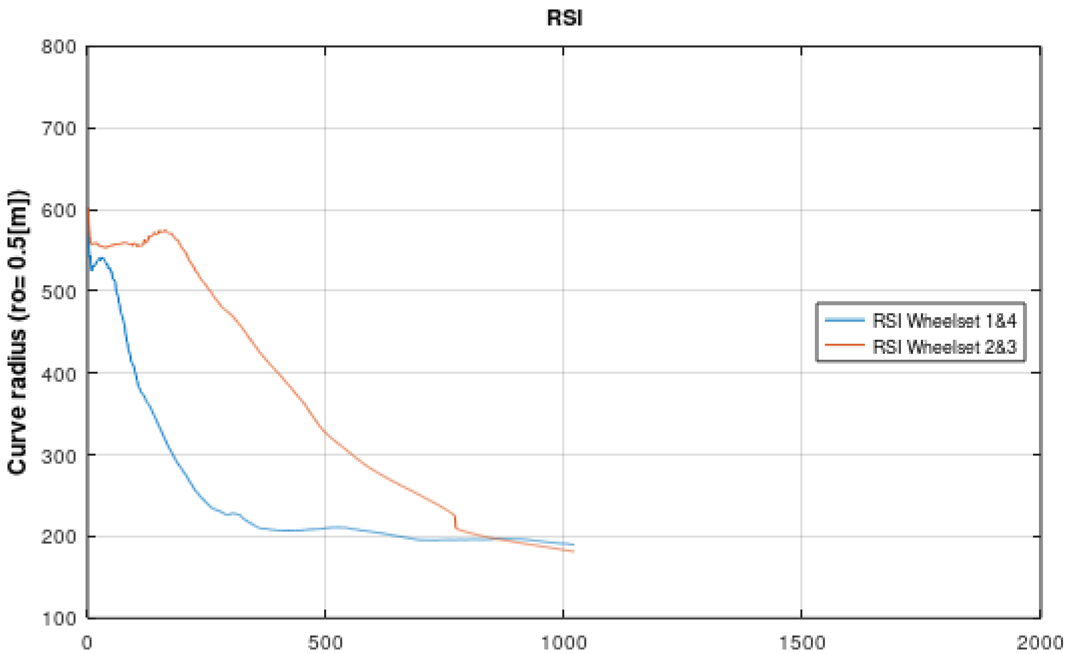

In the beginning the wheelset steering ability is as good as in the reference case 9.8, but the asymptotic value in the end seems to be a little bit higher in this case.

E.7 Development of the risk for RCF

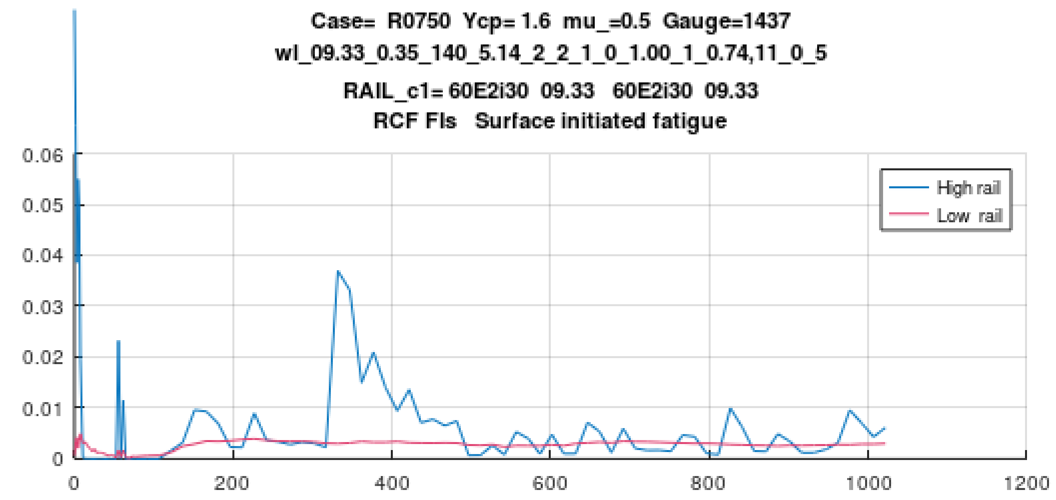

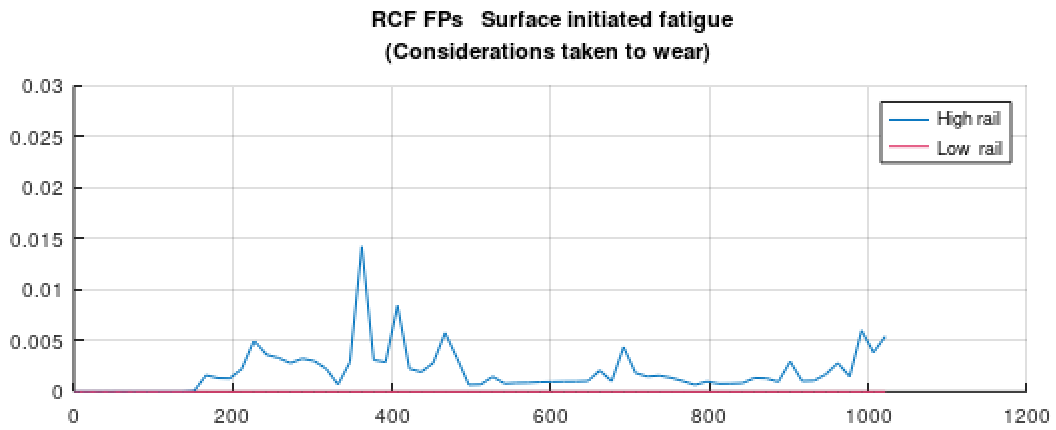

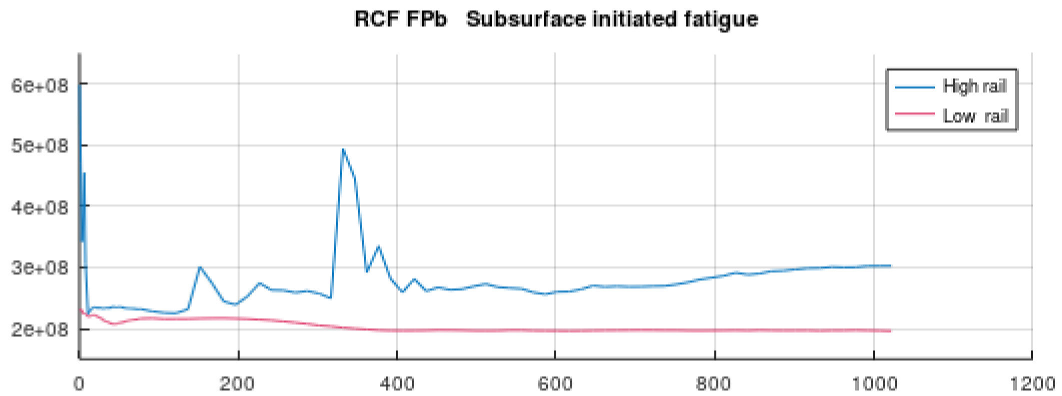

Compared to the reference case 9.9 this case is better for both RCF FPs and RCF FPb.

Appendix F. Softer longitudinal primary stiffnesses in the bogies

This case is denoted:

wl_09.33_0.30_167_5.14_2_2_1_0_1.00_1_0.74,11_0_5

All data are the same as the reference case 9, except the longitudinal stiffness in the primary suspension. In this case the bogie steering ability is SAb= 167. For the definition of SAb, see section 5 and ref [2].

F.1 Development of conicity wheelset 1&4

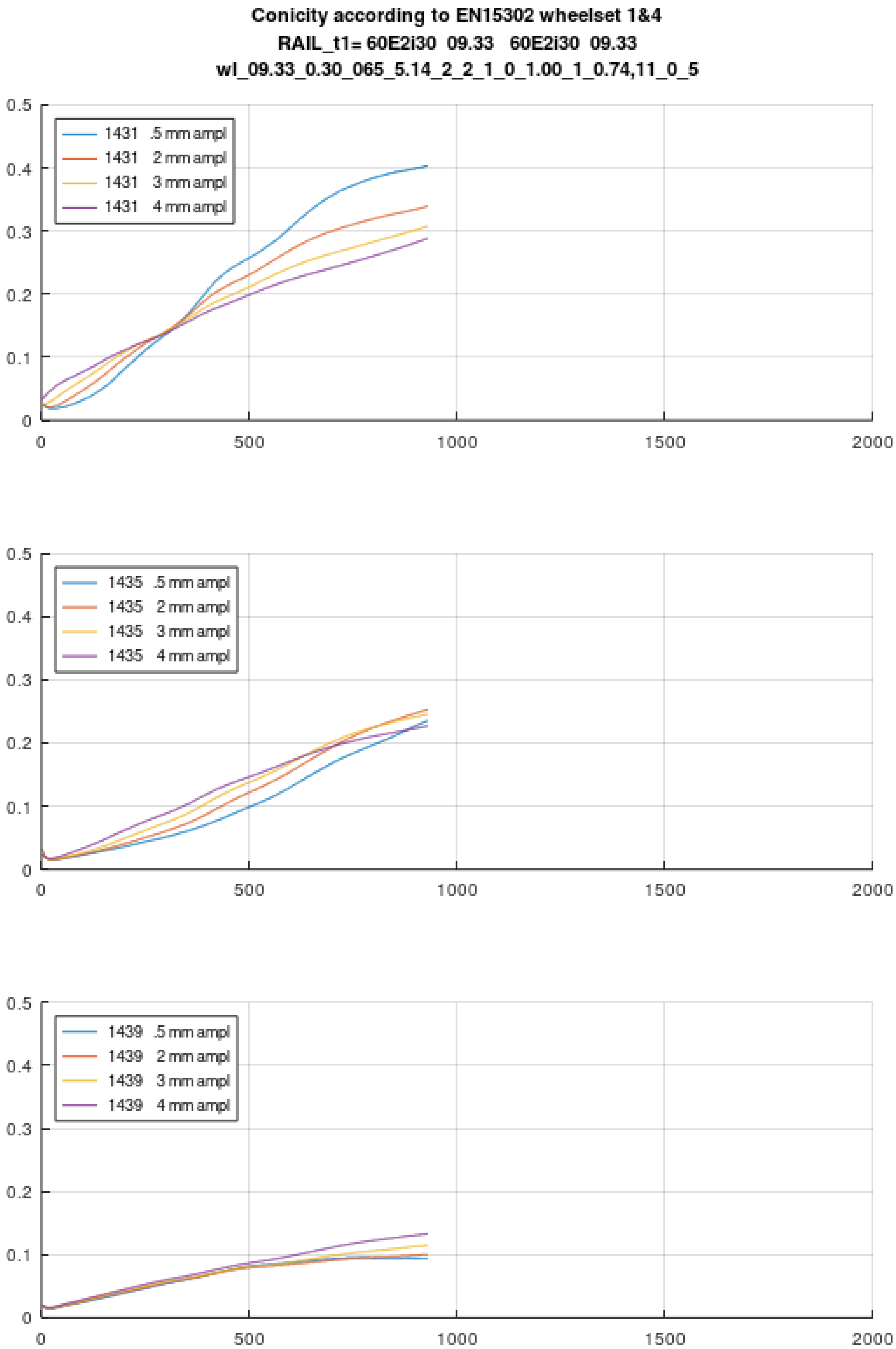

Compared to the reference case 9.1 the conicity here increases faster. The conicity become so high so the wear prediction loop was be stopped prematurely.

F.2 Development of wheel profile shapes wheelset 1&4

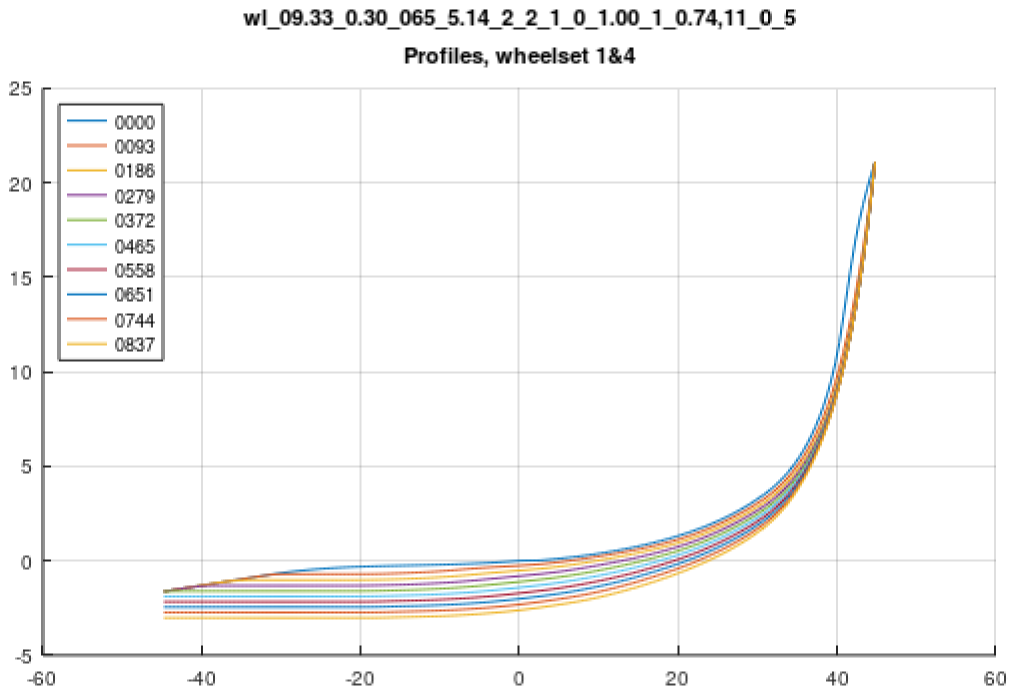

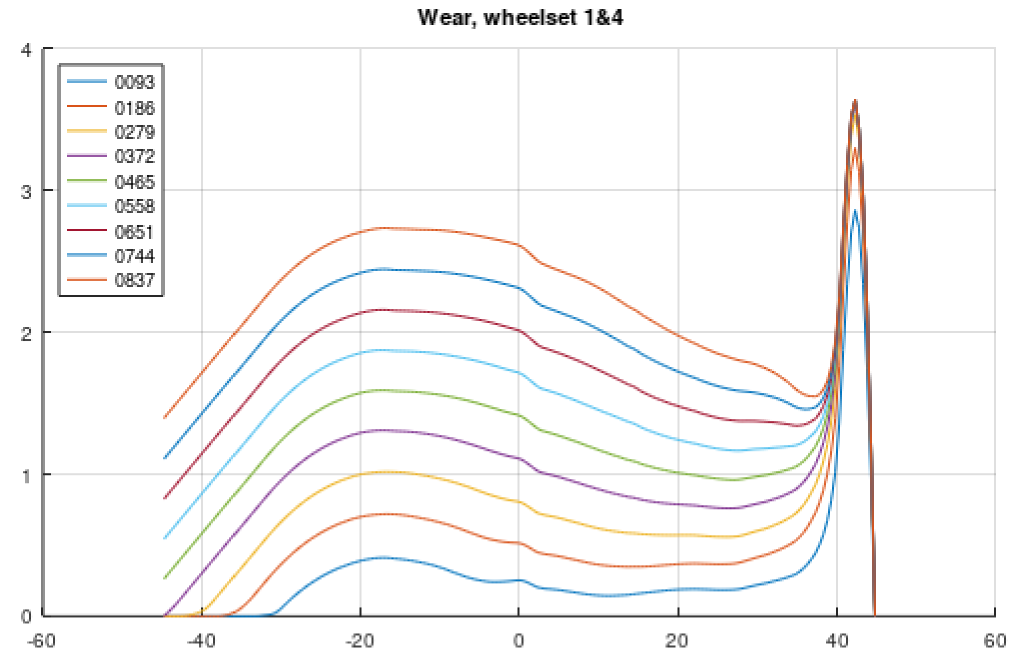

Compared to the reference case 9.3, the flange wear is lower for this case.

F.3 Development of GIPw

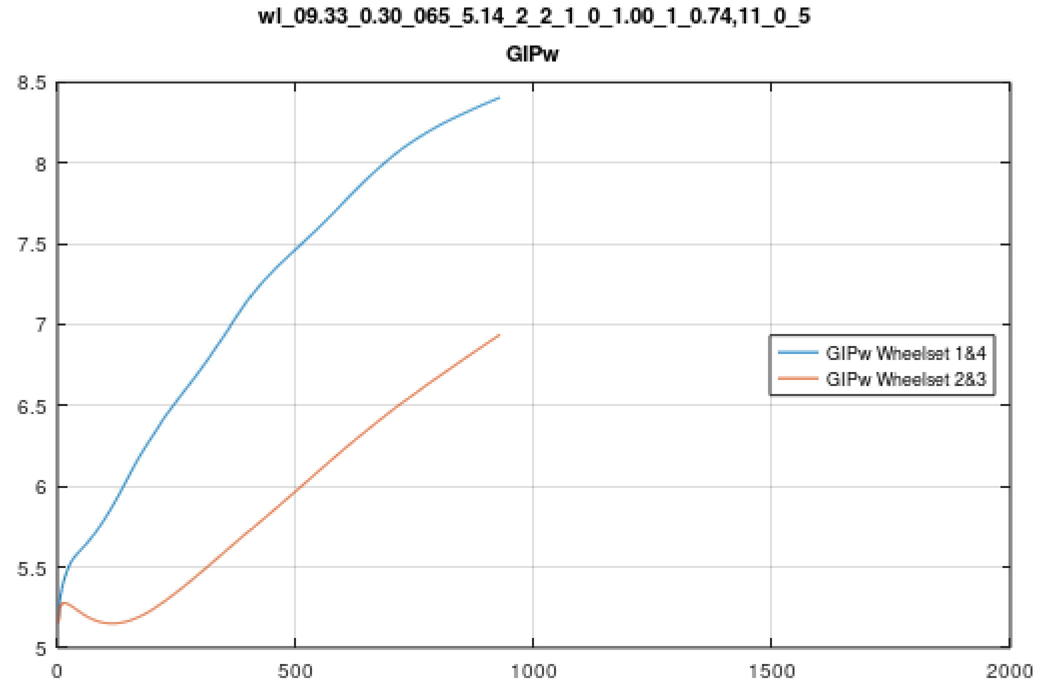

Compared to the reference case 9.5, GIPw increases much faster in this case.

F.4 Development of the Flange Thickness

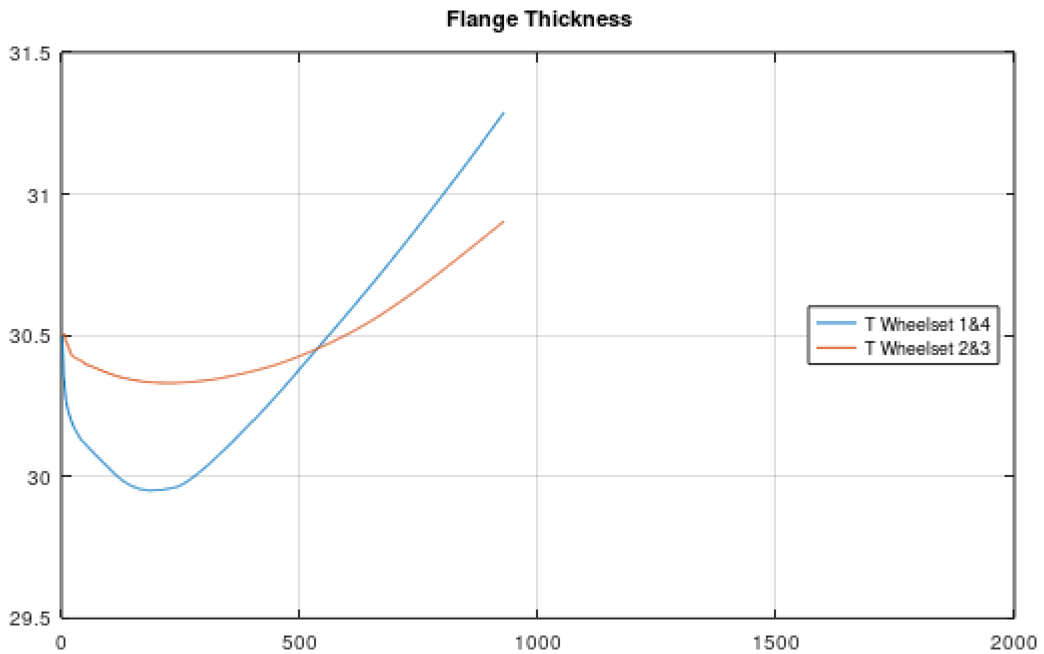

Compared to the reference case 9.6, the flange thickness goes down and up much faster.

F.5 Development of the Flange Flank qR

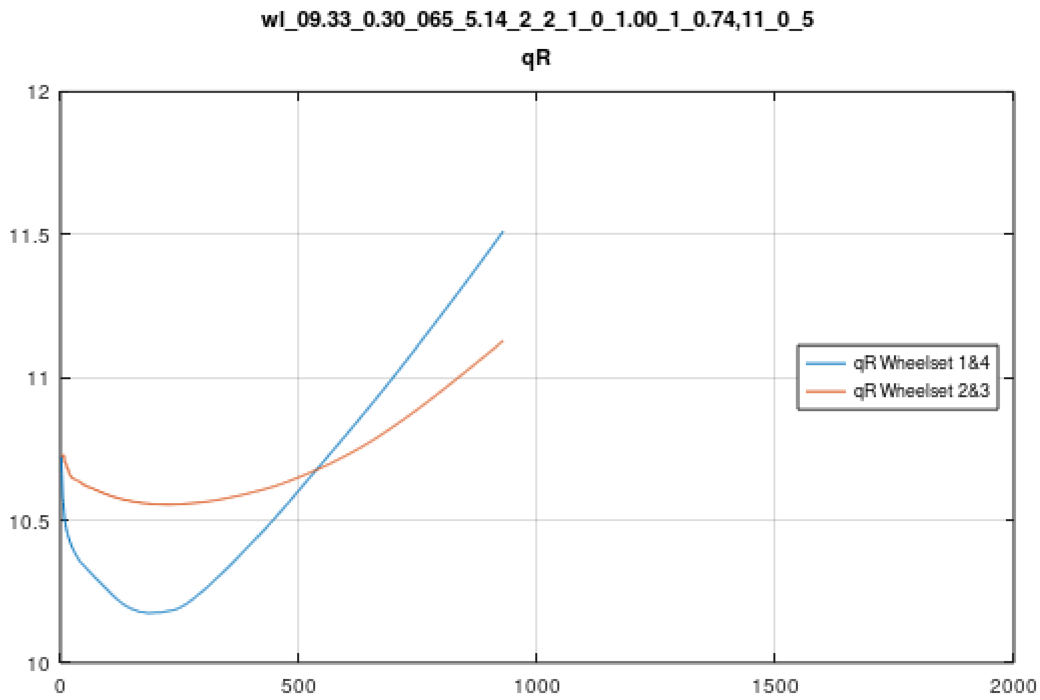

Compared to the reference case 9.7, the flange flank qR goes down and up much faster. The results are OK, the value of qR is over 6.5 at all times.

F.6 Development of the Wheelset Steering Ability

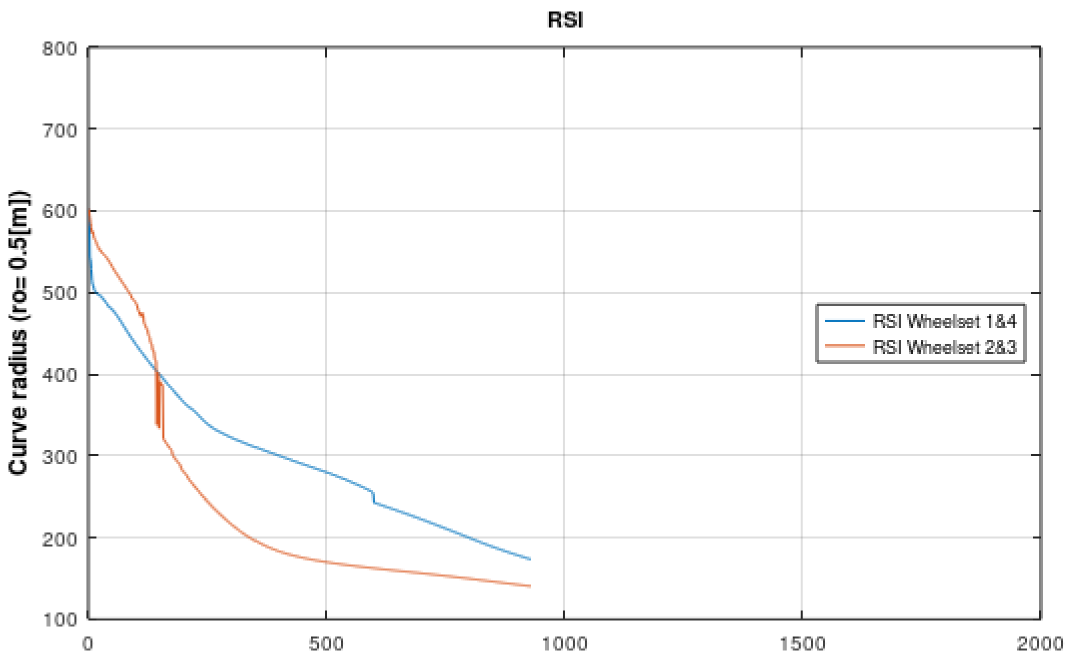

The result is similar to the reference case 9.8. However, it seems that the asymptotic value is reached faster for this case.

F.7 Development of the risk for RCF

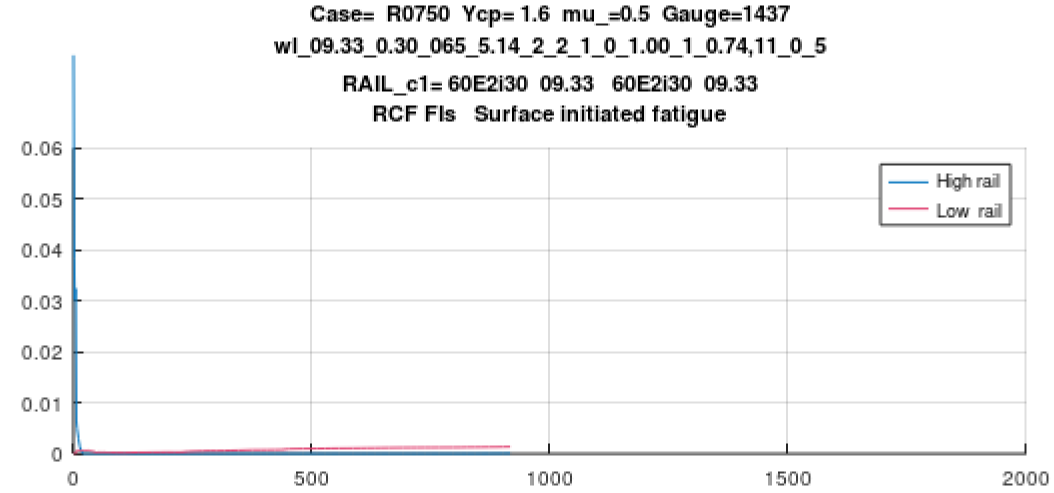

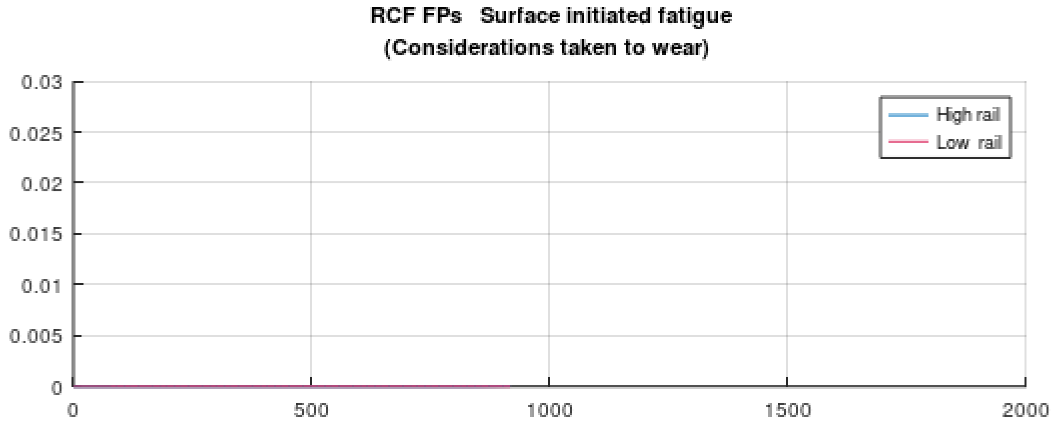

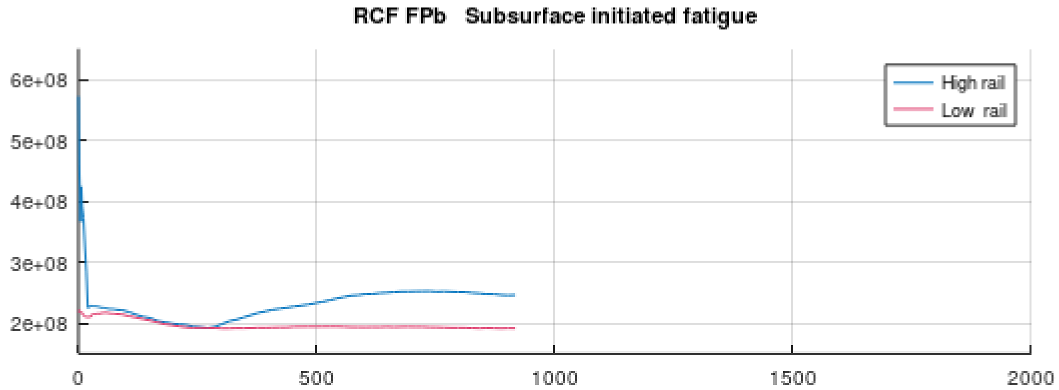

Compared to the reference case 9.9, the bogie with soft primary suspension behaves very well. No risk for RCF FPs and RCF FPb.

Appendix G. Stiffer longitudinal primary stiffnesses in the bogies

This case is denoted:

wl_09.33_0.30_900_5.14_2_2_1_0_1.00_1_0.74,11_0_5

All data are the same as the reference case 9, except the longitudinal stiffness in the primary suspension. In this case the bogie steering ability is SAb= 900. For the definition of SAb, see section 5 and ref [2].

G.1 Development of conicity wheelset 1&4

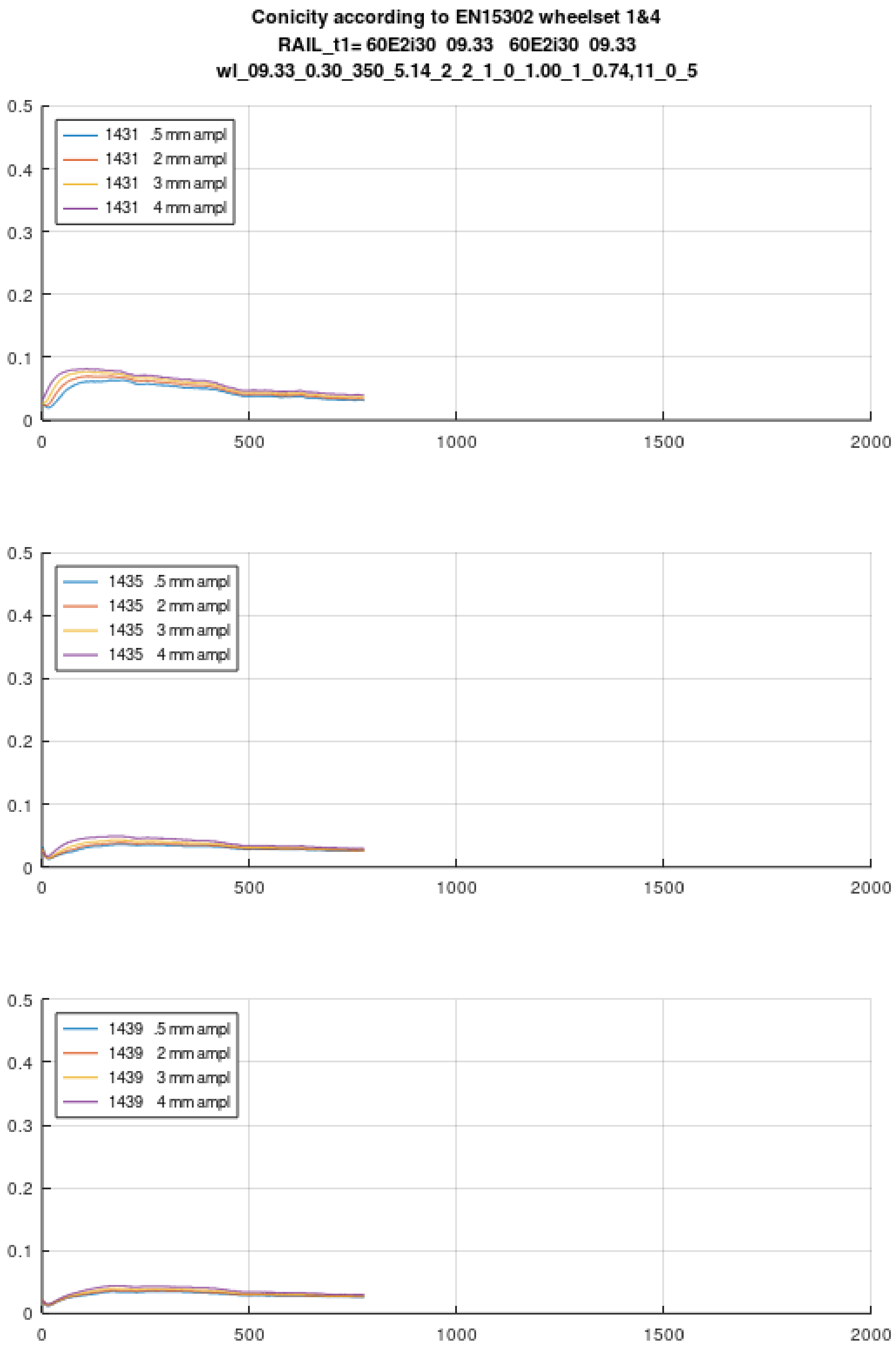

Compared to the reference case 9.1, this bogie type behaves very different. In this bogie design the conicities are low at all times. The wear loop was stopped prematurely because of low qR values.

G.2 Development of wheel profile shapes wheelset 1&4

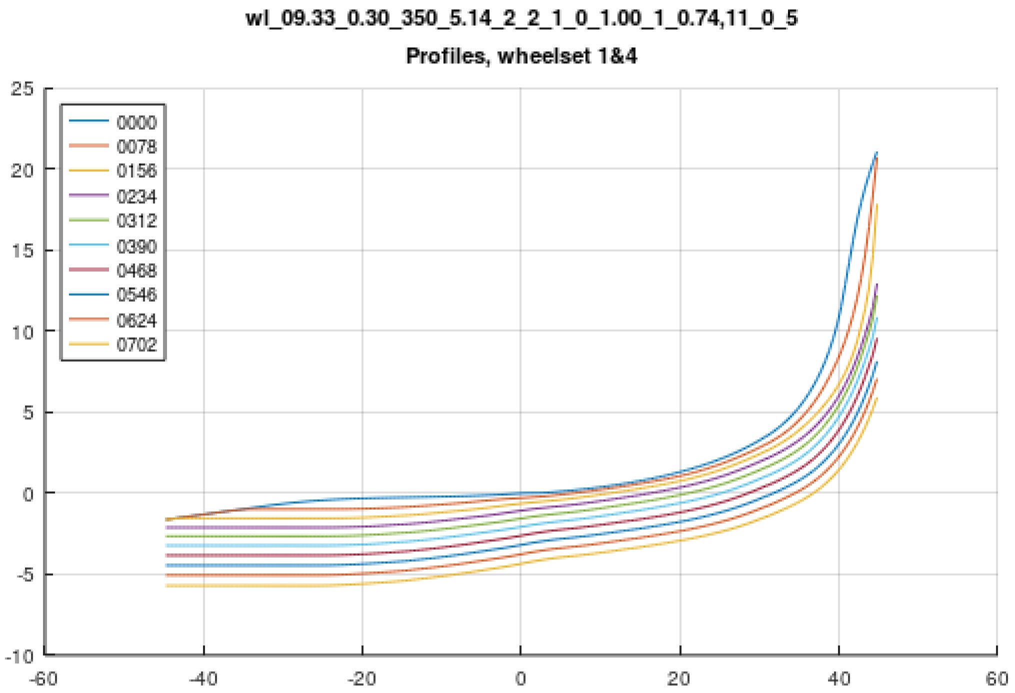

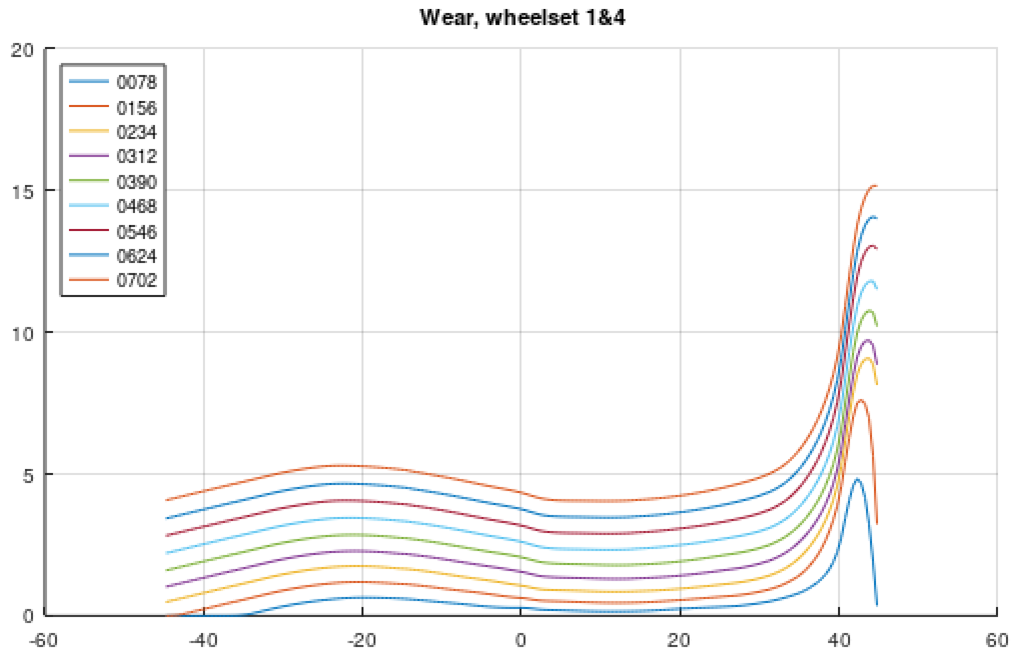

Compared to the reference case 9.3, the flange wear is more in this case.

G.3 Development of GIPw

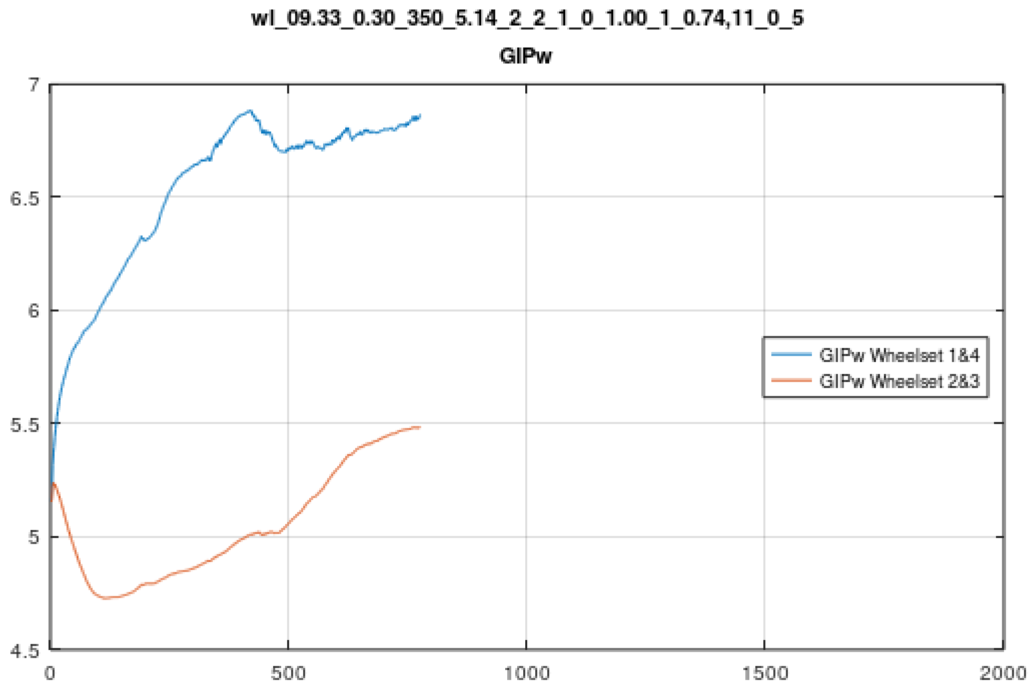

Compared to the reference case 9.5, it seems that GIPw reaches its asymptotic value faster, and that the asymptotic value is lower than in the reference case.

G.4 Development of the Flange Thickness

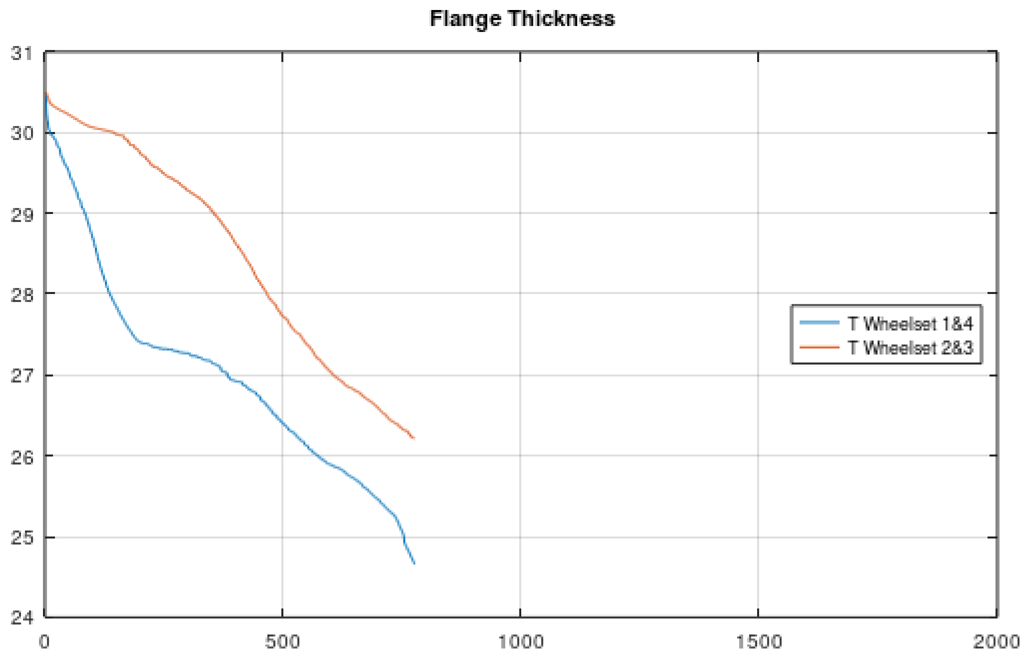

In contrast to the reference case 9.6, the flange doesn't grow in this case. The flange thickness just gets thinner and thinner. The wear prediction loop was stopped because of thin flanges.

G.5 Development of the Flange Flank qR

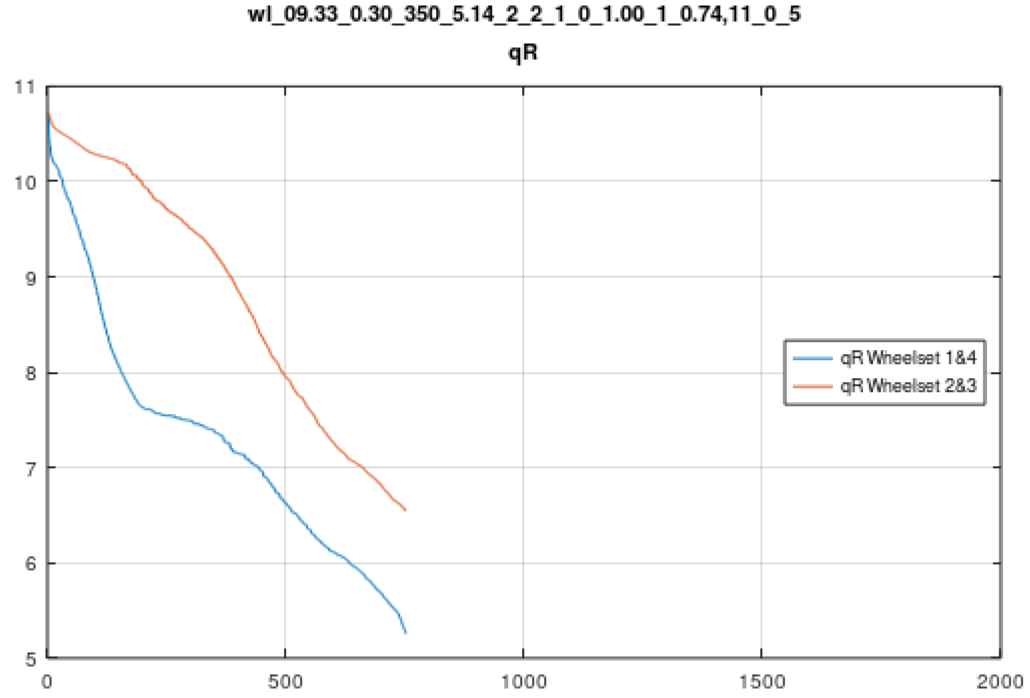

In contrast to the reference case 9.7, the flange flank qR doesn't grow in this case. The qR value just gets lower and lower. The wear prediction loop was stopped because qR was lower than its limit value 6.5.

.

G.6 Development of the Wheelset Steering Ability

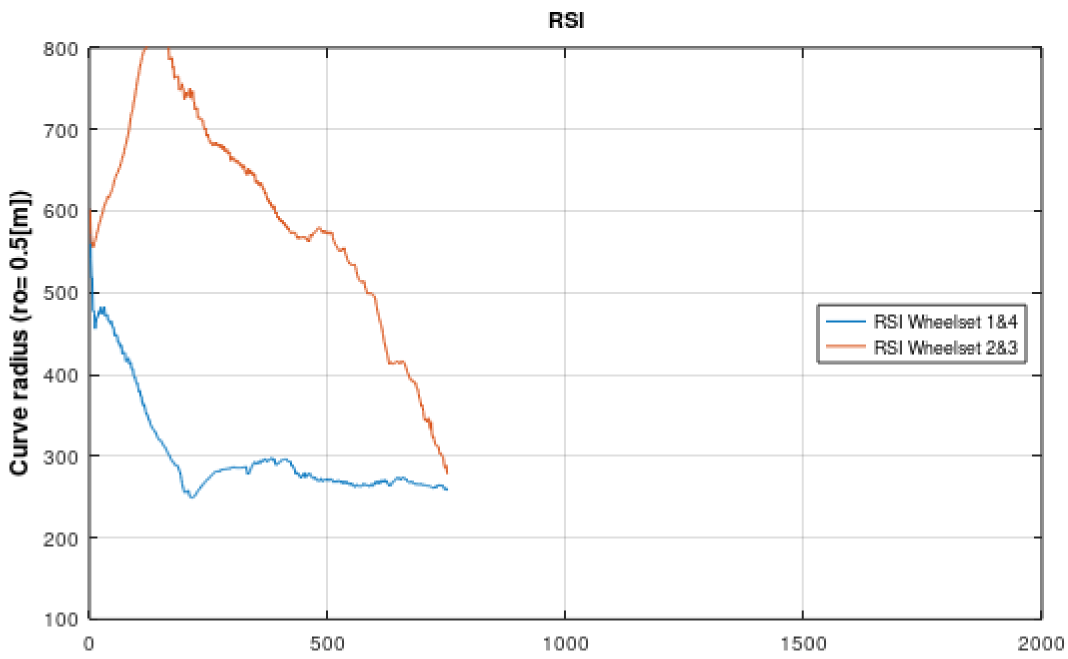

In contrast to the reference case 9.8, the wheelset steering ability doesn't improve so much. The asymptotic value for wheelset steering ability seems to be ~270m.
.

G.7 Development of the risk for RCF

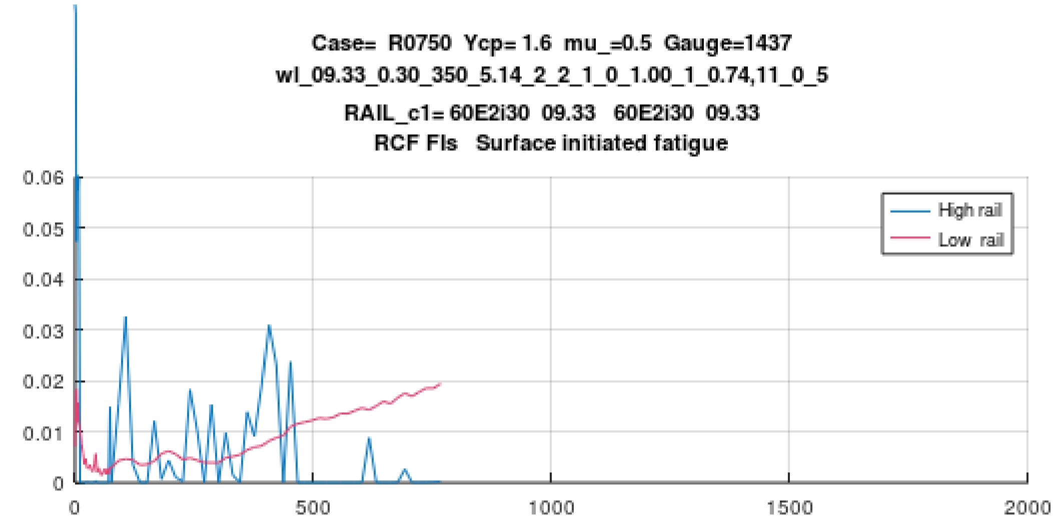

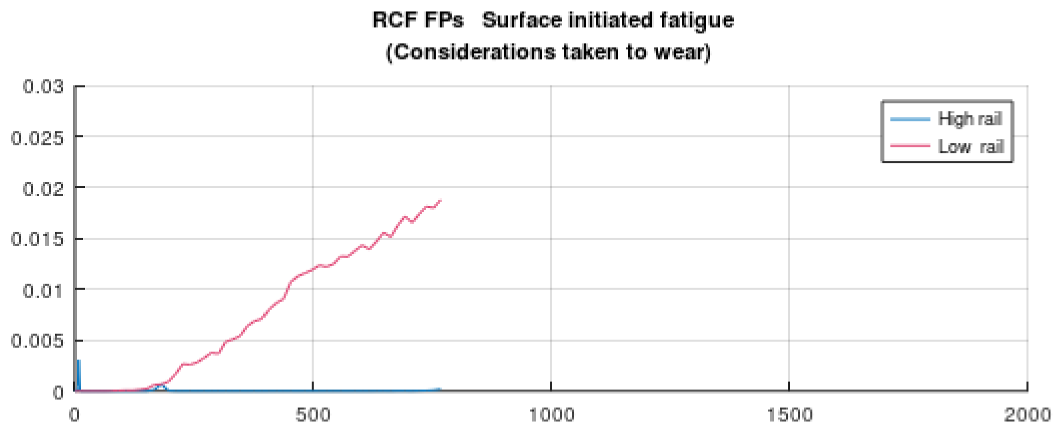

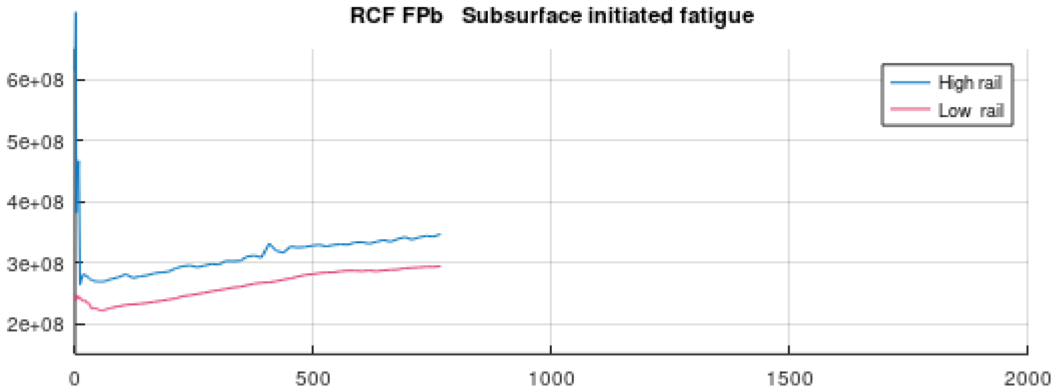

Compared to the reference case 9.9, the risk for RCF behaves quite differently. Because of the high flange wear, there is very little risk for RCF FPs on the high rail. However, on the low rail the risk for RCF FPs just keeps to increase with travelled distance.
The risk for RCF FPb looks good. The value of RCF FPb is lower than the limit value 450e6 at all times.

Appendix H. Initial wheel profile with 0.87 lower GIPw

This case is denoted:

wl_09.33_0.30_360_4.27_2_2_1_0_1.00_1_0.74,11_0_5

All data are the same as the reference case 9, except the initial wheel profile. For a description of the used initial wheel profiles please see section 6.

H.1 Development of conicity wheelset 1&4

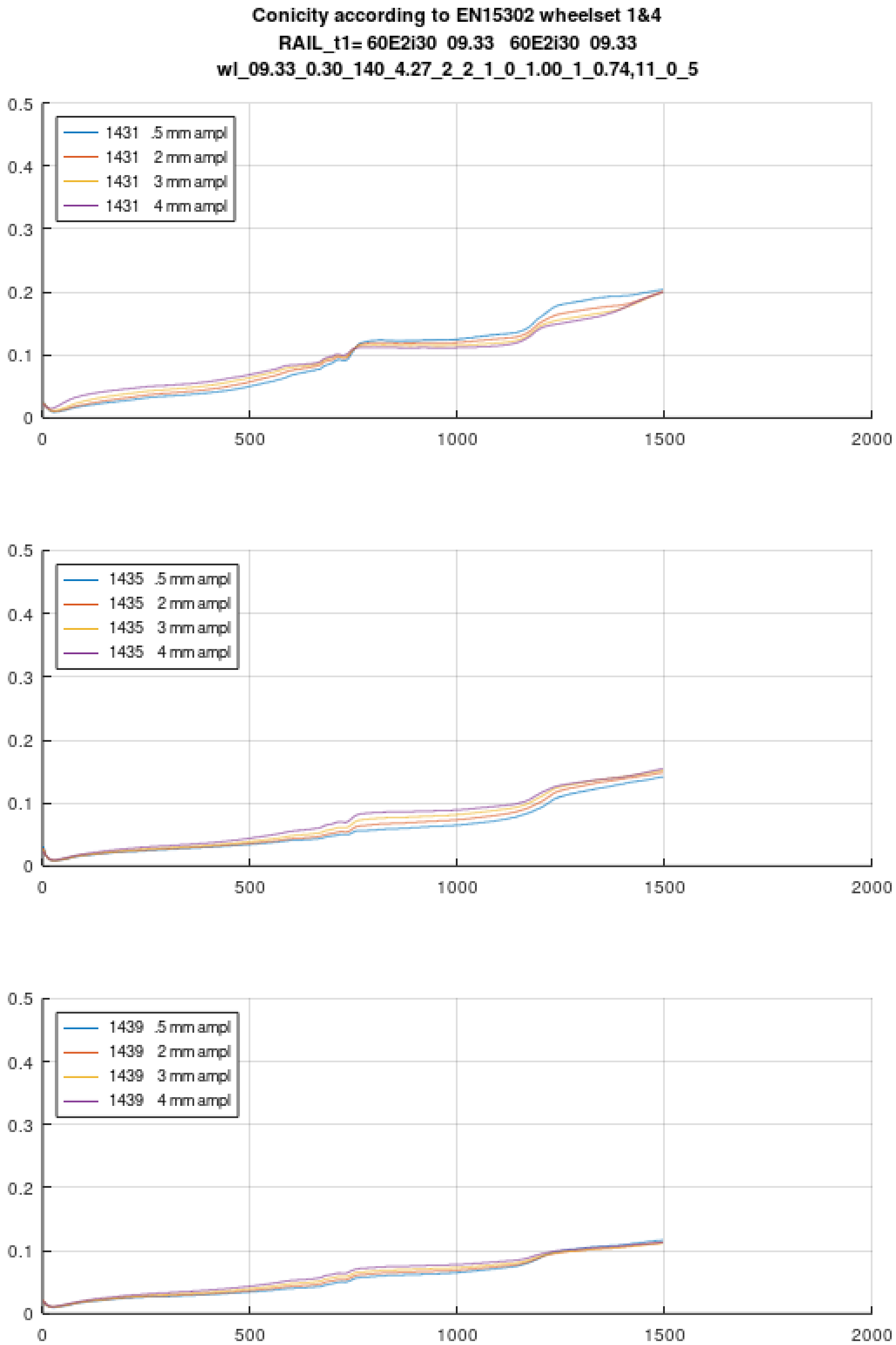

Compared to the reference case 9.1, this profile starts with a lower conicity, so it takes longer time before the conicity gets high. There is a step in the conicity curve at ~1200 wear steps. This step can also be seen in the reference case, but in the reference case this step occurs after ~800 wear steps.

H.2 Development of wheel profile shapes wheelset 1&4

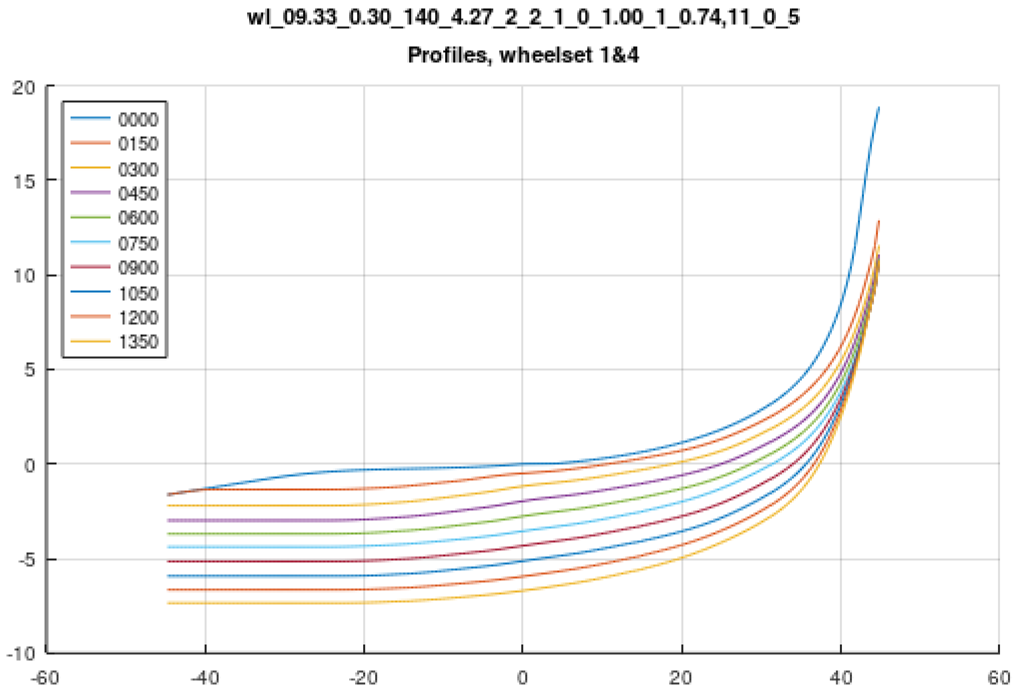

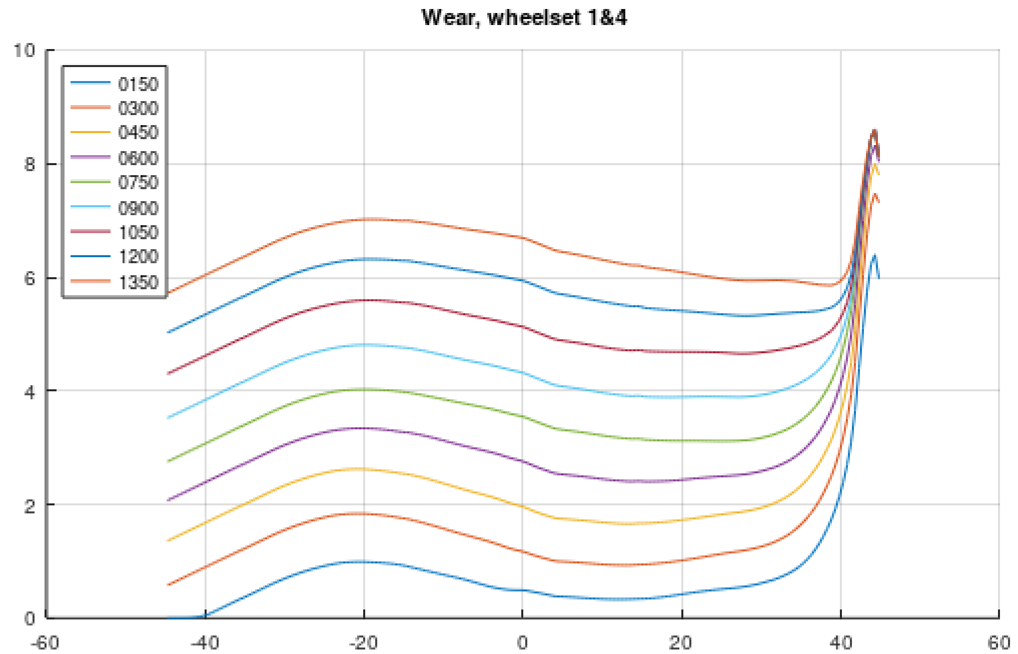

Compared to the reference case 9.3, it can be seen that the flange is thinner already for the initial profile.

H.3 Development of GIPw

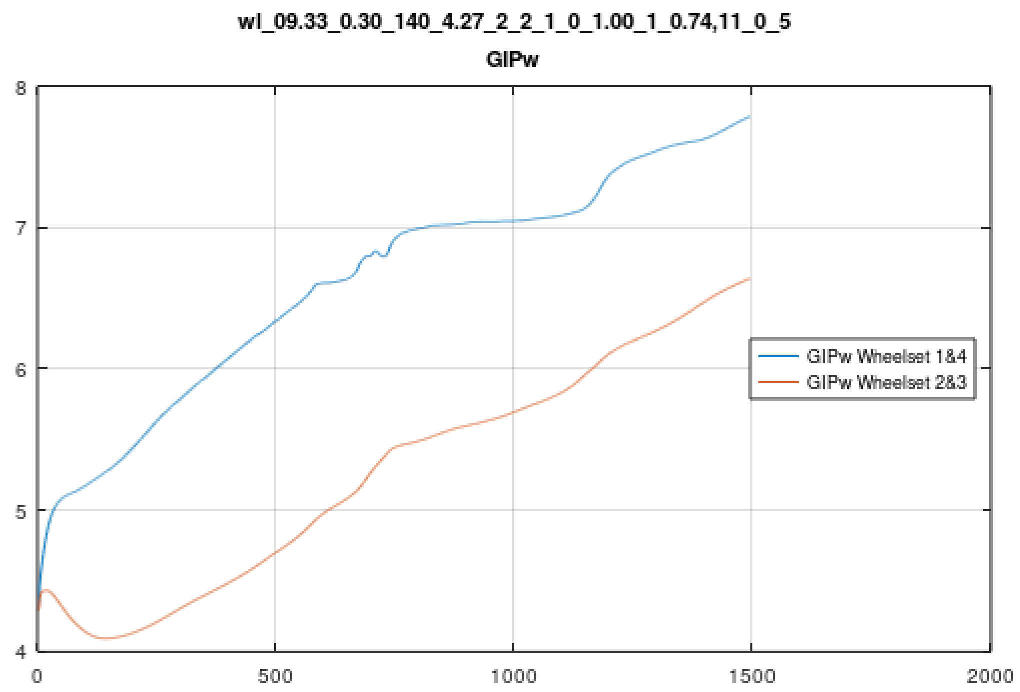

Compared to the reference case 9.5, it can be seen that the initial wheel profile has a lower GIPw value. However, GIPw is increasing with travelled distance in a similar way as in the reference case, it just takes a little longer time until the GIPw values get very high. There is a step in GIPw in wheelset 1&4 at ~1200 wear steps, this step can also be seen in the reference case, but here the step occurs already after ~800 wear steps.

H.4 Development of the Flange Thickness

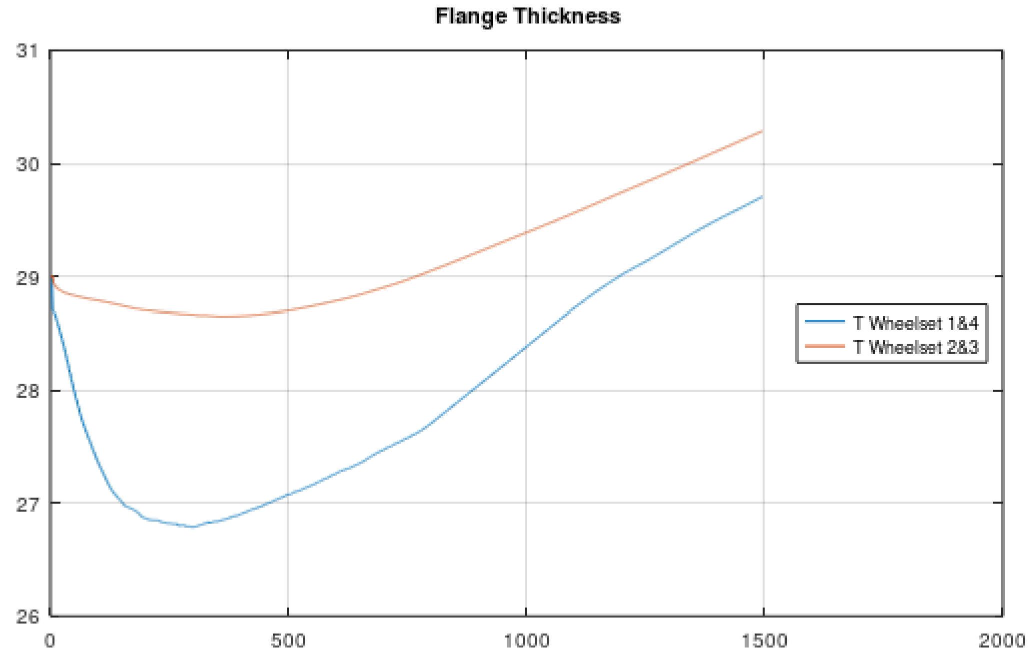

Compared to the reference case 9.6, the flange thickness starts with a lower value 29mm. Also, the minimum point has a lower value 26.8mm compared to the reference case. However, a flange thickness of 26.8mm should be acceptable. If two wheels on the same wheelset wears equally, the sum of the two flange thicknesses becomes 53.6mm, which fulfils the requirement that the sum of the two flange thicknesses should be over 45mm.

H.5 Development of the Flange Flank qR

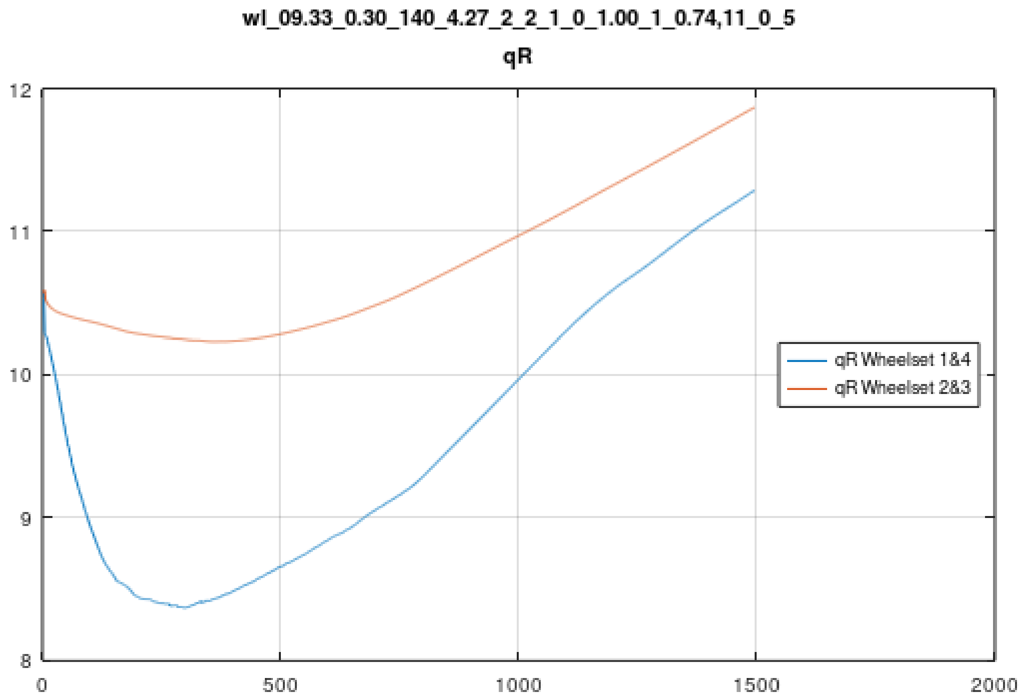

Compared to the reference case 9.7 the qR value goes down and up faster. The results are OK, the value of qR is over 6.5 at all times.

H.6 Development of the Wheelset Steering Ability

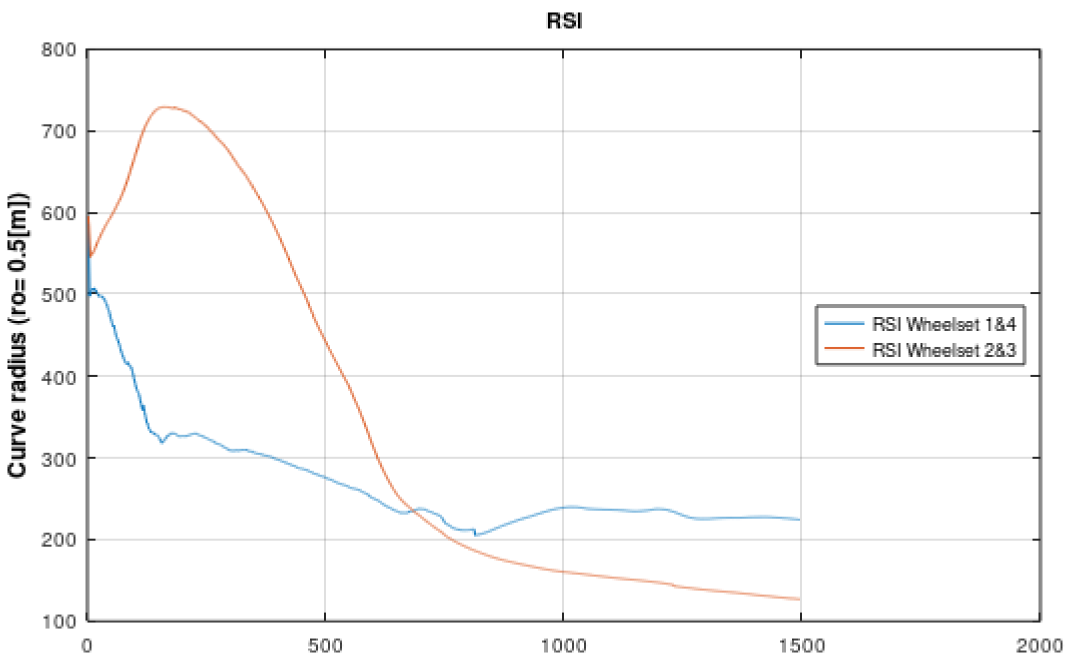

Compared to the reference case 9.8 the wheelsets steering ability don’t improves as fast. The wear prediction loop was stopped after 1500 wear steps, so it is difficult to say if the asymptotic value is the same as in the reference case.

H.7 Development of the risk for RCF

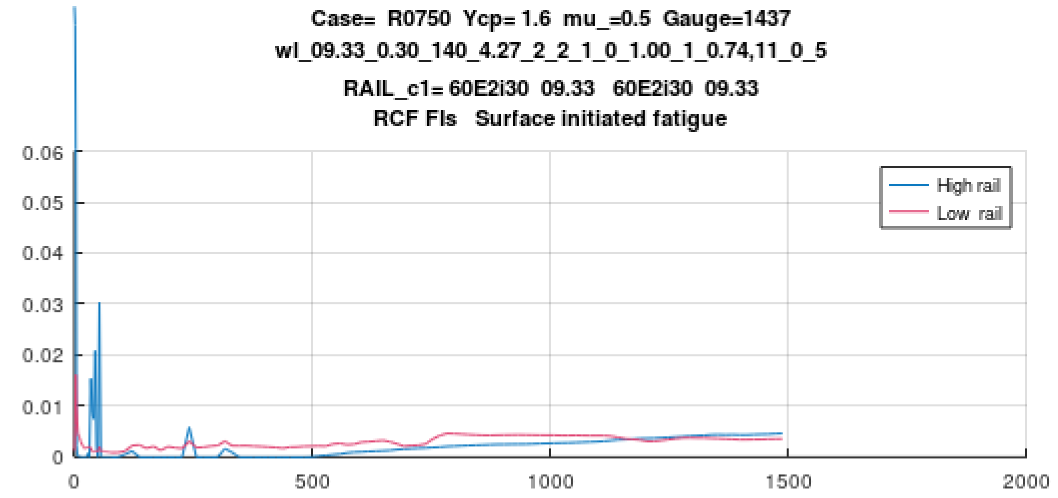

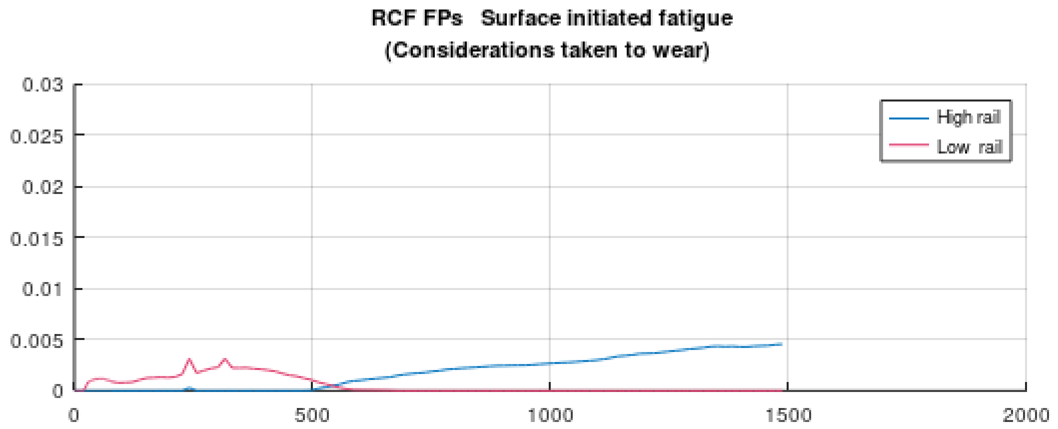

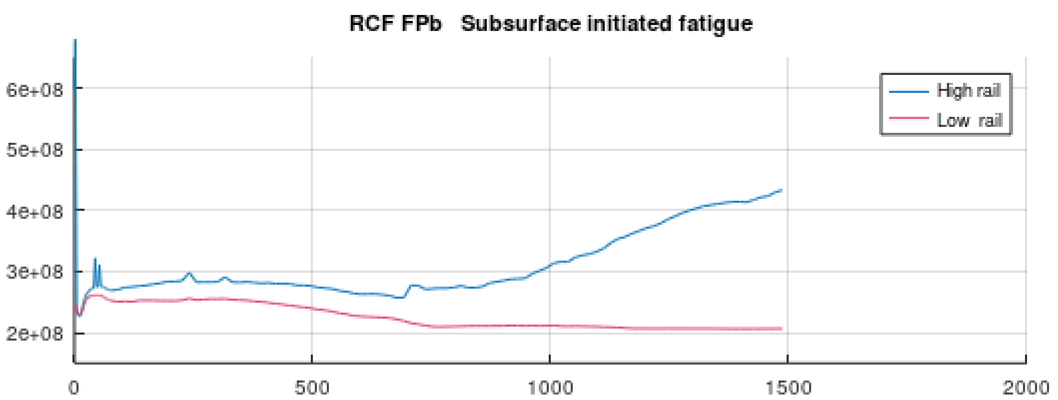

Compared to the reference case 9.9, the risk for RCF FPs looks good. However, in the end of the wear prediction loop RCF FPs starts to increase a little.

RCF FPb is below the limit value 450e6, but the increasing trend in the end doesn't look good.

Appendix I. Initial wheel profile with 0.30 lower GIPw

This case is denoted:

wl_09.33_0.30_360_4.84_2_2_1_0_1.00_1_0.74,11_0_5

All data are the same as the reference case 9, except the initial wheel profile. For a description of the used initial wheel profiles please see section 6.

I.1 Development of conicity wheelset 1&4

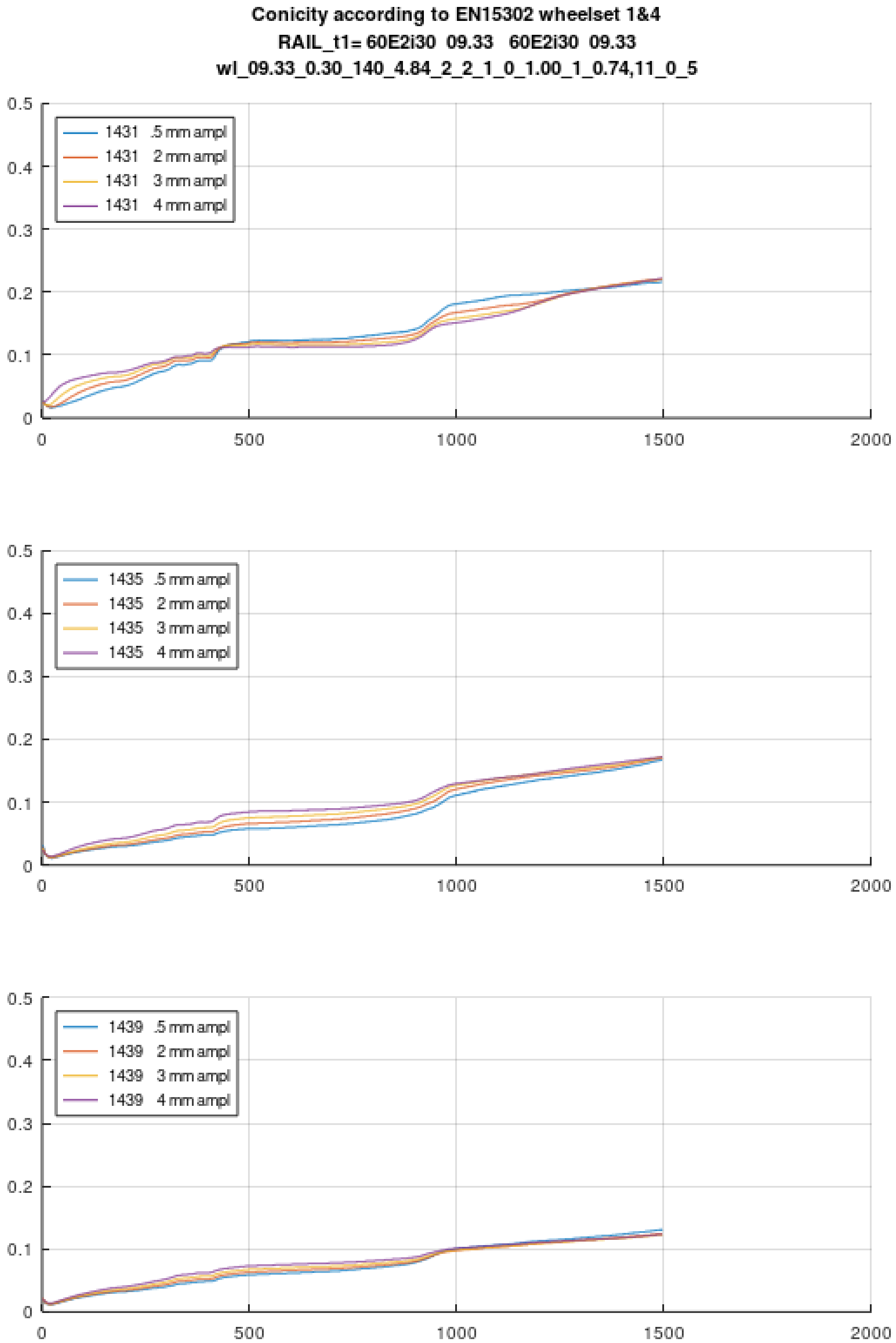

Compared to the reference case 9.1, this profile starts with a lower conicity, so it takes a little longer time before the conicity gets high. There is a step in the conicity curve at ~950 wear steps. This step can also be seen in the reference case, but in the reference case this step occurs after ~800 wear steps.

I.2 Development of wheel profile shapes wheelset 1&4

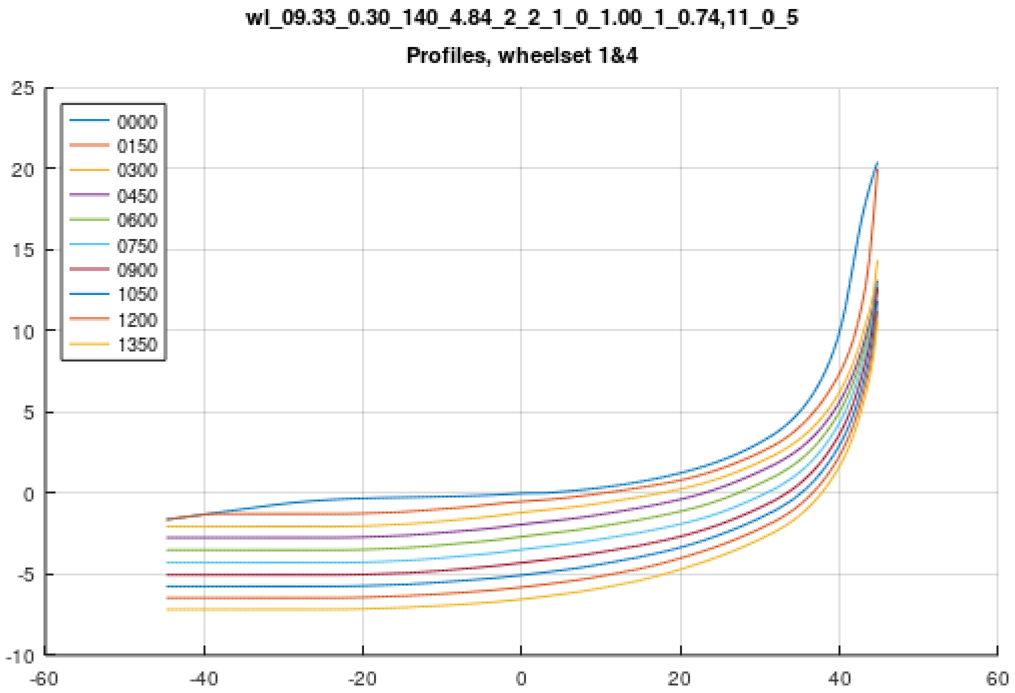

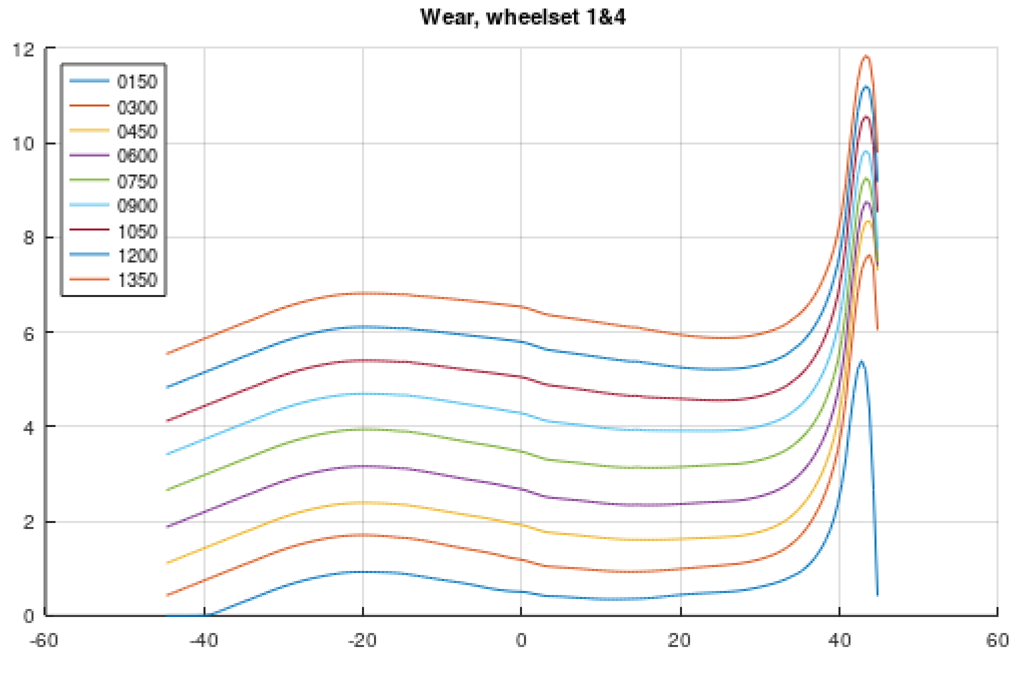

The worn wheel profiles are very similar to the reference case 9.3, it is difficult to see the differences with the eyes only.

I.3 Development of GIPw

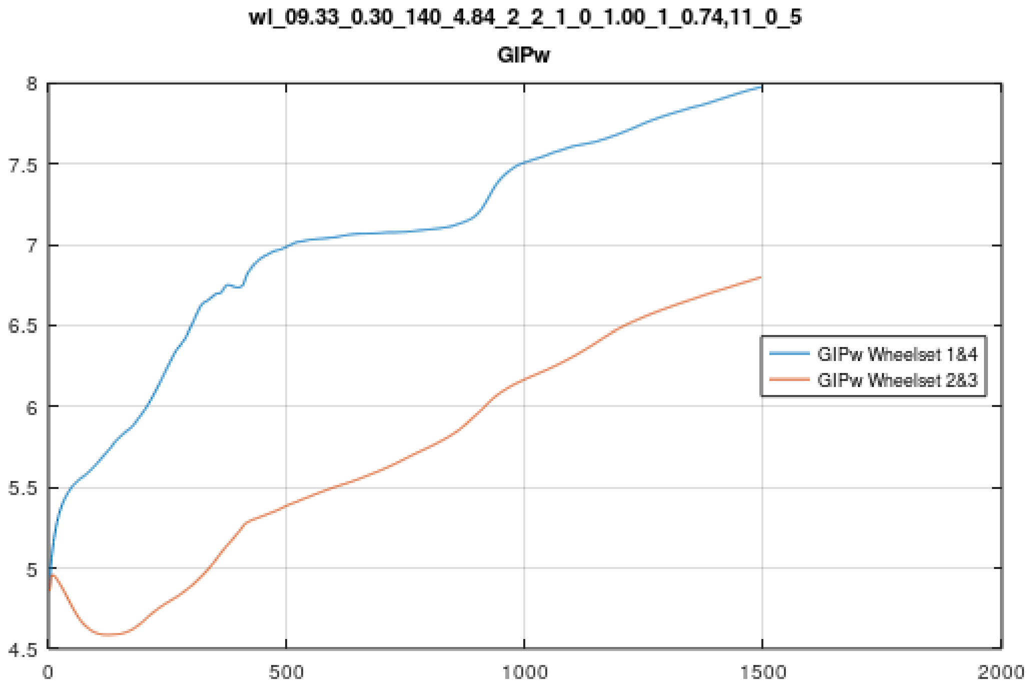

Compared to the reference case 9.5, it can be seen that the initial wheel profile has a lower GIPw value. However, GIPw is increasing with travelled distance in a similar way as in the reference case, it just takes a little longer time until the GIPw values get very high. There is a step in GIPw in wheelset 1&4 at ~950 wear steps, this step can also be seen in the reference case, but here the step occurs already after ~800 wear steps.

I.4 Development of the Flange Thickness

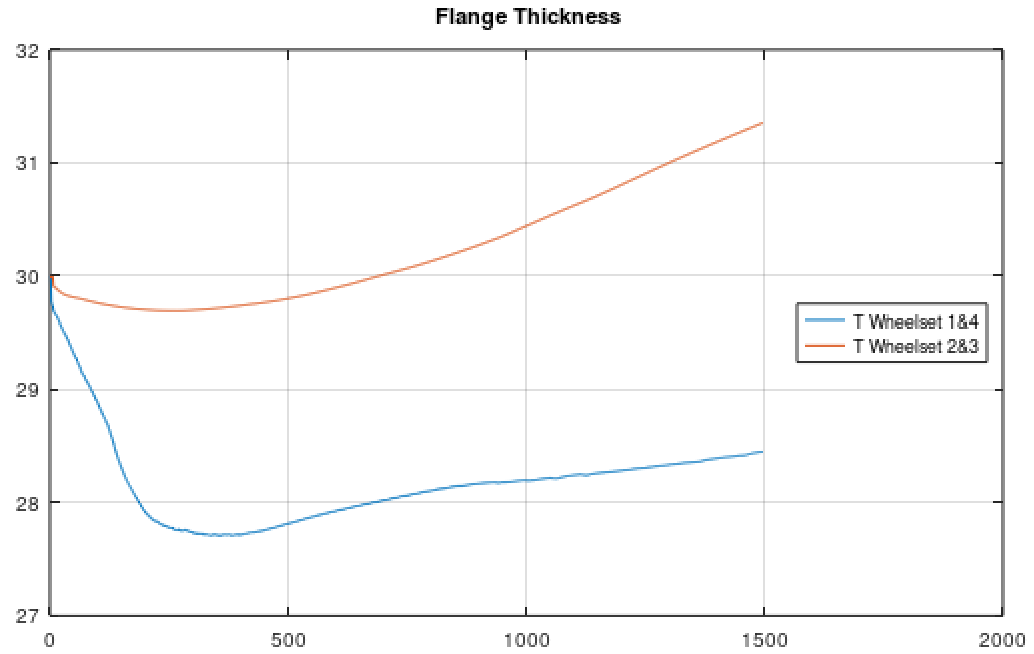

Compared to the reference case 9.6, the flange thickness starts with a lower value 30mm. Also, the minimum point has a little bit lower value 27.7mm compared to the reference case.

I.5 Development of the Flange Flank qR

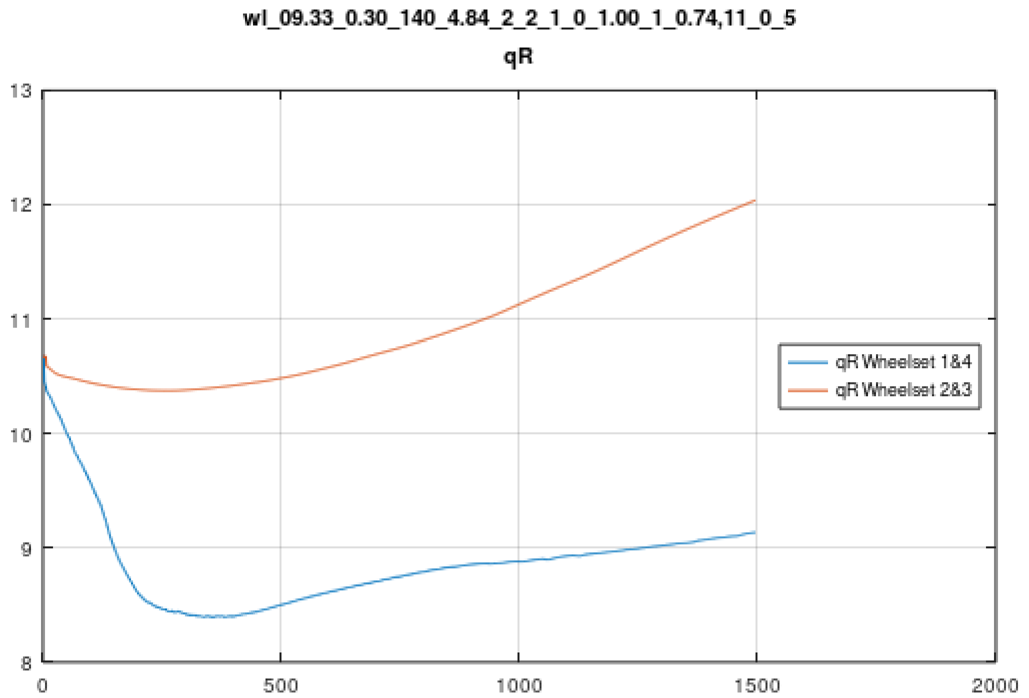

Compared to the reference case 9.7 the qR value goes down and up a little bit faster. The results are OK, the value of qR is over 6.5 at all times.

I.6 Development of the Wheelset Steering Ability

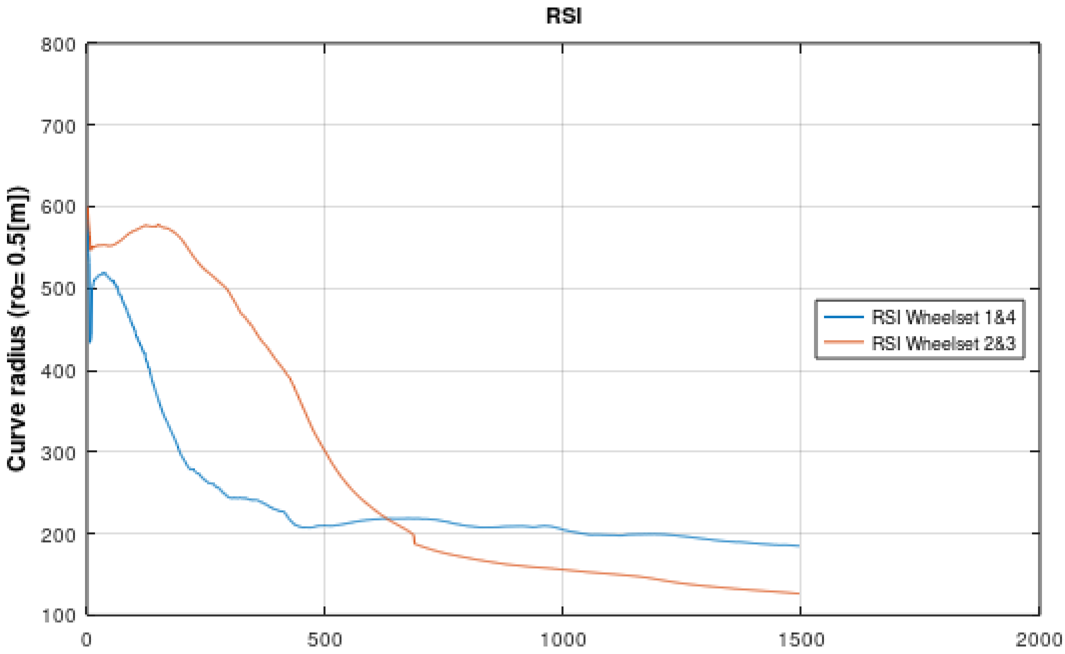

The behaviour of the wheelset steering ability is very similar to the reference case 9.8.

I.7 Development of the risk for RCF

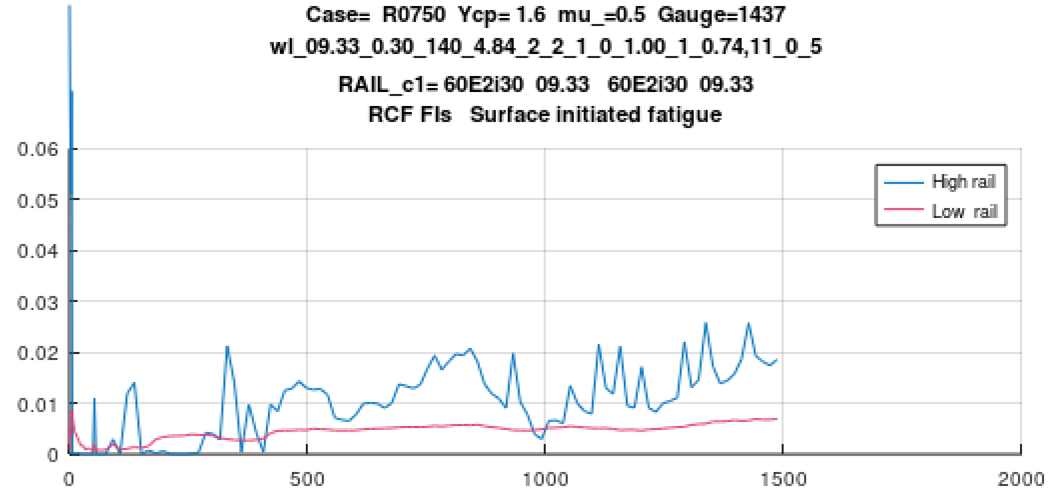

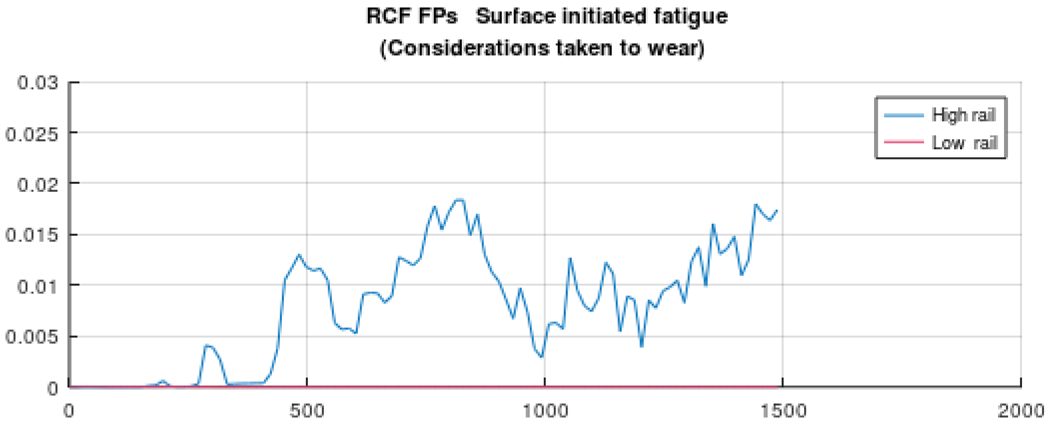

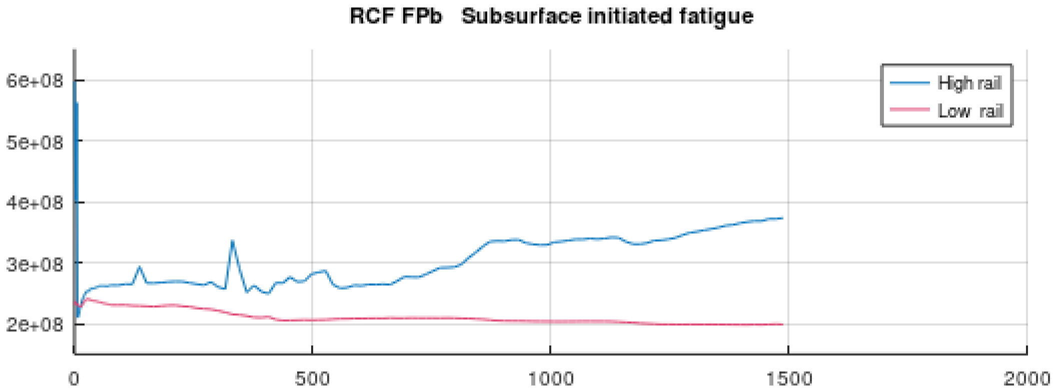

The behaviour of the RCF FPs and RCF FPb is similar to the reference case 9.9. The risk for RCF is quite low when the wheels are newly turned, but increases with travelled distance.

Appendix J. Initial wheel profile with 0.39 higher GIPw

This case is denoted:

wl_09.33_0.30_360_5.53_2_2_1_0_1.00_1_0.74,11_0_5

All data are the same as the reference case 9, except the initial wheel profile. For a description of the used initial wheel profiles please see section 6.

J.1 Development of conicity wheelset 1&4

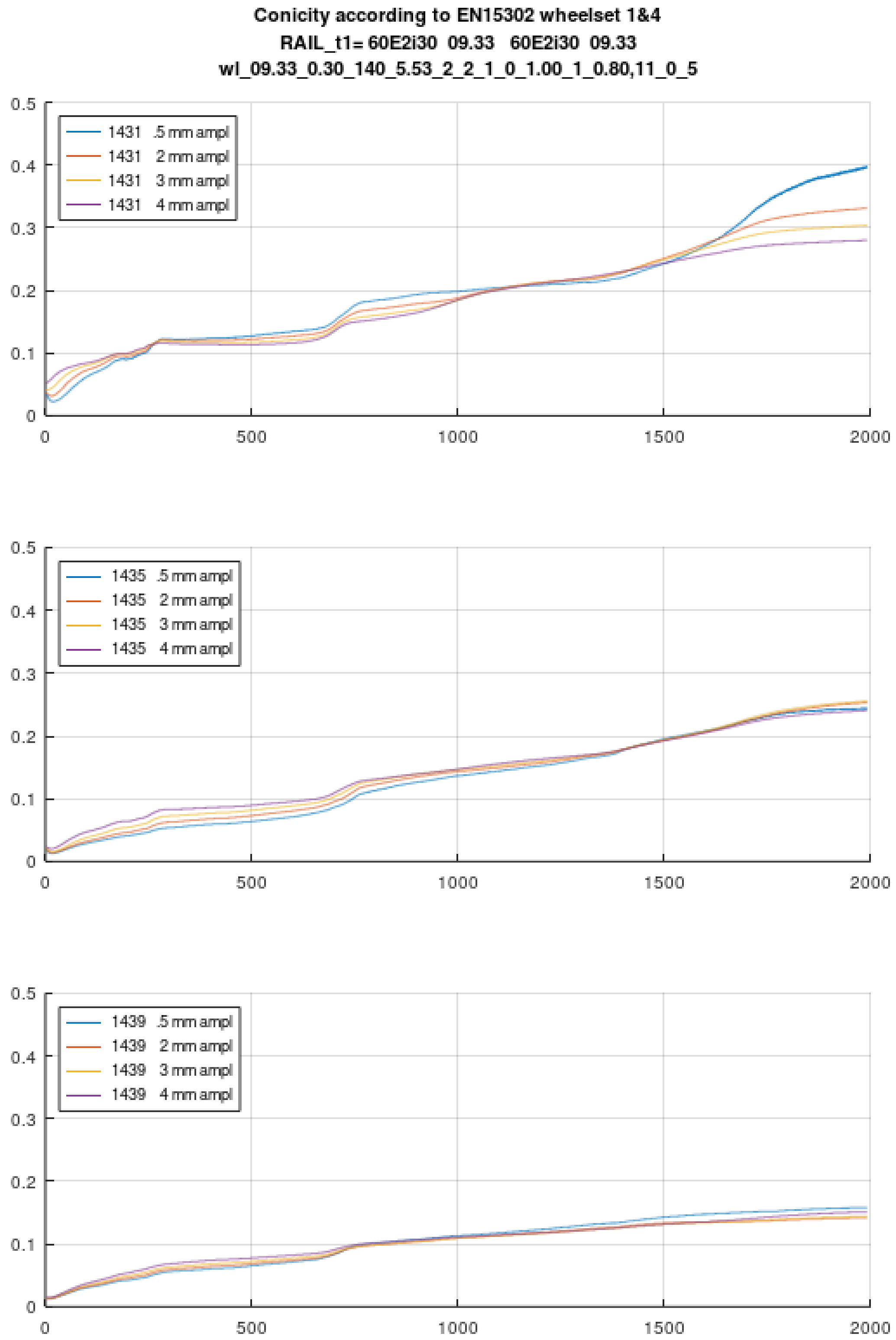

Compared to the reference case 9.1, this profile starts with a somewhat little higher conicity, so it starts a little bit up on the conicity curve. The step in the conicity curve comes here after ~740 wear steps. In the reference case this step come after ~800 wear steps.

J.2 Development of wheel profile shapes wheelset 1&4

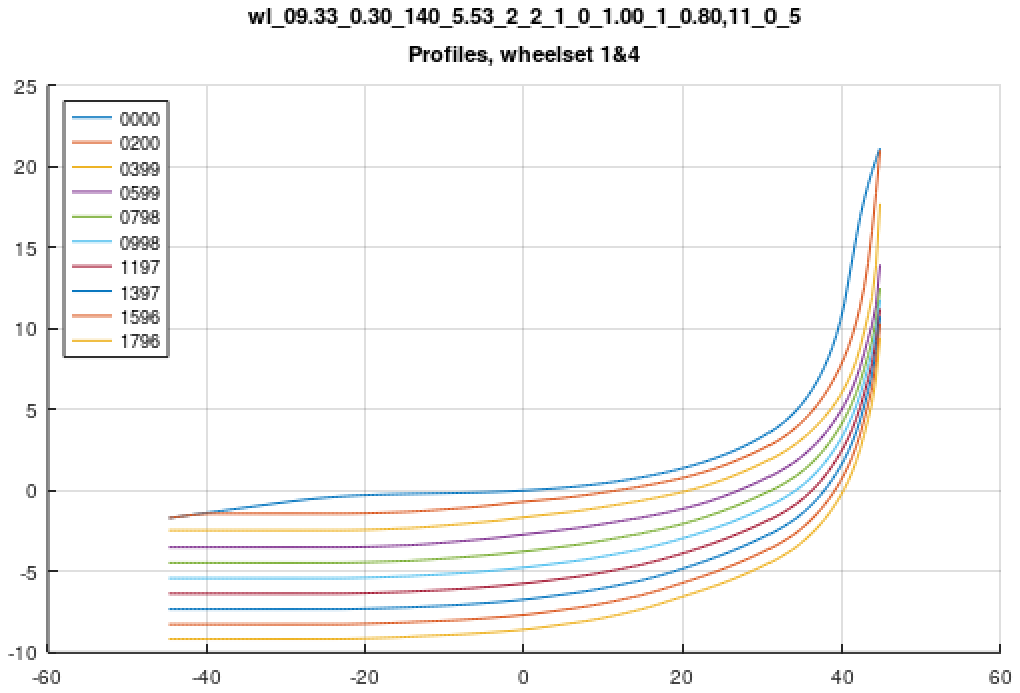

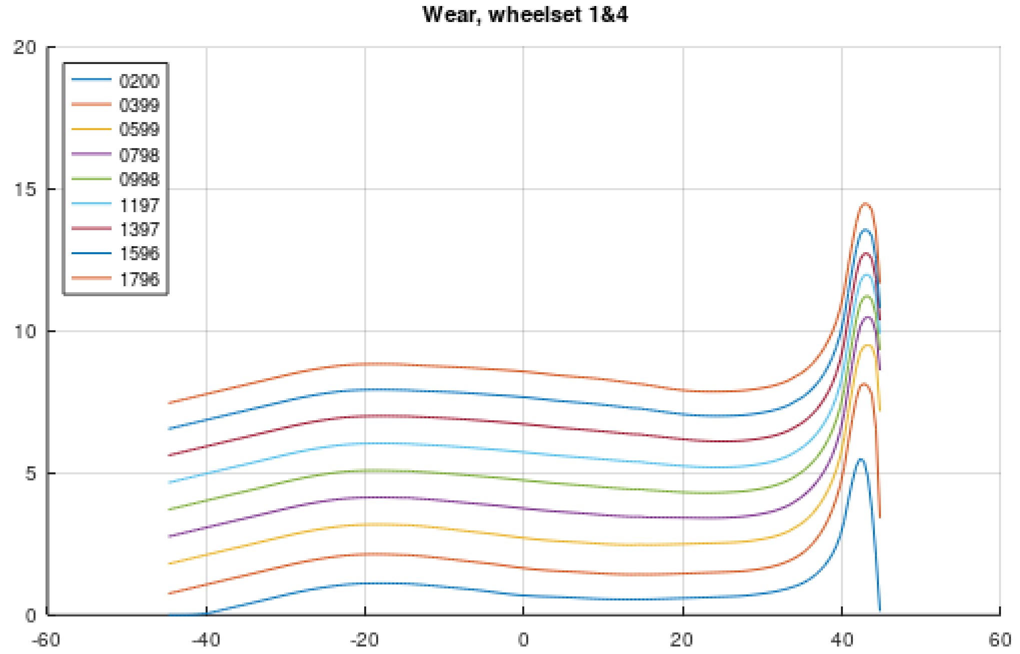

The worn wheel profiles are very similar to the reference case 9.3, it is difficult to see the differences with the bare eye.

J.3 Development of GIPw

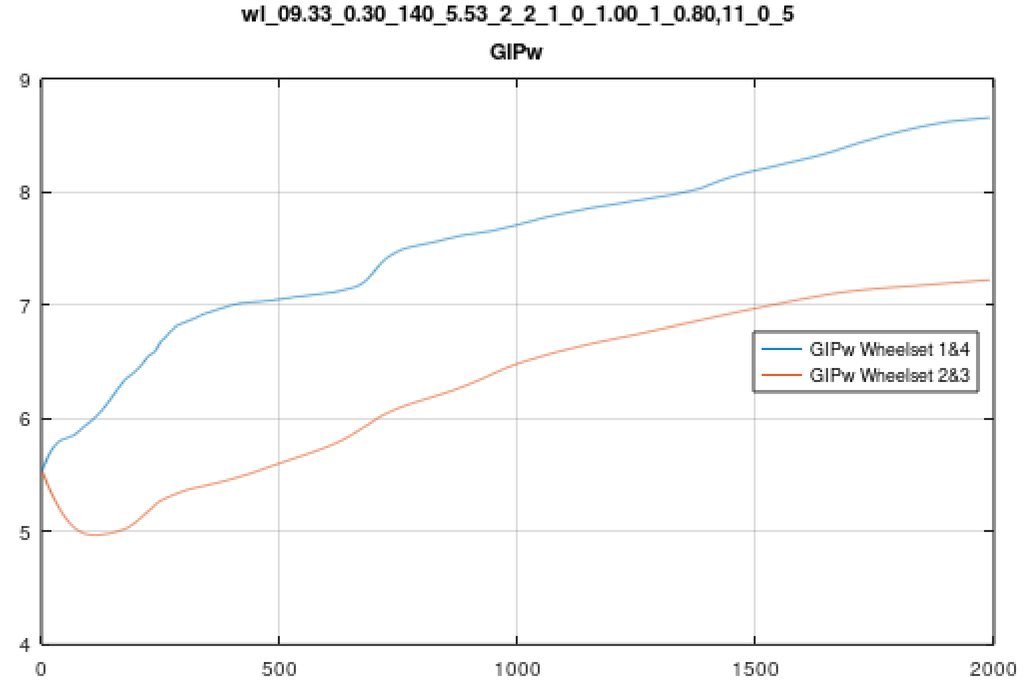

Compared to the reference case 9.5, it can be seen that the initial wheel profile has a higher GIPw value. However, GIPw is increasing with travelled distance in a similar way as in the reference case. There is a step in GIPw in wheelset 1&4 at ~740 wear steps, this step can also be seen in the reference case, but here the step occurs after ~800 wear steps.

J.4 Development of the Flange Thickness

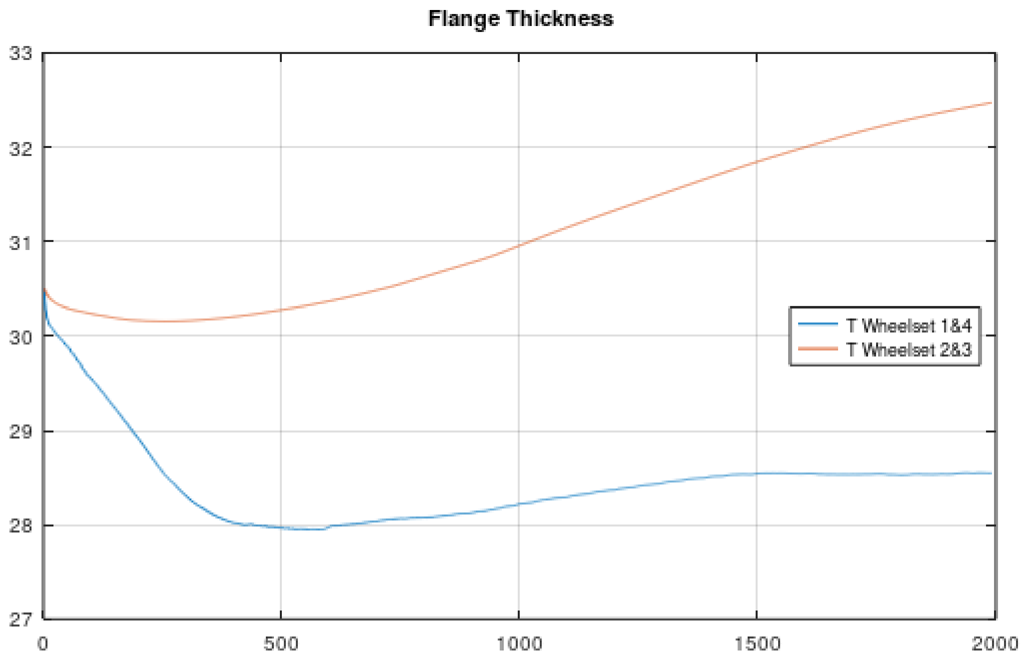

Compared to the reference case 9.6, the flange thickness starts with a little lower value 30mm, but otherwise the flange thickness is very similar to the reference case.

J.5 Development of the Flange Flank qR

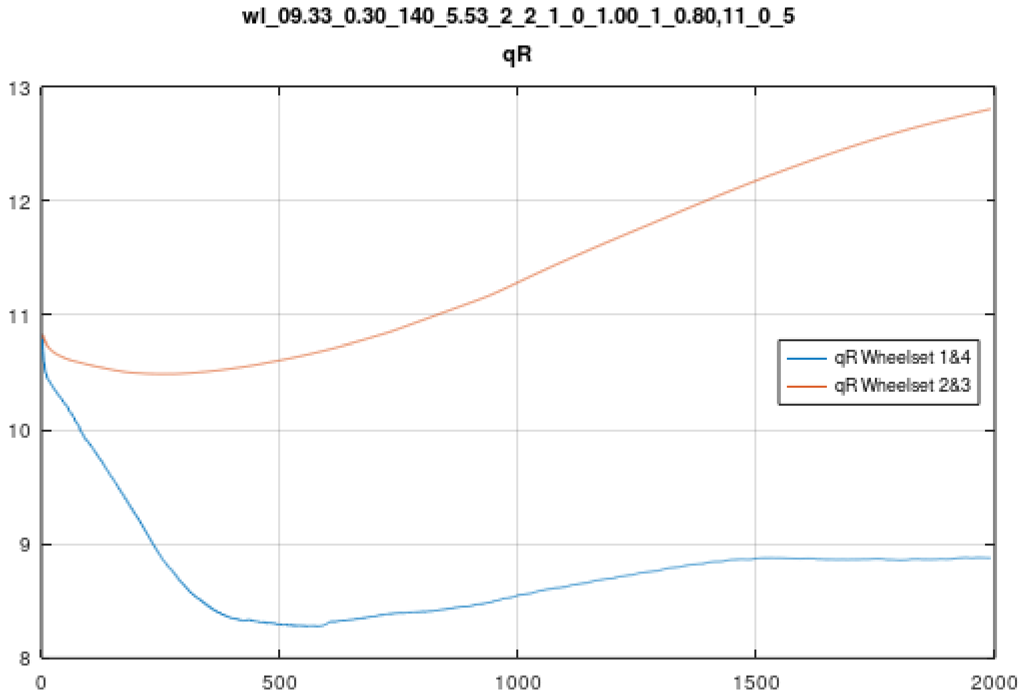

Compared to the reference case 9.7 the flange flank qR is very similar to the reference case.

J.6 Development of the Wheelset Steering Ability

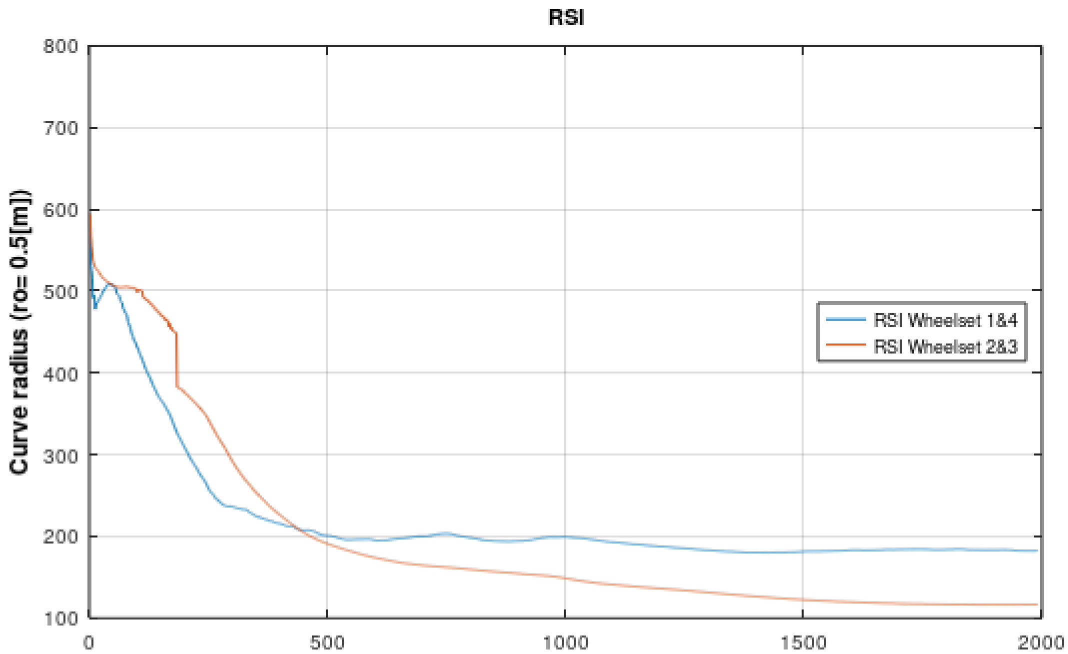

The behaviour of the wheelset steering ability is very similar to the reference case 9.8.

J.7 Development of the risk for RCF

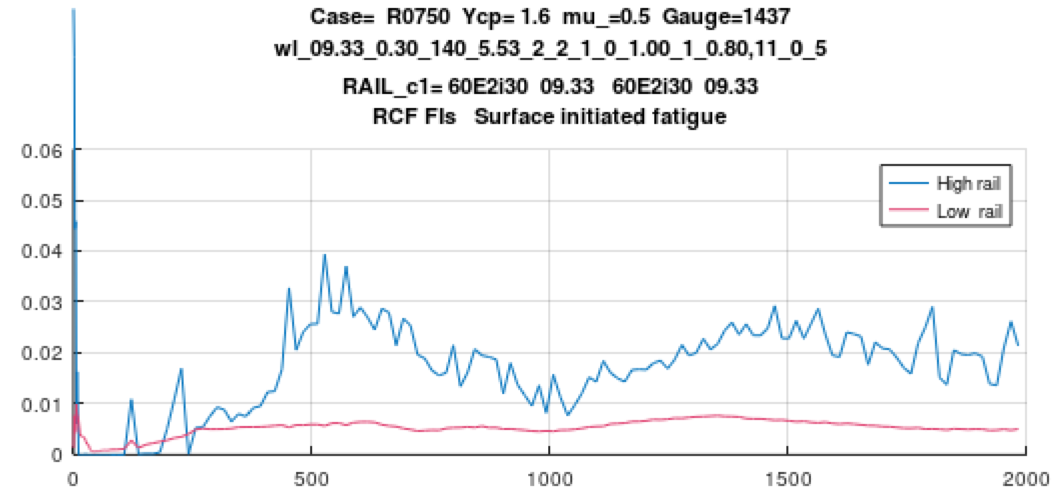

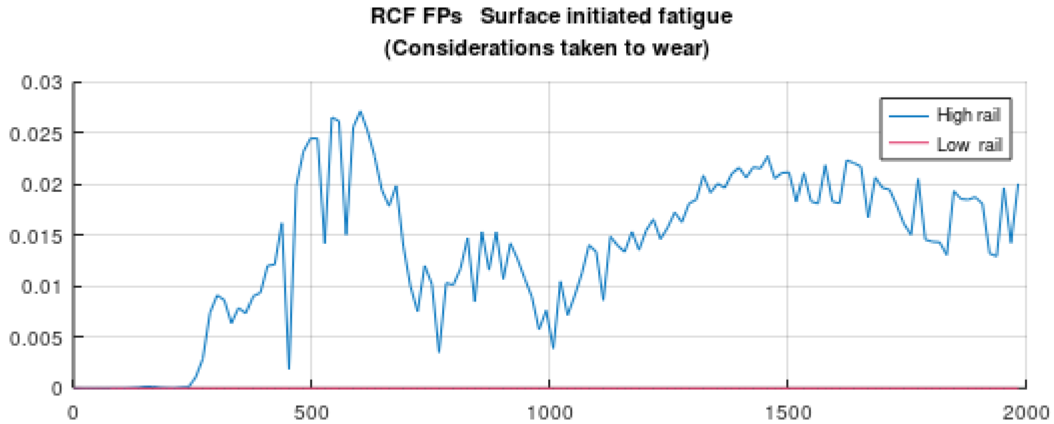

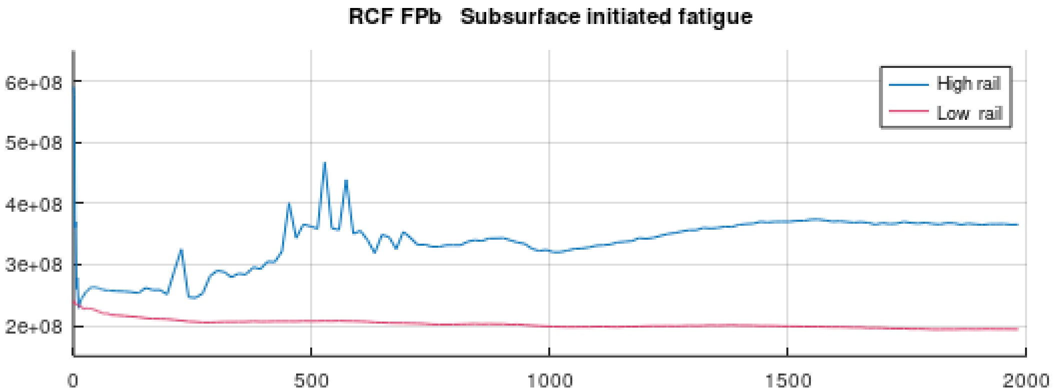

Regarding the risk for RCF, this wheel profile is very similar to the reference case 9.9.

Appendix K. Initial wheel profile with 0.52 higher GIPw

This case is denoted:

wl_09.33_0.30_360_5.66_2_2_1_0_1.00_1_0.74,11_0_5

All data are the same as the reference case 9, except the initial wheel profile. In this case the initial wheel profile is a mix of the two profiles ENS1002t30 and EPSt30, 75% of the profile comes from ENS1002t30 and 25% comes from EPSt30. The shape of the flanges is the same for both ENS1002t30 and EPSt30, so the mixed profile will also have the same flange, it is only the tread that will differ a little. See selection of initial wheel profiles 6.

K.1 Development of conicity wheelset 1&4

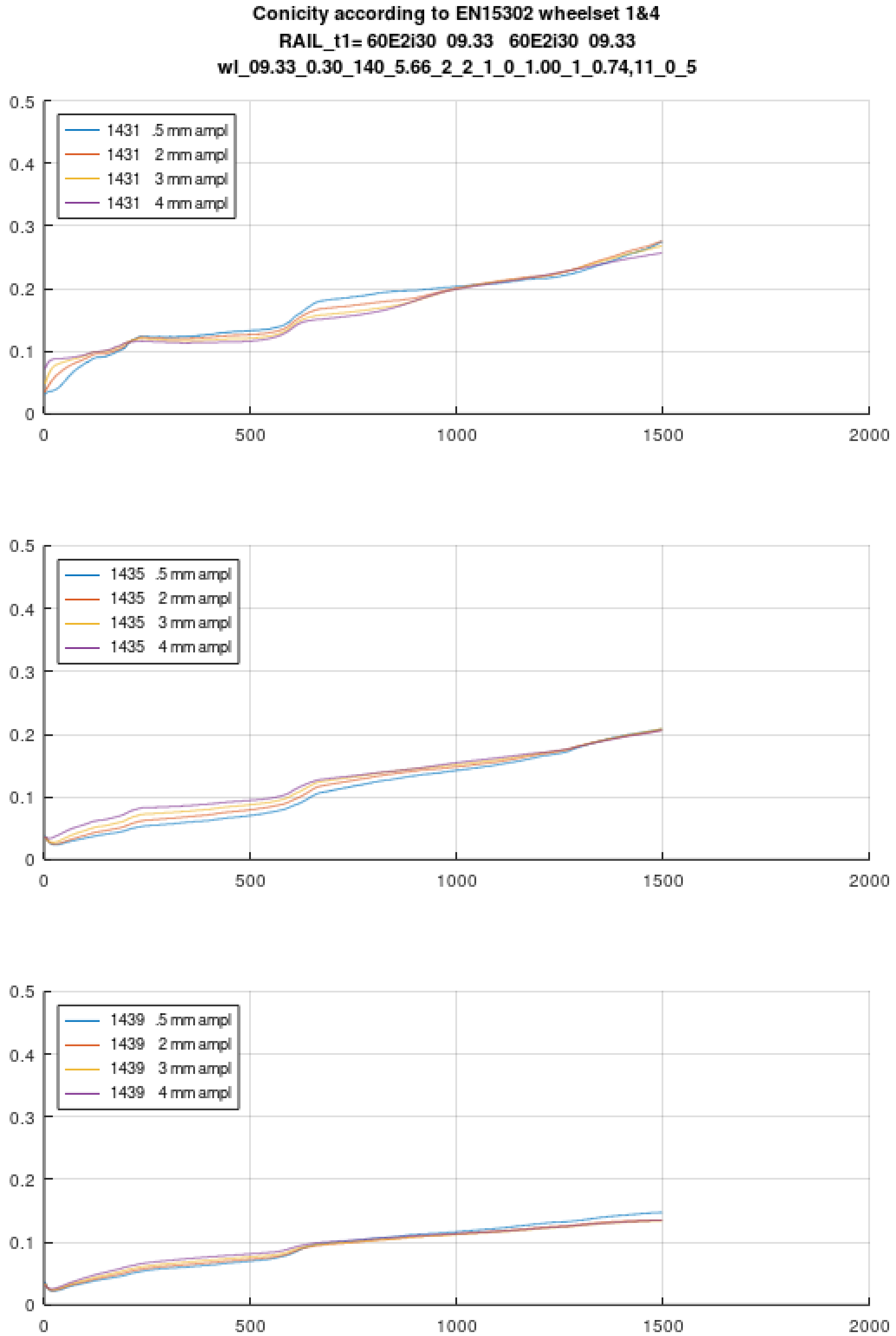

Compared to the reference case 9.1, this profile starts with a little higher conicity, so it starts a little bit up on the conicity curve. The step in the conicity curve comes here after ~650 wear steps. In the reference case this step come after ~800 wear steps.

K.2 Development of wheel profile shapes wheelset 1&4

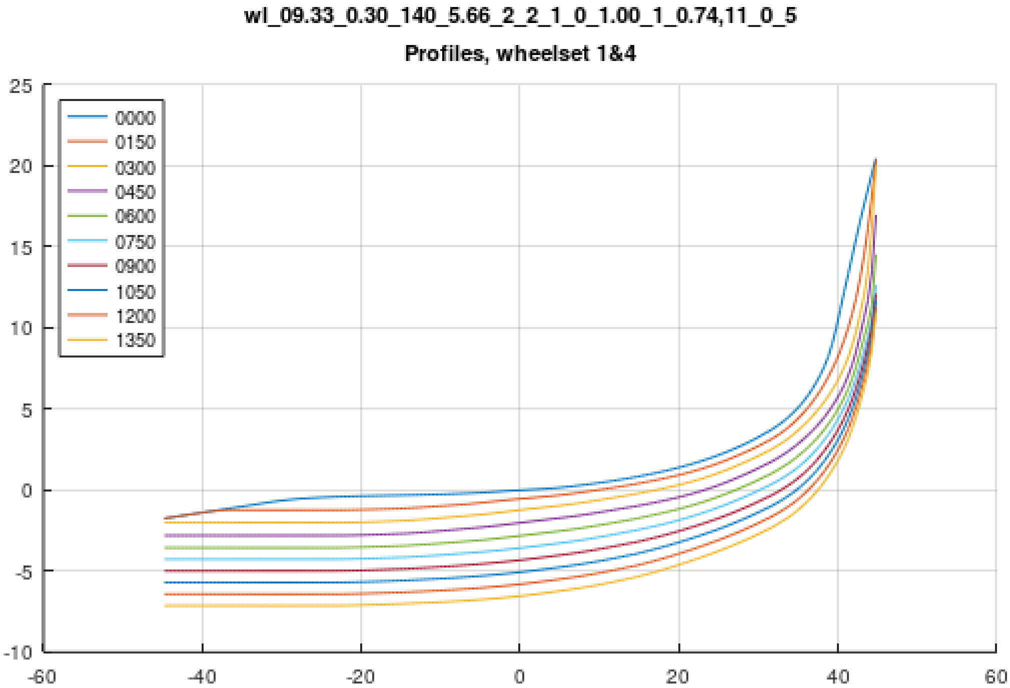

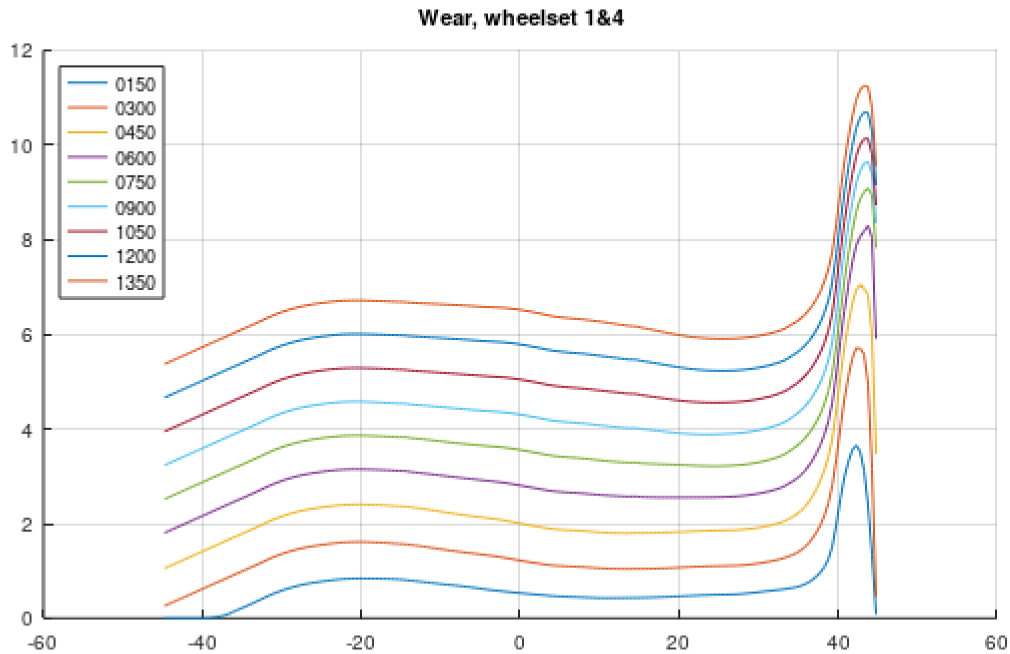

The worn wheel profiles are very similar to the reference case 9.3, it is difficult to see the differences with the bare eye.

K.3 Development of GIPw

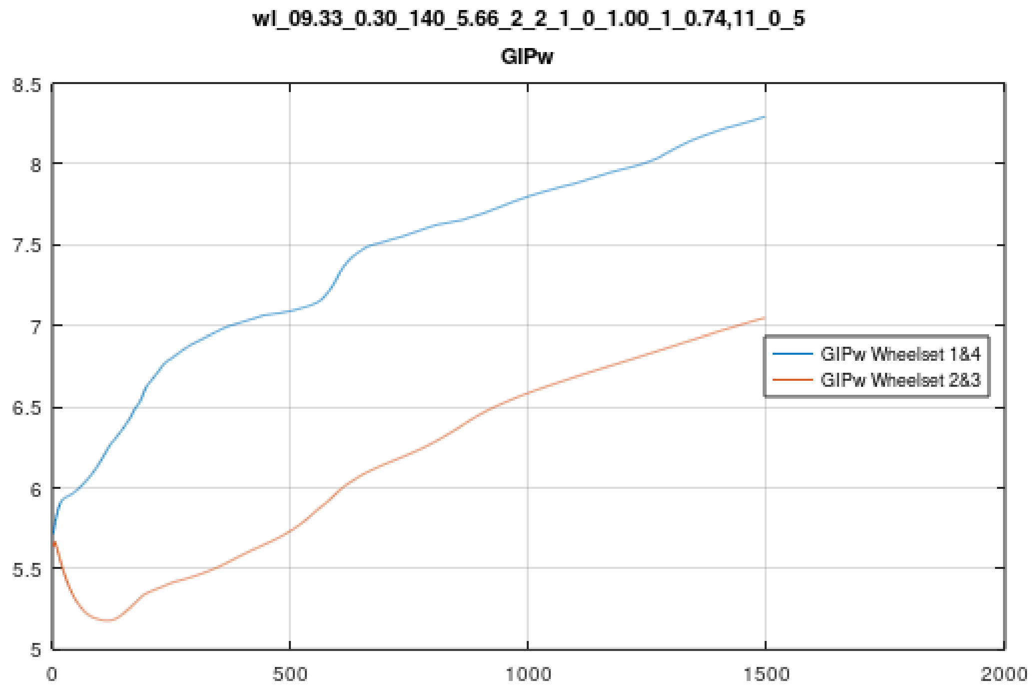

Compared to the reference case 9.5, it can be seen that the initial wheel profile has a higher GIPw value. However, GIPw is increasing with travelled distance in a similar way as in the reference case. There is a step in GIPw in wheelset 1&4 at ~650 wear steps, this step can also be seen in the reference case, but here the step occurs after ~800 wear steps.

K.4 Development of the Flange Thickness

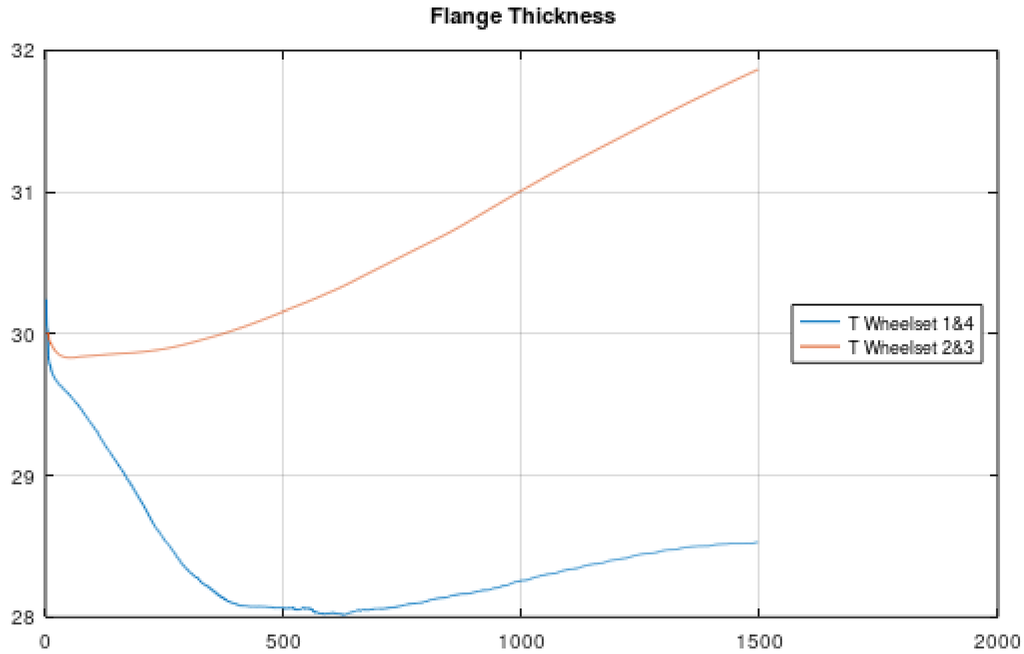

Compared to the reference case 9.6, the flange thickness is a little thinner in the beginning, but in the end, they are quite similar.

K.5 Development of the Flange Flank qR

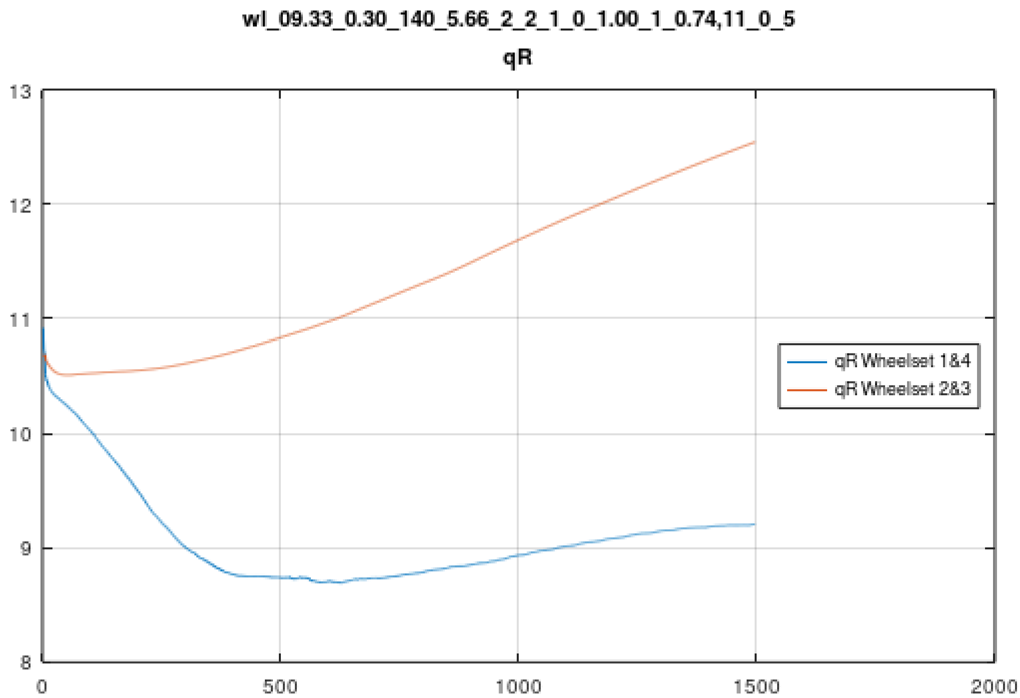

Compared to the reference case 9.7 the flange flank qR is practically equal in the beginning, but in the end qR increases more than the reference case.

K.6 Development of the Wheelset Steering Ability

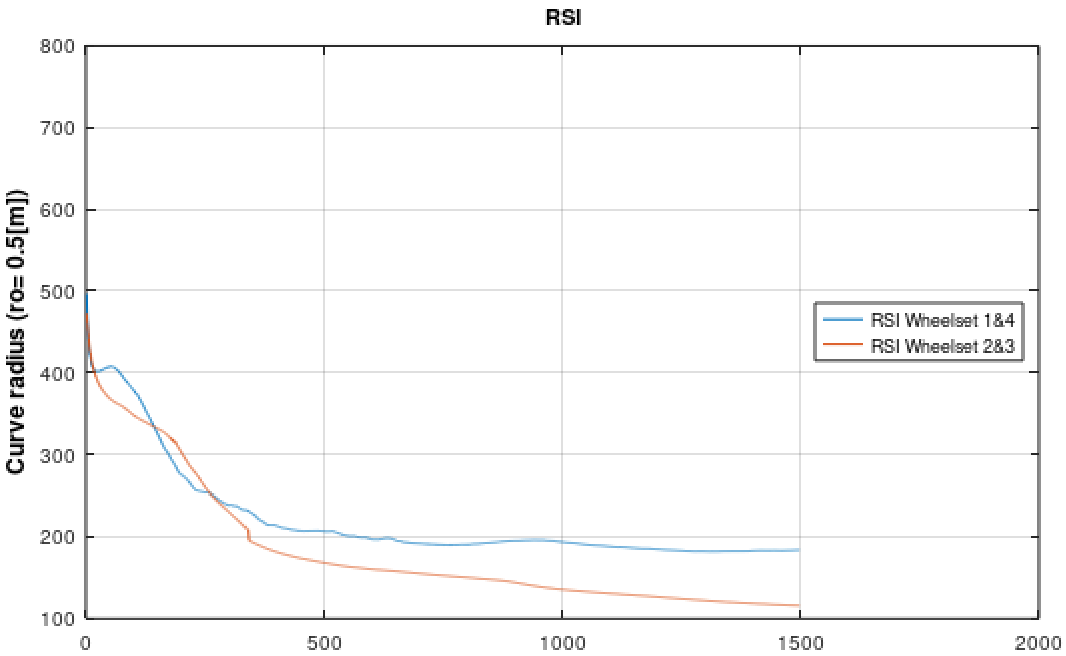

The wheelset steering ability improves faster than the reference case 9.8.

K.7 Development of the risk for RCF

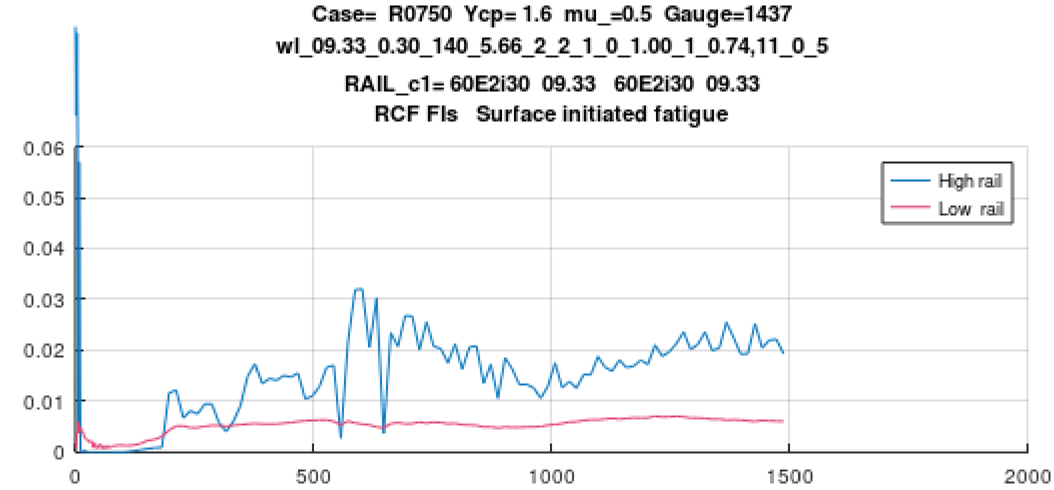

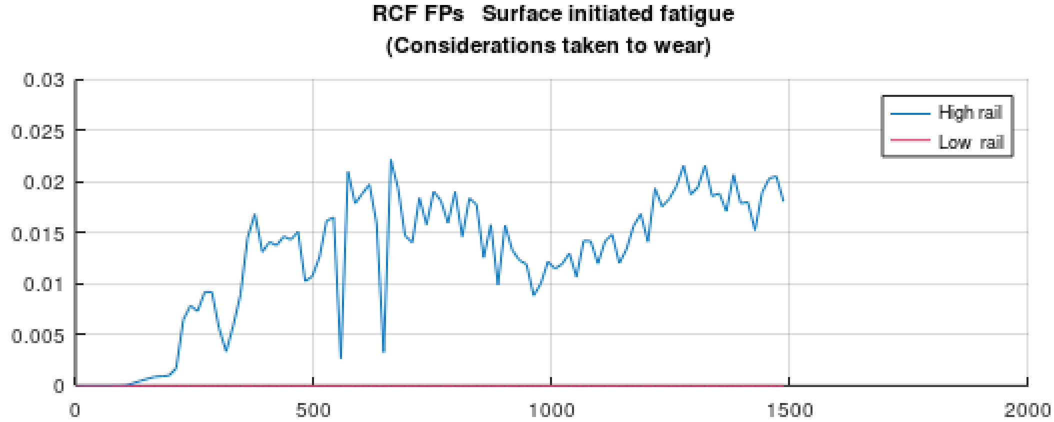

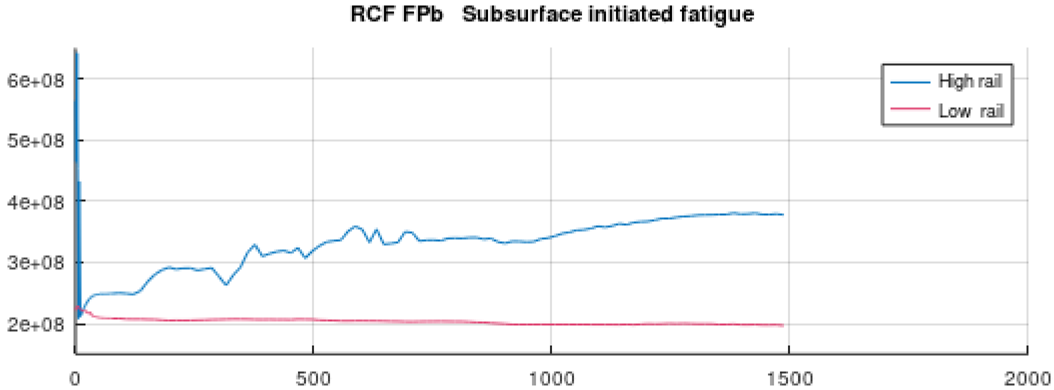

Regarding the risk for RCF, this wheel profile is very similar to the reference case 9.9.

Appendix L. Initial wheel profile with 1.72 higher GIPw

This case is denoted:

wl_09.33_0.30_360_6.86_2_2_1_0_1.00_1_0.74,11_0_5

All data are the same as the reference case 9, except the initial wheel profile. In this case the initial wheel profile is ENXt30.3. See selection of initial wheel profiles 6.

L.1 Development of conicity wheelset 1&4

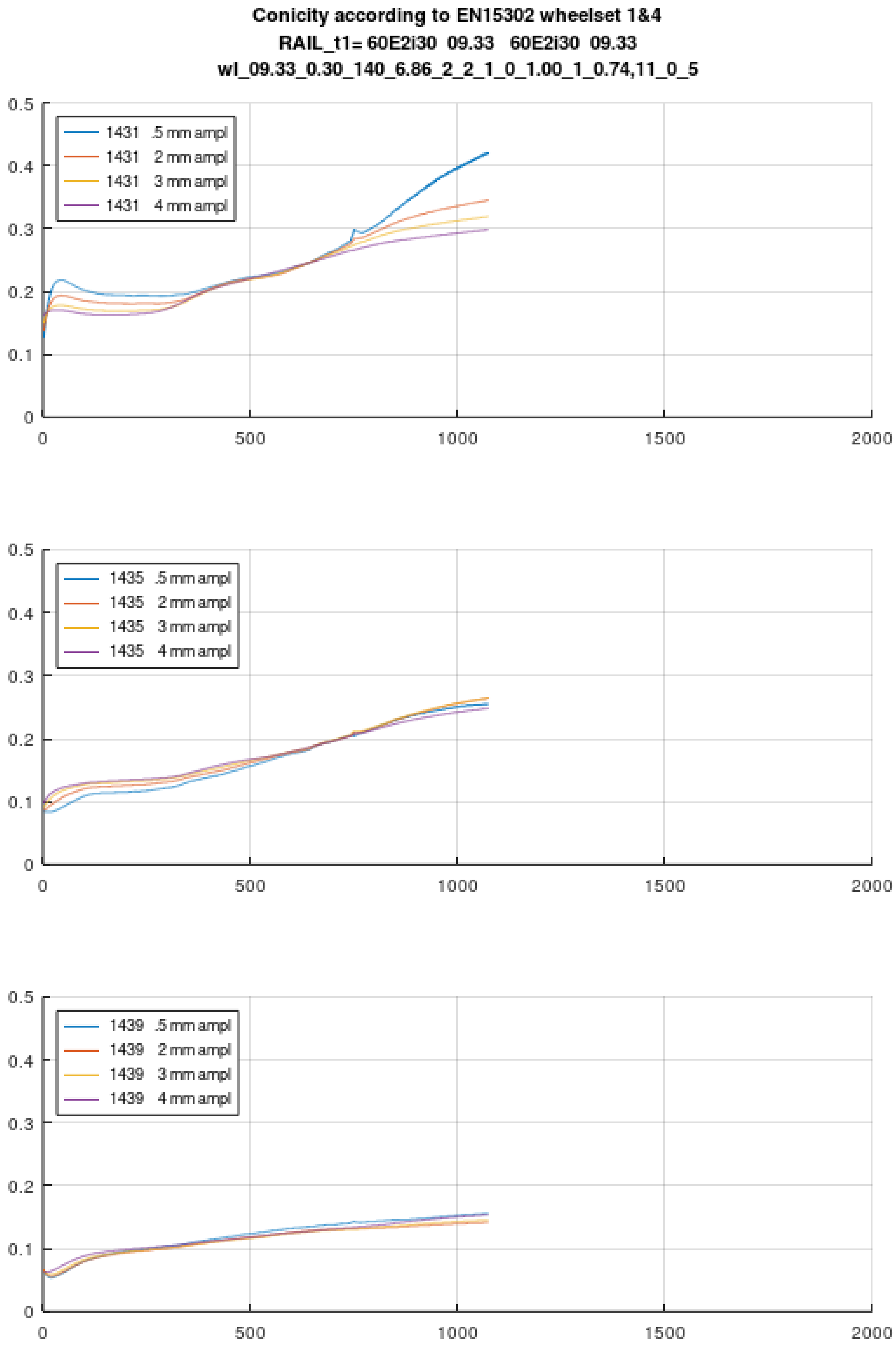

When this diagram is compared with the reference case it can be seen that the conicity here starts at a higher level, and it increases faster than the reference case 9.1. I.e. the profile is starter higher up on the conicity curve. The wear prediction loop was interrupted when the conicity become higher than 0.4.

Our understanding is that a higher conicity gives better steering and more concentrated wear. If the initial wheel profile initially gives a higher conicity the growth rate of the conicity will be higher compared to the reference case. Until the vehicle starts to be unstable. When the vehicle starts to be unstable the wheelsets will move more violate in the track, which will spread out the wear and reduces the increase of the conicity.

L.2 Development of wheel profile shapes wheelset 1&4

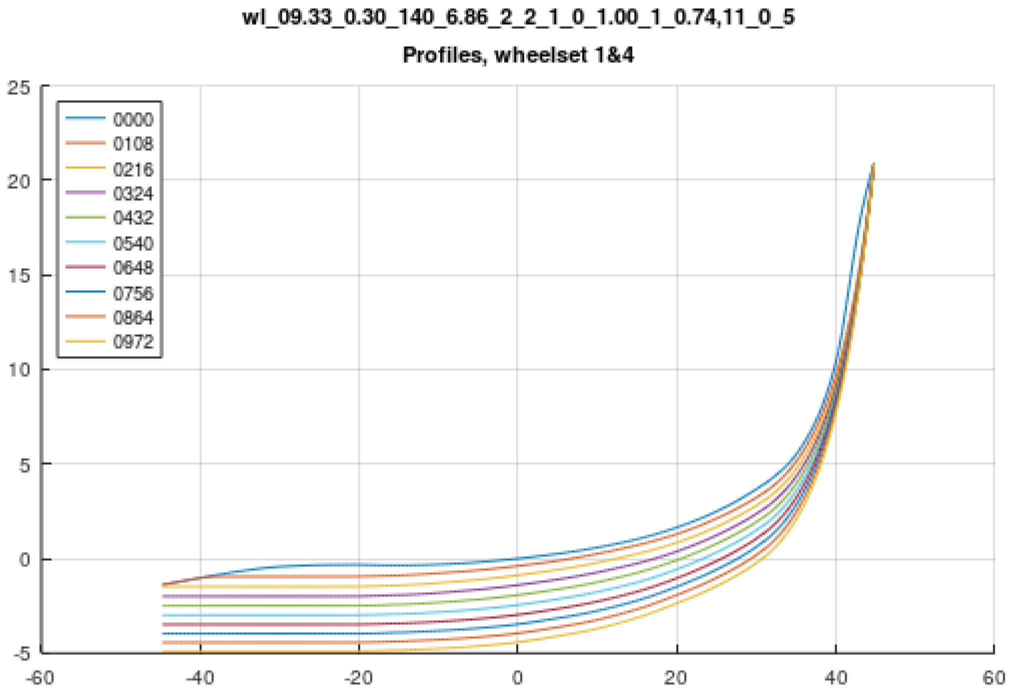

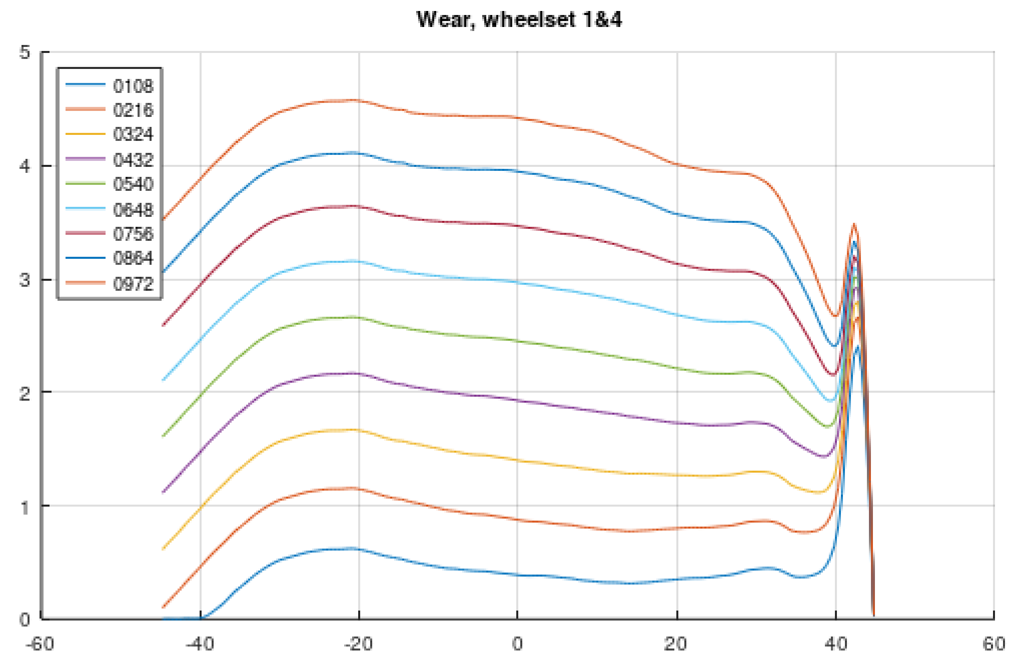

Compared to the reference case 9.3, this wheel steers very well. There is very little flange wear.

L.3 Development of GIPw

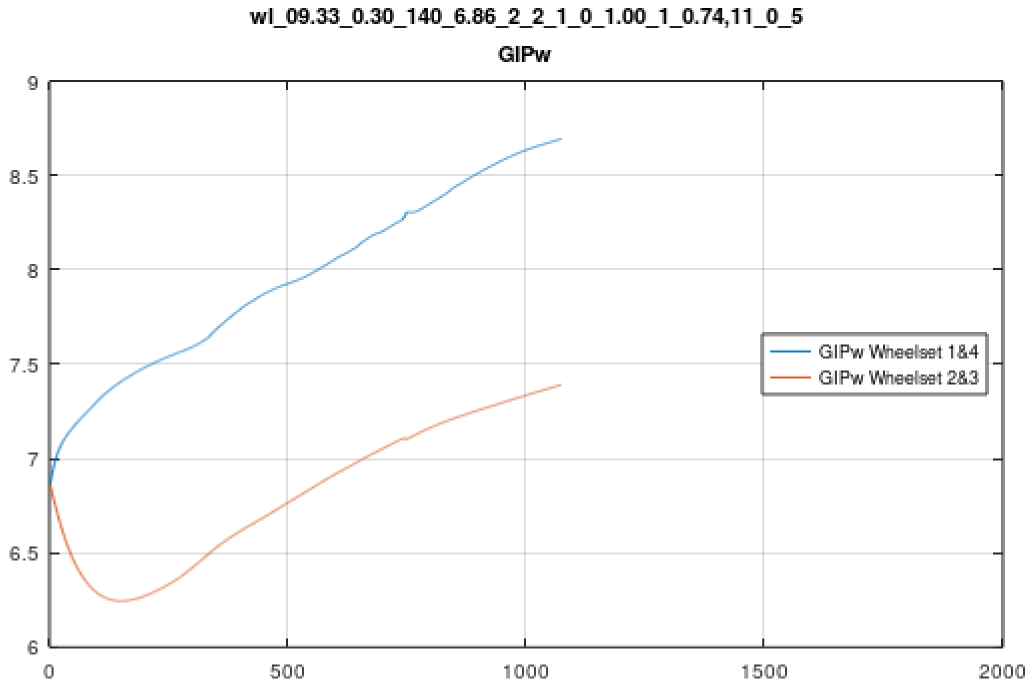

Compared to the reference case 9.5, it can be seen that the initial wheel profile has a higher GIPw value, and from that value it increases further, which leads to the high conicity. Our understanding is that a higher GIPw gives better steering and more concentrated wear, which in its turn leads to even higher conicities.

L.4 Development of the Flange Thickness

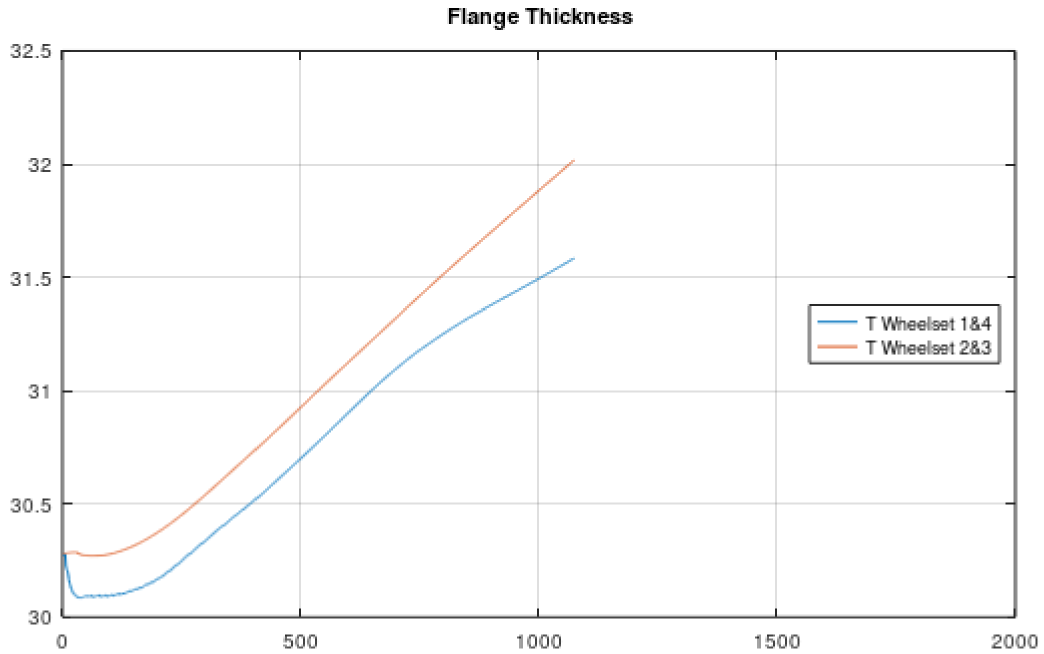

Compared to the reference case 9.6, the flange thickness is a little bit thinner in the beginning, but when the wheels start to get worn the flanges grows fast.

L.5 Development of the Flange Flank qR

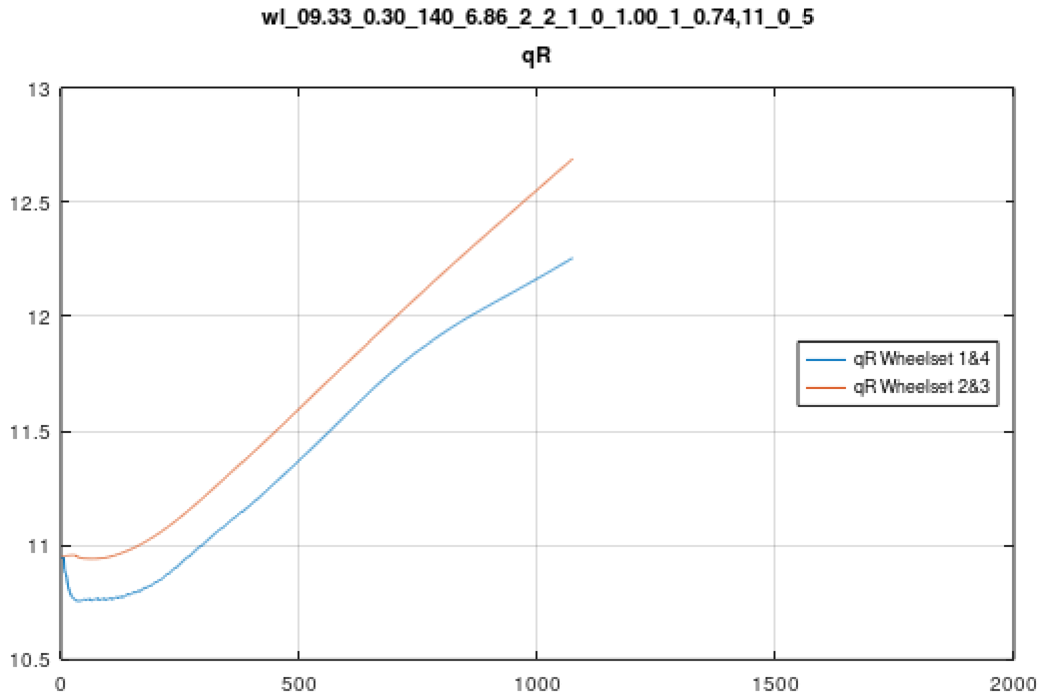

Compared to the reference case 9.7 the flange flank qR is approximately the same in the beginning, but when the wheels start to get worn qR grows fast.

L.6 Development of the Wheelset Steering Ability

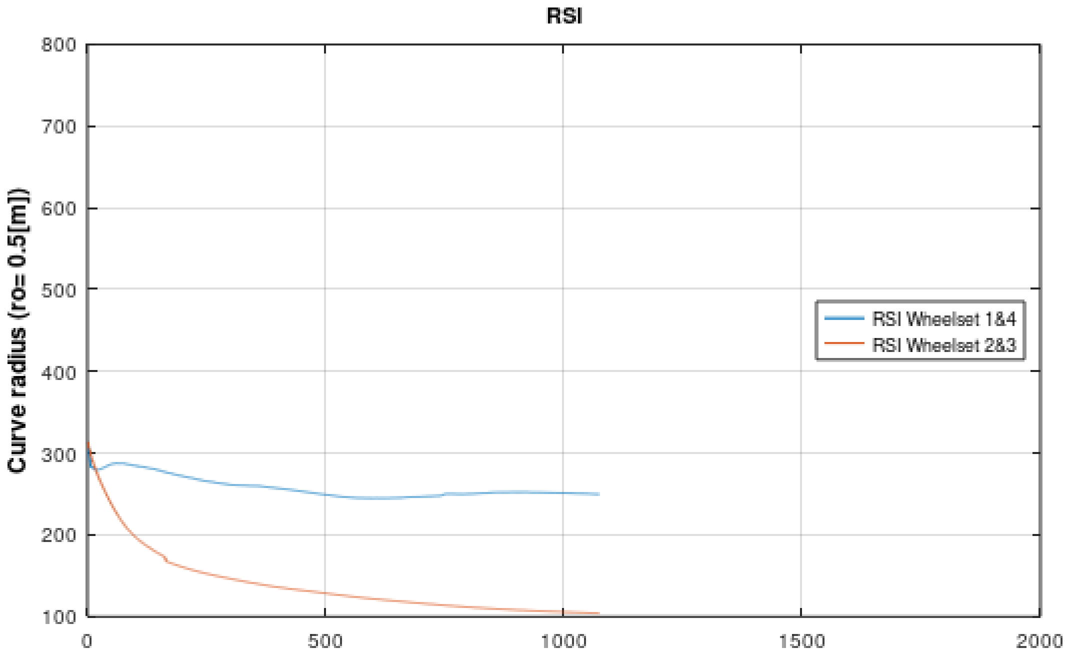

Compared to the reference case 9.8 the wheelset steering ability is already very good for newly turned wheels, and after that the steering ability improves further.

L.7 Development of the risk for RCF

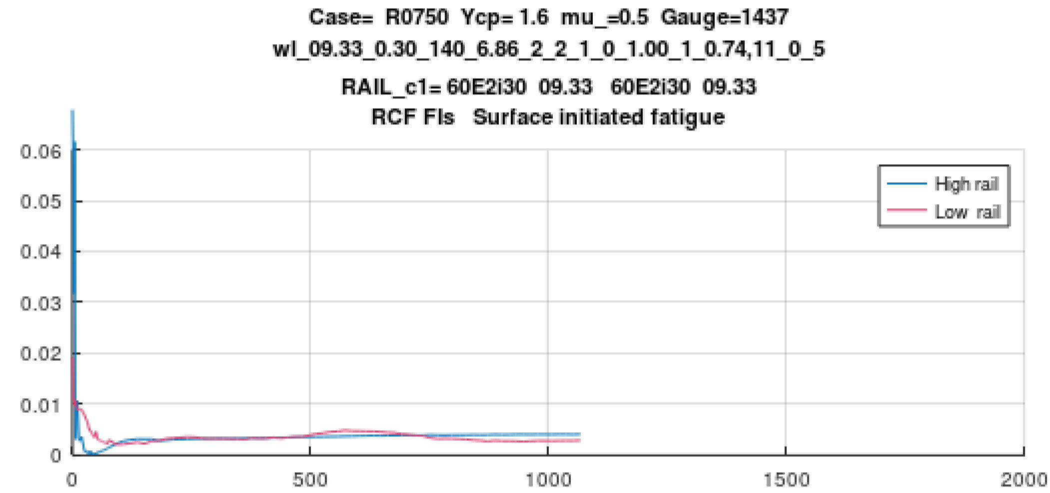

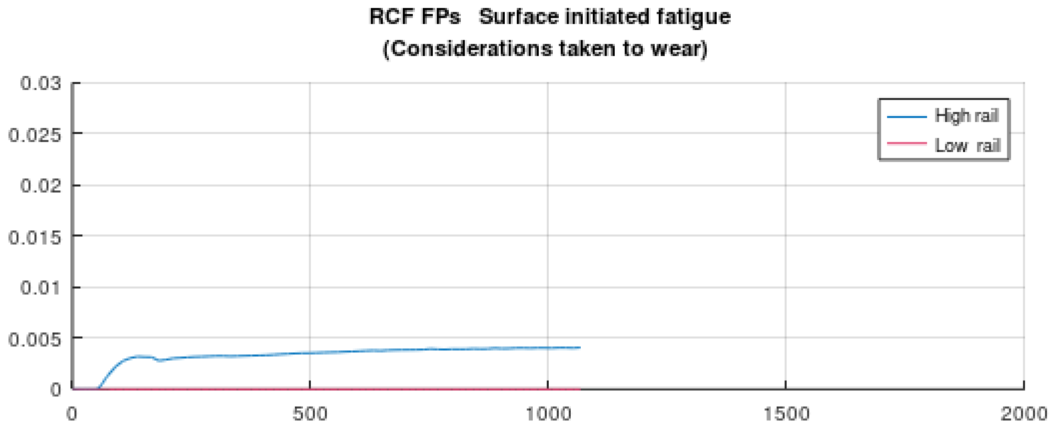

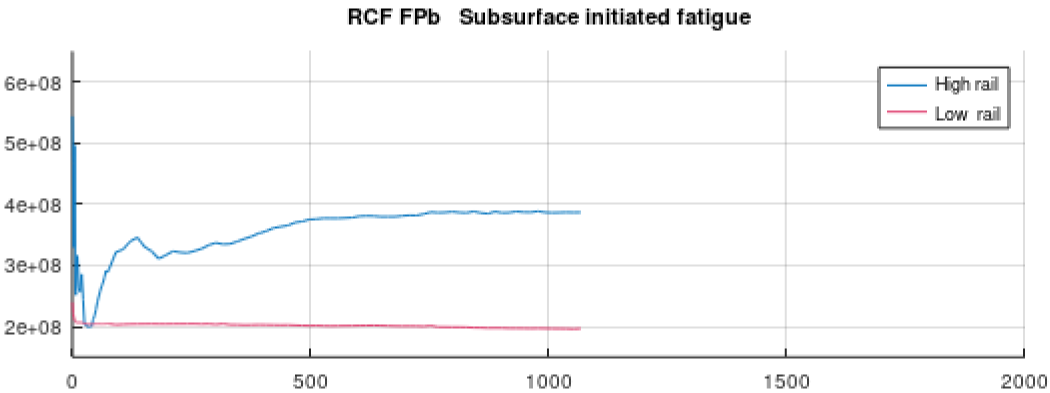

Compared to the reference case 9.9, the risk for RCF looks very good both for RCF FPs and RCF FPb.

Appendix M. Initial wheel profile with GIPw-2.64 pure conical wheels

This case is denoted:

wl_09.33_0.30_360_2.50_2_2_1_0_1.00_1_0.74,11_0_5

All data are the same as the reference case 9, except the initial wheel profile. In this case the initial wheel profile is 1i40t32.5. See selection of initial wheel profiles 6. This profile has a pure conical tread, and there is no or very short transition zone in the flange root. These type wheel profiles has a great portion of flange wear when the wheels are newly turned. Therefore, this profile has an initial flange thickness of 32.5mm.

M.1 Development of conicity wheelset 1&4

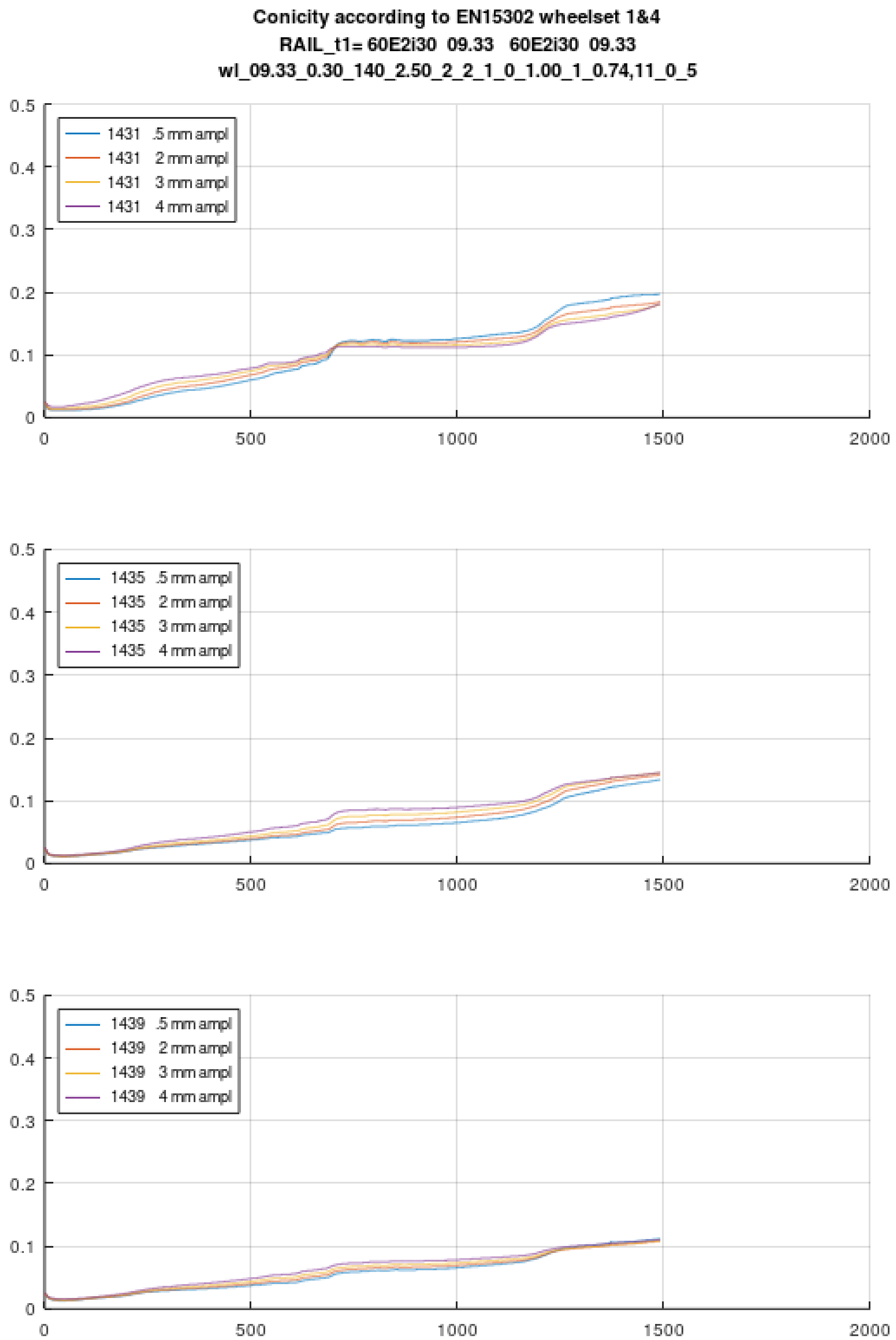

Compared to the reference case 9.1, this profile starts with a lower conicity, so it takes a little longer time before the conicity gets high. There is a step in the conicity curve at ~1250 wear steps. This step can also be seen in the reference case, but in the reference case this step occurs after ~800 wear steps.

M.2 Development of wheel profile shapes wheelset 1&4

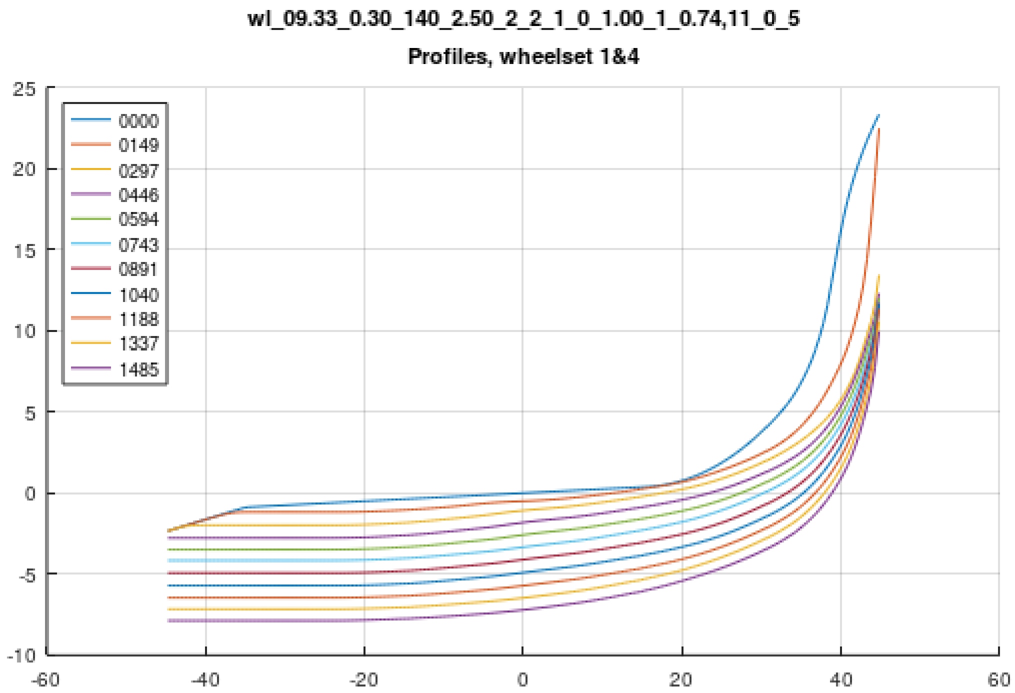

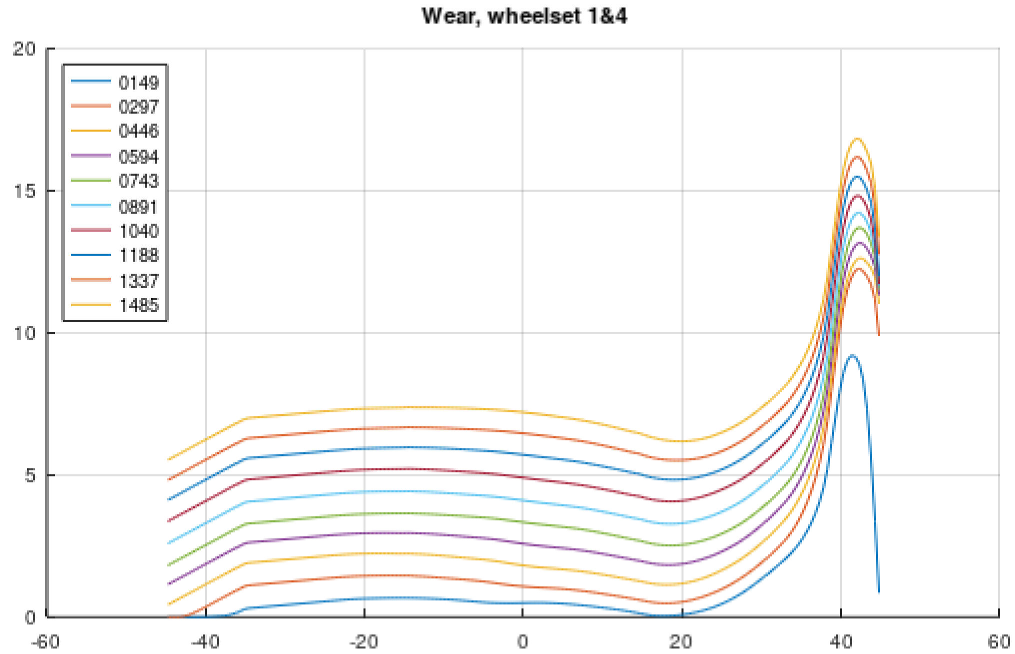

Compared to the reference case 9.3, it can be seen that the flange is thicker for the initial profile. It can also be seen that the flange wear is severe in the beginning.

M.3 Development of GIPw

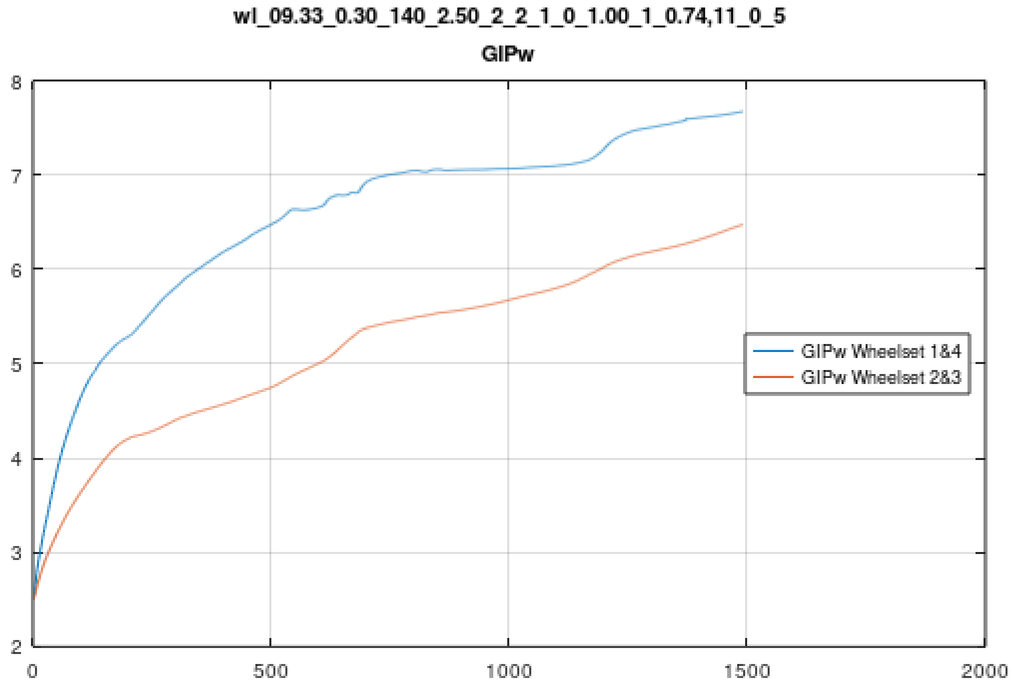

Compared to the reference case 9.5, it can be seen that the initial wheel profile has a much lower GIPw value. However, GIPw is increasing with travelled distance in a similar way as in the reference case, it just takes longer time until the GIPw values get high. There is a step in GIPw in wheelset 1&4 at ~1250 wear steps, this step can also be seen in the reference case, but here the step occurs already after ~800 wear steps.

M.4 Development of the Flange Thickness

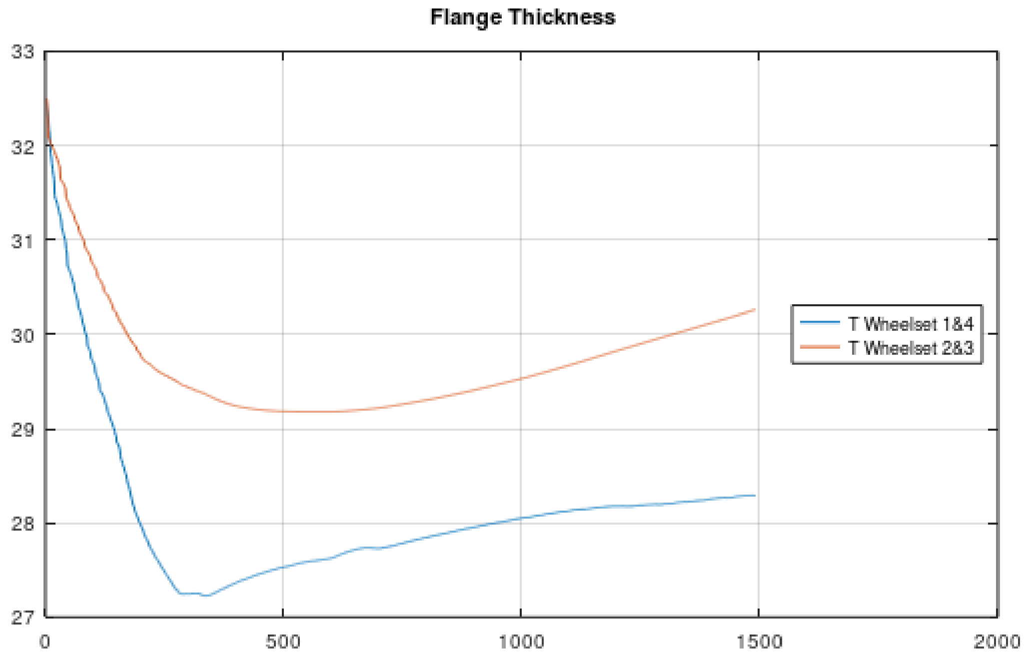

Compared to the reference case 9.6, the flange thickness starts with a higher value 32.5mm. The flange thickness decreases very fast, and after ~300 wear steps the flange thickness is even lower than 28mm which was the minimum flange thickness in the reference case. However, after the minimum flange thickness has been reached, the flange thickness starts to grow again in a similar way as in the reference case.

M.5 Development of the Flange Flank qR

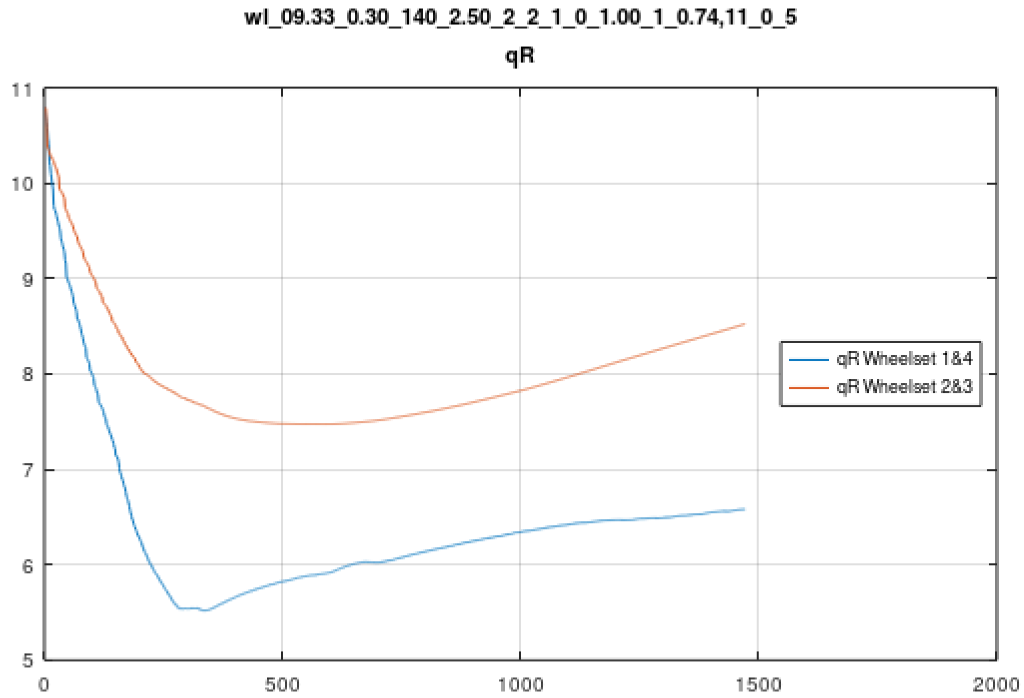

Compared to the reference case 9.7 the qR value doesn't look good. The minimum value for qR here is 5.5 which is below the limit value of 6.5.

M.6 Development of the Wheelset Steering Ability

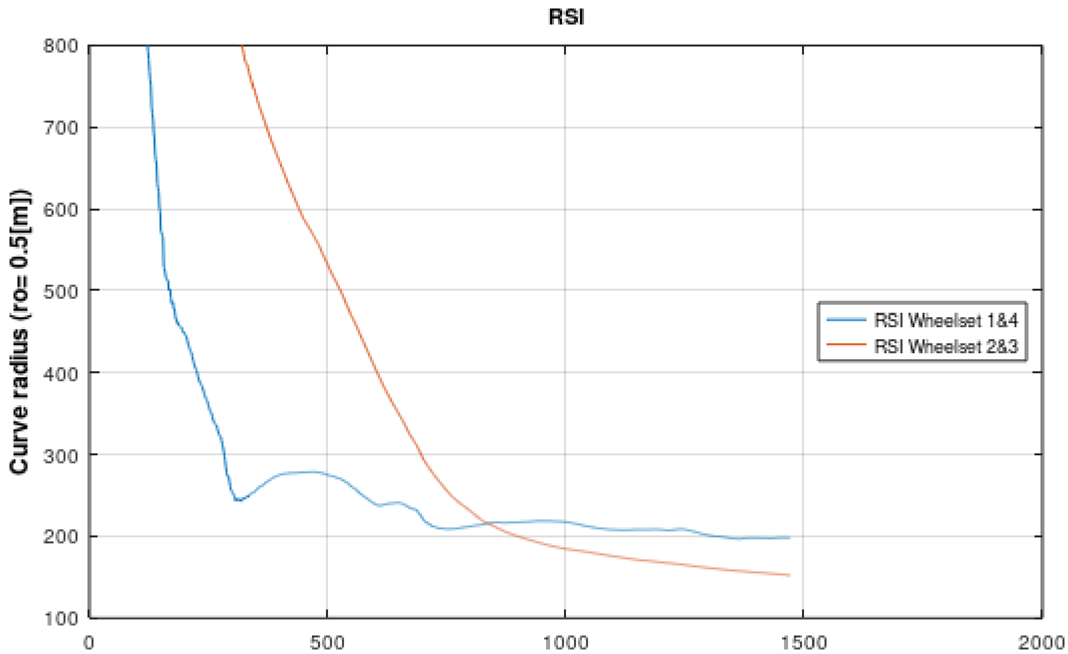

Compared to the reference case 9.8 the wheelsets steering is very bad in the beginning. However, after a while the wheelset steering ability increases, so in the end the results are similar to the reference case.

M.7 Development of the risk for RCF

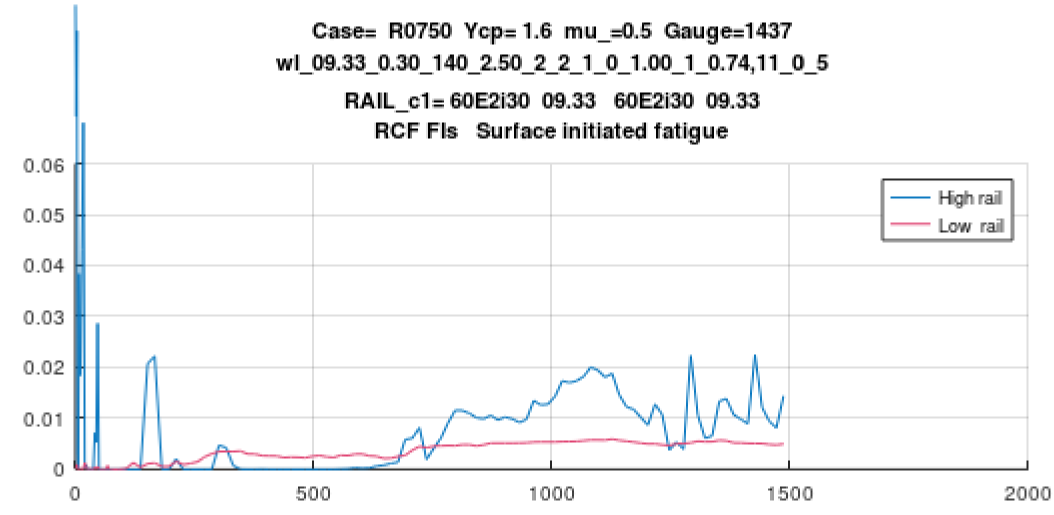

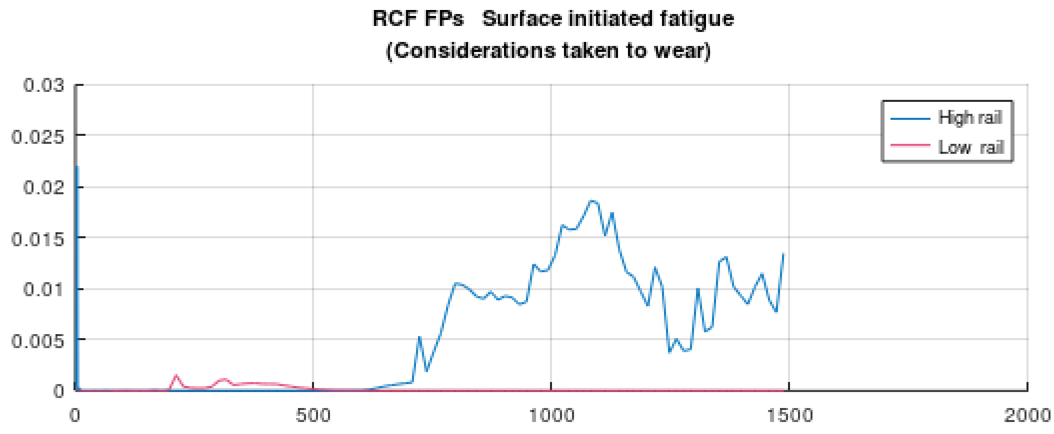

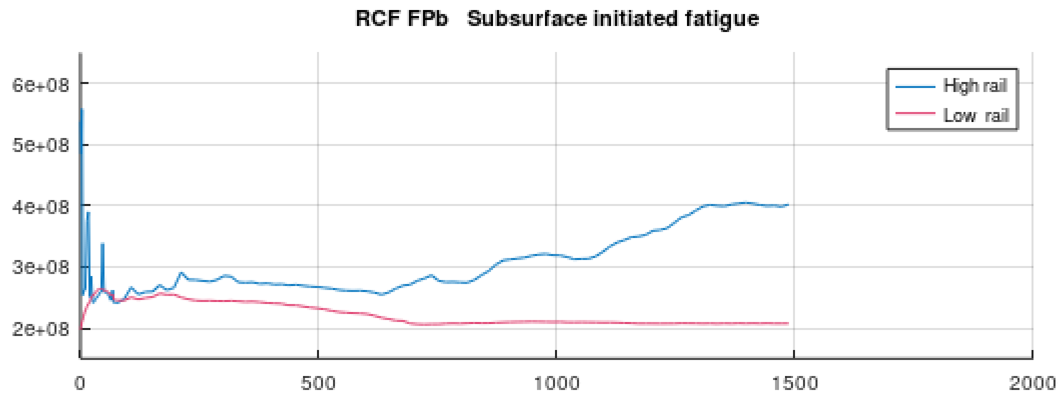

Regarding the risk for RCF, this wheel profile is also quite similar to the reference case 9.9. However, it takes a longer time until RCF gets high.

Appendix N. Initial wheel profile with GIPw+0.10 pure conical wheels

This case is denoted:

wl_09.33_0.30_360_5.24_2_2_1_0_1.00_1_0.74,11_0_5

All data are the same as the reference case 9, except the initial wheel profile. In this case the initial wheel profile is n33t32.8 which is an old Swedish wheel profile called ”Normalprofil”. See selection of initial wheel profiles 6. This profile has a pure conical tread, and there is no or very short transition zone in the flange root. These type wheel profiles has a great portion of flange wear when the wheels are newly turned. Therefore, this profile has an initial flange thickness of 32.5mm.

N.1 Development of conicity wheelset 1&4

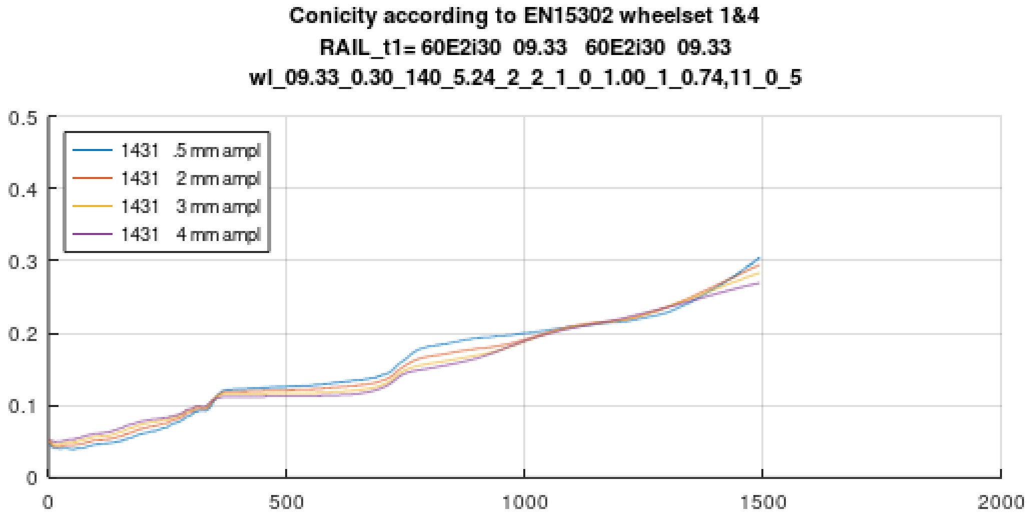

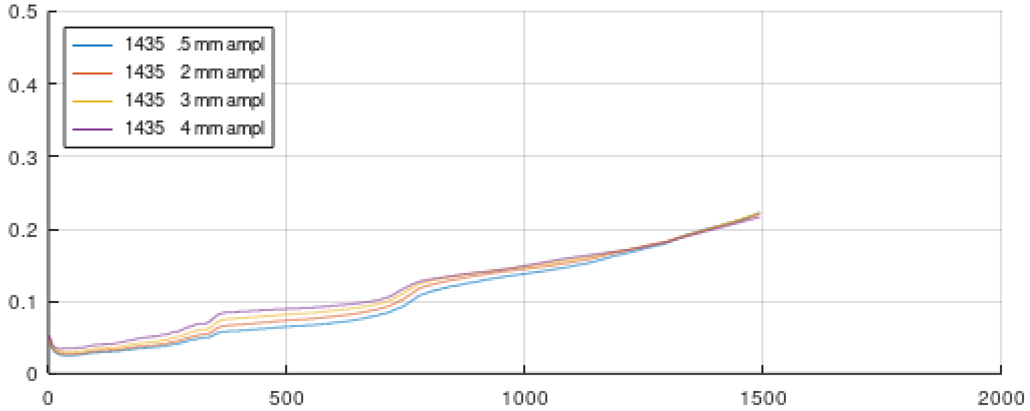

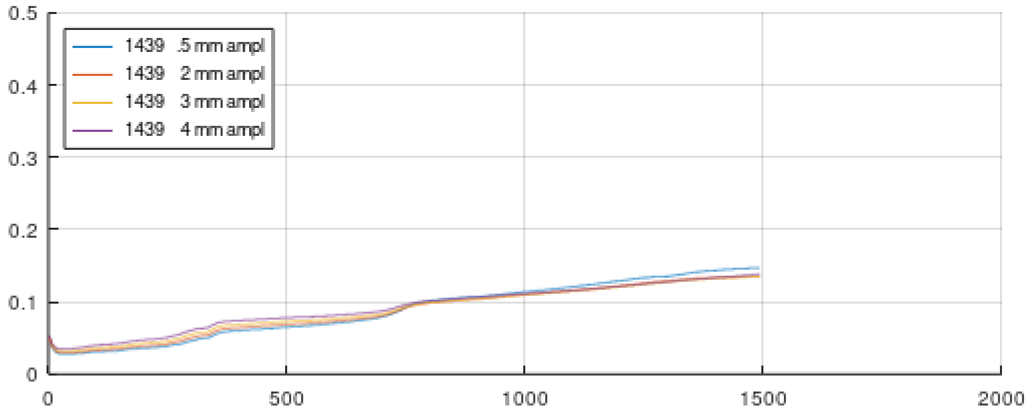

Compared to the reference case 9.1, this profile starts with approximately the same conicity. However, after the initial wear steps, it seems that the increase rate of this wheel profile is a little bit higher than for the reference case. The step in the reference curve that occurred at ~800 wear steps occur here at ~750 wear steps.

N.2 Development of wheel profile shapes wheelset 1&4

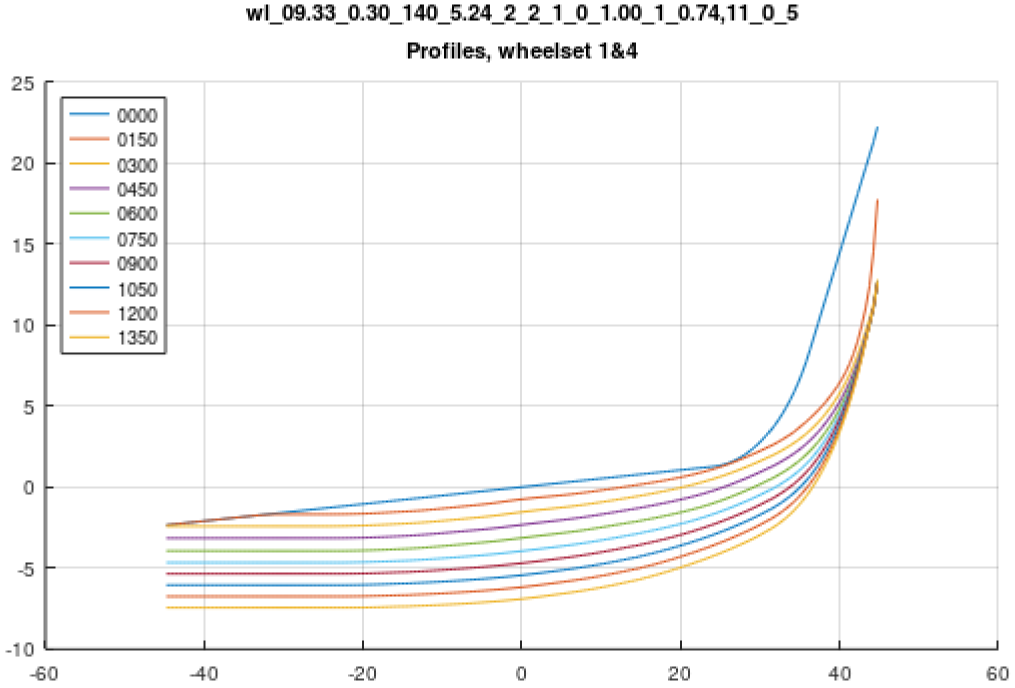

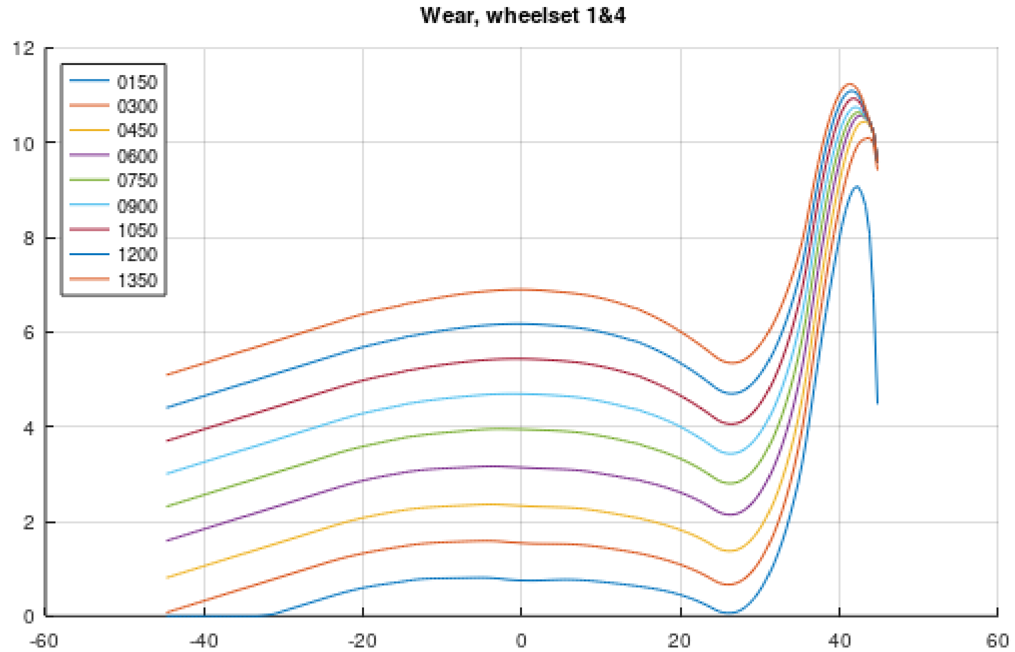

Compared to the reference case 9.3, it can be seen that the flange is thicker for the initial profile. It can also be seen that the flange wear is severe in the beginning.

N.3 Development of GIPw

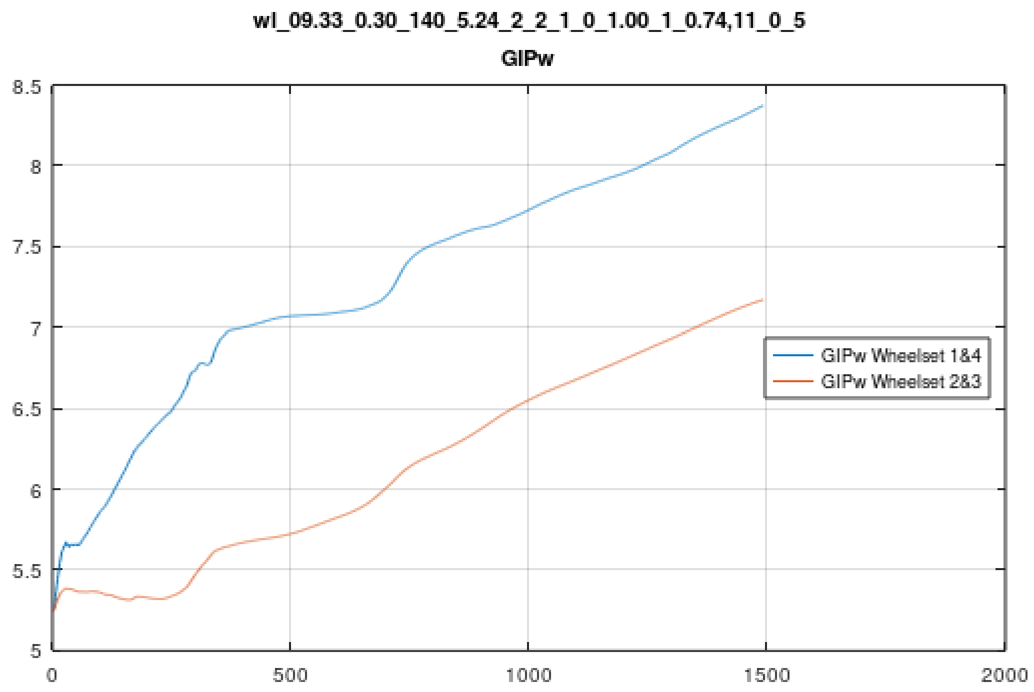

Compared to the reference case 9.5, it can be seen that GIPw starts at approximatively the same point as the reference profile, but after a while it seems that GIPw increases a little bit faster for this wheel profile. The step in the reference curve that occurred at ~800 wear steps occur here at ~750 wear steps.

N.4 Development of the Flange Thickness

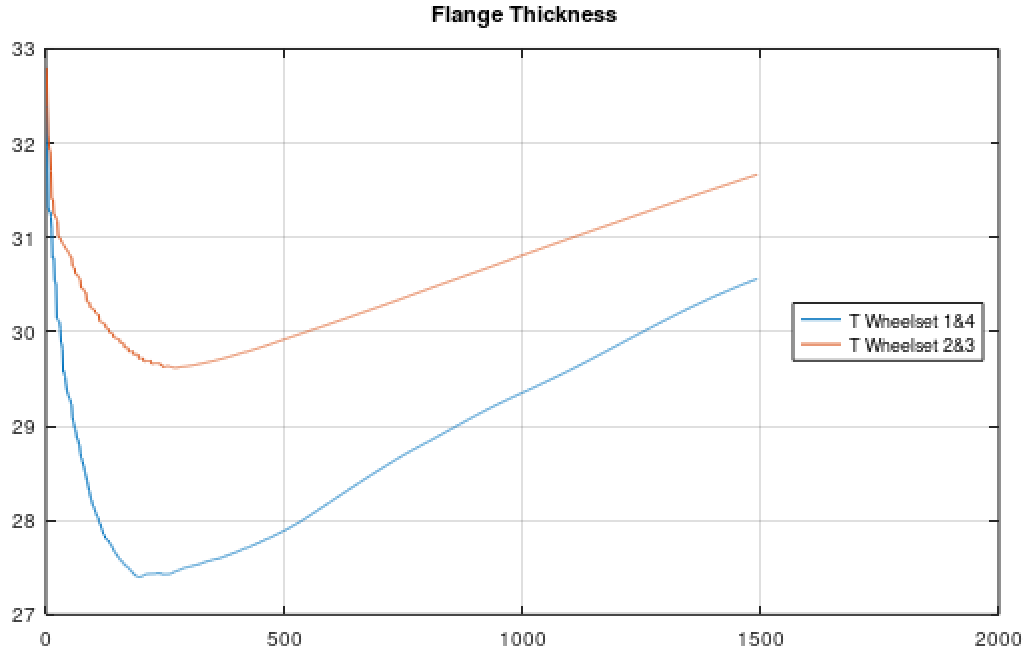

Compared to the reference case 9.6, the flange thickness starts with a higher value 32.5mm. The flange thickness decreases very fast, and after ~300 wear steps the flange thickness is even lower than 28mm which was the minimum flange thickness in the reference case. However, after the minimum flange thickness has been reached, the flange thickness starts to grow again in a similar way as in the reference case.

N.5 Development of the Flange Flank qR

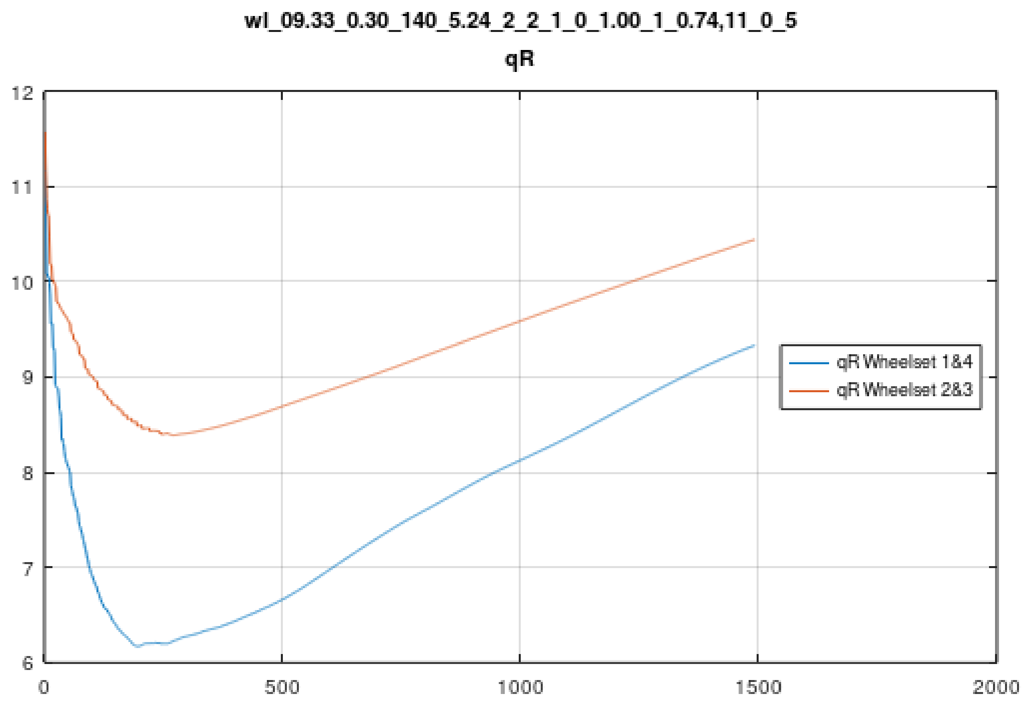

Compared to the reference case 9.7 the qR value doesn't look good. The minimum value for qR is below the limit value of 6.5.

N.6 Development of the Wheelset Steering Ability

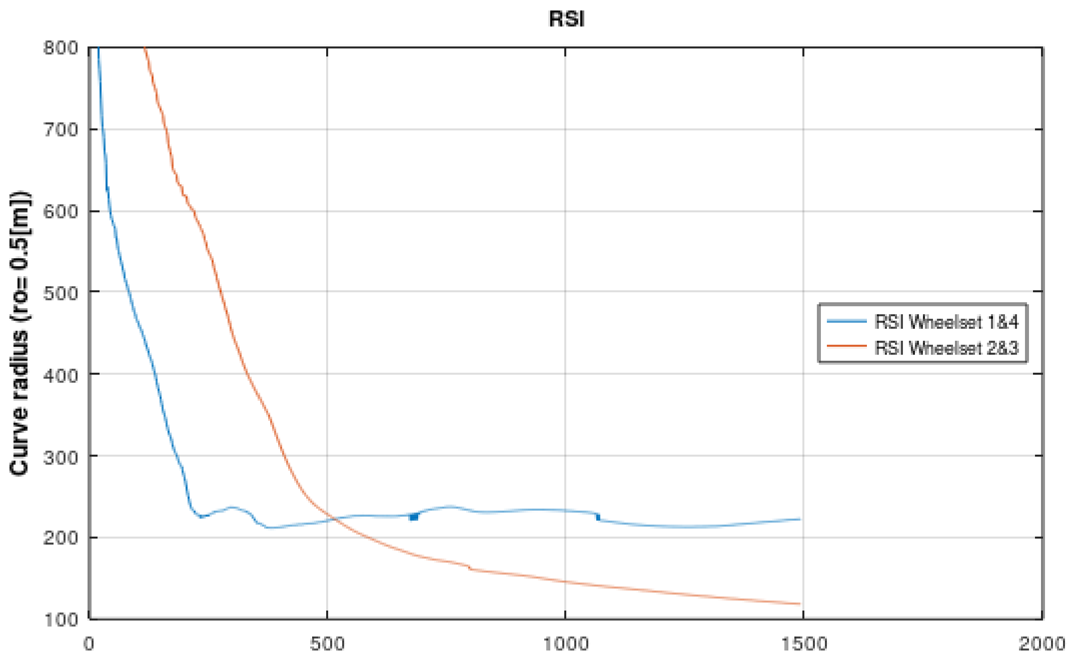

Compared to the reference case 9.8 the wheelsets steering is very bad in the beginning. However, the wheelset steering ability inproves fast and in the end the results are relatively similar to the reference case.

N.7 Development of the risk for RCF

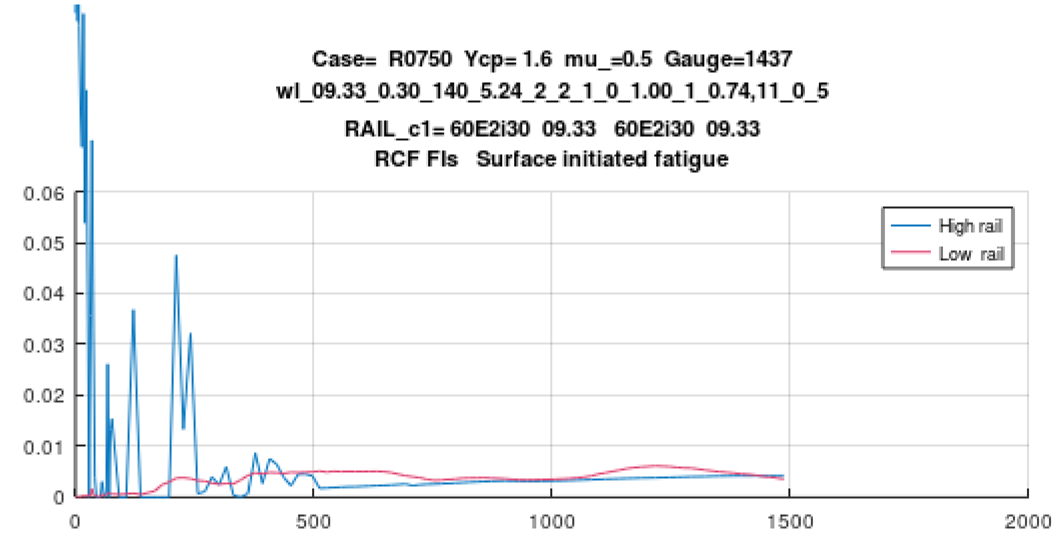

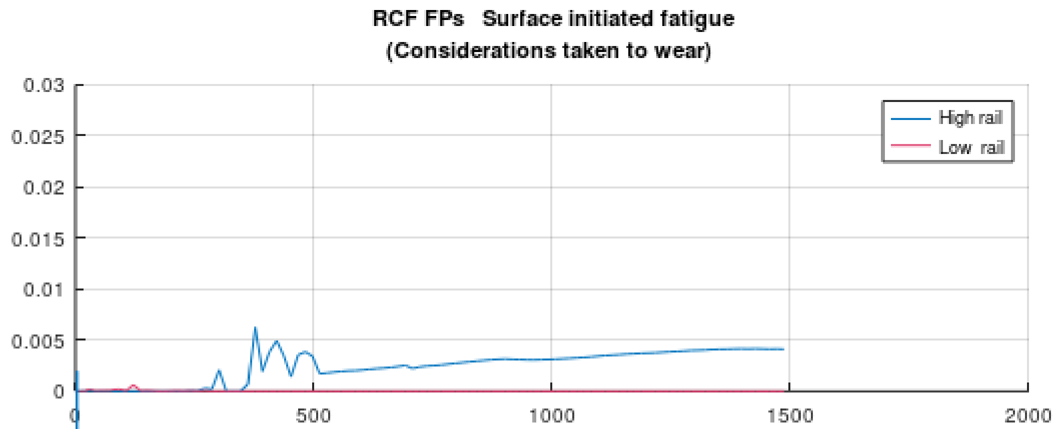

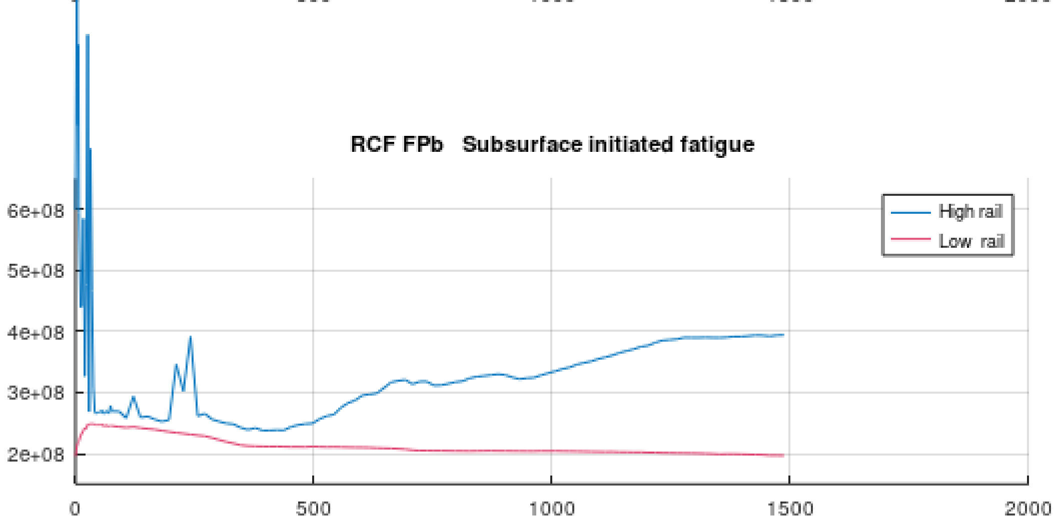

Compared to the reference case 9.9, the risk for RCF looks very good both for RCF FPs and RCF FPb.

Appendix O. Lower amplitudes for the track irregularities

This case is denoted:

wl_09.33_0.30_360_5.14_2_2_1_1_1.00_1_0.74,11_0_5

All data are the same as the reference case 9, except the amplitudes of the track irregularities 7.4. On tangent track the track amplitude for this case is 50% lower than the reference case.

O.1 Development of conicity wheelset 1&4

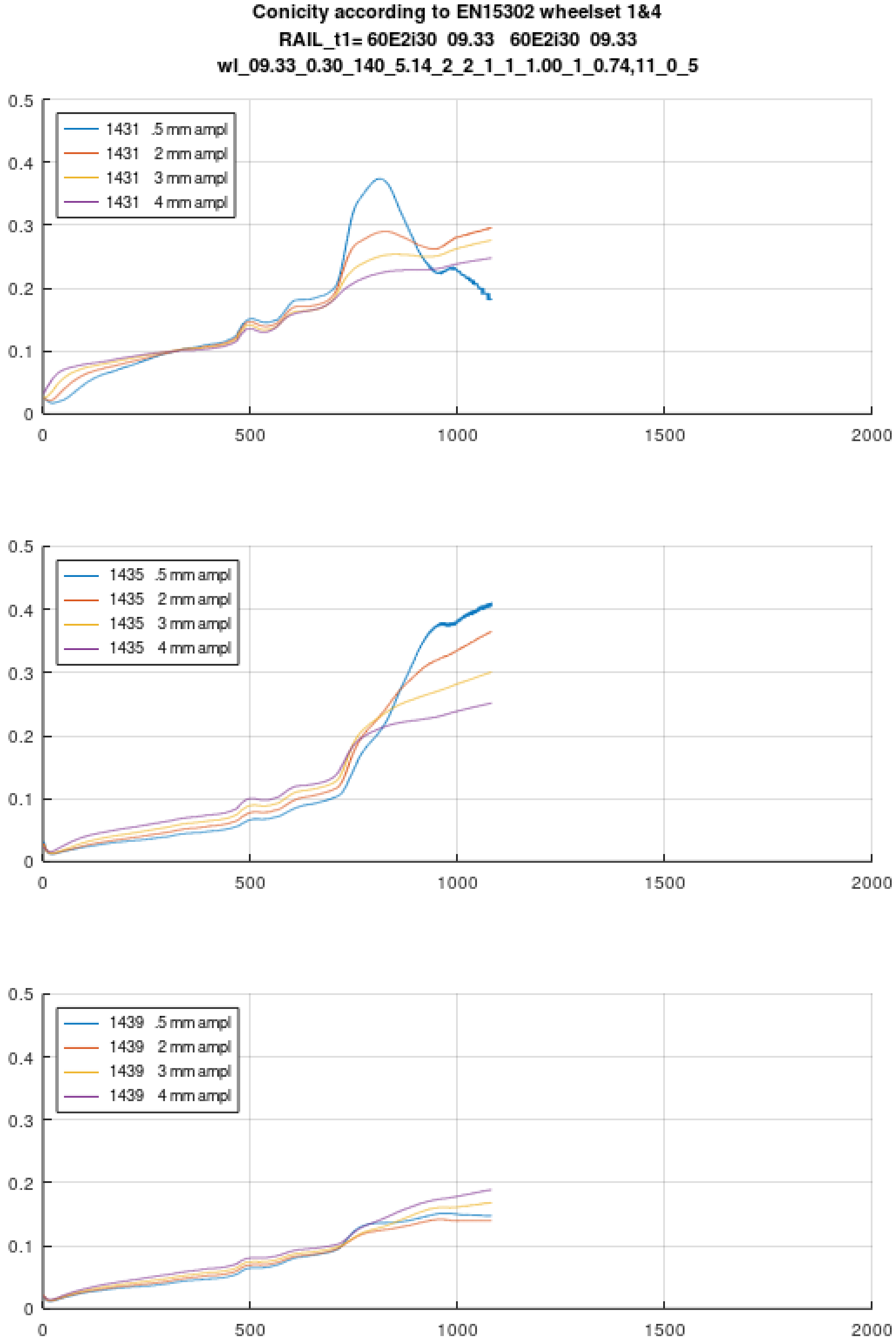

Compared to the reference case 9.1 the conicities for this rail profile increases very fast. The conicity become so high so the wear prediction loop was be stopped prematurely.

Our understanding is that a better track alignment causes more concentrated wear on the tread of the wheel, and the shape of the wheel therefore gets closer to the shape of the rail profile. Which implies that for a small lateral displacement of the wheelset the contact patches can move very far, which leads to high conicities.

O.2 Development of wheel profile shapes wheelset 1&4

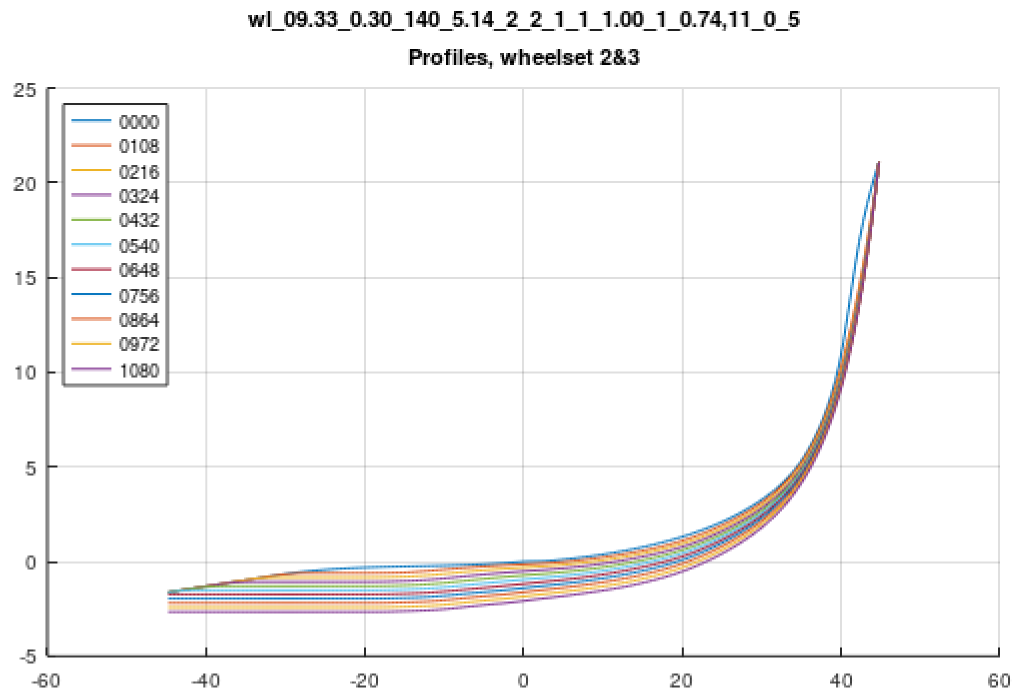

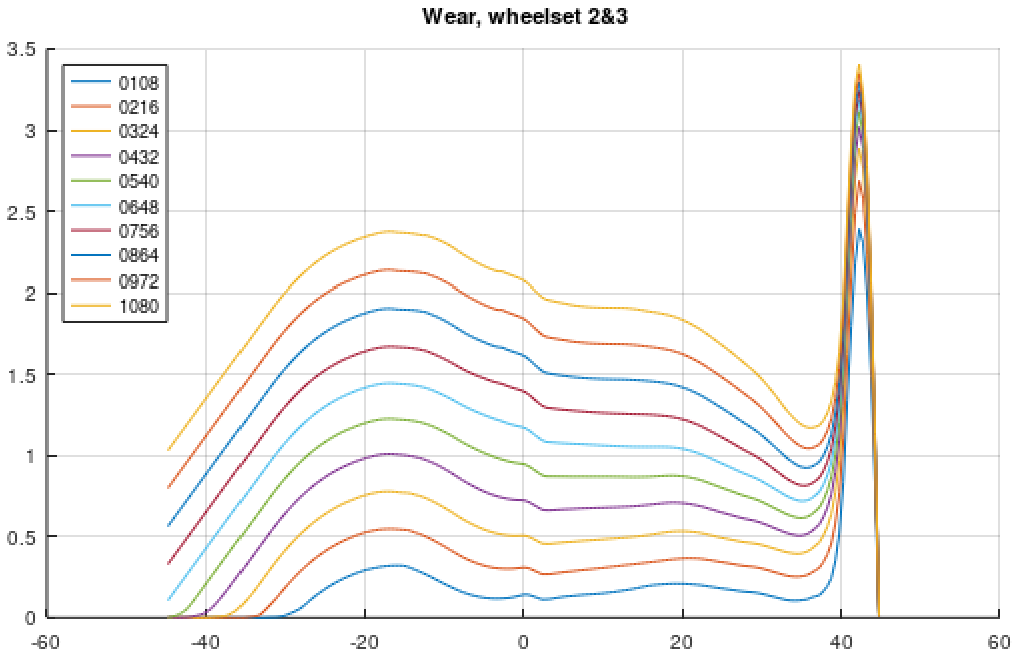

Compared to the reference case 9.3, it can be seen that the tread wear around approx. -20mm is more concentrated.

O.3 Development of GIPw

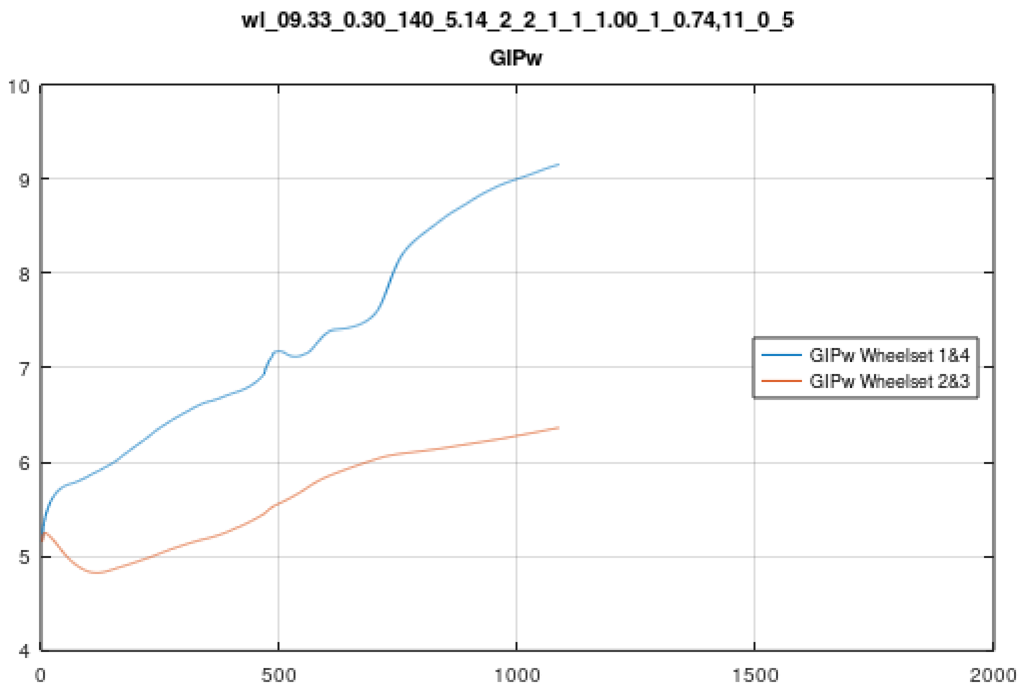

Compared to the reference case 9.5, GIPw increases much faster in this case.

O.4 Development of the Flange Thickness

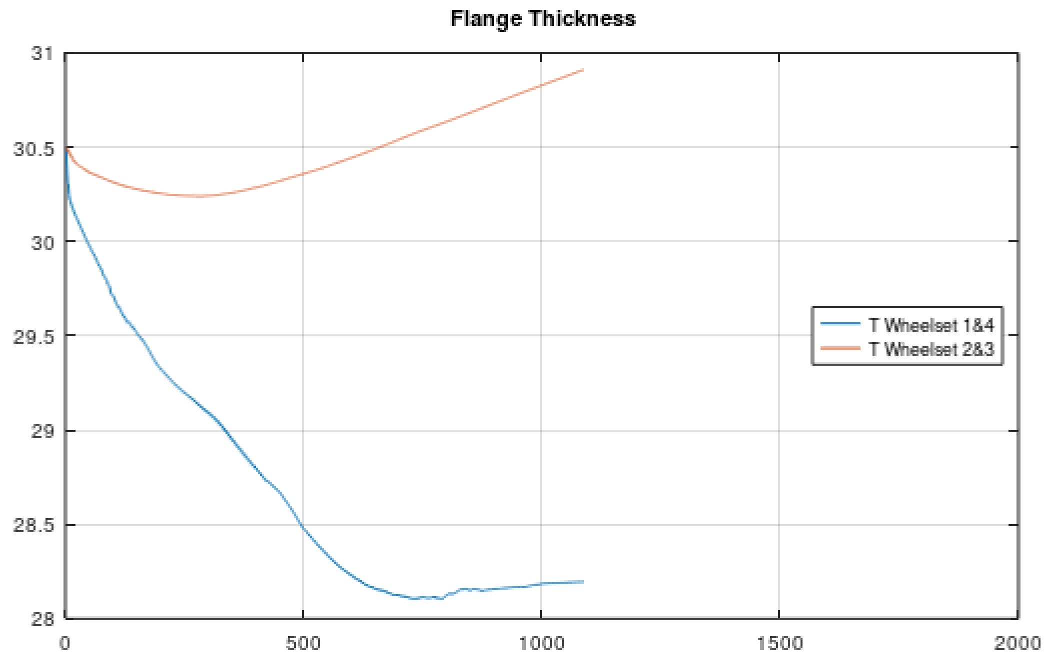

The flange thickness behaves in a similar way as the reference case 9.6. The dip in the flange thickness curve occurs at a later time compared to the reference case.

O.5 Development of the Flange Flank qR

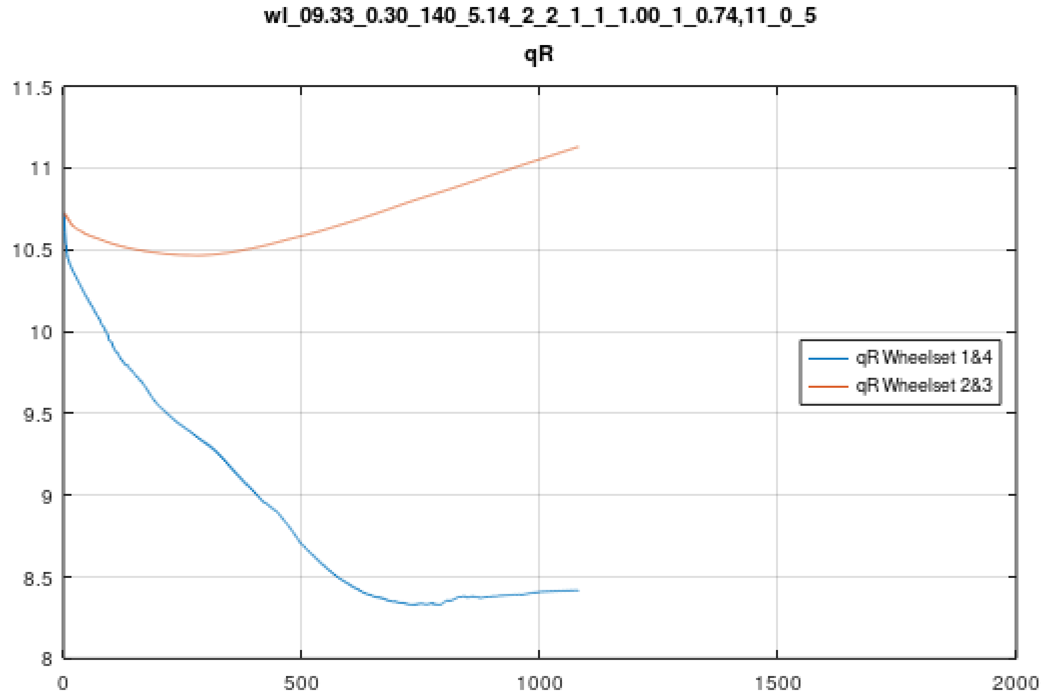

Compared to the reference case 9.7 the qR value goes down and up slower. The results are OK, the value of qR is over 6.5 at all times.

O.6 Development of the Wheelset Steering Ability

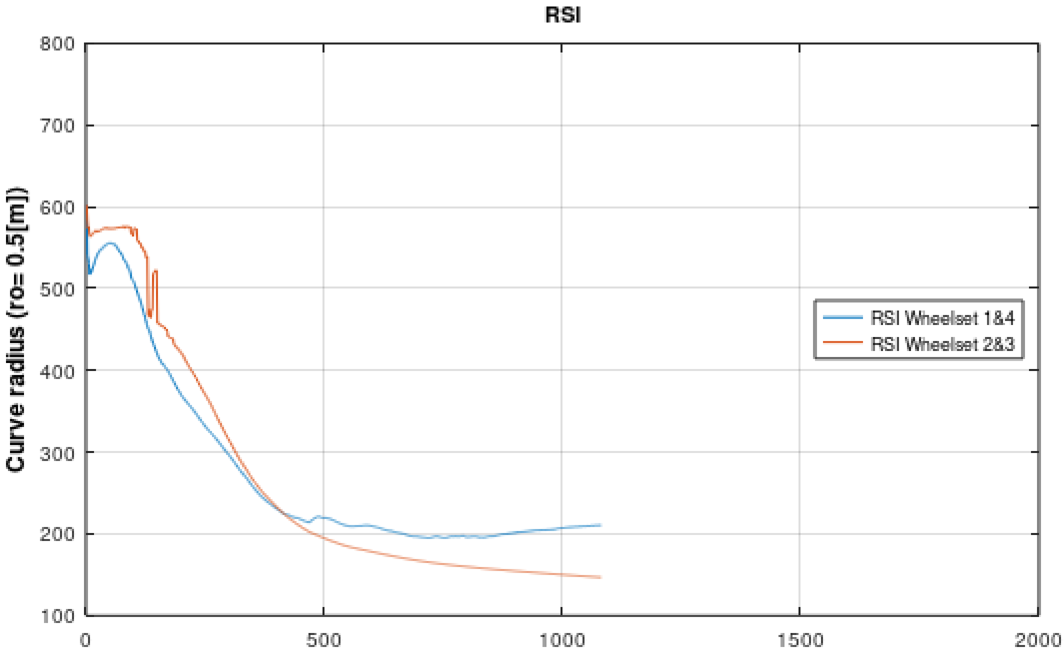

In the beginning the wheelset steering ability is as good as in the reference case 9.8, but the asymptotic values in the end seems to be similar.

O.7 Development of the risk for RCF

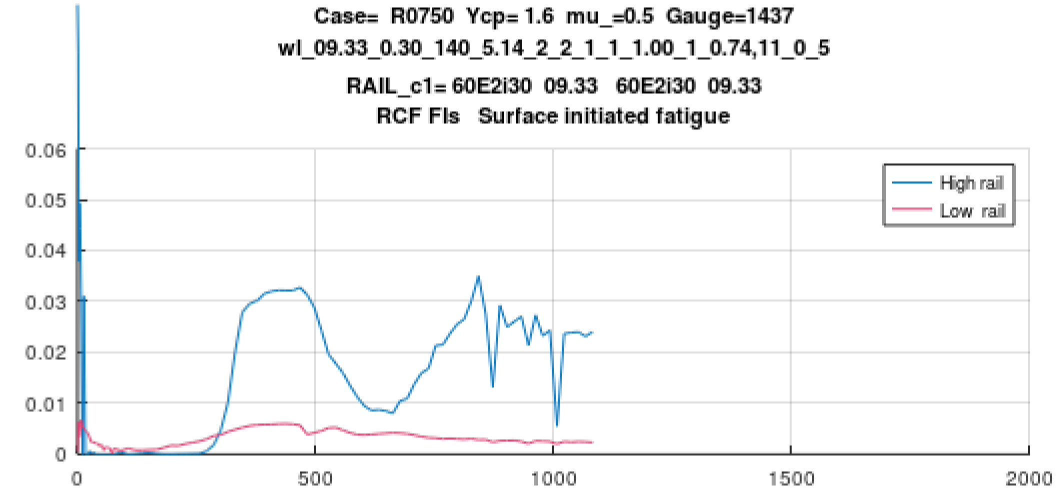

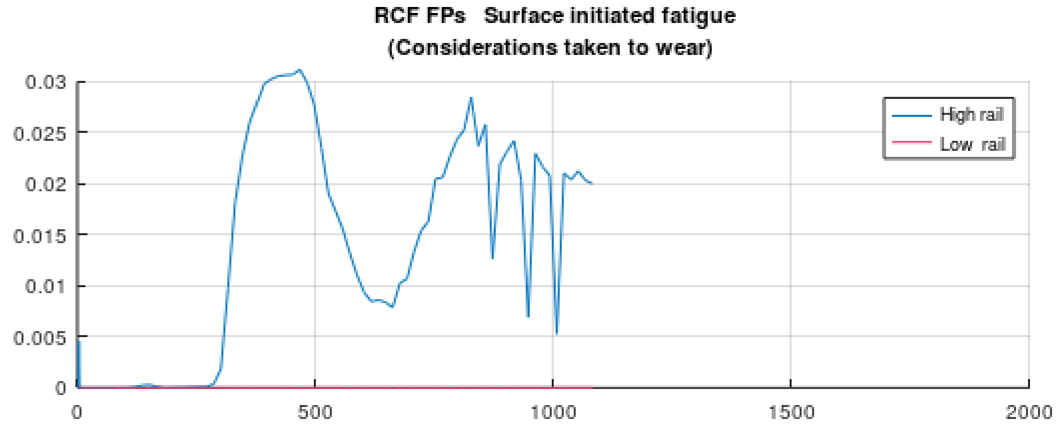

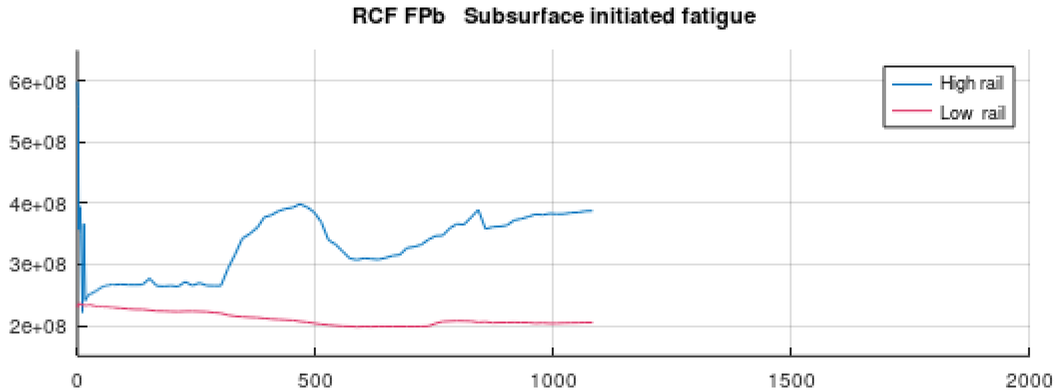

As in the reference case 9.9, the risk for RCF FPs is low for newly turned wheels, but after a while the risk for RCF FPs builds up. After ~350 wear steps the results are even a bit worse than the reference case.

RCF FPb also is low when the wheels are newly turned, but over time the risk for RCF FPb also increases. However, RCF FPb is below the limit value 450e6 at all times.

Appendix P. Lateral uncompensated acceleration 0.65

This case is denoted:

wl_09.33_0.30_360_5.14_2_2_1_0_0.65_1_0.74,11_0_5

All data are the same as the reference case 9, except the uncompensated lateral acceleration, which is here equal to 0.65[m/s^2] (same as 100[mm] cant deficiency) , see section 8.

P.1 Development of conicity wheelset 1&4

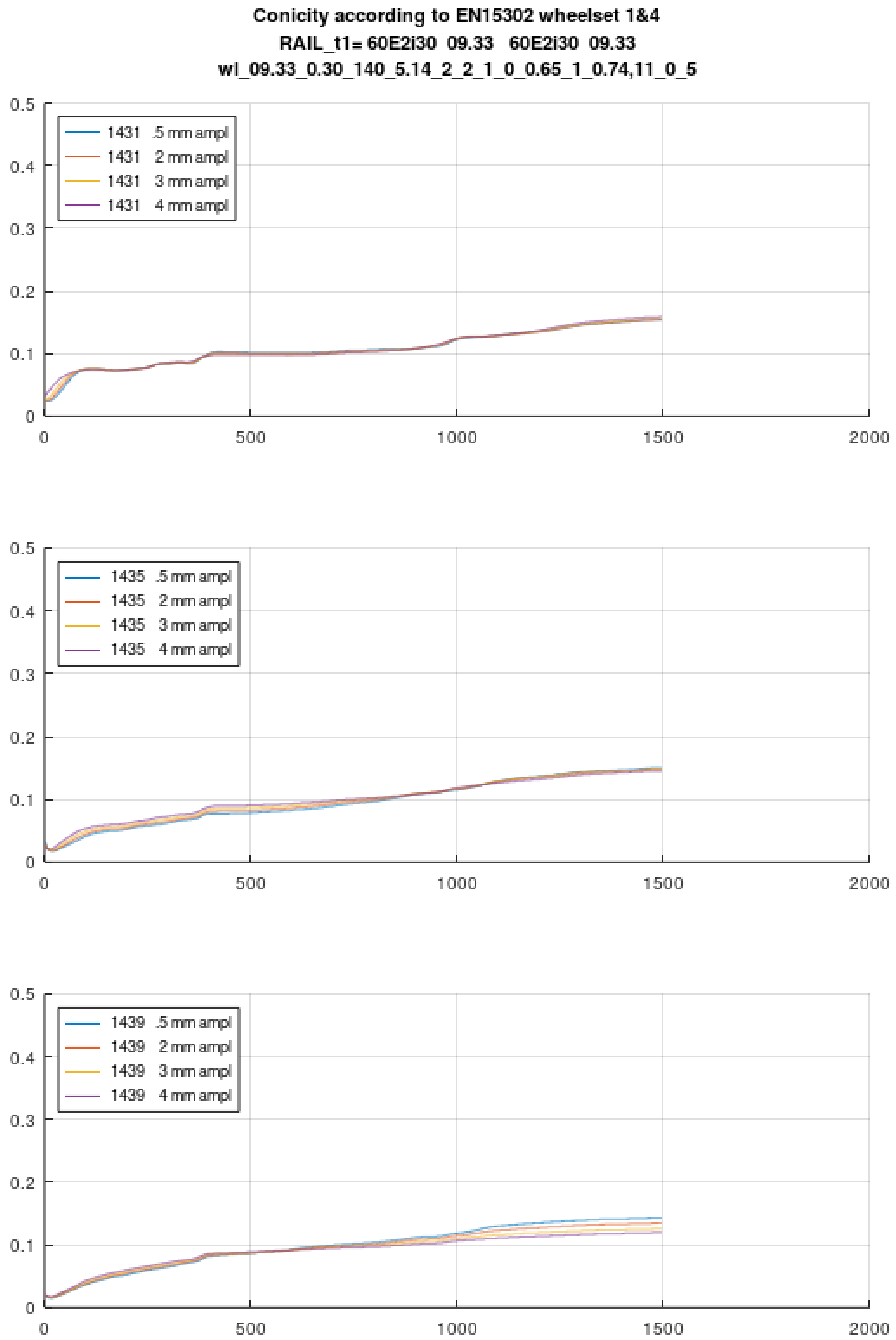

P.2 Development of wheel profile shapes wheelset 1&4

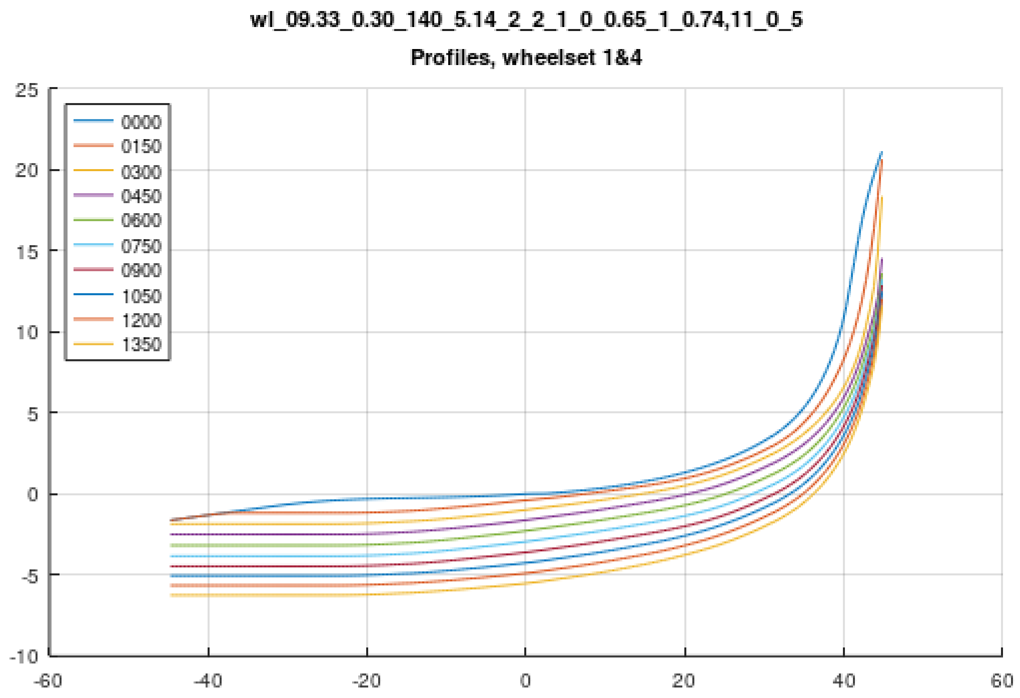

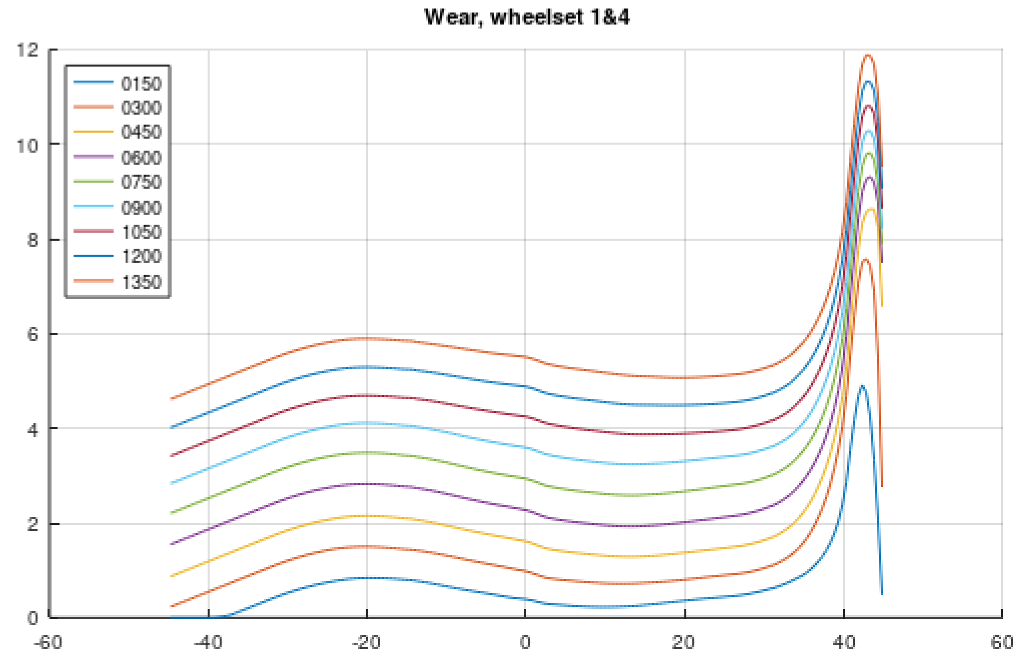

P.3 Development of GIPw

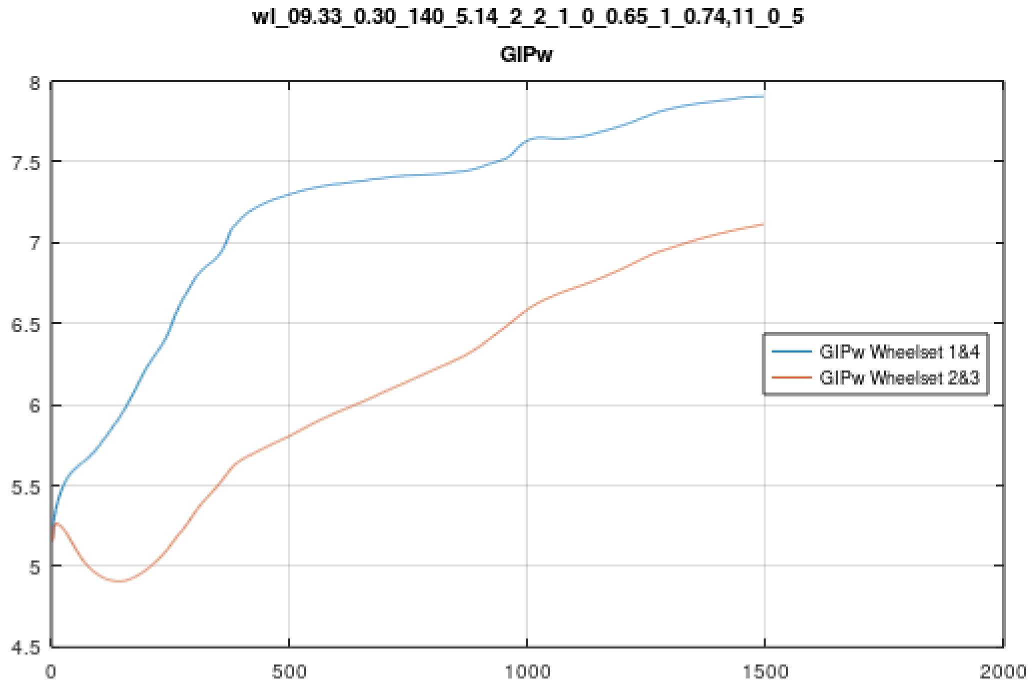

P.4 Development of the Flange Thickness

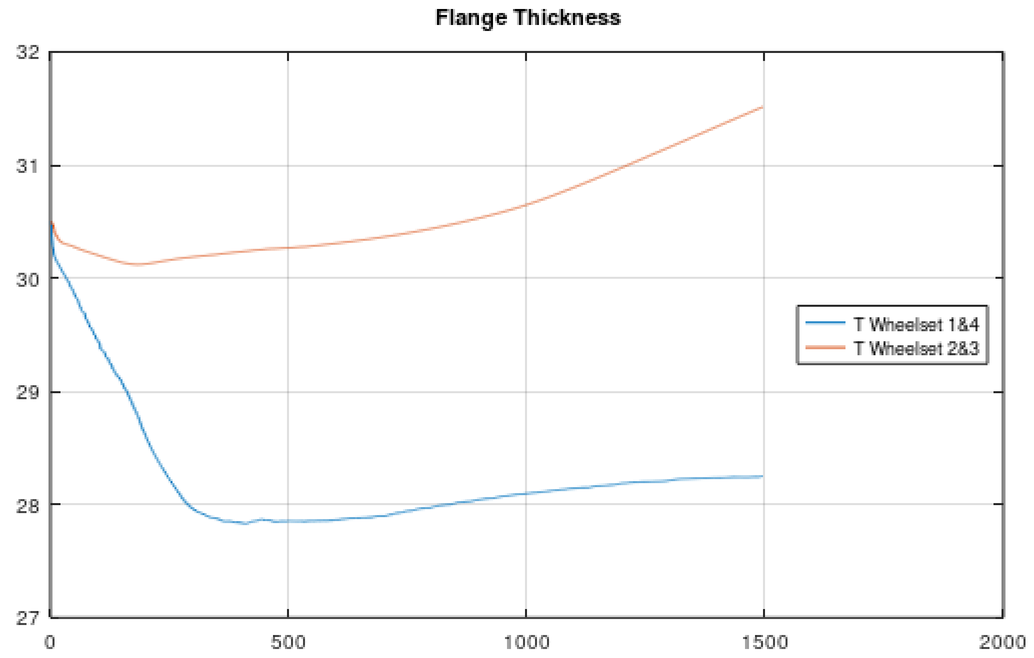

P.5 Development of the Flange Flank qR

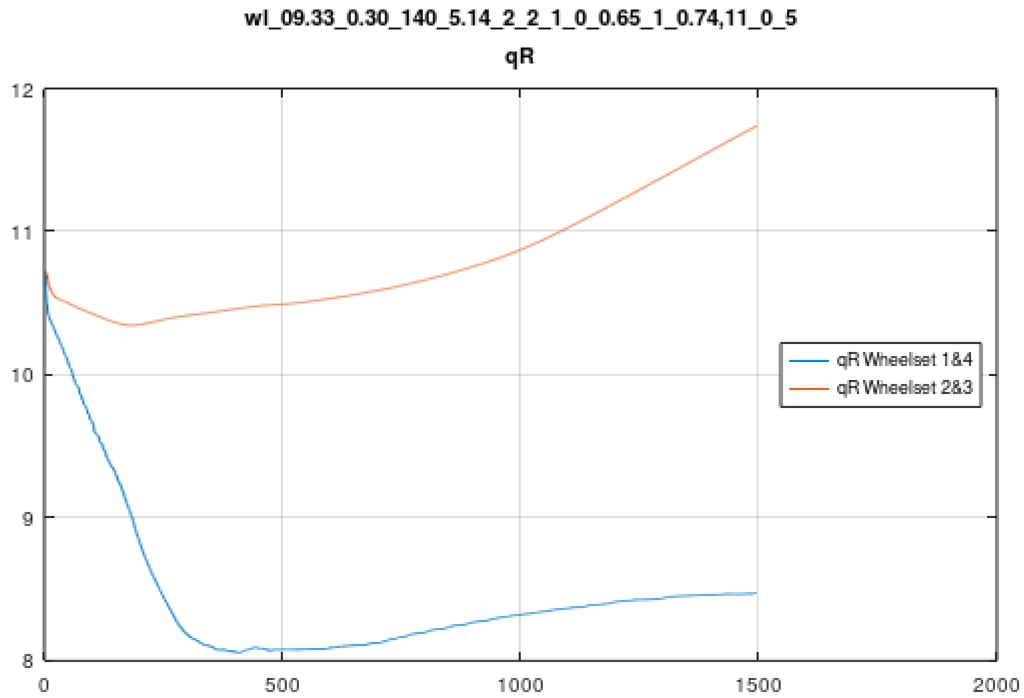

P.6 Development of the Wheelset Steering Ability

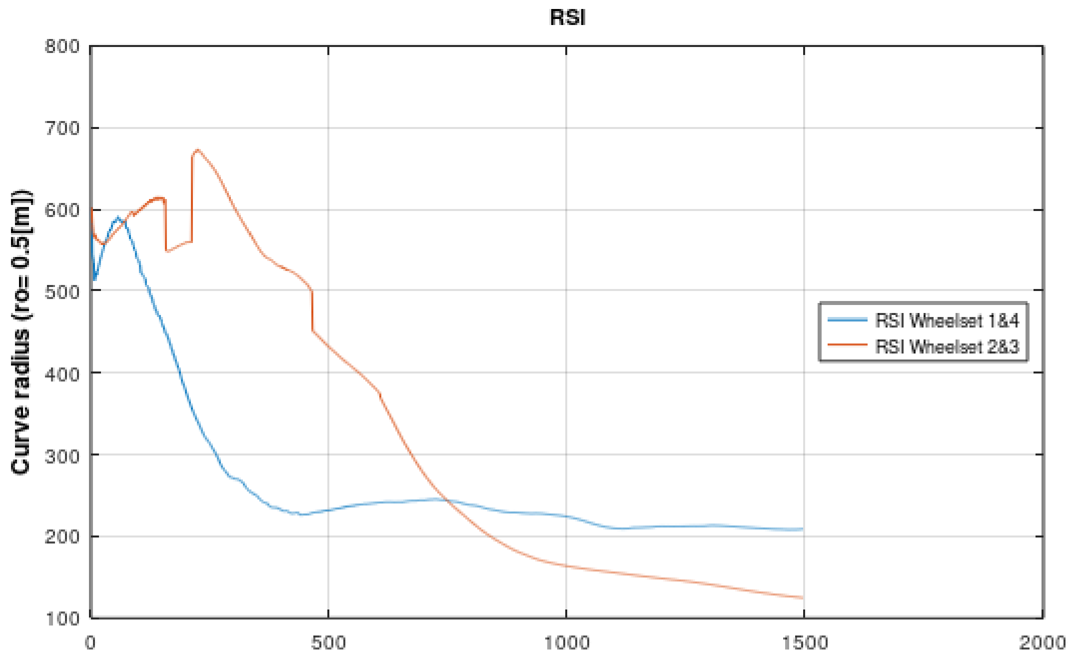

P.7 Development of the risk for RCF

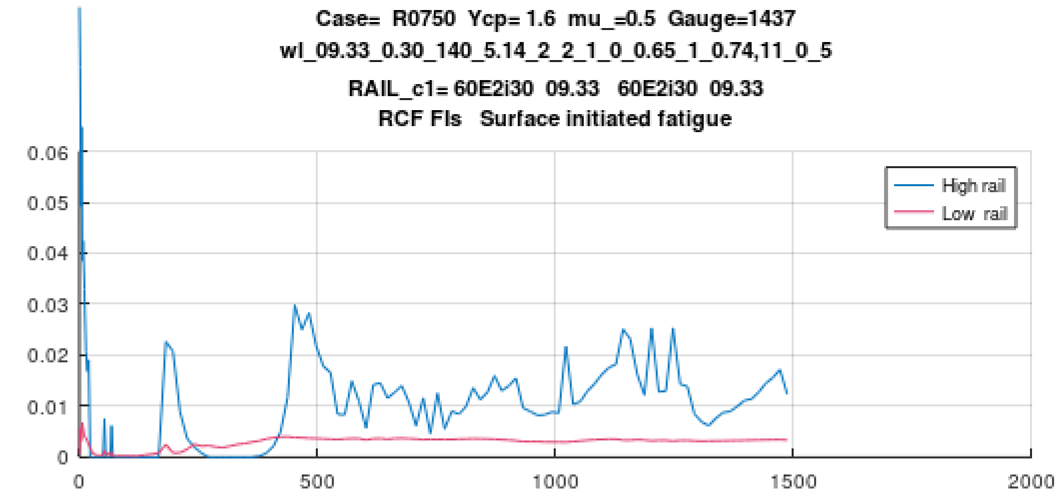

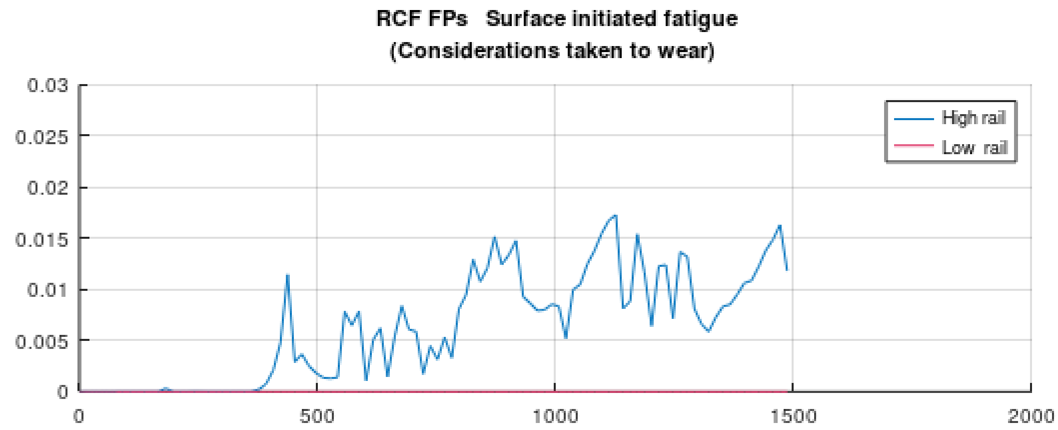

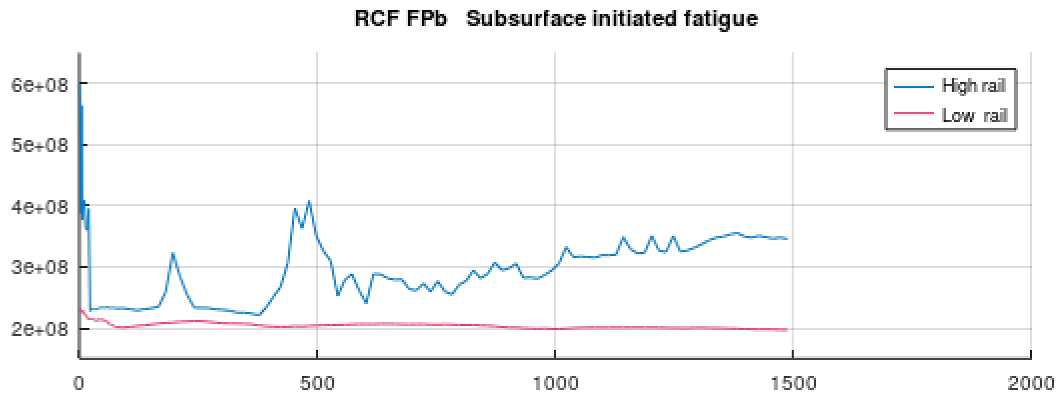

Appendix Q. Lateral uncompensated acceleration 1.17

This case is denoted:

wl_09.33_0.30_360_5.14_2_2_1_0_1.17_1_0.74,11_0_5

All data are the same as the reference case 9, except the uncompensated lateral acceleration, which is here equal to 1.17[m/s^2] (same as 180[mm] cant deficiency), see section 8.

Q.1 Development of conicity wheelset 1&4

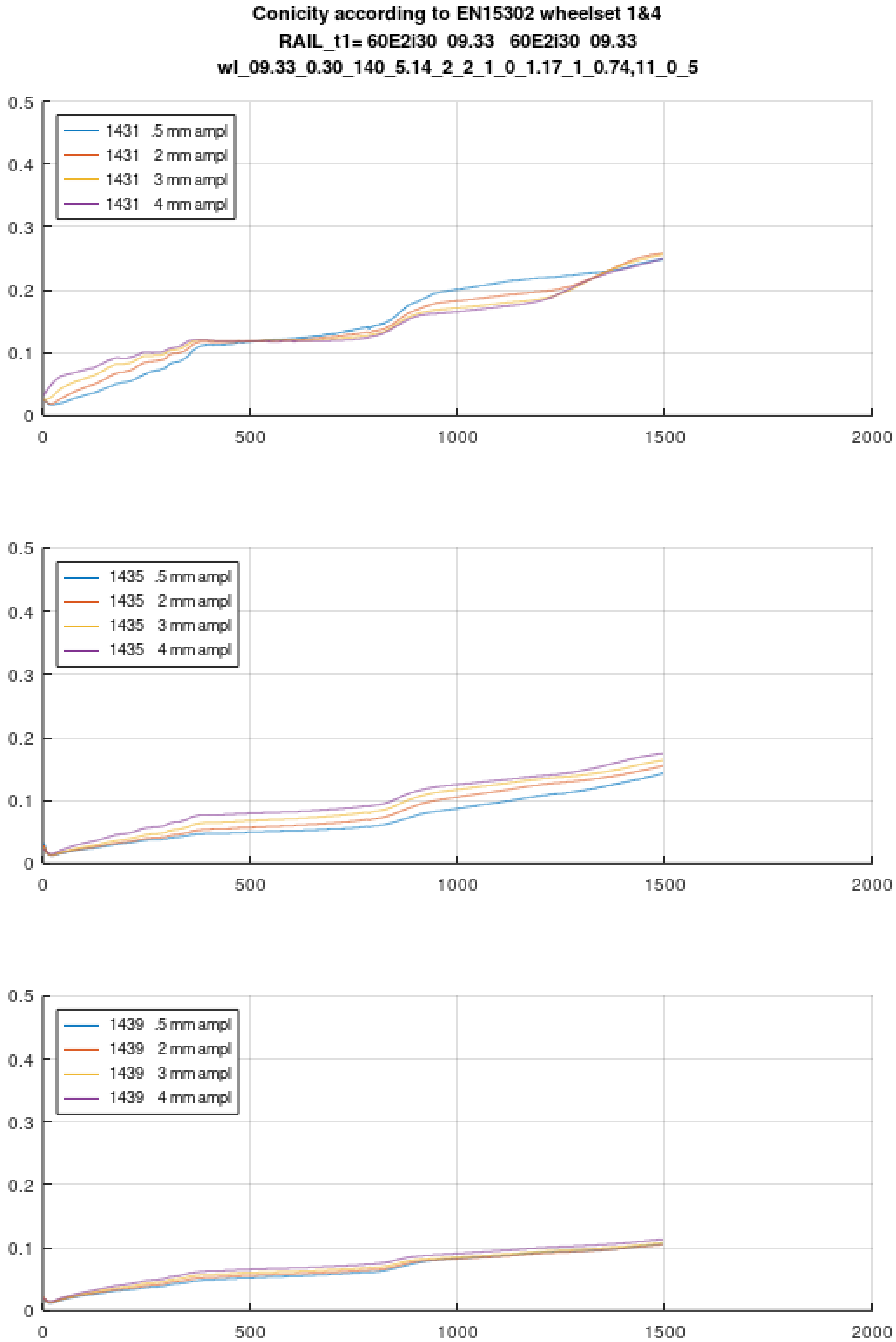

This case is quite similar to the reference case 9.1, the conicity is only increasing a little bit more.

Q.2 Development of wheel profile shapes wheelset 1&4

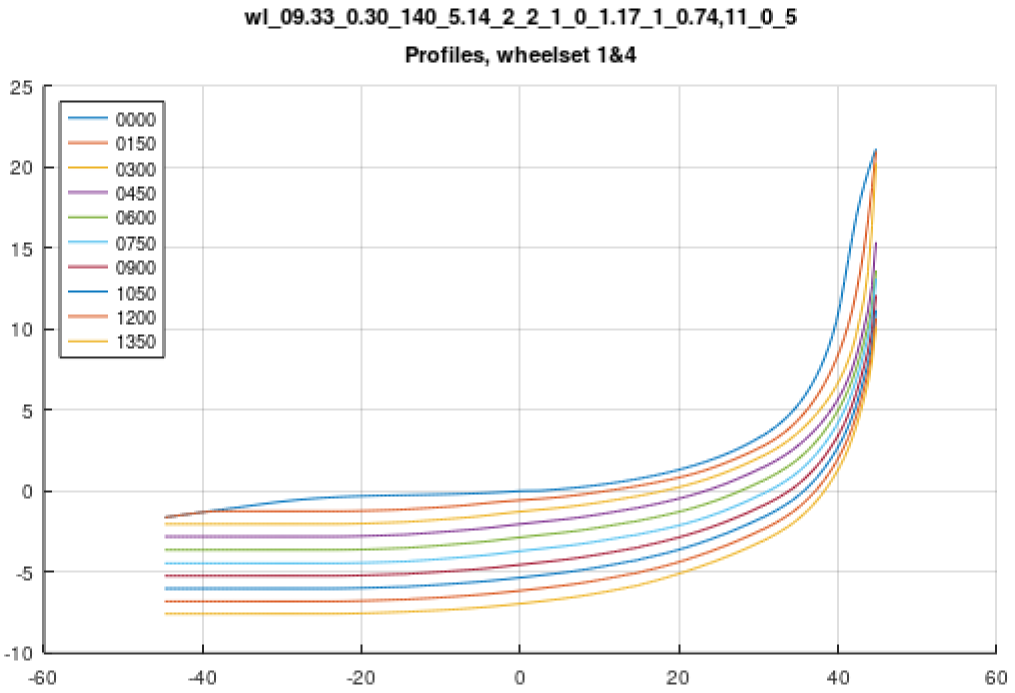

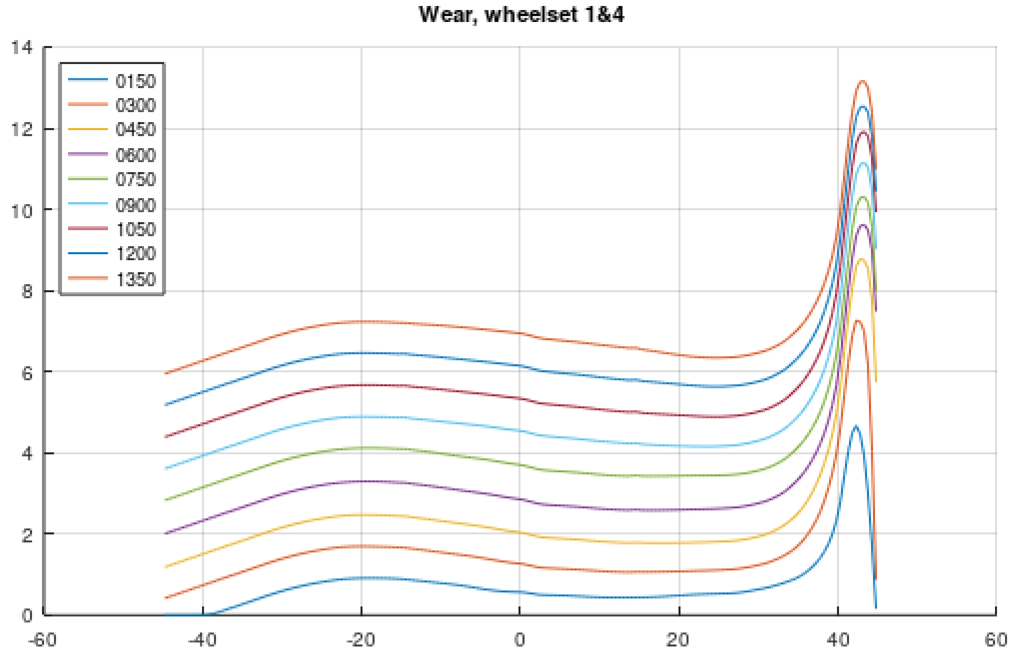

The worn wheel profiles are very similar to the reference case 9.3, it is difficult to see the differences with the bare eye.

Q.3 Development of GIPw

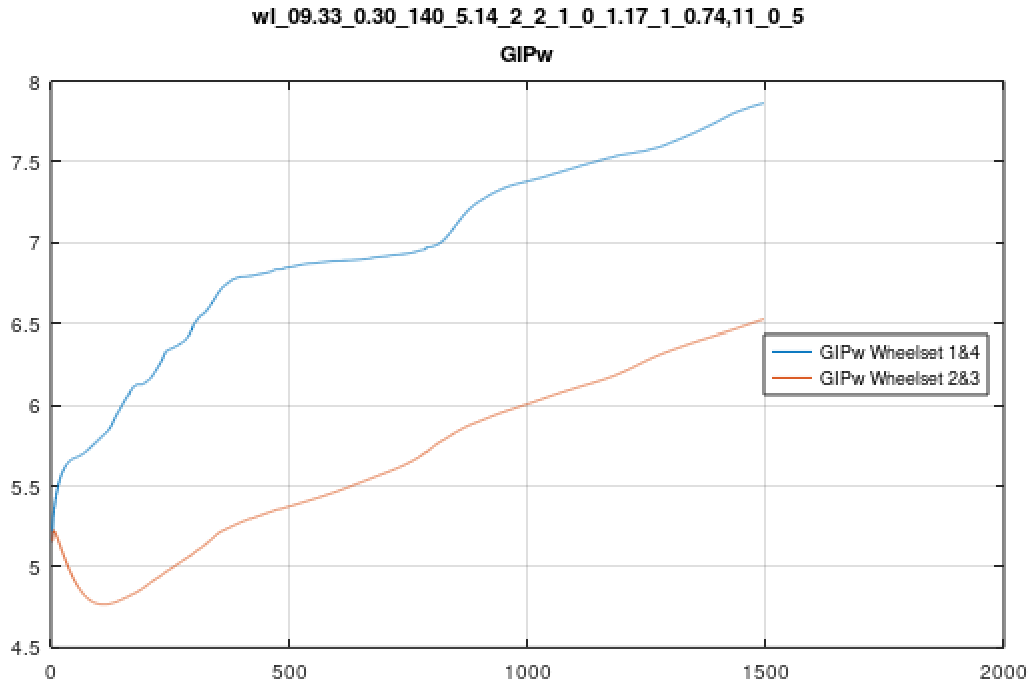

GIPw is quite similar to the reference case 9.5, it only increases a little bit slower, and the step in GIPw occurs a little bit later.

Q.4 Development of the Flange Thickness

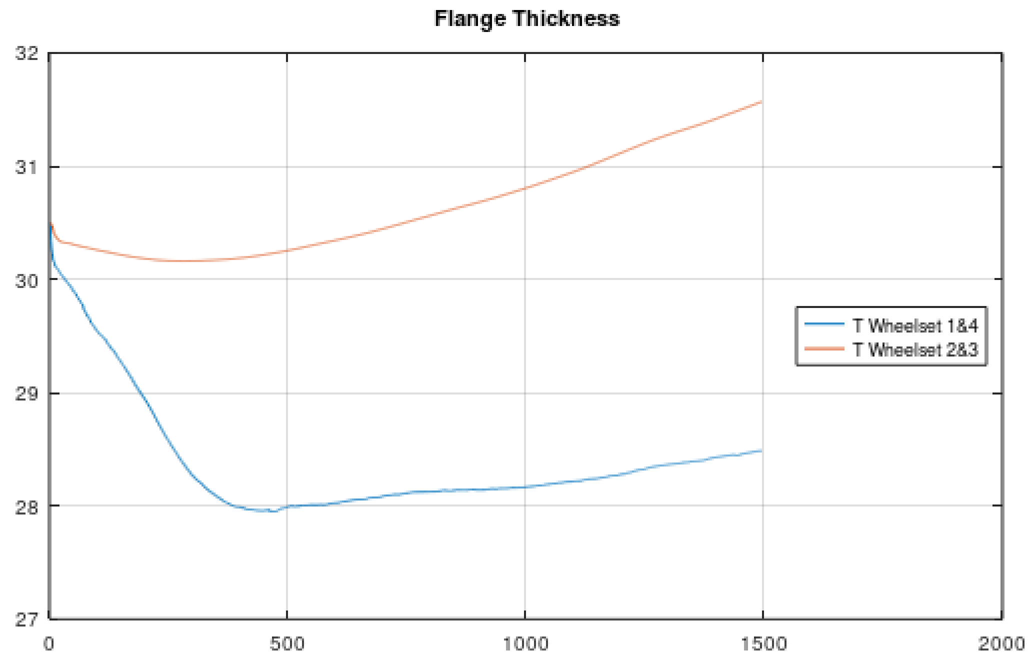

The flange thickness is very similar to the reference case 9.6.

Q.5 Development of the Flange Flank qR

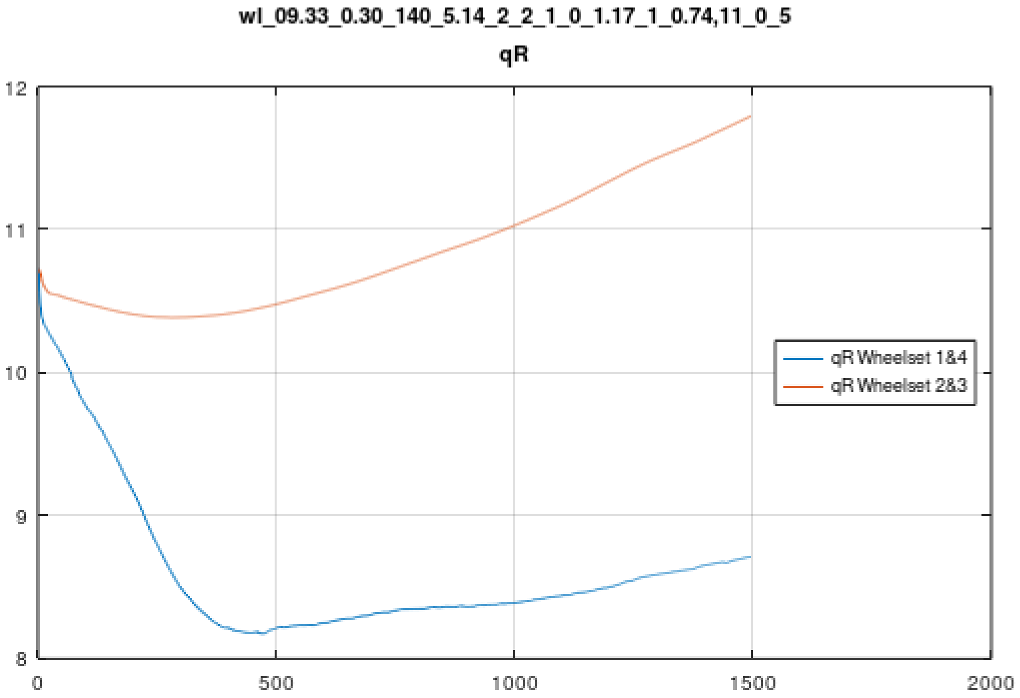

The flange flank qR is also very similar to the reference case 9.7, just a little bit lower.

Q.6 Development of the Wheelset Steering Ability

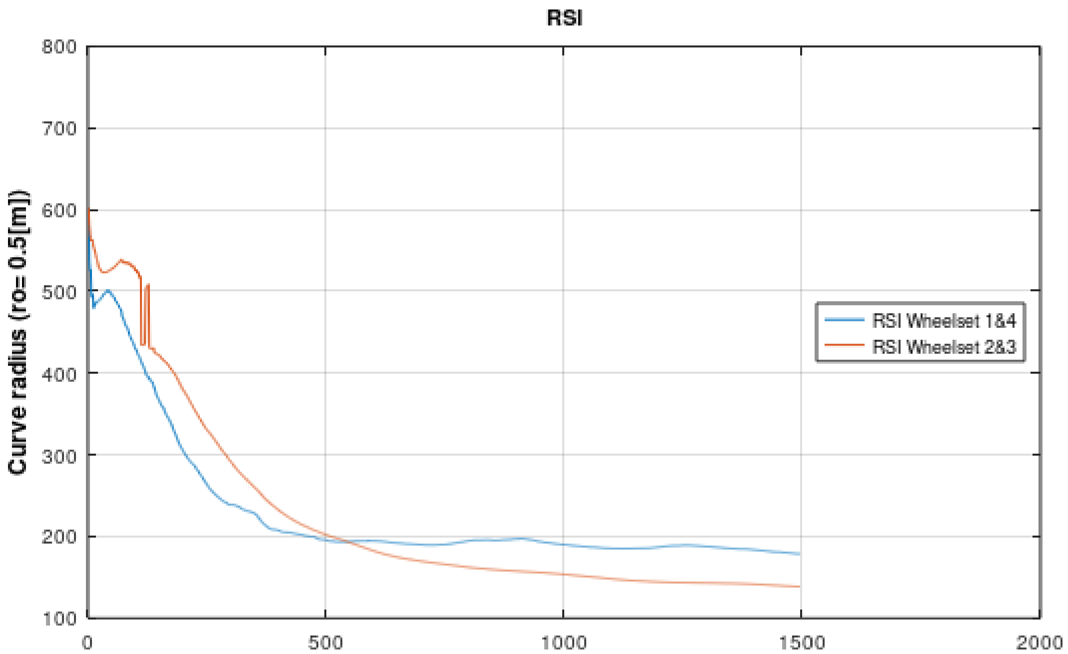

The wheelset steering ability is also very similar to the reference case 9.8.

Q.7 Development of the risk for RCF

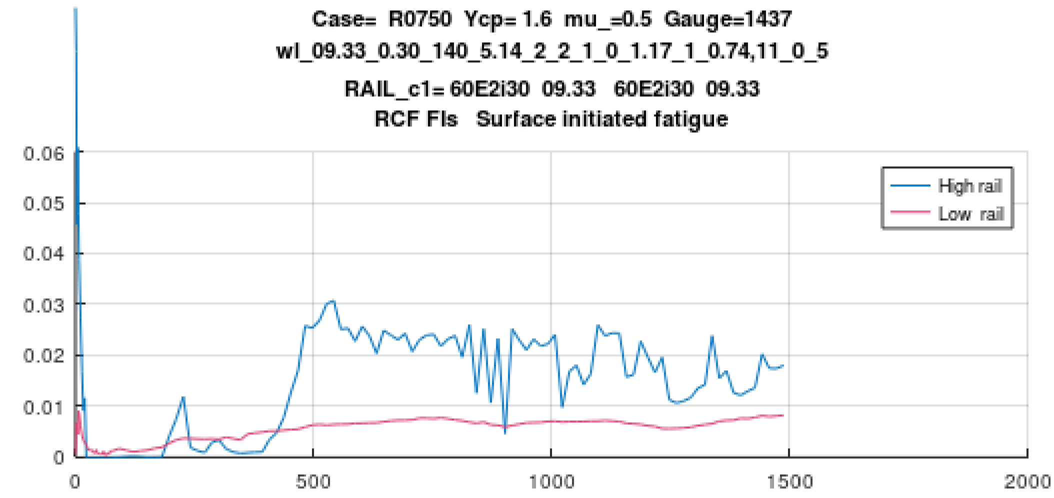

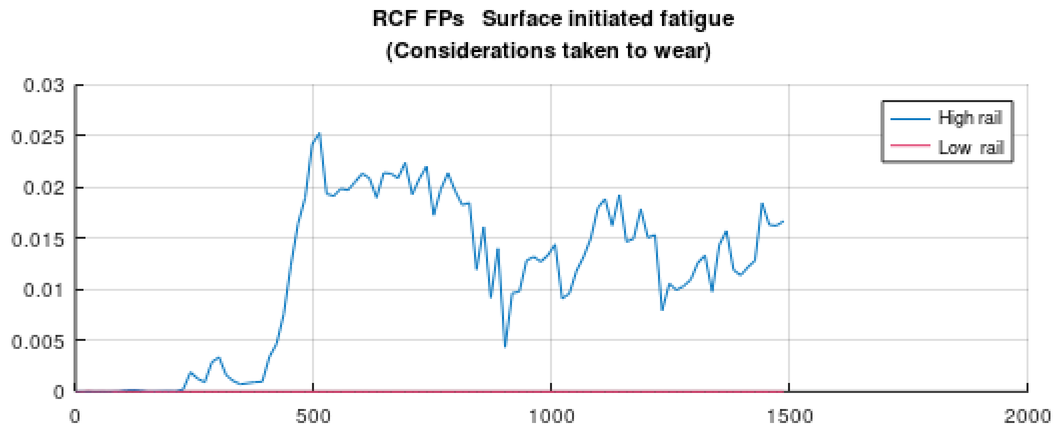

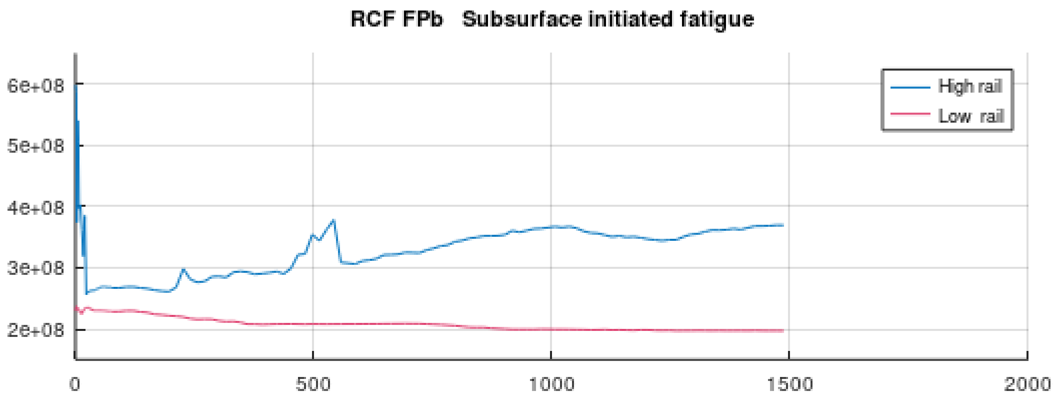

The risk for RCF is also very similar to the reference case 9.9.

Appendix R. Lateral uncompensated acceleration 1.60

This case is denoted:

wl_09.33_0.30_360_5.14_2_2_1_0_1.60_1_0.74,11_0_5

All data are the same as the reference case 9, except the uncompensated lateral acceleration, which is here equal to 1.60[m/s^2] (same as 245[mm] cant deficiency) , see section 8.

R.1 Development of conicity wheelset 1&4

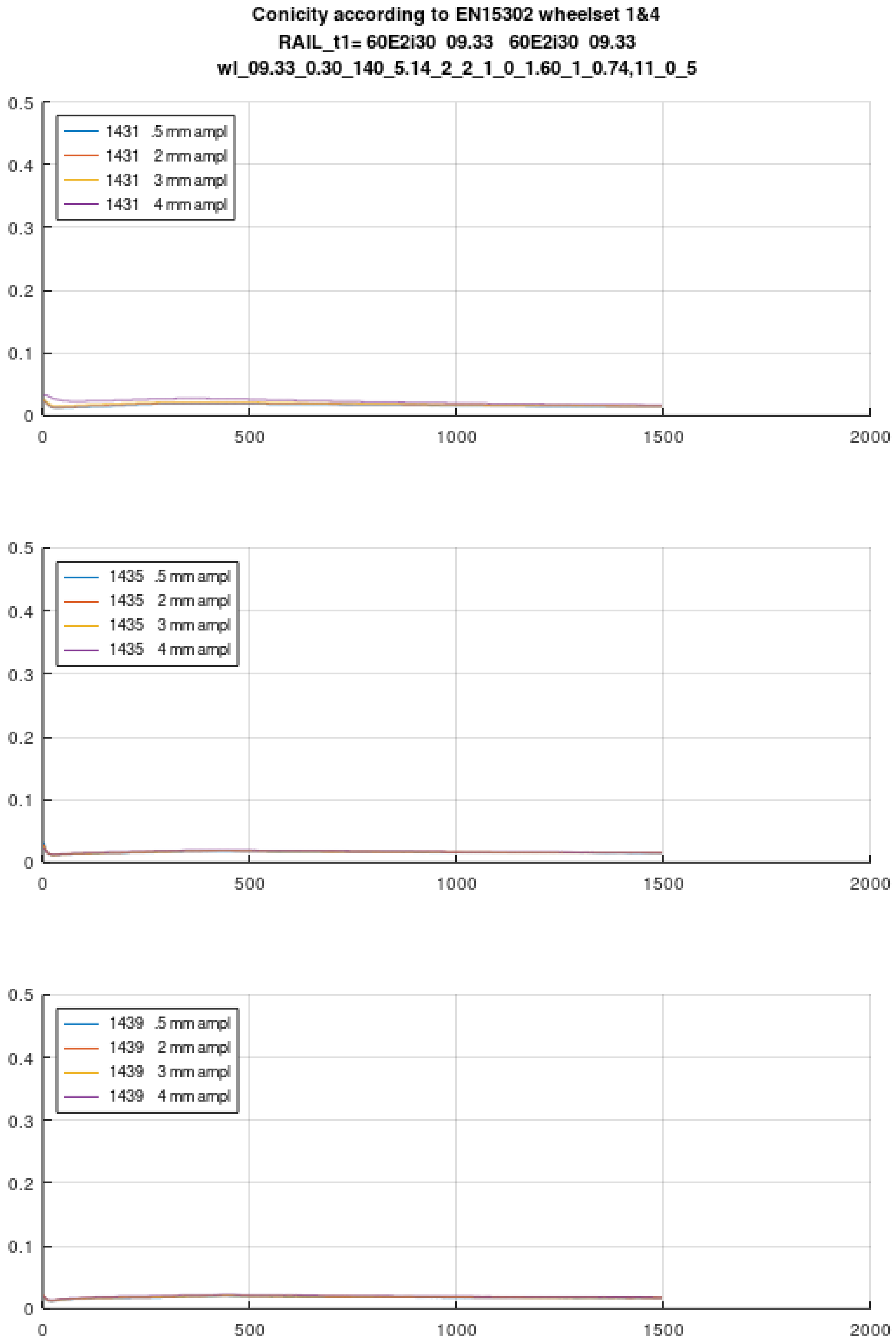

The wheel/rail conicity is very low for this case, during the whole lifetime of the wheel. Our understanding is that the lateral acceleration is so high that the load on the lower rail is so low that the wheelset cannot steer very well.

R.2 Development of wheel profile shapes wheelset 1&4

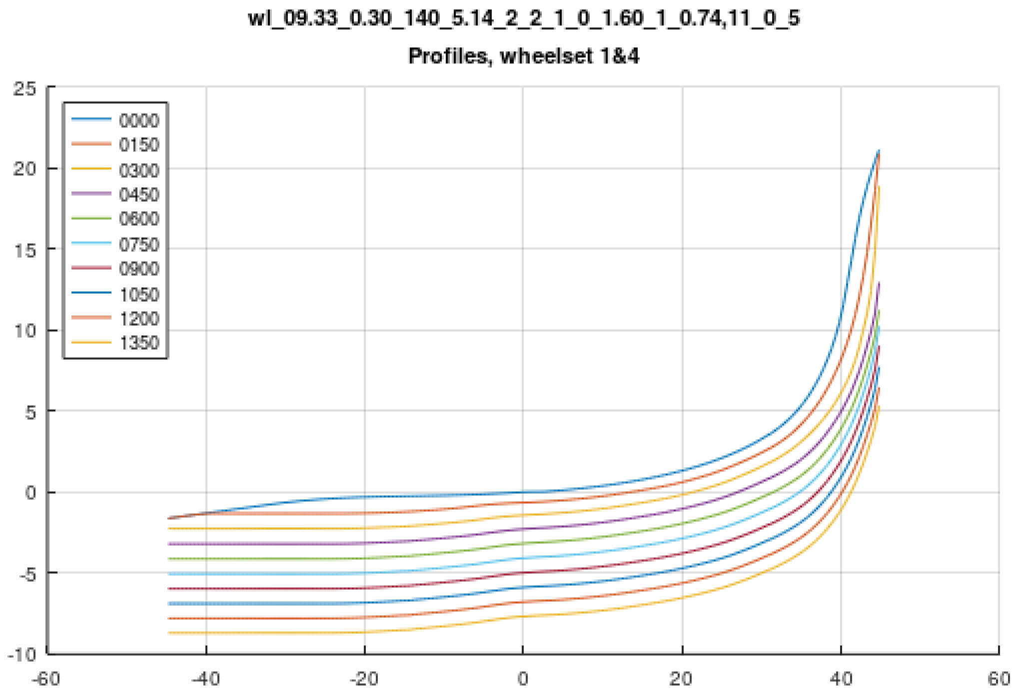

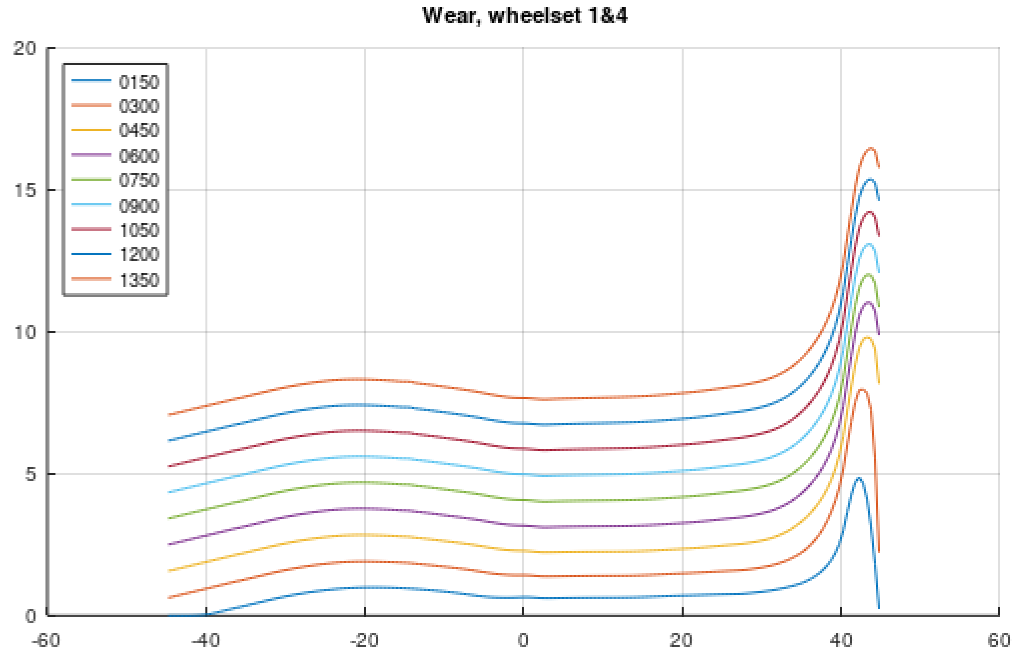

Compared to the reference case 9.3, this case has an more even wear over the whole surface of the wheel.

R.3 Development of GIPw

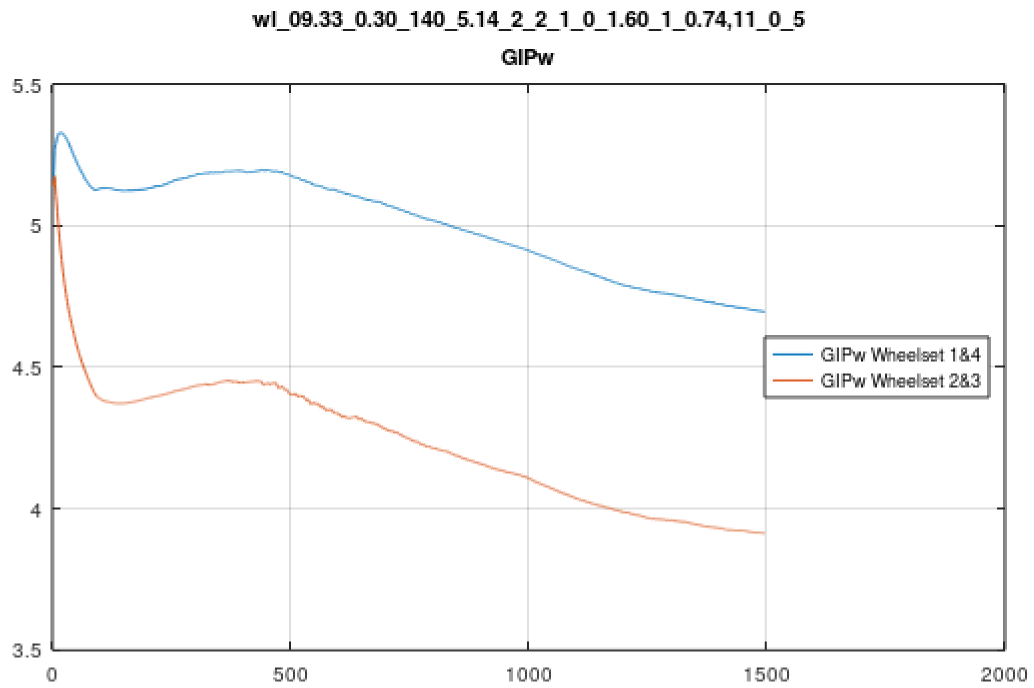

GIPw behaves quite differently compared to the reference case 9.5. In this case GIPw is decreasing.

R.4 Development of the Flange Thickness

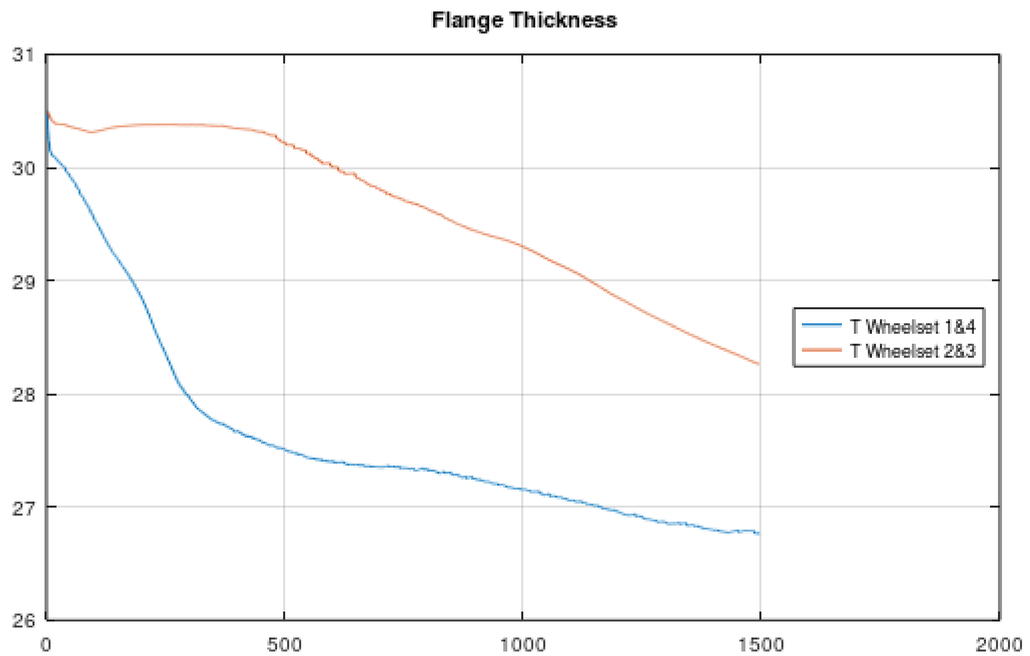

The flange thicknesses are decreasing all the time, in contrast to what they do in the reference case 9.6.

R.5 Development of the Flange Flank qR

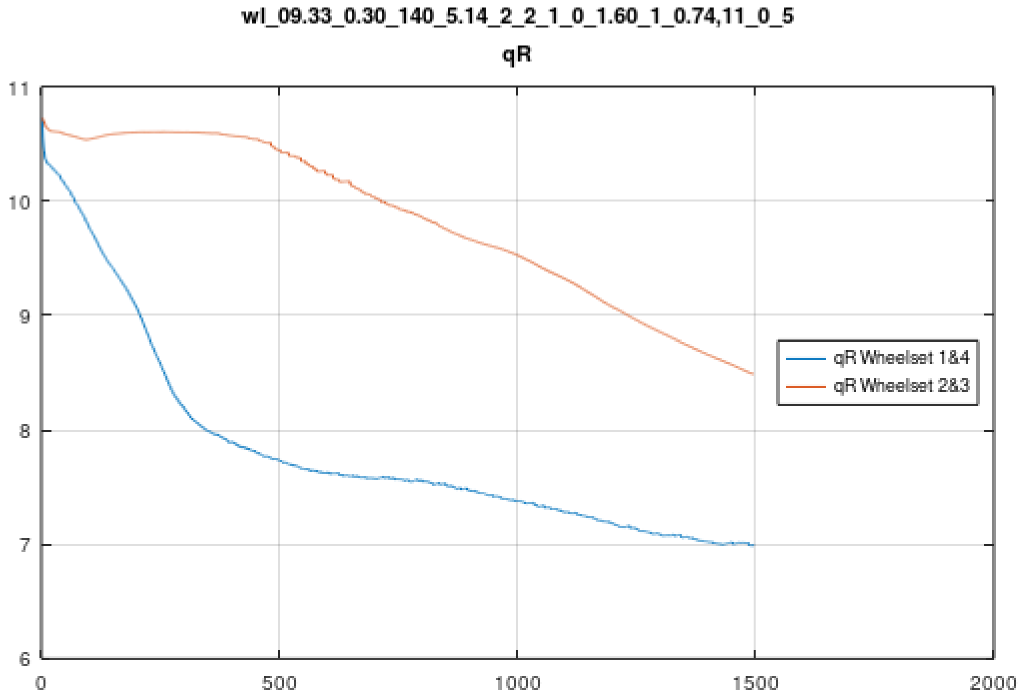

The flange flanks are also decreasing, in contrast to what they do in the reference case 9.7.

R.6 Development of the Wheelset Steering Ability

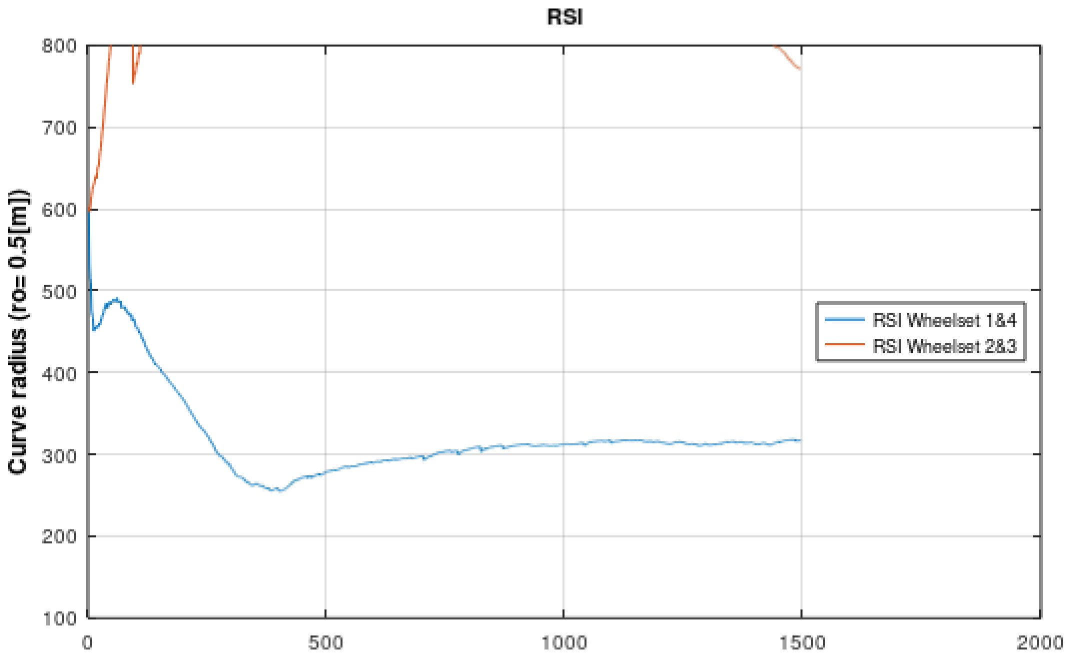

The wheelset steering ability for wheelset 1&4 is relatively constant ~300m, but the wheelset steering ability for wheelset 2&3 becomes quickly very bad. The curve for wheelset 2&3 can only be seen the first initial wear steps, after a little while the curve disappears. If the diagram is plotted with automatic scales. The curve will look like this:

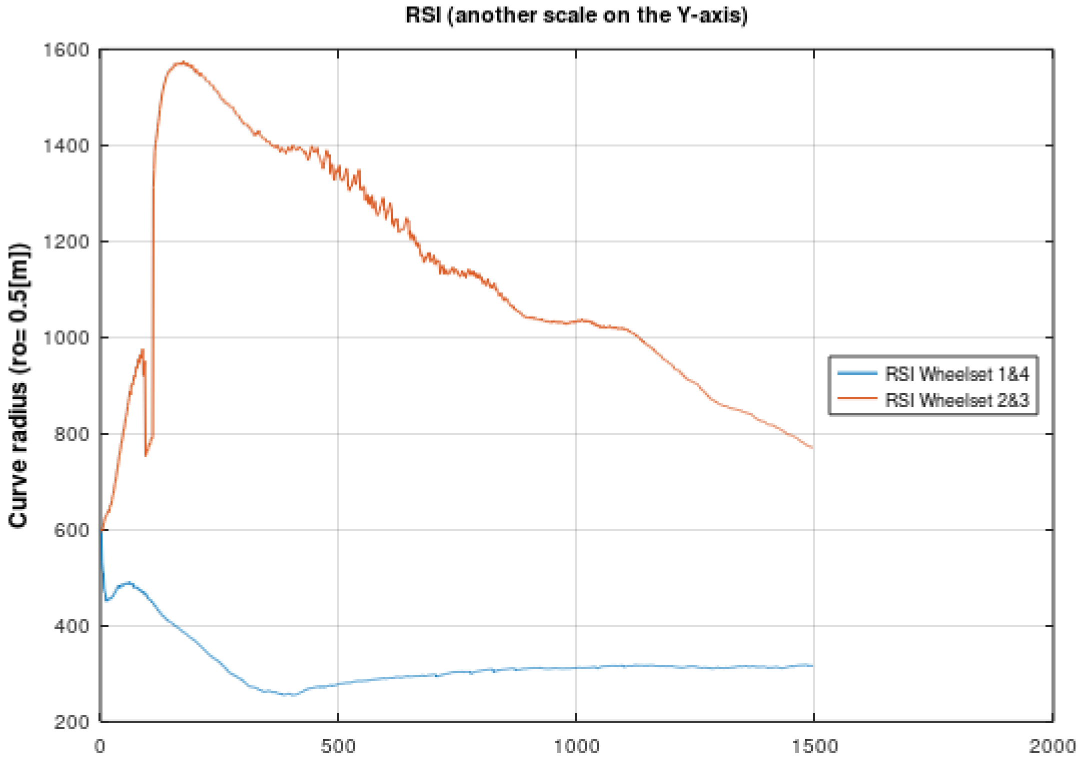

R.7 Development of the risk for RCF

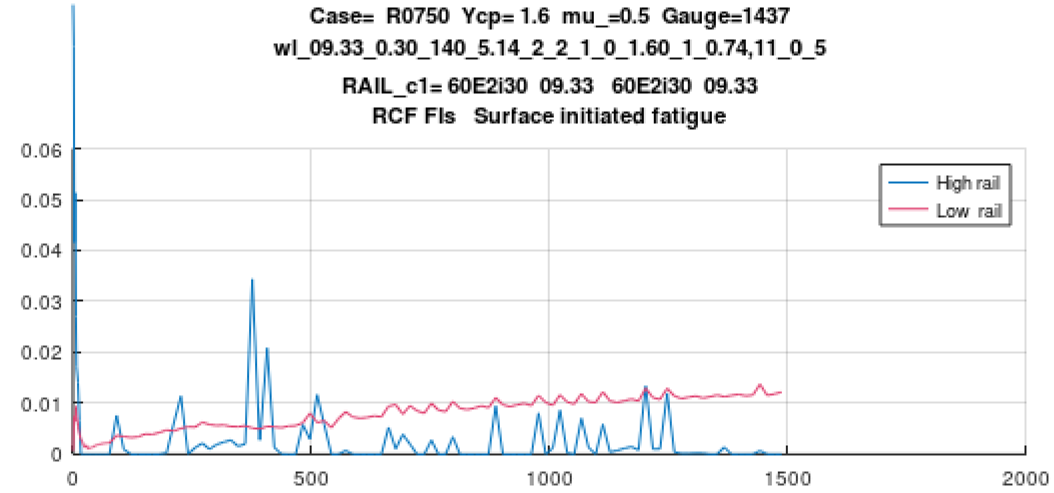

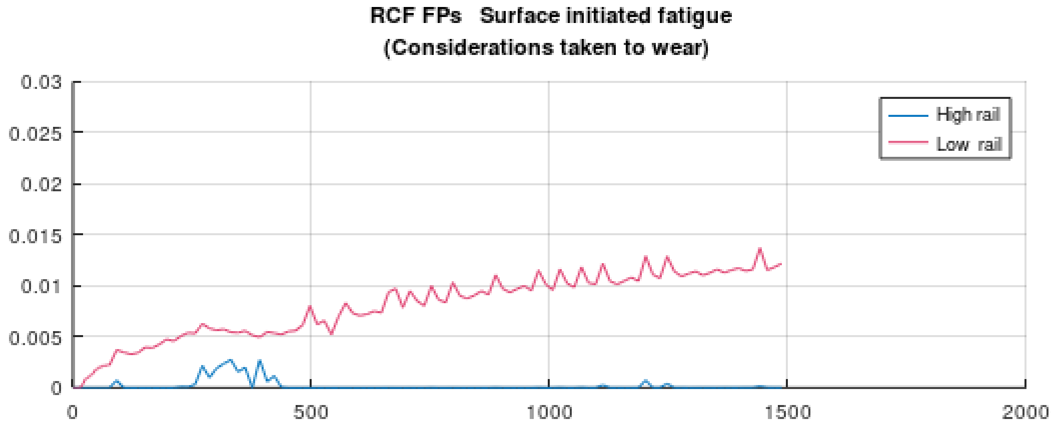

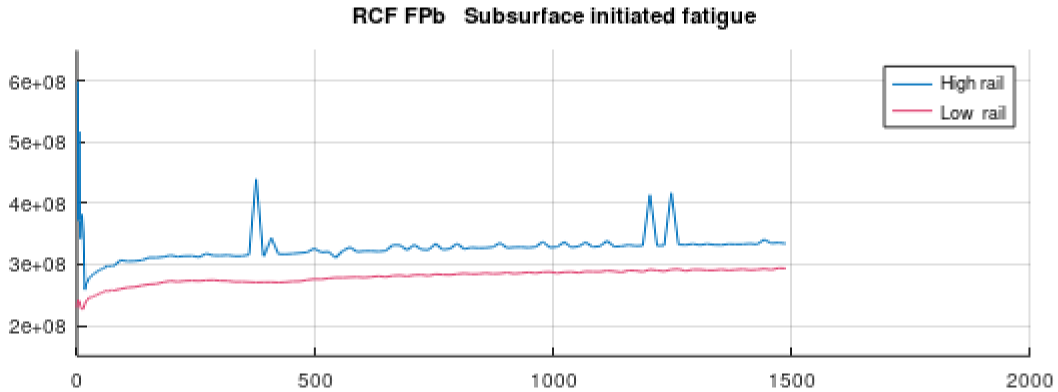

Compared to the reference case 9.9 the RCF curves look very differently. In this case the risk for RCF FPs occurs on the lower rail rather than the high rail. Regarding RCF FPb it is a little better on the high rail and much better on the low rail.

Appendix S. Different rail profiles in curves

This case is denoted:

wl_08.34t_09.33c_0.30_360_5.14_2_2_1_0_1.00_1_0.74,11_0_5

All data are the same as the reference case 9, except that two different rail profiles has been used. On tangent tracks and in very tight curves profile 60E1i30 has been used, in curves between 400-1400m rail profile 60E2i30 has been used. More information about rail profiles can be found in section 4.

S.1 Development of conicity wheelset 1&4

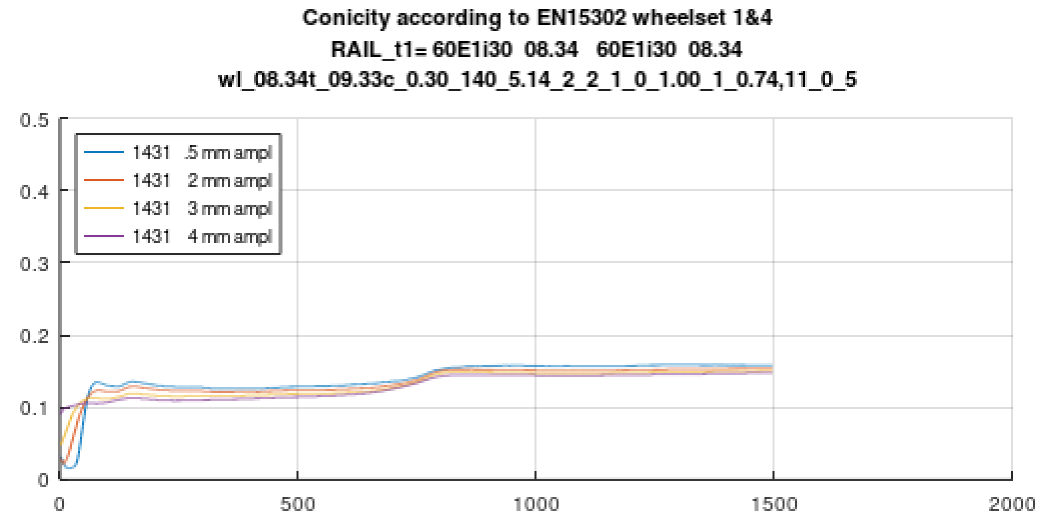

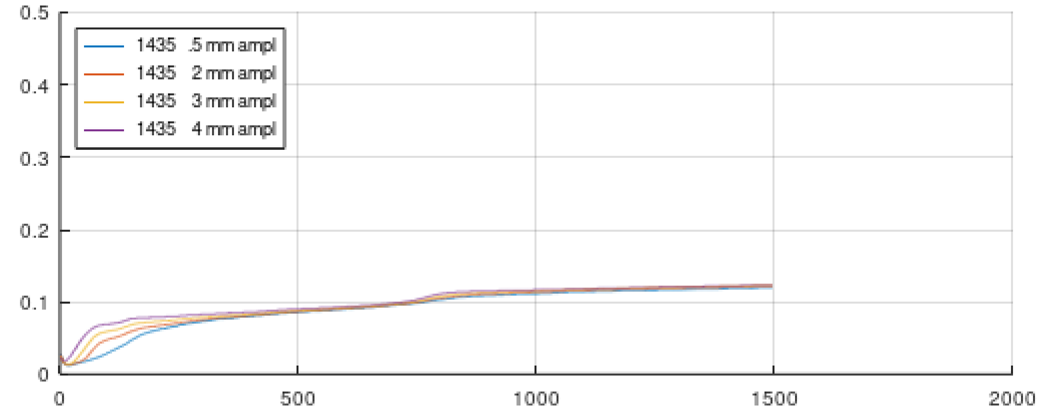

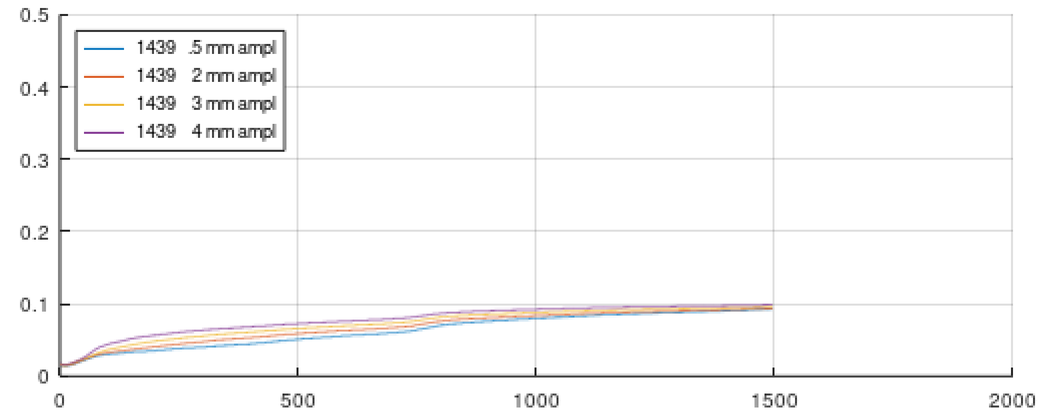

The development of the conicity looks very good. The conicity is well below 0.3 and is almost constant during the whole lifetime of the wheel. For comparisons see the reference case 9.1.

S.2 Development of wheel profile shapes wheelset 1&4

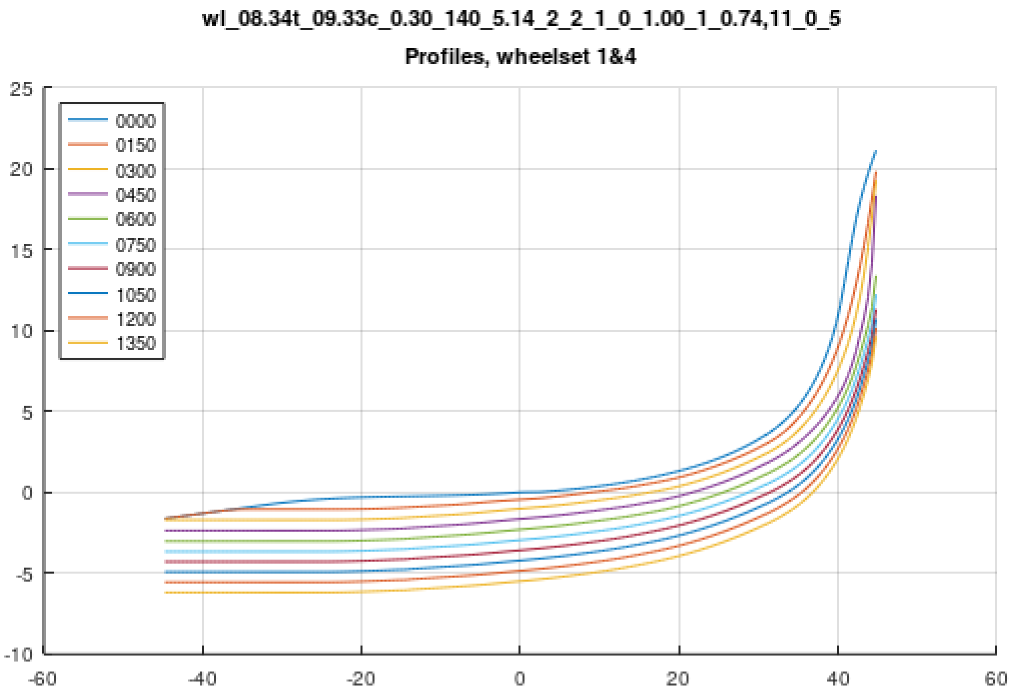

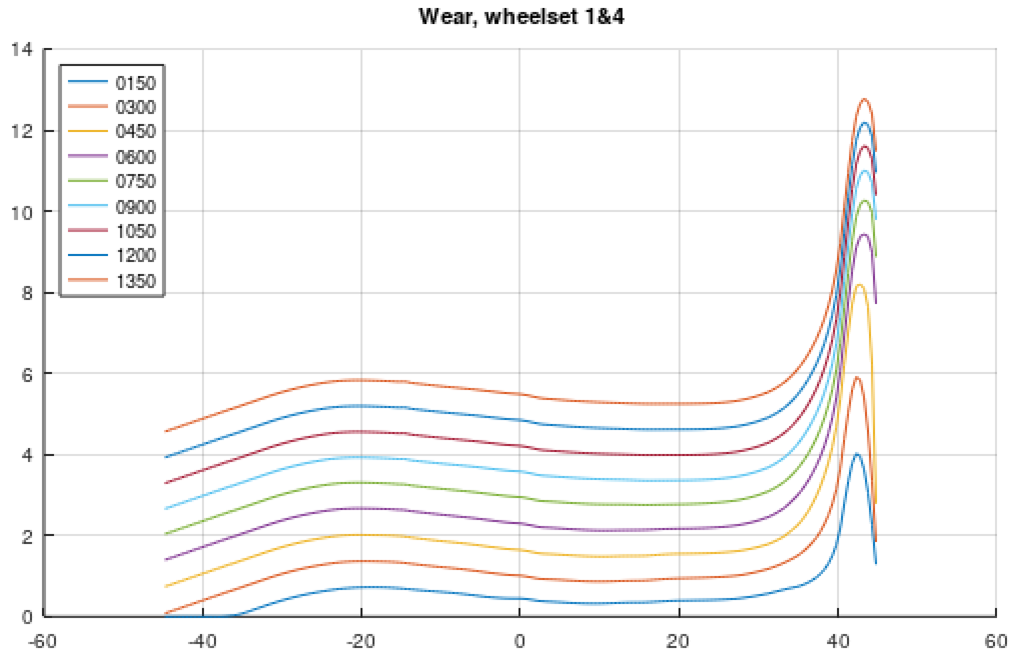

The worn wheel profiles are relatively similar to the reference case 9.3, it is difficult to see the differences with the bare eye.

S.3 Development of GIPw

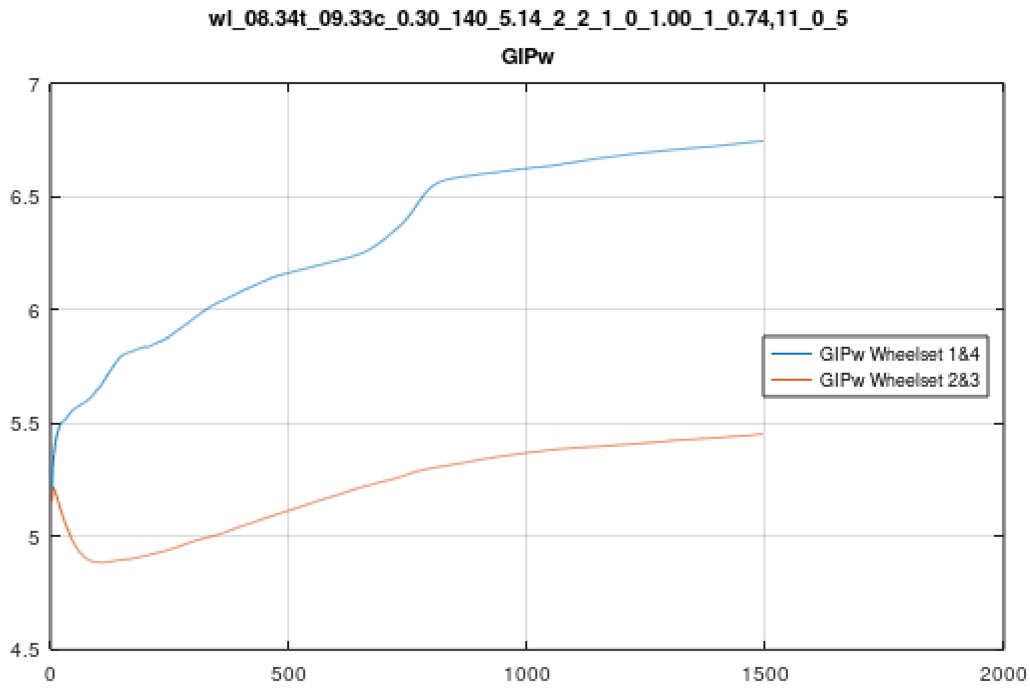

The development of GIPw looks very good. It increases with travelled distance but not as much as in the reference case 9.5.

S.4 Development of the Flange Thickness

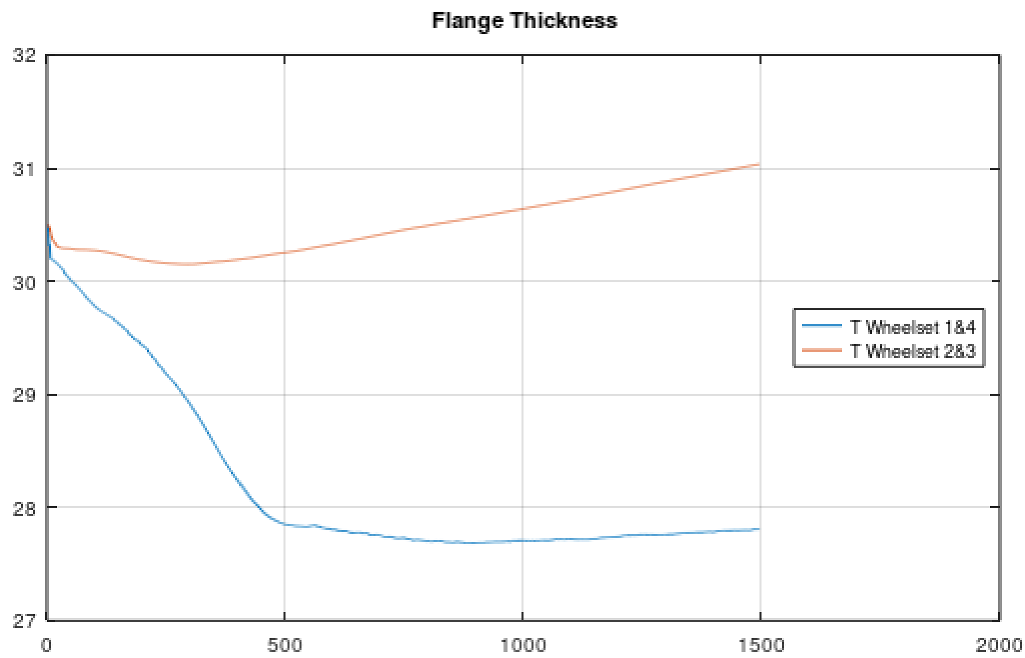

The flange thicknesses look very good. They are quite constant during the whole lifetime of the wheel. For comparisons see the reference case 9.6.

S.5 Development of the Flange Flank qR

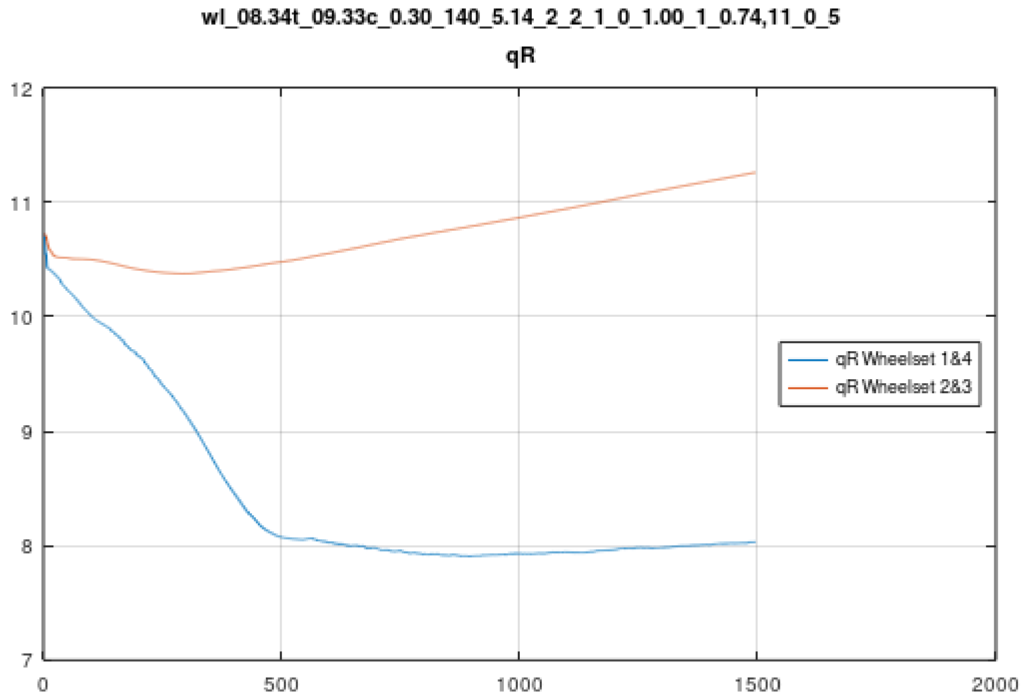

The flange flank qR looks very good. They are quite constant during the whole lifetime of the wheel. For comparisons see the reference case 9.7.

S.6 Development of the Wheelset Steering Ability

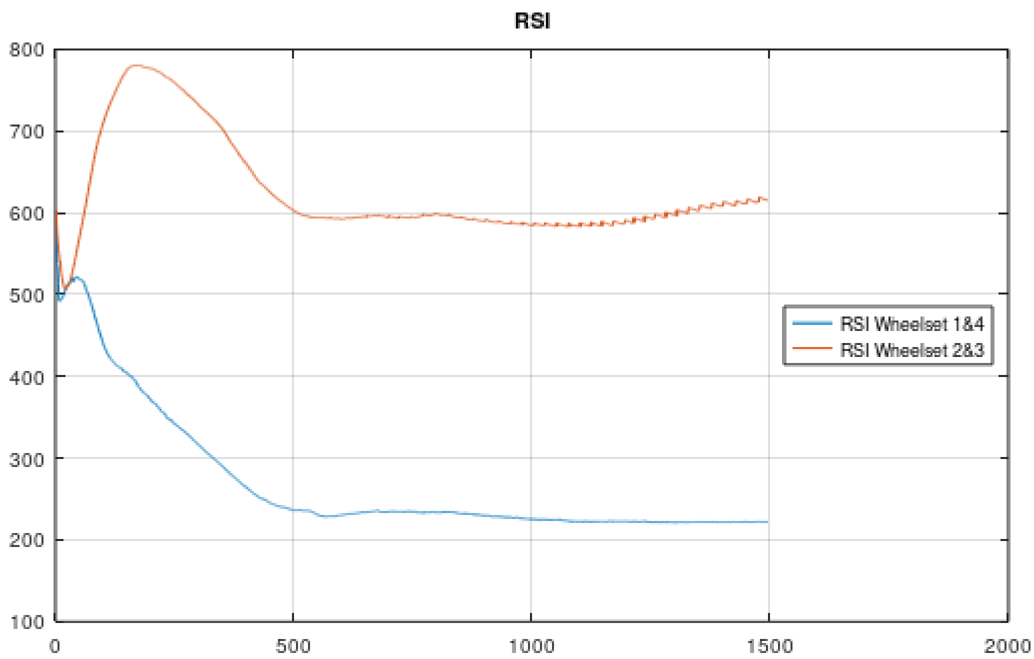

The figure above shows the wheelset steering ability against the curve rail. Relative to this rail the steering ability doesn't look very impressive, but this is also the purpose of this rail. The steering should not be so good in curves 400-1400m because we want to have a wear rate that is greater than the crack propagation rate.

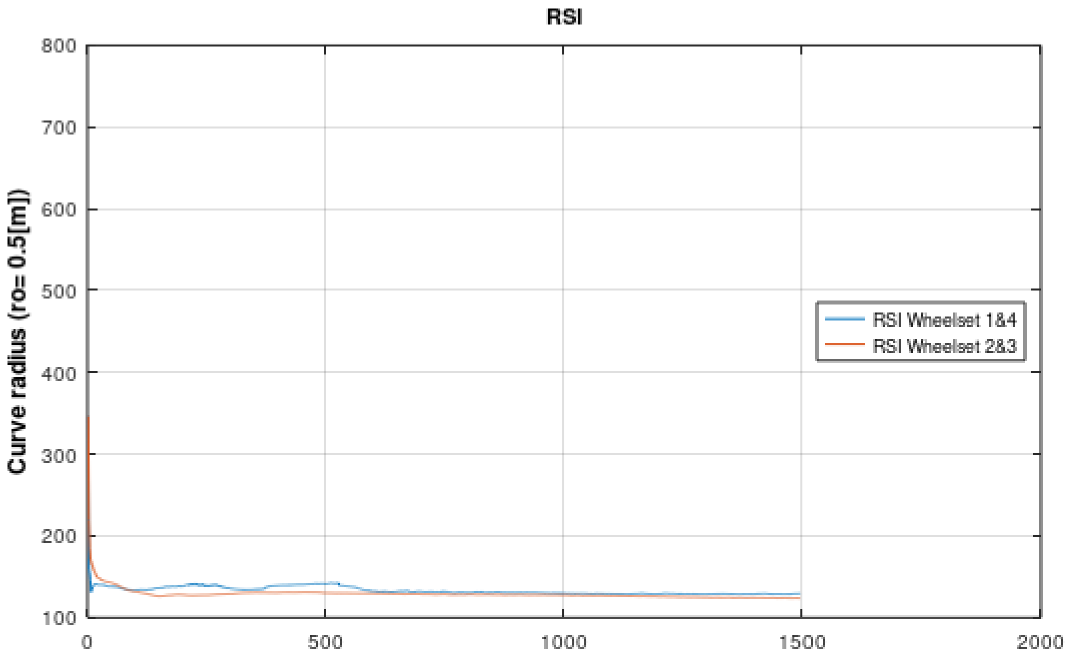

The figure above shows the wheelset steering ability against the tangent track rail. Relative to this rail the steering ability looks very good. For comparisons see the reference case 9.8.

S.7 Development of the risk for RCF

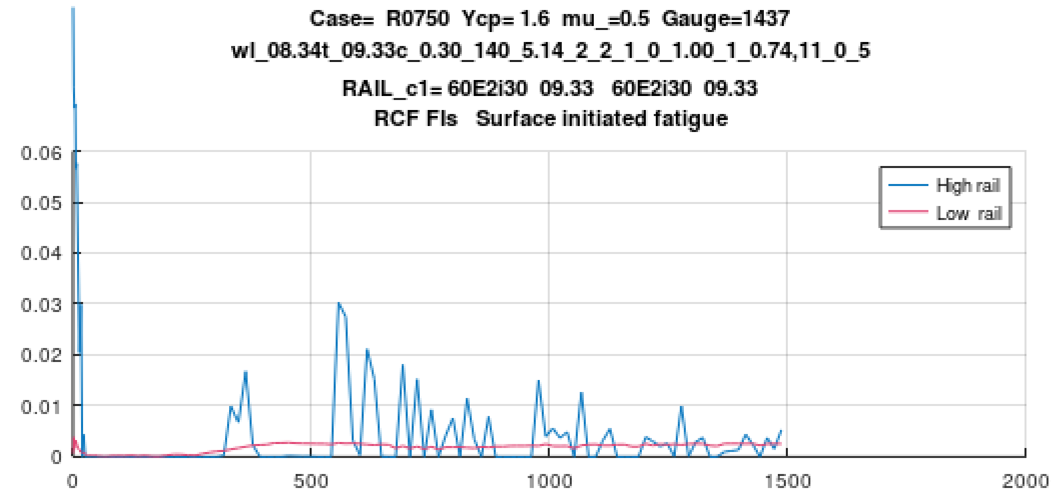

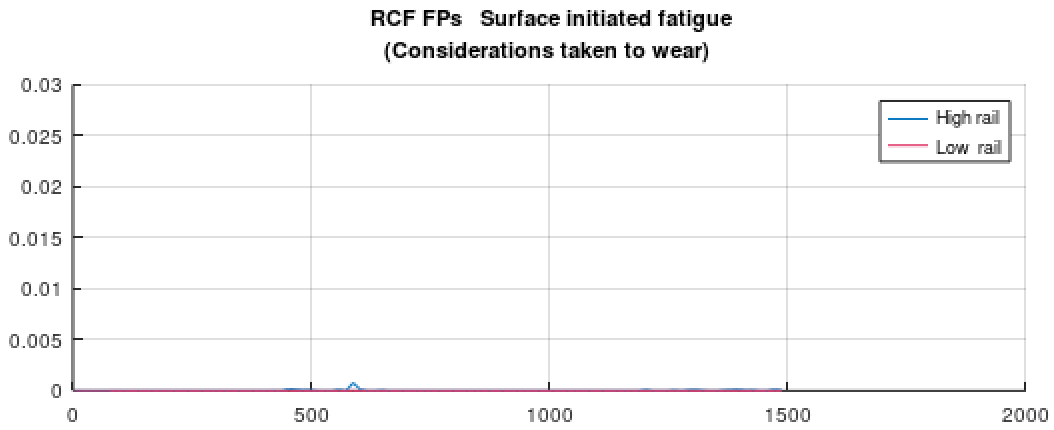

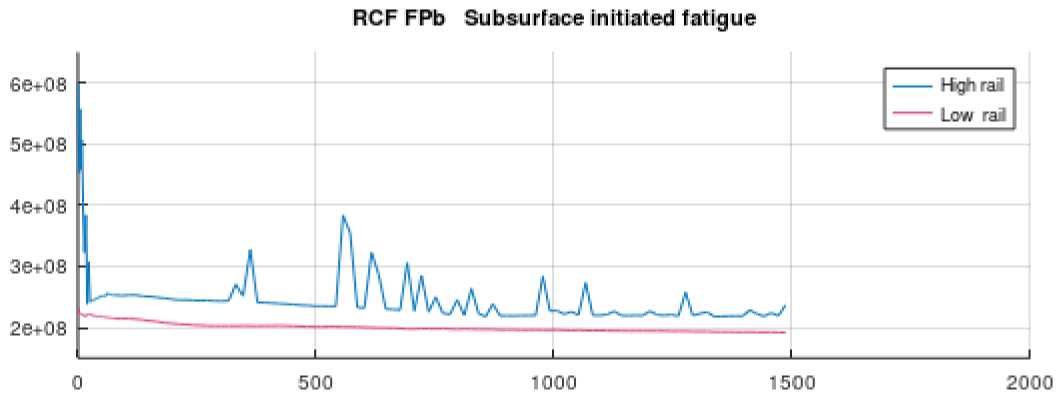

The risk for RCF FPs and RCF FPb are both very low, both on the high rail and the low rail.

For the chosen track section Stockholm-Gothenborg 7.1.2 this solution works well because this track section contains of a great portion of tangent track 65.4%, this means that it is mainly the tangent track sections that governs the shape of the wheels. The risk for RCF on tangent track sections are low, therefore the tangent track rail can mainly focus in shaping the wheel profiles so the conicities don’t becomes very high. The rails in the curves on the other hand can mainly focus in minimizing the risk for RCF.